Lantibiotic resistance in human pathogens

Inaugural-Dissertation

For the attainment of the title of doctor in the
Faculty of Mathematics and Natural Sciences at the
Heinrich Heine University Duesseldorf

Presented by

Julia Schumacher
née Zaschke-Kriesche

Duesseldorf, November 2019

From the Institute of Biochemistry
At the Heinrich Heine University Duesseldorf

Published by permission of the
Faculty of Mathematics and Natural Science
At Heinrich Heine University Duesseldorf

Supervisor: Dr. Sander H. J. Smits
Co-supervisor: Prof. Dr. Holger Gohlke

Date of oral examination: 16.12.2019

“Have no fear of perfection; you’ll never reach it.“

(Marie S. Curie)

Abstract

The need for new compounds, which can be used as antibiotics is rising. Antimicrobial peptides are excellent candidates to fulfill this. The subclass of lantibiotics contain unusual amino acids and lanthionine rings, which ensure their high stability and high potency. They are active in the nanomolar range and exhibit two main modes of action: Binding to the cell wall precursor lipid II as well as in some cases pore formation within the bacterial membrane, which leads to cell death. Commercial usage is, however hampered by the presence of genes in human pathogenic strains which, when expressed, confer resistance. The human pathogen *Streptococcus agalactiae* COH1 for example is resistant against different lantibiotics due to the nsr-operon encoding a two-component system NsrRK, the nisin resistance protein (NSR) and a BceAB-type ABC transporter NsrFP (1). Interestingly, this operon appears to be evolutionary conserved in several other human pathogenic bacteria.

The nisin resistance protein *Sa*NSR is a C-terminal processing peptidase (CTP) and has a specific catalytic dyad mechanism consisting of a serine and a histidine residue (2, 3). It was shown that *Sa*NSR confers resistance against nisin by degrading the lantibiotic at its C-terminus resulting in a 100 fold less active nisin fragment (4, 5). The crystal structure of *Sa*NSR was solved and shows a 10 Å width tunnel, which is hydrophobic, negatively charged and binds the last two (methyl–) lanthionine rings D and E of nisin (3). In this thesis I discovered how to overcome the resistance mediated by *Sa*NSR by two approaches. The first approach was to bypass the protein by a nisin derivate, which is still active but the serine protease is not able to cleave this variant *in vivo.* The second approach was based on molecular modelling and revealed a small molecule which specifically inhibits *Sa*NSR.

The ABC transporter NsrFP from *Streptococcus agalactiae* belongs to the BceAB-type transporters (6). Several BceAB-type transporters are known which confer resistance against more than one antimicrobial peptide (7-10). In this thesis I elucidated the mechanism of *Sa*NsrFP and demonstrated that the BceAB-type transporter flips the cell wall precursor lipid II inside of the cytoplasm. Further a specific inhibitor of the transporter was detected by screening of natural compounds and their derivatives.

Zusammenfassung

Der Bedarf an neuen Wirkstoffen, die als Antibiotika eingesetzt werden können, steigt. Antimikrobielle Peptide sind ausgezeichnete Kandidaten, um dies zu erfüllen. Die Unterklasse der Lantibiotika enthält ungewöhnliche Aminosäuren und Lanthioninringe, die für ihre hohe Stabilität und hohe Wirksamkeit sorgen. Sie sind im nanomolaren Bereich aktiv und weisen zwei Hauptwirkungsweisen auf: Bindung an die Zellwandvorstufe Lipid II, sowie in manchen Fällen Porenbildung innerhalb der Bakterienmembran, die zum Zelltod führt. Die kommerzielle Nutzung wird jedoch durch das Vorhandensein von Genen in humanpathogenen Stämmen behindert, die, wenn sie exprimiert werden, Resistenz verleihen. Der humane Erreger *Streptococcus agalactiae* COH1 ist beispielsweise resistent gegen verschiedene Lantibiotika, da das nsr-Operon für ein Zweikomponentensystem NsrRK, das Nisin-Resistenzprotein (NSR) und einen BceAB-Typ ABC Transporter NsrFP kodiert (1). Interessanterweise scheint dieses Operon evolutionär in mehreren anderen humanpathogenen Bakterien konserviert zu sein.

Das Nisin-Resistenzprotein *Sa*NSR ist eine C-Terminal verarbeitende Peptidase (CTP) und weist einen spezifischen katalytischen Paar-Mechanismus auf, der aus einem Serin- und einem Histidinrest besteht (2, 3). Es wurde gezeigt, dass *Sa*NSR Resistenz gegen Nisin vermittelt, indem es das Lantibiotikum an seinem C-Terminus abbaut, was zu einem 100-fach weniger aktiven Nisinfragment führt (4, 5). Die Kristallstruktur von *Sa*NSR wurde gelöst und zeigt einen 10 Å breiten Tunnel, der hydrophob, negativ geladen ist und die letzten beiden (Methyl-) Lanthioninringe D und E von Nisin bindet (3). In dieser Arbeit habe ich entdeckt, wie man die von *Sa*NSR vermittelte Resistenz durch zwei Ansätze überwindet. Der erste Ansatz bestand darin, das Protein durch ein Nisinderivat zu umgehen, das noch aktiv ist, aber die Serinprotease ist nicht in der Lage, diese Variante *in vivo* zu spalten. Der zweite Ansatz basierte auf molekularer Modellierung und zeigte ein kleines Molekül, das *Sa*NSR spezifisch hemmt.

Der ABC Transporter NsrFP von *Streptococcus agalactiae* gehört zu den Transportern vom Typ BceAB (6). Es sind mehrere Transporter vom Typ BceAB bekannt, die Resistenz gegen mehr als ein antimikrobielles Peptid verleihen (7-10). In dieser Arbeit habe ich den Mechanismus von *Sa*NsrFP aufgeklärt und gezeigt, dass der Transporter vom Typ BceAB die Zellwandvorstufe Lipid II in das Zytoplasma umdreht. Weiterhin wurde ein spezifischer Inhibitor des Transporters nachgewiesen indem Naturstoffe und deren Derivate überprüft wurden.

Table of contents

List of figures

Abbreviations

ATP	Adenosine-5-triphosphate
Å	Angström
AMP	antimicrobial peptide
ABC	ATP-binding cassette
B. subtilis	*Bacillus subtilis*
CTPs	C-terminal processing peptidase
CL	cardiolipin
C. difficile	Clostridium difficile
Dha	dehydroalanine
Dhb	dehydroamminobutyric acid
DNA	desoxyribonucleic acid
3d	drei dimensional
ECD	extracellular domain
HPLC	high pressure liquid chromatography
kDa	kilo dalton
L. lactis	*Lactococcus lactis*
Lan	lanthionine
L. monocytogenes	*Listeria monocytogenes*
L-PG	lysyl-phosphatidylglycerol
mRNA	messegner ribonucleic acid
MeLan	methyl-lanthionine
µM	micro molar
mM	milli molar
MprF	multipeptide resistance factor
M. tuberculosis	*Mycobacterium tuberculosis*
GlcNAc	N-acetylglucosamine
MurNAc	N-acteylmuramic acid
nm	nano meter
nM	nano molar
NSR	nisin resistance protein
NBD	nucleotide binding domain
NMR	nulear magnetic resonance
PBP	penicillin-binding proteins
PGN	peptidoglycan
PC	phosphatidylcholine
PE	phosphatidylethanolamine
PG	phosphatidylglycerol
RP	reverse phase
RNA	ribonucleic acid

S. aureus	*Staphylococcus aureus*
S. epidermidis	*Staphylococcus epidermidis*
S. gallinarium	*Staphylococcus gallinarium*
S. mutans	*Streptococcu mutans*
S. agalactiae	*Streptococcus agalactiae*
Sa	*Streptococcus agalactiae*
S. coelicolor	*Streptomyces coelicolor*
S. venezuelae	*Streptomyces venezuelae*
TSP	tail specific protease
TMD	transmembrane domain
TMH	transmembrane helix
tRNA	transfer ribonucleic acid
TCS	two-component system
UP	undecaprenyl phosphate
UPP	undecaprenyl pyrophosphate
UDP	uridine diphosphate

amino acid	three letter code	one letter code
Alanine	Ala	A
Arginine	Arg	R
Asparagine	Asn	N
Aspartic acid	Asp	D
Cysteine	Cys	C
Glutamic acid	Glu	E
Glutamine	Gln	Q
Glycine	Gly	G
Histidine	His	H
Isoleucine	Ile	I
Lysine	Lys	K
Methionine	Met	M
Phenylalanine	Phe	F
Proline	Pro	P
Serine	Ser	S
Threonine	Thr	T
Tryptophan	Trp	W
Tyrosine	Tyr	Y
Valine	Val	V

1. Introduction

1.1. Antibiotics

Nearly one century ago the first antimicrobial substance penicillin was discovered (11), which drastically changed our era. Life expectancy increased due to antibiotic treatments, which cure bacterial infections (12). In the following decades several antibiotics and antibiotic classes were discovered, subdivided due to their mechanism of action (12, 13). The four main targets of antibiotics are nucleic acid synthesis, protein synthesis, the metabolic pathway and the cell wall synthesis.
Inhibiting the nucleic acid synthesis is the mechanism of, for example, quinolones, which target the enzymes DNA gyrase and topoisomerase IV. DNA gyrase and topoisomerase IV are responsible for untwisting of double stranded DNA and relaxing of positive supercoils, allowing DNA polymerase to continue. Consequently, bacteria cells were killed by the antibiotic quinolone due to prevented DNA replication (14-16).

Another mechanism of antibiotics is the inhibition of protein synthesis. Here, antibiotics target the 30S or 50S subunit of the bacterial ribosome, thereby circumvent the translation of the mRNA (17, 18). Antibiotics targeting the 30S subunit are aminoglycosides, causing misreading of the mRNA and preterm termination of the translation, and tetracyclines, preventing the binding of tRNA (17, 19). Inhibitors of the 50S subunit are chloramphenicol, macrolides and oxazolidinones (19). Chloramphenicol prevents binding of tRNA to the ribosome, whereas macrolides cause early detachment of uncompleted peptide chains (17, 19, 20). Oxazolidinones are synthetic antibiotics and impede the formation of the 70S ribosome (21).
The metabolic pathway is target of sulfonamides and trimethoprim, which inhibit the folic acid metabolism, essential for nucleotide synthesis those antibiotics disturb cell replication (17, 19).

Cell wall synthesis targeting antibiotics

Glycopeptides, lipodepsipeptides and ß-lactam antibiotics target the cell wall synthesis of bacteria. The cell wall of all bacteria is composed of the peptidoglycan, a polymer of N-acteylmuramic acid (MurNAc) and N-acetylglucosamine (GlcNAc) cross-linked by a pentapeptide. Briefly, lipid I is built in the cytoplasm by MraY attaching UDP-MurNAc-

pentapeptide to the lipid carrier undecaprenyl phosphate (UP), sequentially UDP-GlcNAc is attached through MurG resulting in lipid II. The peptidoglycan precursor is afterwards flipped to the extracellular space (or periplasm in Gram-negativ bacteria), still anchored to the membrane *via* undecaprenyl. Subsequently the GlcNAc-MurNAc-pentapeptide subunit is incorporated into the peptidoglycan by penicillin-binding proteins (PBP), which catalyze the transpeptidation, remaining undecaprenyl pyrophosphate (UPP). This UPP is then dephosphorylated to UP, which can be flipped back into the cytoplasm to reenter the peptidoglycan synthesis cycle (Figure 1).

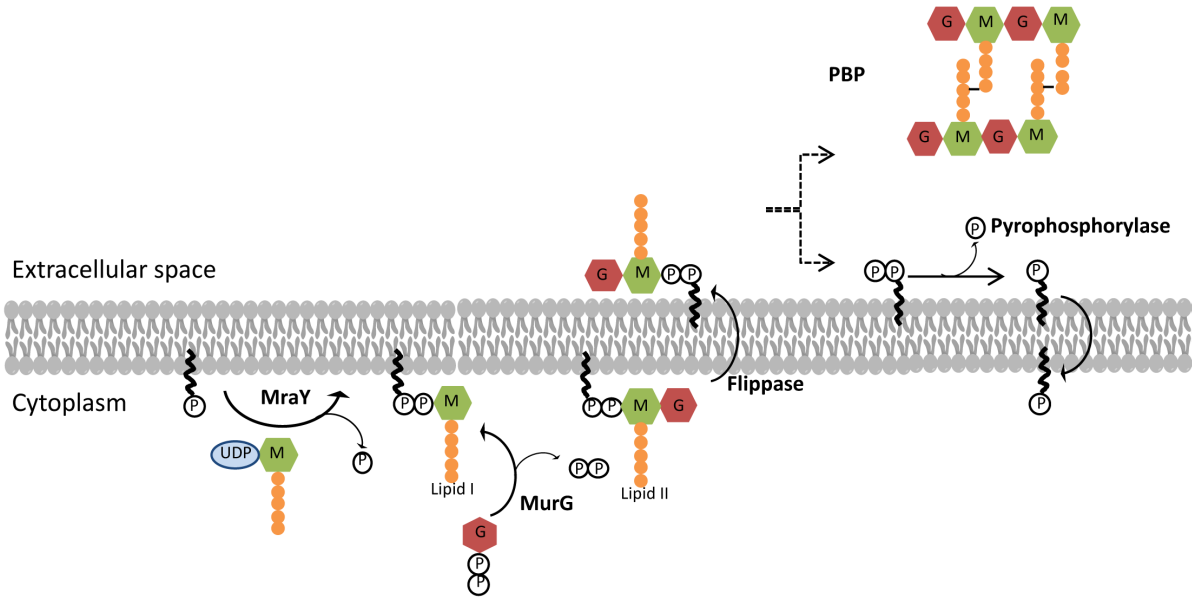

Figure 1: Schematic view of peptidoglycan synthesis.

Synthesis of Lipid II in the cytoplasm and incorporation into the peptidoglycan. Phosphate atoms are marked with a P, undecaprenyl as a black curved line, uridine phosphate (UDP) in blue, GlcNAc in red, MurNAc in green and aminoacids of the pentapeptide in orange (Adapted from (22)).

Glycopeptide antibiotics are synthesized by non-ribosomal peptide synthase (NRPS) assembly lines in *actinomycete*s (23). The glycopeptide antibiotic vancomycin, produced by *Streptomyces orientalis*, is active against Gram-positive bacteria (24). Vancomycin binds to the D-Ala-D-Ala sequence of the pentapeptide of lipid II (25-27), thereby inhibiting the crosslink of the peptidoglycan (Figure 2A).

The best-known exemplar of lipoglycodepsipeptide antibiotics is ramoplanin, which is produced by *Actinoplanes sp.* ATCC 33076. Ramoplanin A2, which only differs in the N-terminal part to ramoplanin A1 and A3, was found to be the most abundant variant and is active against Gram-positive bacteria (28, 29). It was shown to bind the pyrophosphate and the muramic acid moiety of lipid II as a dimer (30-32) (Figure 2A).

A member of the acylcyclodepsipeptides is lysobactin, also known as katanosin B. The antibiotic lysobactin was first isolated from a *Lysobacter* species and is active against several Gram-positive bacteria (33, 34), inhibiting the peptidoglycan synthesis by binding lipid II in a 1:1 ratio (35). Lysobactin was shown to bind to the reducing end of lipid-linked cell wall precursors (35) (Figure 2A).

In 2015 a novel depsipeptide antibiotic named teixobactin was discovered, which is produced by Gram-negative *Eleftheria terrae*. Teixobactin was shown to bind to the phosphate moiety and the MurNAc of lipid II and shows antimicrobial activity against human pathogens like *M. tuberculosis,* methicillin resistant *S. aureus* and vancomycin resistant *Enterococci* (36) (Figure 2A).

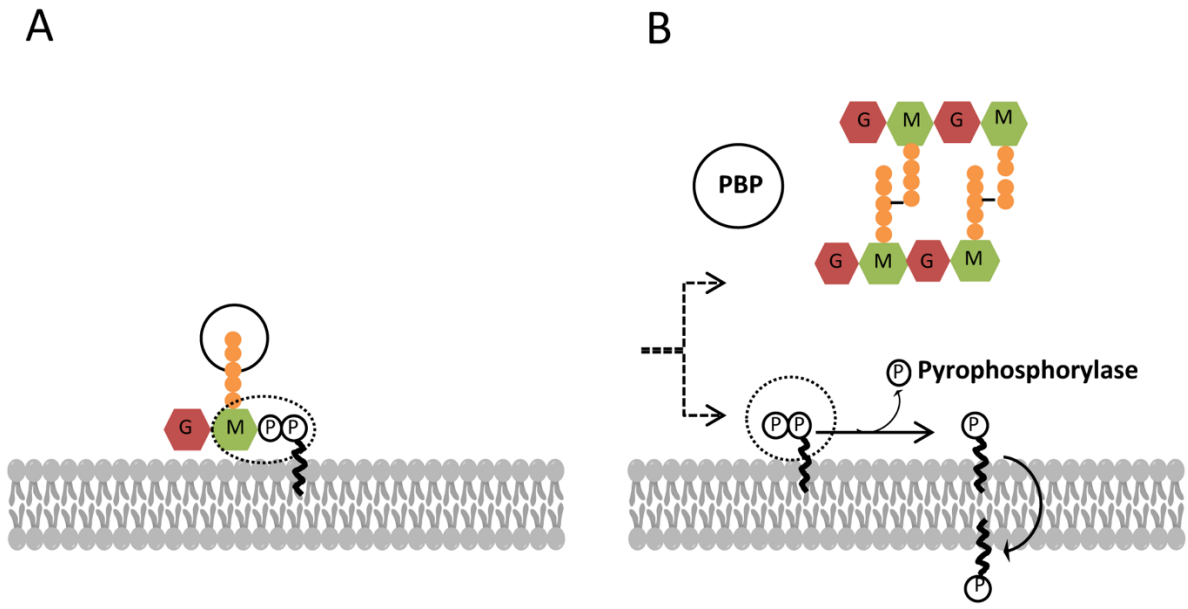

Figure 2: A) Lipid II and B) Peptidoglycan with targets of antibiotics.
A) Lipid II with target of vancomycin (black circle) and ramoplanin, lysobactin and teixobactin (dashed circle). **B) Peptidoglycan** with target of ß-lactams (black circle) and bacitracin (dashed circle). Phosphates are marked with a P, undecaprenyl as a black curved line, GlcNAc in red, MurNAc in green and aminoacids of the pentapeptide in orange.

The first discovered antibiotics are ß-lactams, which characteristically contain a ß-lactam ring. The most prominent ß-lactam antibiotic is penicillin, but also cephalosporin and carbapenems belong to this subclass of antibiotics. ß-lactam antibiotics inhibit the cell wall synthesis by binding to the PBP, thereby preventing the cross-linking of the peptidoglycan (11, 37, 38) (Figure 2B).

In addition also other components of the peptidoglycan synthesis were shown to be effective targets for antibiotics. One of those targeting antibiotics is the cyclic peptide bacitracin. Produced by some *Bacillus* species bacitracin is used in medicinal treatments since decades (39-42). The target was shown to be undecaprenyl-pyrophosphate (UPP) and further a high-resolution crystal structure demonstrated that bacitracin sequesters this and thereby prevents the recycling of the lipid carrier resulting in an interrupted peptidoglycan synthesis (43, 44) (Figure 2B).

1.2. Antimicrobial peptides

Antimicrobial peptides (AMPs) are found in all organisms as a conserved part of the innate immune response (45, 46). The first discovered AMP is lysozyme, found by Alexander Flemming in 1922 followed by hundreds of other AMPs in the last century (47). Antimicrobial peptides are relatively short (< 60 amino acids), amphipathic molecules with a positive net charge of +2 to +9 but differ in their antimicrobial activity and modes of action (48-50). They have an antimicrobial effect against Gram-positive and Gram-negative bacteria, fungi, parasites and also against viruses (49). The effect of most AMPs is given by an interaction with the cellular membrane or cell surface, subsequently permeation of the membrane, resulting in loss of cellular integrity. Here the effect can be either given by disruption of the cell membrane, leading to cell lysis, or due to interaction with the membrane, resulting in pore formation (51). Furthermore, those small peptides also have intracellular targets, like nucleic acids, cell wall synthesis, protein synthesis and proteins (52, 53).
AMPs can be classified due to several properties like their biological source or function, their net charge, size and hydrophobicity, their molecular targets or most likely their three-dimensional structure, which can be linear, α-helices, ß-sheet and loop-like (45, 48, 54).

Bacteriocins

Bacteriocins are ribosomally synthesized AMPs produced by bacteria, which have a broad activity spectrum and kill related bacteria or non-related bacteria (55). The group of bacteriocins are differentiated between those produced by Gram-negative bacteria and those produced by Gram-positive bacteria (56).

Bacteriocins produced by Gram-negative bacteria

The bacteriocins produced by Gram-negative bacteria are called colicins and microcines. Colicins have an antimicrobial effect against host related bacteria, which is mediated due to pore-formation, nuclease activity or peptidoglycanase activity (56, 57). They are relatively large and contain three domains, an N-terminal translocation domain, necessary for the transport to the extracellular space, a receptor-binding domain and a C-terminal cytotoxic domain, responsible for the antimicrobial activity (56-58). Microcins are small (< 10 kDa) ribosomally synthesized AMPs with a broad bactericidal activity including pore-formation, nuclease activity, inhibition of protein synthesis and inhibition of DNA replication (56). Microcins are hydrophobic peptides and can either be post-translationally modified or not, since they are transported as core peptides with a leader peptide (59) (Figure 3A).

Bacteriocins produced by Gram-positive bacteria

Bacteriocins produced by Gram-positive bacteria can be subdivided in three classes: The class I are lantibiotics, class II are non-lantibiotics and class III are bacteriolysins (60, 61).
Lantibiotics are post-translationally modified small (< 5 kDa) antimicrobial peptides, which contain lanthionine or methyl-lanthionine rings. Lantibiotics interact with bacterial membranes and show their activity in a low nanomolar range (62-64). The best known lantibiotic is nisin, produced by *Lactococcus lactis* and *Streptococcus uberis* strains (61, 65, 66) (Figure 3B).
Class II bacteriocins are non-lantibiotics, which do not undergo post-translational modifications and do not contain lanthionine rings. They contain 30 to 60 amino acids (<10 kDa), are positively charged and share a distinct heat tolerance. These peptides are active in a nanomolar range and induce membrane permeabilization due to insertion into the membrane (56, 60, 61). Class II bacteriocins can have a cyclic structure, like the non-lantibiotic gassericin A, or can be pediocin-like, like leucocin A (Figure 3C). Further two peptides can combine their activity which can be enhanced or synergistic (60, 67-69).
Class III bacteriocins are large (>30 kDa), thermolabile antimicrobial proteins, which are named bacteriolysins or non-bacteriocin lytic proteins. Bacteriolysins, like enterolisin A, catalyze cell-wall hydrolysis, resulting in cell lysis, whereas some class III bacteriocins, like caseicin 80 are non-lytic proteins (56, 60, 61).

Figure 3: Structure of representatives for bacteriocins.

Structure of representatives for bacteriocins produced by Gram-negative bacteria A) Microcin J25 in green (PDB:1pp5) and bacteriocins produced by Gram-positive bacteria B) nisin A in red (Adapted from PDB: 1wco) and C) leucocin A in blue (PDB:1cw6).

1.3. Lantibiotics

Lantibiotics are small, ribosomally synthesized and post-translational modified antimicrobial peptides, mostly produced by Gram-positive bacteria (55, 64). They are produced as prepeptides and mature in the cytosol of the bacteria. Specific amino acid residues, serine and threonine, in the core peptide get intrinsically dehydrated and form the amino acids 2,3-didehydroalanine (Dha) and 2,3-didehydrobutyrine (Dhb). Those formed amino acids are subsequently covalently linked with a neighbored cysteine side chain, due to a Michael-type addition. Those originated thioether bridges are called (methyl-)lanthionine rings and are eponymous for the **lan**thionine containing an**tibiotics** (70-72)**.** The family of known lantibiotics is steadily increasing, mainly due to the opportunity to detect encoding genes by computational techniques such as BAGEL4 (73). They can be subdivided in four classes depending on their post-translational modification enzymes (70, 74, 75).

Class I lantibiotics are peptides with a small size of less than 5 kDa and are post-translationally modified by two enzymes, LanB and LanC (Figure 3). The dehydratase LanB dehydrates serine and threonine residues and therefore generates the amino acids Dha and Dhb (76, 77). The cyclase LanC, which forms thioether bridges between Dha/Dhb and the thiol of the neighbored cysteine (71, 72), has a characteristic zinc binding motif (78, 79). After maturation the modified prepeptide is secreted by the transporter LanT and activated by cleaving off the leader peptide by a specific protease LanP (80, 81). The fully modified peptides, like nisin, gallidermin (Figure 4) and subtilin, possess antimicrobial activity in a low nanomolar range against mainly Gram-positive bacteria (71, 74).

Class II lantibiotics are bigger in size (5-10 kDa) than class I lantibiotics and are maturated by a single enzyme LanM (Figure 3). This bifunctional synthetase consists of an N-terminal dehydratase and a C-terminal cyclase domain and therefore combines the dehydration and cyclization reaction (70, 74). LanM shows no homology with LanB but low sequence homology with the class I cyclase LanC, including the zinc binding motif (70). After maturation by LanM the enzyme LanT exports the prepeptide and cleaves off the leader peptide (82). Prominent class II lantibiotics are lacticin 481 (Figure 4) and mersacidin, showing antimicrobial activity against Gram-positive bacteria (74).

The class III lantibiotics contain a tri-functional synthetase LanKC (Figure 3), which is composed of an N-terminal lyase domain, a central kinase domain an C-terminal putative cyclase domain. Latter lacks the zinc binding motif, the active site, found in class I and class II cyclase enzymes and domains, respectively (74). Class III lantibiotics are for example sapB (Figure 4) and sapT, which do not possess any antimicrobial activity (70).
A fourth class of lantibiotics was discovered in 2010 and includes the peptide venezuelin (Figure 4). Those lantibiotics are also matured by a tri-functional synthetase, consisting of a lyase, a kinase and a cyclase domain (Figure 3). Latter contains, unlike class III, the zinc binding motif (70, 75, 83).

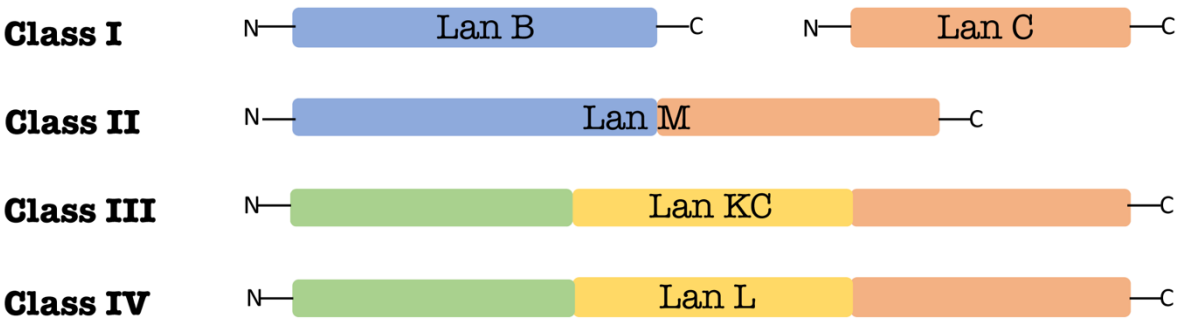

Figure 3: Lanthionine modification enzymes.
The four classes of lanthionines and their modification enzymes with dehydratase domains (blue), cyclase domains (orange), lyase domains (green) and kinase domains (yellow) (Adapted from (70)).

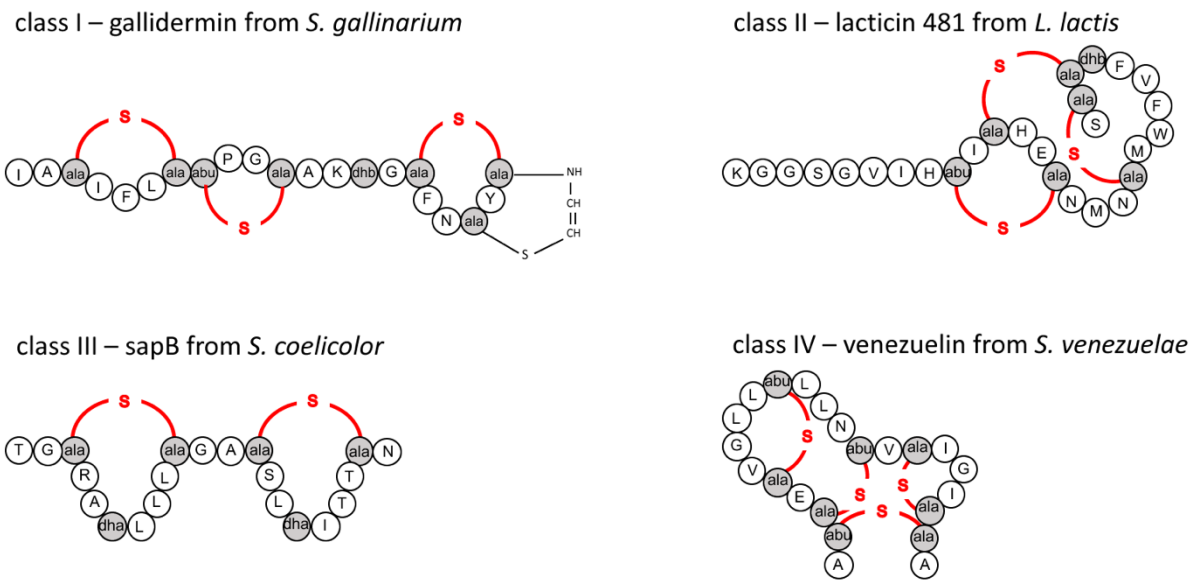

Figure 4: Representative lantibiotics and their classes.

Schematically view of structural examples for class I: gallidermin, Class II: lacticin 481, class III: sapB and classIV: venezuelin. Dehydrated amino acids as well as cysteines are highlighted in grey, (methyl-) lanthionine rings are shown in red.

Nisin

The best studied bacteriocin is nisin, produced by *Lactococcus lactis* and *Streptococcus uberis* strains, which was discovered 1928 and is used in the food and dairy industry since decades (61, 65, 66). Nisin is an amphipathic, 34 amino acids long peptide, consisting of a hydrophobic N-terminus and a hydrophilic C-terminus (84, 85). It has a broad antimicrobial activity against Gram-positive bacteria like staphylococci, streptococci, bacilli and enterococci. The structure of nisin was solved in 1991 with NMR spectroscopy (86) and shows it can be subdivided in three parts. The N-terminal region of nisin is composed of three (methyl-)lanthionine rings A, B and C, followed by flexible hinge region and the C-terminal region consisting of two intertwined (methyl-)lanthionine rings D and E and the last 6 amino acids (86-88) (Figure 5A). Nisin has, at least, a dual mode of action. First the N-terminal part of nisin binds to the pyrophosphate moiety of the cell wall precursor lipid II, detected *via* NMR in 2004, and thereby inhibiting peptidoglycan synthesis (89, 90) (Figure 5B). Secondly, nisin forms pores of 2-2.5 nm diameter into the membrane which leads to rapid cell death due to the efflux of nutrients and ions and subsequently to a collapse of the membrane potential. This complex, consisting of eight nisin and four lipid II molecules, is built if the concentration of nisin reaches a certain

threshold (91). When nisin binds to lipid II *via* the first two (methyl-)lanthionine rings the flexible hinge region between the rings C and D mediated the pore formation by flipping the last two rings D and E inside of the membrane (87, 90, 92, 93) (Figure 5C). Due to this dual mode of action nisin is active in a low nanomolar range (94). A putative third mode of action for nisin was discussed in 2006, proposing a sequestration of lipid II (95).

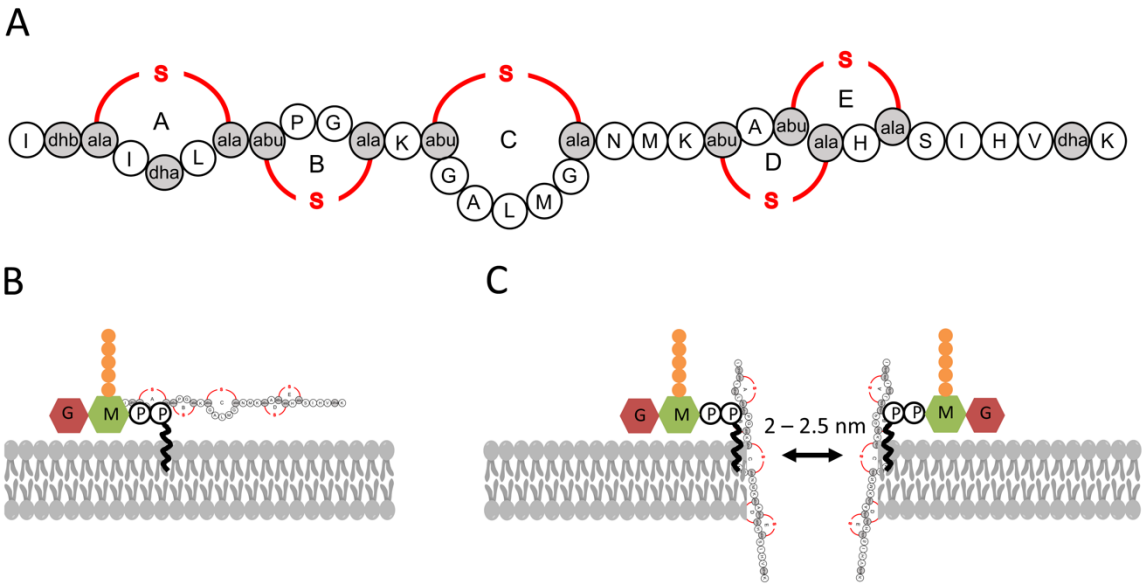

Figure 5: Nisin and its dual mode of action.

A) Nisin with the N-terminal rings A, B and C and the C-terminal intertwined rings D and E. Dehydrated amino acids as well as cysteines are highlighted in grey, (methyl-) lanthionine rings are shown in red. **B) Nisin binding lipid II** *via* the first two rings A and B. **C) Pore formation** of nisin by binding lipid II and flipping the hinge region inside of the membrane. Pores have a diameter of 2 – 2.5 nm (96).

1.4. Lantibiotic resistance

The bacteriocin subgroup lantibiotics are active in the nanomolar range and target the bacterial cell wall and membranes of mainly Gram-positive bacteria, including multi-drug resistant pathogenic bacteria (97, 98). Pharmaceutical usage of lantibiotics is however hampered by resistance mechanisms against lantibiotics. Those resistance mechanisms could be modifications in the cell membrane or in the cell wall, but also resistance operons containing a two-component system and an ATP-dependent transporter are known (51, 99-102).

Modifications of the cell membrane

Changes in the composition of the bacterial membrane, which consists of different phospholipids, can lead to lantibiotic resistance. Cell membrane composition differs between species and growth phases. Although the total amount is variable per species, most bacterial membranes contain phosphatidylglycerol (PG), a phospholipid with a negatively charged head group (103). Resistance against lantibiotics can occur by an increase or decrease of the PG levels in the membrane (104-106). Besides PG membranes contain lipids like cardiolipin (CL), phosphatidylethanolamine (PE) and phosphatidylcholine (PC). It was shown that the lantibiotic nisin is able to penetrate membranes with a higher concentration of CL more effectively than PG, PE or PC high concentrated membranes (99). Furthermore, it could be shown that resistant cells contain more saturated fatty acids than unsaturated and rather long chain fatty acids. Those modifications lead to a decreased membrane fluidity and a more rigid conformation of the membrane, thereby hindering the lantibiotics to access the membrane (51, 107-109).

Additionally, some Gram-positive bacteria developed the ability to modify the negative charge of the phospholipid PG. Those cells express the integral lysyl-phosphatidylglycerol synthetase **m**ulti**p**eptide **r**esistance **f**actor (MprF), which synthesizes one of the hydroxyl groups of PG *via* a lysine esterification. Subsequently the originated lysyl-phosphatidylglycerol (L-PG) is translocated to the external membrane layer, decreasing the total negative charge of the membrane due to the positive charge of the free amino group (51, 110-112). Lantibiotic resistance mediated by MprF has been observed in several Gram-positive bacteria like *Staphylococcus aureus* (112, 113), *Bacillus subtilis* (114), *Enterococcus faecalis* (115), *Enterococcus faecium* (116) and *Mycobacterium tuberculosis* (117).
Furthermore, a mechanism to obtain resistance against lantibiotics is provided by the fabDG1G2Z1Z2 (*fab*) operon, present in some Gram-positive bacteria. Fab is involved in the membrane synthesis steps of saturation and elongation of phospholipids. It was shown that a decreased expression results in lantibiotic resistance due to a less dense packed membrane which has an impact of lantibiotic interaction (118, 119).

Modifications of the cell wall

The cell wall of Gram-positive bacteria is composed of the peptidoglycan (PGN) and teichoic acids, which are polymers of alternating phosphate and alditol groups. Those teichoic acids are

either wall teichoic acids (WTA), which are covalently linked to the MurNAc of the PGN due to phosphodiesters or lipoteichoic acids (LTA), which are linked to the membrane glycolipids (120, 121). Since the phospholipids and teichoic acids include anionic components the cell wall is negatively charged, which attracts the positively charged lantibiotics (122). Therefore, changing the negative charge of the cell wall by changing its composition is a strategy to prevent the lantibiotics from interaction with the cell wall, hence to gain resistance against lantibiotics. A method to change the net charge is the D-alanylation of the teichoic acids mediated by the *dltABCD* operon, which has been found in many different bacteria like *Staphylococcus, Listeria, Enterococcus, Bacillus, Clostridium, Streptococcus, Lactobacillus* and *Lactococcus* (123-130).
Bacteria can also gain resistance against lantibiotics by increasing the expression of the penicillin-binding protein (PBP). This bifunctional enzyme catalyzes the glycosyltransfer to the PGN and the transpeptidation between the PGN subunits (131). PBP related resistance could be observed in *Listeria* and *Lactococcus* (119, 132).

Lantibiotic resistance operon

Lantibiotic resistance can be mediated by resistance operons, which consist of a two-component system (TCS), with a histidine kinase and a response regulator, and an **A**TP-**b**inding **c**assette transporter (ABC transporter) (Figure 6).

Two-component system

The histidine kinase of the TCS is anchored to the membrane and acts as a sensor for the lantibiotic, activated by the histidine kinase the response regulator mediates the signal intracellular which leads to expression of corresponding genes (133, 134). Lantibiotic resistance related TCS can be subdivided into two groups, the BceRS-like and the LiaRS-like. The BceRS-like TCS was first discovered in *B. subtilis* and is involved in resistance against actagardine and mersacidin (7). The BceS-like kinase is an intermembrane sensing kinase, since it lacks the characteristic large extracellular sensor domain (134-136). Therefore those kinases are functionally linked to BceAB-type ABC transporters (134, 137). Other examples for the BceRS-like TCS are BraRS from *S. aureus* and NsrRK from *S. agalactiae* (138). The structure of the response regulator NsrR has been solved and it was classified as a member of

the OmpR/PhoB subfamily. Further conserved amino acids in lantibiotic resistance regulators were found to be involved in posphorylation, dimerization and DNA-binding (139).
The LiaRS-like TCS was first discovered in *B. subtilis* and contains three proteins, the kinase LiaS, the response regulator LiaR and additional LiaF, which acts as a negative regulator of the LiaR mediated gene expression (140). Examples for this type of TCS are LiaRS from *L. monocytogenes*, VraRS from *S. aureus* and CeaRS from *L. lactis* (141-144) .

ABC transporter

ABC transporters of lantibiotic resistance operons in Gram-positive bacteria mediate an active resistance by transporting or effluxing lantibiotics. ABC transporter consist of a transmembrane domain (TMD) with a permease function and a nucleotide binding domain (NBD), which is able to hydrolyze ATP to generate the energy for the transport (145). For lantibiotic resistance two main classes of ABC transporter are known, the homodimeric and the heterodimeric (51, 137).

The homodimeric resistance ABC transporter are BceAB-type transporter, the **b**a**c**itracin **e**fflux transporter, which was first discovered in *B. subtilis* (146). Those transporter are encoded on one operon with the BceRS-like TCS and confer resistance against more than one substrate. BceAB of *B. subtilis* confers resistance against bacitracin, actagardine and mersacidin (7, 8), whereas VraDE of *S. aureus* together with the TCS BraRS mediates resistance against bacitracin, daptomycin and nisin (9, 10). The *S. agalactiae* resistance transporter NsrFP confers resistance against the lantibiotics nisin and gallidermin (1, 147). Those transporter contain a large (620-670 aa) TMD with ten transmembrane helices (TMH) and a characteristic large extracellular domain (ECD) between TMH VII and VIII, as well as an NBD of 225-300 amino acids (1, 137, 148, 149). Although it has been assumed that BceAB-type transporter are involved in antimicrobial peptide removal from the membrane (150), operate as an exporter (147) or flip undecaprenyl pyrophosphate (151) the resistance mechanism of the ABC transporter family remains unsolved.

Heterodimeric lantibiotic resistance transporter consist of two TMDs and one NBD (145), and are rather immunity than resistance transporter since they are mostly found in lantibiotic producing strains. Those transporter are named LanFEG-like and are found in the nisin producing strain *L. lactis* (NisFEG), in the epidermin producing strain *S. epidermidis* (EpiFEG)

and in the subitilin producing strain *B. subtilis* (SpaFEG) (137, 152-154). Till date the only known **c**ationic antimicrobial **p**eptide **r**esistance transporter, not used as a self-protection mechanism in producer strains, is CprABC from *C. difficile*, which confers resistance against nisin, gallidermin and subtilin (99, 137, 155).

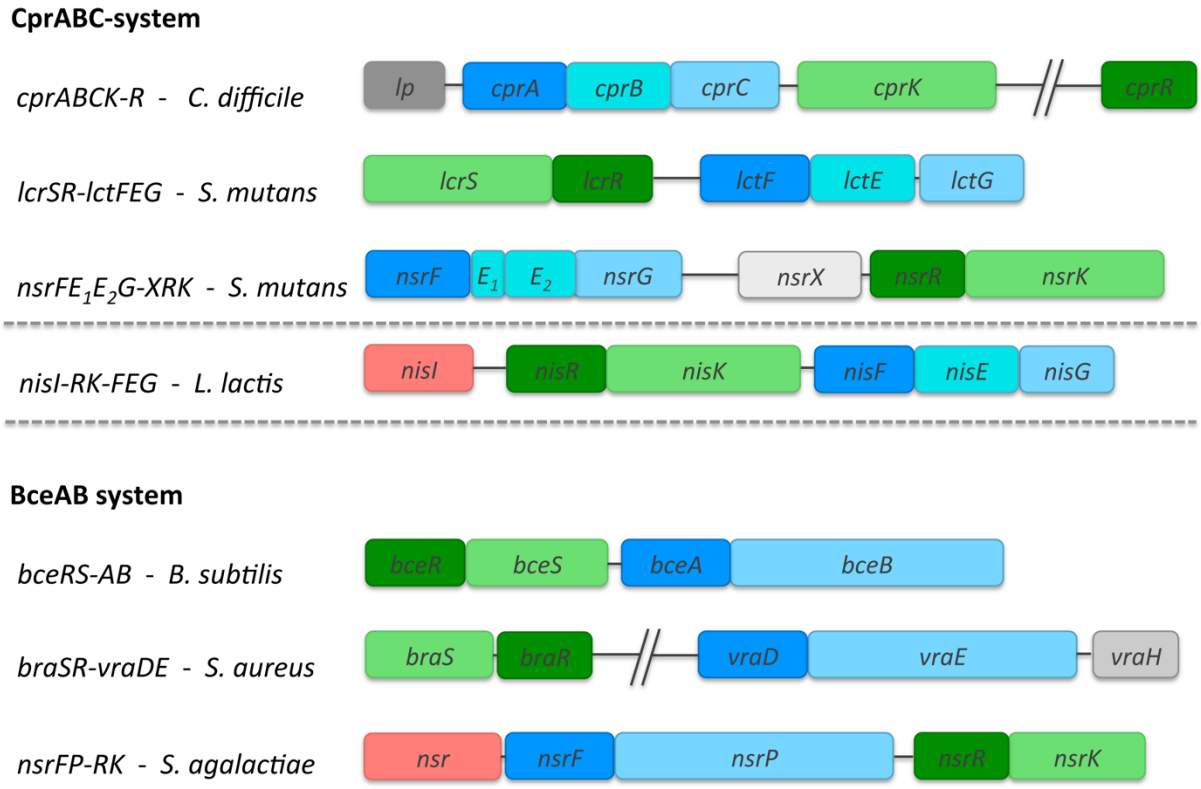

Figure 6: Overview of lantibiotic resistance operons.

Three operon structures for the cprABC system and the BceAB system as well as the NisFEG system as a representative for LanFEG are shown. For CprABC system cprABCK-R from *C. difficile*, nsrFE1E2G-XRK and lcrSR-lctFEG from *S. mutans* are shown. The nisRK-FEG system from *L. lactis* involved in nisin immunity is also highlighted. For BceAB system bceRS-AB from *B. subtilis*, braSR-vraDE from *S. aureus* and the nsrFP-RK system from *S. agalactiae* are shown. The size of the genes corresponds directly with the gene length as deposited in the NCBI database. The TCSs with response regulator (dark green) and histidine kinase (light green); and the ABC transporters are shown in different shades of blue. In the bceAB system, the NBD is dark blue while the TMD is shown in light blue. The additional TMD present in the cprABC systems is shown in cyan. The proteins, which are part of the operon but the function has not been determined so far are shown in grey. In case of the nis and nsr operons, an additional membrane associated protein is present which is colored in red. Taken from Clemens *et al.* (138).

Other lantibiotic resistance proteins

In almost all lantibiotic producing strains a LanI protein is found, which confers self-immunity (156). This membrane associated protein is on one operon with the LanFEG transporter, together those proteins protect the producer strain from the produced lantibiotic. In the nisin producer strain *L. lactis* the NisI protein together with NisFEG is expressed to gain immunity against nisin (152, 157, 158). Further this protein is found in the subtilin producer strain *B.subtilis* (SpaI), the gallidermin producer strain *S. gallinarium* (GdmH) and the epidermin producer strain *S. epidermidis* (EpiH) (153, 154, 159). A well-known LanI protein is NisI from *L. lactis*, which confers resistance against nisin and held two different immunity systems. NisI is able to bind nisin to protect the cell from pore formation mediated by nisin (152, 157). The other mode of action of NisI is clustering the cells in the presence of nisin, thereby forming long cell chains and prevent the cell from nisin. This process is reversible, if nisin is removed from the cells they start to behave normal again (157).

Some Gram-positive bacteria, which contain the BceRSAB-type operon additionally contain a gene on this operon responsible for degrading lantibiotics. One of those proteins is the **ni**s**i**n **r**esistance protein NSR produced by *S. agalactiae*. The membrane associated serine protease *Sa*NSR confers resistance against nisin by cleaving off the last 6 amino acids of nisin and thereby decreasing its activity 100 fold (4, 157).

Further the protein MlbQ is known, which is produced by *Microbispora* and confers resistance against NAI-107- like lantibiotics (160, 161).

Additionally some Gram-positive bacteria are able to express a nisinase, which is a nisin inactivating enzyme. This enzyme is produced by *E. faecalis* but also by some *Bacillus, Lactobacillus, Lactococcus, Enterococcus, Leuconostoc, Staphylococcus* and *Streptococcus* specia and is supposed to reduce the C-terminal dehydroalanyl-lysine of nisin (99, 162-164).

1.5. NSR operon

Like described in 1.4.3. some strains confer resistance against lantibiotics due to an lantibiotic resistance operon, composed of four or five genes, which encode for a two-component system, an ABC transporter and some operons additionally hold a gene for a serine protease or a protein of unknown function (1, 138, 155, 165). These operons are often found in human pathogenic bacteria like *S. aureus* and *S. agalactiae* (138). Latter confers resistance against nisin *via* the nisin resistance protein operon (nsr operon), which is composed of a serine protease, an ABC transporter and a two-component system (1) (Figure 6 & 7).

The Nisin resistance protein

The 36.2 kDa NSR protein of *S. agalactiae* is anchored to the membrane with the N-terminal part and has a high hydrophobicity (Figure 7). The hydrophobic N-terminus holds a transmembrane sequence of 21 amino acids (166). NSR belongs to peptidases of the S41 family, further to the C-terminal processing peptidases (CTPs) and has a specific catalytic dyad mechanism consisting of a serine and a histidine residue (2, 3). NSR confers resistance against nisin by degrading the lantibiotic *via* cleavage between MeLan28 and Ser29 of nisin (4). Although it still contains the five characteristically (methyl-) lanthionine rings the originated, reduced $nisin_{1-28}$ has a 100 fold less antimicrobial activity due to a reduced affinity for the cell membrane as well as a decreased effective pore formation (4, 5). If NSR is expressed in a nisin sensitive *L. lactis* strain a 18-20 fold resistance against nisin can be observed (1). The crystal structure of NSR was solved and shows three domains: An N-terminal helical bundle, the protease cap and a core domain. Those domains form a 10 Å width tunnel, which is hydrophobic, negatively charged and binds nisin (3). It was shown that the catalytic dyad is in the protease core domain and further that the last two (methyl–) lanthionine rings D and E of nisin are necessary for the interaction of the lantibiotic and the protease (3).

The ABC transporter NsrFP

The ABC transporter NsrFP from *Streptococcus agalactiae* consists of a nucleotide binding domain NsrF and a transmembrane domain NsrP (1) (Figure 7). NsrFP belongs to the BceAB-type transporter and has a high sequence similarity (45 %) to MbrAB from *S. mutans* (6). The NBD NsrF has a size of 28 kDa, whereas the TMD NsrP has 74 kDa, including ten transmembrane helices and a characteristic large extracellular domain of 220 amino acids (1, 138). Like described before several BceAB-type transporter are known which confer resistance against more than one antimicrobial peptide (1.4.3.2.). If expressed in a nisin sensitive *L .lactis* strain NsrFP was shown to confer a 16 fold of resistance against nisin A and 12 fold of resistance against another natural nisin variant nisin H and the lantibiotic gallidermin. As nisin and gallidermin are similar in the N-terminal part it was assumed that NsrFP also recognizes the N-terminal part of nisin. Further it was shown that NsrFP prevents the cells from pore formation mediated by nisin and an efflux mechanism of the transporter was postulated based on an peptide release assay (147). Despite this the mechanism and the structure of NsrFP from *S. agalactiae* remain elusive.

The Two-component system NsrRK

In all lantibiotic immunity and resistance operons genes encoding a TCS are present. In *S. agalactiae* the TCS of the nsr operon is composed of the response regulator NsrR (25 kDa) and the histidine kinase NsrK (31 kDa) (1) (Figure 7).

The response regulator NsrR belongs to the OmpR subfamily and its structure was solved with X-ray crystallography. This structure postulates a DNA-binding response regulator and shows the typical helix-turn-helix motif which is characteristic for OmpR type response regulators. Although the putative residues responsible for the DNA binding were identified, the distinct promoters for the nsr operon remain unknown (139).

The histidine kinase NsrK belongs to the intermembrane sensing kinase (IMSK) family and is composed of a short sensory domain and a characteristic kinase domain (167). NsrK lacks additional domains which would be needed for cytoplasmic signal detection, so it is assumed that the ABC transporter NsrFP is necessary to gain full resistance against nisin (1).

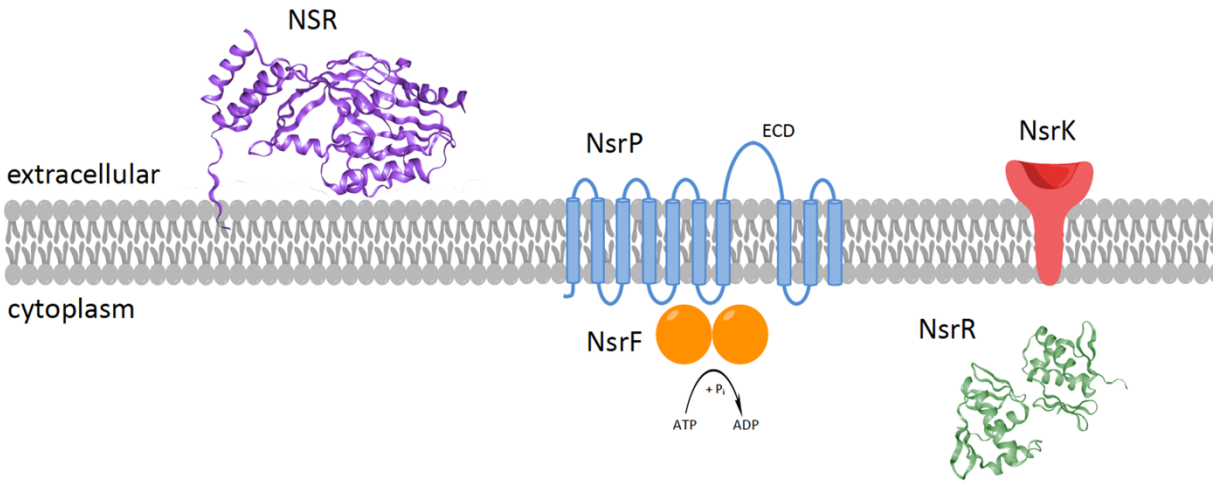

Figure 7: Proteins of the nsr operon.

The structure of NSR in purple (PDB: 4Y68), the ABC transporter NsrFP with the TMD in blue and the NBD in orange, the histidine kinase in red and the response regulator in green (PDB: 5DCM).

2. Aims

Elucidating and overcoming the nisin resistance mediated by the proteins NSR and NsrFP of *S. agalactiae* was the overall aim of this thesis.

Since antibiotic resistance has become a great challenge in our era, it gets more and more important to overcome the evolved resistance mechanisms. One of those evolved mechanisms are the serine protein NSR and the ABC transporter NsrFP of the human pathogenic strain *S. agalactiae.*

The nisin resistance protease *Sa*NSR is a C-terminal processing peptidase (CTP) and has a specific catalytic dyad mechanism consisting of a serine and a histidine residue (2, 3). It was shown that NSR confers resistance against nisin by degrading the lantibiotic at its C-terminus resulting in a 100 fold less active nisin fragment (4, 5) . The crystal structure of *Sa*NSR was solved and shows a 10 Å width tunnel, which is hydrophobic, negatively charged and binds the last two (methyl–) lanthionine rings D and E of nisin (3). Since the structure and the mechanism of *Sa*NSR are known the first aim of this thesis was to overcome this nisin resistance by finding inhibiting compounds: Those compounds either derived from natural sources or virtual screenings, further effective nisin derivatives to bypass this resistance were investigated.

The ABC transporter NsrFP from *Streptococcus agalactiae* belongs to the BceAB-type transporter (6). Several BceAB-type transporter are known which confer resistance against more than one antimicrobial peptide (7-10). The second aim of this thesis was to clarify the resistance spectrum of *Sa*NsrFP.

Although there have been a lot of studies about BceAB-type transporter and it has been assumed that they are involved in antimicrobial peptide removal from the membrane (150), operate as an exporter (147) or flip undecaprenyl pyrophosphate (151) the resistance mechanism of the ABC transporter family remains unsolved. The third aim of this thesis was to elucidate the mechanism of *Sa*NsrFP as a model system for BceAB-type transporter.

Additional several rational designed nisin variants as well as natural compounds and their derivatives were tested to subsequently overcome the resistance mediated by *Sa*NsrFP.

3. Publications

Chapter I	The nisin resistance ABC Transporter NsrFP **The N-terminal Region of Nisin Is Important for the BceAB-Type ABC Transporter NsrFP from Streptococcus agalactiae COH1** Frontiers in Microbiology
Chapter II	Insight into Two ABC Transporter Families **Insight into Two ABC Transporter Families Involved in Lantibiotic Resistance** Frontiers in Molecular Bioscience
Chapter III	Bypassing the Nisin Resistance Protein **Bypassing lantibiotic resistance by an effective nisin derivative** Bioorganic and Medicinal Chemistry
Chapter IV	Lantibiotic immunity and resistance proteins **Influence of nisin hinge-region variants on antibiotic immunity and resistance proteins** Bioorganic and Medicinal Chemistry
Chapter V	Bypassing the nisin resistance of the *Sa*NSR protein **Small-molecule inhibitors of nisin resistance protein NSR from the human pathogen Streptococcus agalactiae** Bioorganic and Medicinal Chemistry
Chapter VI	Mechanism of the ABC Transporter NsrFP **Mechanism of the BceAB-type transporter NsrFP from *Streptococcus agalactiae***
Chapter VII	Natural compounds against nisin resistance **Natural compounds against nisin resistance**

3.1. Chapter I - The nisin resistance ABC Transporter NsrFP

Published in : Frontiers in Microbiology

Impact factor: 4.26

Own Work: 10 %

Preparation of the figures

The N-terminal Region of Nisin Is Important for the BceAB-Type ABC Transporter NsrFP from *Streptococcus agalactiae* COH1

Jens Reiners, Marcel Lagedroste, Katja Ehlen, Selina Leusch, **Julia Zaschke-Kriesche** and Sander H. J. Smits

frontiers in Microbiology

ORIGINAL RESEARCH
published: 29 August 2017
doi: 10.3389/fmicb.2017.01643

The N-terminal Region of Nisin Is Important for the BceAB-Type ABC Transporter NsrFP from *Streptococcus agalactiae* COH1

*Jens Reiners†, Marcel Lagedroste†, Katja Ehlen, Selina Leusch, Julia Zaschke-Kriesche and Sander H. J. Smits**

Institute of Biochemistry, Heinrich Heine University Düsseldorf, Düsseldorf, Germany

Lantibiotics are (methyl)-lanthionine-containing antimicrobial peptides produced by several Gram-positive bacteria. Some human pathogenic bacteria express specific resistance proteins that counteract this antimicrobial activity of lantibiotics. In *Streptococcus agalactiae* COH1 resistance against the well-known lantibiotic nisin is conferred by, the nisin resistance protein (NSR), a two-component system (NsrRK) and a BceAB-type ATP-binding cassette (ABC) transporter (NsrFP). The present study focuses on elucidating the function of NsrFP via its heterologous expression in *Lactococcus lactis*. NsrFP is able to confer a 16-fold resistance against wild type nisin as determined by growth inhibition experiments and functions as a lantibiotic exporter. Several C-terminal nisin mutants indicated that NsrFP recognizes the N-terminal region of nisin. The N-terminus harbors three (methyl)-lanthionine rings, which are conserved in other lantibiotics.

Keywords: ABC transporter, lanthionine ring, lantibiotic, nisin, resistance

OPEN ACCESS

Edited by:
Helen Zgurskaya,
University of Oklahoma, United States

Reviewed by:
Rajeev Misra,
Arizona State University, United States
Karl Hassan,
Macquarie University, Australia

****Correspondence:***
Sander H. J. Smits
sander.smits@hhu.de

†These authors have contributed equally to this work.

Specialty section:
This article was submitted to Antimicrobials, Resistance and Chemotherapy, a section of the journal Frontiers in Microbiology

Received: *26 April 2017*
Accepted: *15 August 2017*
Published: *29 August 2017*

Citation:
Reiners J, Lagedroste M, Ehlen K, Leusch S, Zaschke-Kriesche J and Smits SHJ (2017) The N-terminal Region of Nisin Is Important for the BceAB-Type ABC Transporter NsrFP from Streptococcus agalactiae COH1. Front. Microbiol. 8:1643. doi: 10.3389/fmicb.2017.01643

INTRODUCTION

Lantibiotics are ribosomally synthesized antimicrobial peptides of approximately 19–38 amino acids, which are mainly produced by Gram-positive bacteria (Klaenhammer, 1993). They are characterized by extensive post-translational modifications, which result in the presence of dehydrated amino acids, lanthionine and methyl-lanthionine rings (Chatterjee et al., 2005). Lantibiotics are considered to be promising candidates as antibiotic alternatives due to their capability to inhibit various multidrug-resistant pathogenic bacteria such as Staphylococci, Enterococci, Streptococci and Clostridia species (Dischinger et al., 2014). Several lantibiotics are also effective against Gram-negative bacteria like species of the *Neisseria* and *Helicobacter* genus (Mota-Meira et al., 2000). The pharmaceutical potential of lantibiotics has been extensively studied and some are already in the preclinical and clinical phases of development (Yang et al., 2014). Lantibiotics exhibit different modes of action including binding to the cell wall, which results in growth inhibition, as well as subsequent pore formation leading to immediate cell death (Brötz et al., 1998a; Hasper et al., 2004, 2006; Islam et al., 2012).

Some bacteria, however, are inherently resistant against lantibiotics due to the expression of various protein systems that can detect and subsequently respond to the presence of lantibiotics in the extracellular medium (reviewed in Draper et al., 2015). These broad range resistance systems can either be unspecific such as changes in bacterial cell wall and membrane (Nawrocki et al., 2014;

de Freire Bastos et al., 2015; Draper et al., 2015) or more specific by proteolytic degradation of the lantibiotic itself (Sun et al., 2009).

In the present study, we focused on the lantibiotic nisin, which is produced by some *Lactococcus lactis* and *Streptococcus uberis* strains (Klaenhammer, 1993; Chatterjee et al., 2005). Nisin has a broad antimicrobial spectrum against a wide range of Gram-positive bacteria and exhibits several different modes of action (Ruhr and Sahl, 1985; Brötz et al., 1998b; Hsu et al., 2004; Hasper et al., 2006). One dominant activity is the binding to lipid II, a precursor molecule of peptidoglycan, thereby inhibiting cell wall synthesis (Wiedemann et al., 2001). Secondly, nisin is able to insert into the membrane to form pores (Hasper et al., 2004), which leads to the efflux of ions, nutrients, and subsequently to cell death. This last activity is a very rapid process and occurs almost instantly. Nisin can be structurally dissected in the N-terminus (containing the (methyl)-lanthionine rings A–C), a hinge region with the amino acids NMK and the C-terminus containing rings D and E (Van de Ven et al., 1991) (**Figure 1**). These rings are crucial for the nM activity and deletion of for example only ring E reduces the activity about eightfold (Alkhatib et al., 2014b).

Within the human pathogen *Streptococcus agalactiae* COH1 the expression of a proteogenous resistance system comprising of NSR (nisin resistance protein; a serine protease), an ATP-binding cassette (ABC) transporter (NsrFP) and a two-component system (TCS) (NsrRK) confers resistance against nisin (Khosa et al., 2013). Recently, this NSR operon has been characterized biochemically and structurally. *In vitro* studies showed that NSR expressed in *L. lactis* confers 20-fold resistance against nisin. This is mediated by cleaving off the last six amino acids from nisin, thereby lowering its activity (Sun et al., 2009; Khosa et al., 2013, 2016a). Another component of this nisin resistance operon is the BceAB-type ABC transporter NsrFP. BceAB-type ABC transporters, are putatively involved in antimicrobial peptide (like lantibiotics) removal from the lipid membrane (Gebhard and Mascher, 2011). They have been named after the BceAB transporter system from *Bacillus subtilis* conferring resistance against the antimicrobial peptide bacitracin (Ohki et al., 2003; Rietkötter et al., 2008). Interestingly, within the genomes the lantibiotic BceAB-type ABC transporter are encoded in close proximity to a TCS (Khosa et al., 2013) which senses the presence of the lantibiotic and subsequently up-regulates the expression of the ABC transporter (Dintner et al., 2011). The BceAB from *B. subtilis* has been shown to form a multicomponent complex with its designated TCS BceRS upon binding of bacitracin (Dintner et al., 2014). This highlights that the BceAB transporter from *B. subtilis* is directly involved in bacitracin sensing and consequently triggering the up-regulation of its own gene by the TCS BceRS.

Within NsrFP from *S. agalactiae* COH1, the transmembrane domain NsrP contains 10 predicted transmembrane helices and harbors a 212 amino acid large extracellular domain (ECD) in between helices VII and VIII (Khosa et al., 2013; **Figure 2**). NsrF is the nucleotide-binding domain delivering the energy for the transport by ATP hydrolysis.

In this study, we determined the function of NsrFP from *S. agalactiae* COH1 in conferring nisin resistance. We expressed only the NsrFP transporter without the corresponding NsrR/NsrK TCS and observe that NsrFP can confer resistance up to 80 nM nisin. In comparison to this, a strain lacking this transporter can only survive a nisin concentration of 5 nM. Above this concentration the cells are suffering from pore formation mediated by nisin. Furthermore, we could show that NsrFP works as a lantibiotic exporter by a peptide release assay. Additionally several mutants of nisin were used to investigate the substrate specificity, which highlights that NsrFP recognizes the N-terminal region of nisin. This was confirmed by the observed resistance against nisin H (O'Connor et al., 2015) and gallidermin (Kellner et al., 1988), which both contain a similar N-terminus but differ in the C-terminal part of the peptide.

MATERIALS AND METHODS

Cloning of *nsrfp*

The *nsrfp* gene from *S. agalactiae* COH1 was amplified from the chromosomal DNA using two primers (NsrFP_for 5′-CA TCACCACCACCACTTATTAGAAATCAATCACTTAG-3′ and NsrFP_rev 5′-GTGGTGGTGGTGGTGCATATAATTCTCCTTTA TTTATTATAC-3) and ligated into *pIL-SV* (*E. coli–L. lactis* shuttle vector) (Alkhatib et al., 2014b). The point mutation $NsrF_{H202A}$ was introduced by a standard mutagenesis protocol using the following primers: forward: 5′-GATGGT AACCGCTTCAGCAAATGCTG-3′; reverse: 5′-CAGCATTTGC TGAAGCGGTTACCATC-3′. The resulting plasmid was verified by sequencing and transformed into the *L. lactis* strain NZ9000 for expression (Holo and Nes, 1989) and the corresponding strains were termed NZ9000NsrFP and NZ9000$NsrF_{H202A}$P. An empty vector *pIL-SVCm* was also transformed into the NZ9000 strain and was used as a control (that excludes any possible effect of induction of the plasmid), and this strain was called NZ9000Cm. The expression of the *nsrfp* gene is regulated by the TCS NisR/NisK present in the NZ9000 strain genome.

Expression of NsrFP and $NsrF_{H202A}$P

The NZ9000NsrFP and NZ9000$NsrF_{H202A}$P strains were grown in GM17 media supplemented with 5 μg/ml chloramphenicol. By the addition of nisin (final concentration of 1 ng/ml, which is equivalent to 0.3 nM), the expression was induced and the culture was further grown overnight. To analyze the expression, the cells were harvested at OD_{600} of 2.0 by centrifuging at 5000 × *g* for 30 min. The resulting pellet was resuspended with R-buffer [50 mM HEPES pH 8.0, 150 mM NaCl, 10% (w/v) glycerol] to an OD_{600} of 200. Then 1/3 (w/v) glass beads (0.3 mm) were added and cells were lysed. A cycle of 1 min disruption and 2 min cooling on ice was repeated five to six times. A low centrifugation step at 10,000 × *g* to collect the cytoplasmic part was performed. Followed by a high spin step (100,000 × *g*) to harvest the membranes. To collected cytoplasmic and membrane fractions SDS-loading dye [0.2 M Tris–HCl, pH 6.8, 10% (w/v) SDS, 40% (v/v) glycerol, 0.02% (w/v) bromophenol and β-mercaptoethanol] was added, samples were

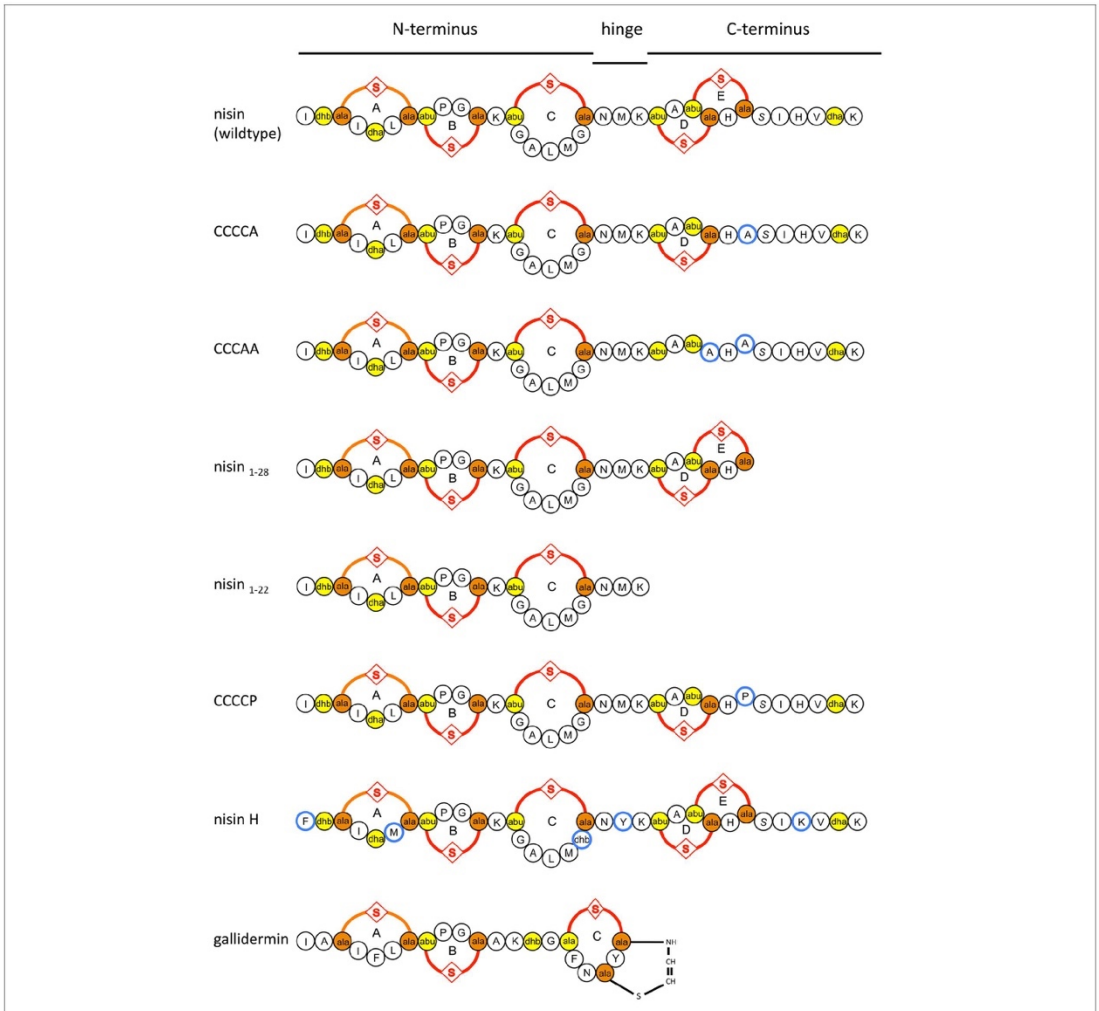

FIGURE 1 | Schematic overview of nisin, the variants of nisin, nisin H, and gallidermin used in this study. Introduced mutations in CCCCA, CCCAA, CCCCP, and the natural variants in nisin H are highlighted in blue. The (methyl)-lanthionine rings (labeled with A, B, C, D, and E) are formed by a dehydrated amino acid residue and a cysteine residue side chain (orange and yellow).

further used for SDS-PAGE and Western blot analysis (20 µl loaded). To detect NsrFP and $NsrF_{H202A}P$ a polyclonal antibody against the large extracellular loop of NsrP was used (Davids Biotechnologie, Regensburg, Germany).

Cloning of the Nisin H and CCCCP Variant

The used variants (CCCCA, CCCAA, $nisin_{1-28}$ and $nisin_{1-22}$) were previously described in Alkhatib et al. (2014b). Nisin H (O'Connor et al., 2015) was created by introducing five point mutations into the *pNZ-SV-nisA* vector (Alkhatib et al., 2014b). For the I_1F-L_6M point mutations we used the following primers (forward: 5′-GTG CATCACCACGCTTTACAAGTATTTCGATGTGTACACCCGG TTG-3′; reverse: 5′-CAACCGGGTGTACACATCGAAATACTT GTAAAGCGTGGTGATGCAC-3′). The $G_{18}T$-$M_{21}Y$ mutations were introduced with the primers (forward: 5′-GTAAAAC AGGAGCTCTGATGACATGTAACTATAAAACAGCAACTTGT CATTG-3′; reverse: 5′-CAATGACAAGTTGCTGTTTTATAGTT ACATGTCATCAGAGCTCCTGTTTTAC-3′) and the last mutation $H_{31}K$ with the primers (forward: 5′-CTTGTCATTG

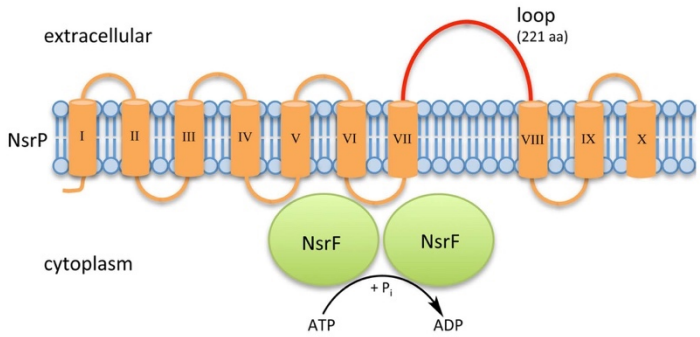

FIGURE 2 | Schematic representation of NsrFP from *S. agalactiae* COH1. NsrFP is an ABC transporter consisting of NsrF (highlighted in green), which hydrolyses ATP and NsrP (highlighted in orange). NsrP is a membrane protein consisting of 10 predicted transmembrane helices with an extracellular domain (depicted in red), which is a characteristic for the BceAB-type of lantibiotic resistance transporters.

TAGTATTAAAGTAAGCAAATAAGCTTTC-3′; reverse: 5′-GAAAGCTTATTTGCTTACTTTAATACTACAATGACAAG-3′). The CCCCP variant, were the last cysteine was exchanged by a proline was created into the *pNZ-SV-nisA* vector with the primers (forward: 5′-CAGCAACTTGTCATCCAAGTATTCACGTAAG-3′; reverse: 5′-CTTACGTGAATACTTGGATGACAAGTTGCTG-3′).

The resulting plasmids were verified by sequencing and transformed into the *L. lactis* strain NZ9000 (already containing the *pIL3-BTC* vector; Rink et al., 2005) for expression by electroporation as described above.

Expression, Purification of Prenisin Variants

Prenisin was purified as described in Alkhatib et al. (2014b). Activation of purified prenisin was done by overnight cleavage at 8°C with purified NisP (Abts et al., 2013). The efficiency of the reaction was monitored and the concentration of active nisin was determined by RP-HPLC as previously described (Abts et al., 2013). The activated nisin variants were then directly used for IC_{50} assays. Gallidermin is commercially available (Enzo Life Sciences).

Purification of Nisin

Nisin was purified as described in Abts et al. (2011). The concentration of nisin was measured by using RP-HPLC as previously described (Abts et al., 2013).

Determination the Activity of Nisin by Growth Inhibition (IC_{50})

Cells from the different expressing strains were grown overnight in GM17 supplemented with 5 μg/ml chloramphenicol in presence of 1 ng/ml nisin. The diluted cells (final OD_{584} was 0.1) were incubated with a serial dilution of nisin in a 96-well plate. The total volume in each well was 200 μl, consisting of 50 μl nisin and 150 μl GM17 containing the corresponding *L. lactis* strain. The highest concentration of nisin used was adapted to the corresponding maximum resistance displayed by each strain.

The plate was incubated at 30°C. After 5 h, the optical density was measured at 584 nm via 96-well plate reader BMG. The normalized optical density was plotted against the logarithm of the nisin concentration in order to calculate the IC_{50} of nisin and the data was evaluated using the following equation (Eq. 1):

$$y = \mathrm{OD}_{\min} + \frac{\mathrm{OD}_{\max} - \mathrm{OD}_{\min}}{1 + 10^{(\log(\mathrm{IC}_{50}) - x) \times p}}$$

The OD_{max} value describes the normalized optical density value where no nisin was added, while the OD_{min} value corresponds to the normalized optical density of the cells grown in the highest nisin concentrations. The y represents the resulted normalized optical density value and x represents the logarithmic of the nisin concentration added. The IC_{50} value is the concentration of nisin where the growth of the *L. lactis* strain is inhibited by 50% (Abts et al., 2011).

Calculation of the Fold of Resistance

We determined the IC_{50} value of nisin against the NZ9000Cm sensitive strain as well as the strain NZ9000NsrFP and NZ9000$NsrF_{H202A}$P. By dividing these two values the fold of resistance is obtained. For example wild type nisin displayed an IC_{50} of 4.9 nM against NZ9000Cm and 82.2 nM against NZ9000NsrFP. Dividing these two values results in a fold of resistance of 16.7. We used this fold of resistance to obtain a quantitative, comparable value for the nisin variants.

Dependency of Nisin Variants on Induced Expression of NsrFP

We verified the expression level of NsrFP in the corresponding strain NZ9000NsrFP by inducing expression with the different nisin variants. Here, we used half the IC_{50} value, which

was determined for each nisin variant against the sensitive NZ9000Cm strain, to exclude an effect on the expression level of NsrFP. The initial OD_{600} of the NZ9000NsrFP strain was 0.1 and we induced each sample with the half IC_{50} value of the corresponding nisin variants. The strains were further grown for 5 h at 30°C. After harvesting the cells, SDS-PAGE samples were prepared as describe above. The expression of NsrFP was analyzed by Western blot using a polyclonal antibody directed against the extracellular loop.

SYTOX Green Nucleic Acids Binding Assay

SYTOX green nucleic acids binding dye possesses a high binding affinity toward nucleic acids. It enters cells, which contain a pore in the plasma membrane and never crosses the intact membranes of living cells (Roth et al., 1997). The cells of NZ9000NsrFP were grown overnight in GM17 supplemented with 5 μg/ml chloramphenicol in presence of 1 ng/ml nisin. The next day, the overnight culture was diluted to an OD_{600} of 0.1 in fresh media supplemented with 5 μg/ml chloramphenicol. The cultures were grown until the OD_{600} reaches 0.5, the SYTOX green dye was added at a final concentration of 2.5 μM and incubated for 5 min according to the manual of the manufacturer (Invitrogen). The fluorescence signal, which was measured at an excitation and emission wavelength of 504 and 523 nm, respectively, was monitored. After a stable baseline is reached, nisin was added and the fluorescence was monitored over an additional time period.

Nisin Transport Assay

To answer the question whether NsrFP is an importer or exporter we performed a well-known nisin transport assay (Stein et al., 2003, 2005).

We grew the cells of NZ9000NsrFP, NZ9000$NsrF_{H202A}$P, and NZ9000Cm in GM17 supplemented with 5 μg/ml chloramphenicol in presence of 1 ng/ml nisin. We harvested the cells and washed them with 50 mM HEPES, pH 7, 500 mM NaCl, 10 % (v/v) glycerol. The cell density was adjusted to an OD_{600} of 10 in 1 ml of the corresponding strain and incubated with 8 μg nisin at 30°C for 30 min under gently shaking. After centrifugation at 10,000 × *g* for 10 min the supernatant was collected and applied to RP-HPLC for the quantification of nisin as described above.

RESULTS

IC_{50} Determination of NZ9000NsrFP and NZ9000$NsrF_{H202A}$P

We cloned NsrFP and $NsrF_{H202A}$P in a *pIL-SVCm* shuttle vector and induced the expression with a sublethal amount of nisin (0.3 nM). To ensure, that there were no side effects from induction with nisin, we compared all experiments with a control strain. This strain was transformed with an empty plasmid and was treated exactly the same. We observed that the induction using 0.3 nM had no influence on the morphology or growth behavior of the *L. lactis* strains. This expression system has been used in the past for several proteins involved in nisin modification as well as immunity and resistance (Kuipers et al., 2004; Plat et al., 2011; AlKhatib et al., 2014a; Khosa et al., 2016a). Nisin was purified as previously described (**Figure 3**; Abts et al., 2011). To address the activity of nisin against the NZ9000Cm, NZ9000NsrFP, and NZ9000$NsrF_{H202A}$P strains, growth experiments were performed using an increasing concentration of nisin. From these the IC_{50} values were determined, which reflects the growth inhibition of the corresponding strain by 50% using Eq. 1.

Nisin is highly active against the NZ9000Cm strain, as observed by the IC_{50} value of 4.9 ± 0.4 nM (**Figure 4** and **Table 1**). The NZ9000NsrFP strain exhibited a higher IC_{50} value of 82.2 ± 6.7 nM (**Figure 4** and **Table 1**). By dividing the two values a 16.7-fold of resistance was calculated (see Materials and Methods). This highlights that NsrFP expressed in *L. lactis* confers resistance against nisin. We cloned a variant of NsrFP termed $NsrF_{H202A}$P, where the histidine at position 202 of NsrF is mutated to an alanine. By sequence alignments this histidine residue was identified as the catalytically important residue for ATP hydrolysis, generally termed as H-loop (Zaitseva et al., 2005). The corresponding NZ9000$NsrF_{H202A}$P strain displayed a lower IC_{50} value of 5.1 ± 0.8 nM, which within experimental error represents the same value as obtained for the NZ9000Cm strain (**Figure 4** and **Table 1**). This suggests that NsrFP relies on ATP hydrolysis to confer resistance against nisin. Here, we have to note that the expression of $NsrF_{H202A}$P led to a reduced final OD (0.8 compared to 1.1 for the wild type strain) in our growth experiments. The observed difference does not rise from different expression levels of NsrFP and the $NsrF_{H202A}$P variant as shown by Western blot analysis using a polyclonal antibody directed against the large ECD of NsrP (Davids Biotechnology, Regensburg, Germany) (**Figure 3A**).

Pore Formation of Nisin in the NZ9000NsrFP Strain

Nisin is able to form pores in the membrane of Gram-positive bacteria initiated by the initial binding to lipid II and subsequently reorientation of the C-terminal part of nisin into the membrane (Hasper et al., 2004). This leads to membrane leakage and rapid cell death. We monitored this pore formation using a SYTOX green nucleic acid dye (Roth et al., 1997). When pores are formed in the membrane the SYTOX dye enters the cells and binds to the DNA, resulting in an increased fluorescence signal. This is an almost instant effect, which can be monitored in real time. We monitored the pore forming action of nisin against the NZ9000NsrFP, using different nisin concentrations, which were based on the IC_{50} values of the corresponding strains determined above. As a control, we added only buffer without nisin, which resulted in no increase of the fluorescence signal as observed by the black line in **Figure 5**. This control indicates that no cells are spontaneously lysed under this experimental setup.

When 40 nM nisin (corresponding to half the IC_{50} value determined for the NZ9000NsrFP strain) was added to the

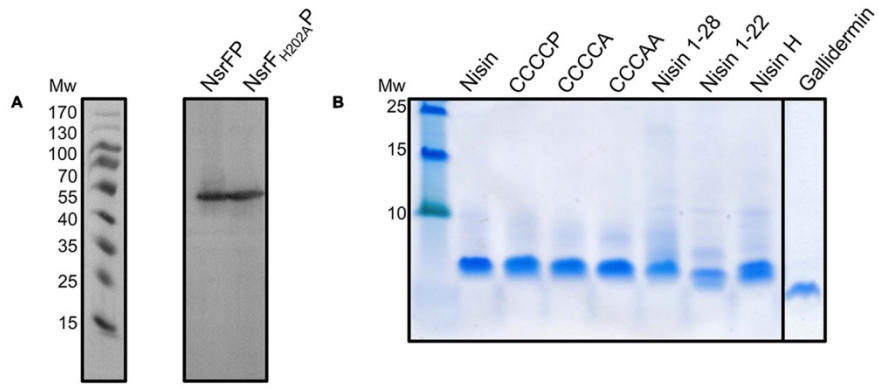

FIGURE 3 | Expression of NsrFP and NsrF$_{H202A}$P in *L. lactis* and purification of nisin variants. **(A)** The expression of NsrFP and NsrF$_{H202A}$P was monitored by Western blot using a polyclonal antibody against the extracellular domain. As observed both proteins are expressed at a similar level in *L. lactis* NZ9000. **(B)** Nisin and its variants were purified and activated by using a standard procedure (see Materials and Methods). All substrates display a similar purity, judged by a 20% Tricine-SDS-PAGE.

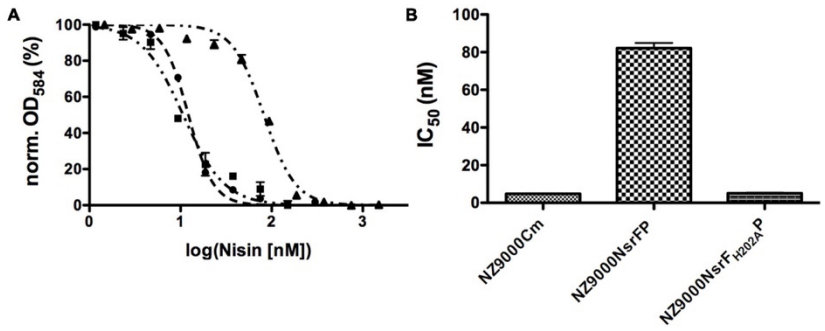

FIGURE 4 | Activity of nisin against the NZ9000Cm, NZ9000NsrFP, and NZ9000NsrF$_{H202A}$P strains. **(A)** The IC$_{50}$ of nisin against the NZ9000Cm (●), NZ9000NsrFP (▲), and strain NZ9000NsrF$_{H202A}$P (■) was determined. As observed the curve shifted to higher nisin concentration indicating that the NZ9000NsrFP strain is more resistant toward nisin. **(B)** The calculated IC$_{50}$ values of nisin against the NZ9000Cm, NZ9000NsrFP, and the NZ9000NsrF$_{H202A}$P strain are highlighted.

NZ9000NsrFP strain, no increase of the fluorescence signal was observed (**Figure 5**, green line). This indicates that the NZ9000NsrFP strain can survive a nisin concentration of 40 nM. Only a small linear increase was visible after 400 s, which reflects to a less extent cell lysis after some time. A nisin concentration equivalent to the IC$_{50}$ value (80 nM) resulted in a slightly stronger increase of the signal after a delay time (**Figure 5**, blue line). Finally, after adding a nisin concentration of two-times the IC$_{50}$ value (e.g., 160 nM to the NZ9000NsrFP strain) a rapid increase of the fluorescence signal was observed and reaches a stable plateau already after a couple of seconds. This shows that NsrFP is not able to confer resistance above the determined IC$_{50}$ concentration (**Figure 5**, red line).

Nisin Transport Assay–Peptide Release Assay

We performed a peptide release assay to verify the transport direction of NsrFP. Previously, the same assay was used to characterize NisFEG and SpaFEG, two exporting systems from lantibiotic producing strains (Stein et al., 2003, 2005). Here, we incubated the NsrFP expressing strain with 8 μg nisin for 30 min. After centrifugation of the cell, the supernatant was analyzed via RP-HPLC to determine the amount of nisin. From 8 μg nisin, 4.3 μg nisin was recovered from the supernatant (**Figure 6**). As a control, we used the NsrF$_{H202A}$P and the sensitive NZ9000Cm strain. There only ∼2 μg nisin was recovered from the supernatant (**Figure 6**). This shows that NsrFP is able to

TABLE 1 | IC_{50} values of nisin and its variants against the NZ9000Cm, NZ9000NsrFP, and NZ9000$NsrF_{H202A}$P strains.

	NZ9000Cm	NZ9000NsrFP		NZ9000$NsrF_{H202A}$P	
Nisin variant	**IC_{50} (nM)**	**IC_{50} (nM)**	**Fold of resistance**	**IC_{50} (nM)**	**Fold of resistance**
Wild type	4.9 ± 0.4	82.2 ± 6.7	16.7	5.1 ± 0.8	1.1
CCCCP	39.7 ± 1.5	238.4 ± 11.7	6.0	37.8 ± 3.9	0.9
CCCCA	64.4 ± 8.4	2023 ± 143	31.4	38.9 ± 5.9	0.6
CCCAA	278.6 ± 18.8	36346 ± 3632	130.5	154.6 ± 30.8	0.5
$Nisin_{1-28}$	157.0 ± 8.7	5243 ± 1225	33.4	65.3 ± 11.4	0.4
$Nisin_{1-22}$	309.9 ± 51.4	12220 ± 804	39.4	209.0 ± 39.9	0.7
Nisin H	7.0 ± 0.4	86.5 ± 3.7	12.3	7.5 ± 0.8	1.1
Gallidermin	67.1 ± 9.1	840 ± 87.0	12.5	59.7 ± 7.3	0.9

Besides the IC_{50} values also the fold of resistance against the nisin variants mediated by NsrFP are shown. The fold of resistance is calculated by the division of the IC_{50} value obtained of the NZ9000NsrFP by the value for the NZ9000Cm strain. The values represent the average and standard deviation of at least four different experiments.

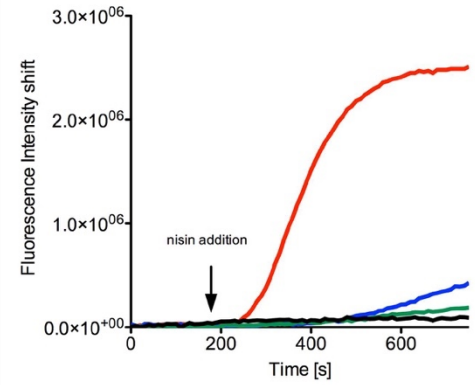

FIGURE 5 | SYTOX green assay to visualize pore formation mediated by nisin. The NZ9000NsrFP strain was grown until OD_{600} of 0.5 and then incubated with the SYTOX dye. After a stable baseline was reached nisin (indicated with an arrow) was added at various concentrations: 40 nM (green line), 80 nM (blue line), and 160 nM (red line). As a control only buffer was added (black line). The fluorescence signal was monitored online using a fluorolog (Horiba III) and the rapid increase indicates pore formation. The curves are representatives of at least four biological replicates.

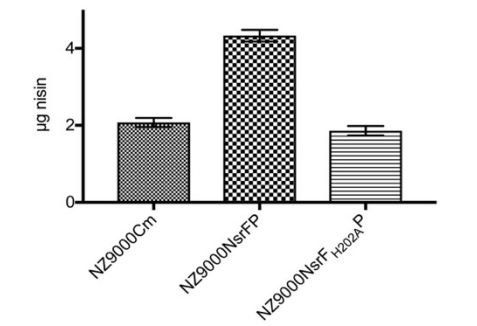

FIGURE 6 | Nisin transport assay. The NZ9000Cm, NZ9000NsrFP, and NZ9000$NsrF_{H202A}$P strain were incubated with 8 µg nisin. After incubation for 30 min the cells were spun down and the amount of nisin in the supernatant was determined using RP-HPLC. The NZ9000Cm and NZ9000$NsrF_{H202A}$P strain showed similar nisin amounts. The NZ9000NsrFP strain revealed a ~2-fold increased nisin amount, highlighting that NsrFP exports nisin from the *L lactis* membrane.

export nisin from the cellular membrane. Our results are similar to the results found for the NisFEG and SpaFEG transporters leading to the same conclusion that NsrFP is exporting nisin from the cellular membrane as well.

Substrate Specificity of NsrFP

In order to investigate the substrate specificity of NsrFP we used a set of nisin variants. Here, the nisin variants CCCCA, CCCAA, $nisin_{1-28}$, and $nisin_{1-22}$ were used (Khosa et al., 2016a). These variants are lacking the last or last two lanthionine rings or display deletions at the C-terminus of nisin, respectively. CCCCP is a variant, where the cysteine at position 28 (important for ring E formation) is exchanged to a proline (for a schematic view see **Figure 1**).

Expression and purification were performed as previously described (Alkhatib et al., 2014b), resulting in high purity (**Figure 3B**). The activities of these variants were determined against the nisin sensitive NZ9000Cm strain and the strains expressing NsrFP or $NsrF_{H202A}$P, respectively (**Table 1**). By comparing these values the fold of resistance was obtained (**Figure 7**) as determined for the wild type nisin (see above and Materials and Methods).

For CCCCP, the fold of resistance was determined to be 6.0 (IC_{50} against NZ9000Cm was 39.7 ± 1.5 nM and against NZ9000NsrFP was 238.4 ± 11.7 nM). For CCCCA, the fold of resistance was determined to be 31.4 (IC_{50} against NZ9000Cm was 64.4 ± 8.4 nM and against NZ9000NsrFP 2023 ± 143 nM). The CCCAA variants displayed a 130.5-fold of resistance (IC_{50} against NZ9000Cm was 278.6 ± 18.8 nM and against NZ9000NsrFP 36346 ± 3632 nM). The two deletion mutants displayed a 33.4 ($nisin_{1-28}$) and 39.4 ($nisin_{1-22}$) fold

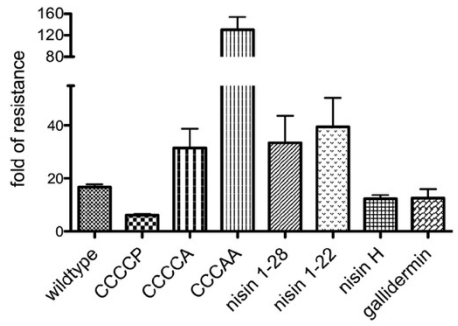

FIGURE 7 | Substrate specificity of NsrFP. Graphical representation of the fold of resistance exhibited by NsrFP with nisin and different nisin variants (CCCCA, CCCAA, CCCCP, $nisin_{1-22}$ and $nisin_{1-28}$) as well as nisin H and gallidermin. The NZ9000Cm and NZ9000NsrFP strains were used to determine the activity of all tested lantibiotics. The error bars indicate the standard error of at least three independent experiments.

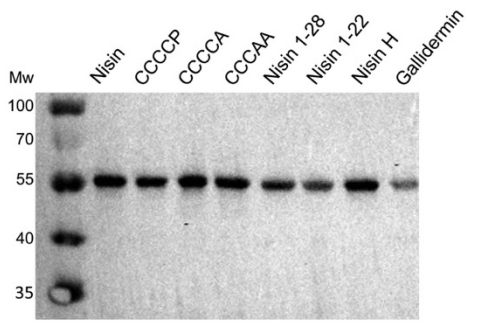

FIGURE 8 | Dependency of nisin variants on induced expression of NsrFP. The expression of NsrFP was monitored by Western blot using a polyclonal antibody against the extracellular domain. As observed, the expression of NsrFP was similar in all cases, independent of the used nisin variant.

of resistance, almost five times higher when compared to wild type. Here IC_{50} were determined to be 157 ± 8.7 nM against NZ9000Cm and 5243 ± 1225 nM against NZ9000NsrFP strain for $nisin_{1-28}$ and 309.9 ± 51.4 nM against NZ9000Cm and 12,220 ± 804 nM against NZ9000NsrFP for $nisin_{1-22}$, respectively.

These results revealed that NsrFP is able to be active as long as the N-terminal region of nisin is present, and since this part is highly conserved in several other lantibiotics, we hypothesized that the NsrFP transporter can besides nisin also recognize other lantibiotics. To test this, we used two other lantibiotics: nisin H (O'Connor et al., 2015) and gallidermin which is produced by *Staphylococcus gallinarum* Tü3928 (Kellner et al., 1988) (schematically shown in **Figure 1**). The latter contains a similar N-terminal part but has in comparison to nisin a structurally non-related C-terminus.

We determined the fold of resistance mediated by NsrFP for these lantibiotics (**Table 1** and **Figure 7**). Here, it was observed that nisin H as well as gallidermin are also recognized and NsrFP confers resistance to these lantibiotics. Our calculated fold of resistance is 12.3 for nisin H and 12.5 for gallidermin (**Table 1**). This strengthens the observation that the N-terminal region plays a predominant role in substrate recognition, since nisin H and gallidermin are recognized as well with similar efficiencies.

We were wondering whether the effect of a higher fold of resistance actually was a result of an increased expression of NsrFP in the membrane. Therefore, we incubated NZ9000NsrFP cells with the corresponding nisin variants (note: the concentration is 1/2 IC_{50} value of each nisin variant) and visualized the expression of NsrFP by Western blot. Here, we observed that the expression levels of NsrFP were similar for each strain and thereby cannot be the reason for the higher increased fold of resistance (**Figure 8**).

DISCUSSION

Lantibiotics possess antimicrobial activity against various bacteria including the well known MRSA, VISA, and VRE strains (Piper et al., 2009). However, various bacteria, especially human pathogens are actually inherently resistant against lantibiotics, which they do not produce themselves. Interestingly, this resistance is often arising from the expression of one or two membrane embedded proteins. Here, one belongs to the BceAB-type ABC transporter family and confer resistance against antimicrobial peptides including lantibiotics (Kallenberg et al., 2013; Kingston et al., 2014). Genetically the BceAB-type transporters are often located next to a TCS in the genome, which regulates the expression of the genes encoded (Dintner et al., 2011). It is thought that especially the ECD, which is a hallmark of BceAB-type ABC transporters is involved in lantibiotic sensing and transferring the signal to the corresponding histidine kinase (Staroń et al., 2011; Kallenberg et al., 2013). We focused on the nisin resistance operon from the *S. agalactiae* COH1, more specifically the BceAB-type ABC transporter NsrFP (Khosa et al., 2013). This transporter is localized on a gene operon together with the membrane associated protease NSR and the TCS NsrR and NsrK (Khosa et al., 2013, 2016b). We heterologously expressed the transporter in *L. lactis*, which lacks the NsrR/NsrK TCS and observed that NsrFP is able to confer resistance by itself. The fold of resistance, which we used as a measure of the activity, revealed that the *L. lactis* cells are able to deal with a 16-fold higher nisin concentration when compared to the same strain lacking NsrFP. The fold of resistance of an ATP hydrolysis deficient mutant of NsrFP is reduced to levels observed for the nisin sensitive NZ9000Cm strain. Like NisFEG (Stein et al., 2003) and SpaFEG (Stein et al., 2005), NsrFP acts as an lantibiotic exporter, which so far has not been conclusively shown for an lantibiotic resistance ABC transporter.

Intriguing is the observation that the N-terminal part of nisin appears to be important for NsrFP. By using C-terminal

variants and deletions of nisin the fold of resistance increased in comparison to the wild type nisin. Only the variant CCCCP displayed a reduced fold of resistance. The recognition of the N-terminal region was further underlined by the observation that nisin H as well as gallidermin were also recognized as substrates. Here, especially the latter is containing a similar N-terminal region but differs structurally completely at the C-terminus (**Figure 1**).

Previously, the recognition of ring A and B was observed for the lantibiotic resistance ABC transporter CprABC from *Clostridium difficile*, which recognizes multiple lantibiotics: for example, nisin, gallidermin, subtilin, and mutacin 1140 (McBride and Sonenshein, 2011; Suárez et al., 2013).

Within the nisin resistance operon in *S. agalactiae* COH1 two proteins, namely the membrane associated protease NSR and NsrFP, are present (Khosa et al., 2013, 2016b). NSR is cleaving off the last six amino acids of nisin resulting in $nisin_{1-28}$, which has a 32-fold lower activity. This product of NSR ($nisin_{1-28}$), however, is still well recognized by NsrFP, as shown by an even increased fold of resistance. This suggests that both proteins are working together to obtain full resistance in *S. agalactiae*. The first line of defense would be NSR and the resulting processed product $nisin_{1-28}$, is transported by NsrFP, once it reaches the membrane with high efficiency. This type of cooperativity would be similar to the natural immunity system observed in the nisin and subtilin (auto)immunity systems from *L. lactis* and *B. subtilis*, respectively. There, a cooperative mode of action of the immunity proteins LanI and LanFEG have been observed by which only full immunity was displayed when both protein are simultaneously expressed (Stein et al., 2003, 2005). Therefore, we suggest that NsrFP and NSR have a similar cooperative mode of action and only when both proteins are expressed simultaneously within the membrane of *S. agalactiae* COH1 full resistance is occurring.

AUTHOR CONTRIBUTIONS

SS conceived and directed this study. JR, ML, SL, and KE conducted the experiments. JZ-K established the mutants of nisin and created the figures. JR, ML, and SS wrote the manuscript with input of all authors. All authors read and approved the manuscript.

FUNDING

This work has been supported by the Graduate School 2158, which is funded by the Deutsche Forschungsgemeinschaft (DFG).

ACKNOWLEDGMENTS

We thank Diana Kleinschrodt and Iris Fey of the Protein Production Facility for excellent support during the initial stages of this project. We thank all members of the Institute of Biochemistry for fruitful discussions. The students of the master course "Fascination Biochemistry" for their initial experiments during their bachelor studies.

REFERENCES

Abts, A., Mavaro, A., Stindt, J., Bakkes, P. J., Metzger, S., Driessen, A. J., et al. (2011). Easy and rapid purification of highly active nisin. *Int. J. Pept.* 2011:175145. doi: 10.1155/2011/175145

Abts, A., Montalban-Lopez, M., Kuipers, O. P., Smits, S. H., and Schmitt, L. (2013). NisC binds the FxLx motif of the nisin leader peptide. *Biochemistry* 52, 5387–5395. doi: 10.1021/bi4008116

AlKhatib, Z., Lagedroste, M., Fey, I., Kleinschrodt, D., Abts, A., and Smits, S. H. (2014a). Lantibiotic immunity: inhibition of nisin mediated pore formation by NisI. *PLoS ONE* 9:e102246. doi: 10.1371/journal.pone.0102246

Alkhatib, Z., Lagedroste, M., Zaschke, J., Wagner, M., Abts, A., Fey, I., et al. (2014b). The C-terminus of nisin is important for the ABC transporter NisFEG to confer immunity in *Lactococcus lactis*. *MicrobiologyOpen* 3, 752–763. doi: 10.1002/mbo3.205

Brötz, H., Bierbaum, G., Leopold, K., Reynolds, P. E., and Sahl, H. G. (1998a). The lantibiotic mersacidin inhibits peptidoglycan synthesis by targeting lipid II. *Antimicrob. Agents Chemother.* 42, 154–160.

Brötz, H., Josten, M., Wiedemann, I., Schneider, U., Götz, F., Bierbaum, G., et al. (1998b). Role of lipid-bound peptidoglycan precursors in the formation of pores by nisin, epidermin and other lantibiotics. *Mol. Microbiol.* 30, 317–327.

Chatterjee, C., Paul, M., Xie, L., and van der Donk, W. A. (2005). Biosynthesis and mode of action of lantibiotics. *Chem. Rev.* 105, 633–684. doi: 10.1021/cr030105v

de Freire Bastos, M. D. C., Coelho, M. L. V., and da Silva Santos, O. C. (2015). Resistance to bacteriocins produced by Gram-positive bacteria. *Microbiology* 161, 683–700. doi: 10.1099/mic.0.082289-0

Dintner, S., Heermann, R., Fang, C., Jung, K., and Gebhard, S. (2014). A sensory complex consisting of an ATP-binding cassette transporter and a two-component regulatory system controls bacitracin resistance in *Bacillus subtilis*. *J. Biol. Chem.* 289, 27899–27910. doi: 10.1074/jbc.M114.596221

Dintner, S., Staroń, A., Berchtold, E., Petri, T., Mascher, T., and Gebhard, S. (2011). Coevolution of ABC transporters and two-component regulatory systems as resistance modules against antimicrobial peptides in Firmicutes bacteria. *J. Bacteriol.* 193, 3851–3862. doi: 10.1128/JB.05175-11

Dischinger, J., Chipalu, S. B., and Bierbaum, G. (2014). Lantibiotics: promising candidates for future applications in health care. *Int. J. Med. Microbiol.* 304, 51–62. doi: 10.1016/j.ijmm.2013.09.003

Draper, L. A., Cotter, P. D., Hill, C., and Ross, R. P. (2015). Lantibiotic resistance. *Microbiol. Mol. Biol. Rev.* 79, 171–191. doi: 10.1128/MMBR.00051-14

Gebhard, S., and Mascher, T. (2011). Antimicrobial peptide sensing and detoxification modules: unravelling the regulatory circuitry of *Staphylococcus aureus*. *Mol. Microbiol.* 81, 581–587. doi: 10.1111/j.1365-2958.2011.07747.x

Hasper, H. E., de Kruijff, B., and Breukink, E. (2004). Assembly and stability of nisin-lipid II pores. *Biochemistry* 43, 11567–11575. doi: 10.1021/bi049476b

Hasper, H. E., Kramer, N. E., Smith, J. L., Hillman, J. D., Zachariah, C., Kuipers, O. P., et al. (2006). An alternative bactericidal mechanism of action for lantibiotic peptides that target lipid II. *Science* 313, 1636–1637. doi: 10.1126/science.1129818

Holo, H., and Nes, I. F. (1989). High-frequency transformation, by electroporation, of *Lactococcus lactis* subsp. *cremoris* grown with glycine in osmotically stabilized media. *Appl. Environ. Microbiol.* 55, 3119–3123.

Hsu, S.-T. D., Breukink, E., Tischenko, E., Lutters, M. A. G., de Kruijff, B., Kaptein, R., et al. (2004). The nisin-lipid II complex reveals a pyrophosphate cage that provides a blueprint for novel antibiotics. *Nat. Struct. Mol. Biol.* 11, 963–967. doi: 10.1038/nsmb830

Islam, M. R., Nishie, M., Nagao, J., Zendo, T., Keller, S., Nakayama, J., et al. (2012). Ring A of nukacin ISK-1: a lipid II-binding motif for type-A(II) lantibiotic. *J. Am. Chem. Soc.* 134, 3687–3690. doi: 10.1021/ja300007h

Kallenberg, F., Dintner, S., Schmitz, R., and Gebhard, S. (2013). Identification of regions important for resistance and signalling within the antimicrobial

peptide transporter BceAB of *Bacillus subtilis*. *J. Bacteriol.* 195, 3287–3297. doi: 10.1128/JB.00419-13

Kellner, R., Jung, G., Horner, T., Zahner, H., Schnell, N., Entian, K. D., et al. (1988). Gallidermin: a new lanthionine-containing polypeptide antibiotic. *Eur. J. Biochem.* 177, 53–59. doi: 10.1111/j.1432-1033.1988.tb14344.x

Khosa, S., Alkhatib, Z., and Smits, S. H. (2013). NSR from *Streptococcus agalactiae* confers resistance against nisin and is encoded by a conserved NSR operon. *Biol. Chem.* 394, 1543–1549. doi: 10.1515/hsz-2013-0167

Khosa, S., Frieg, B., Mulnaes, D., Kleinschrodt, D., Hoeppner, A., Gohlke, H., et al. (2016a). Structural basis of lantibiotic recognition by the nisin resistance protein from *Streptococcus agalactiae*. *Sci. Rep.* 6:18679. doi: 10.1038/srep18679

Khosa, S., Lagedroste, M., and Smits, S. H. (2016b). Protein defense systems against the lantibiotic nisin: function of the immunity protein NisI and the resistance protein NSR. *Front. Microbiol.* 7:504. doi: 10.3389/fmicb.2016.00504

Kingston, A. W., Zhao, H., Cook, G. M., and Helmann, J. D. (2014). Accumulation of heptaprenyl diphosphate sensitizes *Bacillus subtilis* to bacitracin: implications for the mechanism of resistance mediated by the BceAB transporter. *Mol. Microbiol.* 93, 37–49. doi: 10.1111/mmi.12637

Klaenhammer, T. R. (1993). Genetics of bacteriocins produced by lactic acid bacteria. *FEMS Microbiol. Rev* 12, 39–85. doi: 10.1111/j.1574-6976.1993.tb00012.x

Kuipers, A., de Boef, E., Rink, R., Fekken, S., Kluskens, L. D., Driessen, A. J., et al. (2004). NisT, the transporter of the lantibiotic nisin, can transport fully modified, dehydrated, and unmodified prenisin and fusions of the leader peptide with non-lantibiotic peptides. *J. Biol. Chem.* 279, 22176–22182. doi: 10.1074/jbc.M312789200

McBride, S. M., and Sonenshein, A. L. (2011). Identification of a genetic locus responsible for antimicrobial peptide resistance in *Clostridium difficile*. *Infect. Immun.* 79, 167–176. doi: 10.1128/IAI.00731-10

Mota-Meira, M., Lapointe, G., Lacroix, C., and Lavoie, M. C. (2000). MICs of mutacin B-Ny266, nisin A, vancomycin, and oxacillin against bacterial pathogens. *Antimicrob. Agents Chemother.* 44, 24–29. doi: 10.1128/AAC.44.1.24-29.2000

Nawrocki, K. L., Crispell, E. K., and McBride, S. M. (2014). Antimicrobial peptide resistance mechanisms of Gram-positive bacteria. *Antibiotics* 3, 461–492. doi: 10.3390/antibiotics3040461

O'Connor, P. M., O'Shea, E. F., Guinane, C. M., O'Sullivan, O., Cotter, P. D., Ross, R. P., et al. (2015). Nisin H is a new nisin variant produced by the gut-derived strain *Streptococcus hyointestinalis* DPC6484. *Appl. Environ. Microbiol.* 81, 3953–3960. doi: 10.1128/AEM.00212-15

Ohki, R., Giyanto, Tateno, K., Masuyama, W., Moriya, S., Kobayashi, K., et al. (2003). The BceRS two-component regulatory system induces expression of the bacitracin transporter, BceAB, in *Bacillus subtilis*. *Mol. Microbiol.* 49, 1135–1144. doi: 10.1046/j.1365-2958.2003.03653.x

Piper, C., Cotter, P. D., Ross, R. P., and Hill, C. (2009). Discovery of medically significant lantibiotics. *Curr. Drug Discov. Technol.* 6, 1–18. doi: 10.2174/157016309787581075

Plat, A., Kluskens, L. D., Kuipers, A., Rink, R., and Moll, G. N. (2011). Requirements of the engineered leader peptide of nisin for inducing modification, export, and cleavage. *Appl. Environ. Microbiol.* 77, 604–611. doi: 10.1128/AEM.01503-10

Rietkötter, E., Hoyer, D., and Mascher, T. (2008). Bacitracin sensing in *Bacillus subtilis*. *Mol. Microbiol.* 68, 768–785. doi: 10.1111/j.1365-2958.2008.06194.x

Rink, R., Kuipers, A., de Boef, E., Leenhouts, K. J., Driessen, A. J., Moll, G. N., et al. (2005). Lantibiotic structures as guidelines for the design of peptides that can be modified by lantibiotic enzymes. *Biochemistry* 44, 8873–8882. doi: 10.1021/bi050081h

Roth, B. L., Poot, M., Yue, S. T., and Millard, P. J. (1997). Bacterial viability and antibiotic susceptibility testing with SYTOX green nucleic acid stain. *Appl. Environ. Microbiol.* 63, 2421–2431.

Ruhr, E., and Sahl, H.-G. (1985). Mode of action of the peptide antibiotic nisin and influence on the membrane potential of whole cells and on cytoplasmic and artificial membrane vesicles. *Antimicrob. Agents Chemother.* 27, 841–845. doi: 10.1128/AAC.27.5.841

Staroń, A., Finkeisen, D. E., and Mascher, T. (2011). Peptide antibiotic sensing and detoxification modules of *Bacillus subtilis*. *Antimicrob. Agents Chemother.* 55, 515–525. doi: 10.1128/AAC.00352-10

Stein, T., Heinzmann, S., Düsterhus, S., Borchert, S., and Entian, K.-D. (2005). Expression and functional analysis of the subtilin immunity genes spaIFEG in the subtilin-sensitive host *Bacillus subtilis* MO1099. *J. Bacteriol.* 187, 822–828. doi: 10.1128/JB.187.3.822-828.2005

Stein, T., Heinzmann, S., Solovieva, I., and Entian, K.-D. (2003). Function of *Lactococcus lactis* nisin immunity genes nisI and nisFEG after coordinated expression in the surrogate host *Bacillus subtilis*. *J. Biol. Chem.* 278, 89–94. doi: 10.1074/jbc.M207237200

Suárez, J. M., Edwards, A. N., and McBride, S. M. (2013). The *Clostridium difficile cpr* locus is regulated by a noncontiguous two-component system in response to type A and B lantibiotics. *J. Bacteriol.* 195, 2621–2631. doi: 10.1128/JB.00166-13

Sun, Z., Zhong, J., Liang, X., Liu, J., Chen, X., and Huan, L. (2009). Novel mechanism for nisin resistance via proteolytic degradation of nisin by the nisin resistance protein NSR. *Antimicrob. Agents Chemother.* 53, 1964–1973. doi: 10.1128/AAC.01382-08

Van de Ven, F., Van den Hooven, H., Konings, R., and Hilbers, C. (1991). "The spatial structure of nisin in aqueous solution," in *Nisin and Novel Lantibiotics*, eds G. Jung and H.-G. Sahl (Leiden: ESCOM Publishers), 35–42.

Wiedemann, I., Breukink, E., Van Kraaij, C., Kuipers, O. P., Bierbaum, G., De Kruijff, B., et al. (2001). Specific binding of nisin to the peptidoglycan precursor lipid II combines pore formation and inhibition of cell wall biosynthesis for potent antibiotic activity. *J. Biol. Chem.* 276, 1772–1779. doi: 10.1074/jbc.M006770200

Yang, S.-C., Lin, C.-H., Sung, C. T., and Fang, J.-Y. (2014). Antibacterial activities of bacteriocins: application in foods and pharmaceuticals. *Front. Microbiol.* 5:241. doi: 10.3389/fmicb.2014.00241

Zaitseva, J., Jenewein, S., Jumpertz, T., Holland, I. B., and Schmitt, L. (2005). H662 is the linchpin of ATP hydrolysis in the nucleotide-binding domain of the ABC transporter HlyB. *EMBO J.* 24, 1901–1910. doi: 10.1038/sj.emboj.7600657

Conflict of Interest Statement: The authors declare that the research was conducted in the absence of any commercial or financial relationships that could be construed as a potential conflict of interest.

3.2. Chapter II - Insight into Two ABC Transporter Families

Published in: Frontiers in Molecular Bioscience

Impact factor: 3.57

Own Work: 30 %

Writing the manuscript

Insight into Two ABC Transporter Families Involved in Lantibiotic Resistance

Rebecca Clemens, **Julia Zaschke-Kriesche**, Sakshi Khosa and Sander H. J. Smits

frontiers in Molecular Biosciences

REVIEW
published: 22 January 2018
doi: 10.3389/fmolb.2017.00091

Insight into Two ABC Transporter Families Involved in Lantibiotic Resistance

*Rebecca Clemens, Julia Zaschke-Kriesche, Sakshi Khosa and Sander H. J. Smits**

Institute of Biochemistry, Heinrich-Heine-University Duesseldorf, Duesseldorf, Germany

Antimicrobial peptides, which contain (methyl)-lanthionine-rings are called lantibiotics. They are produced by several Gram-positive bacteria and are mainly active against these bacteria. Although these are highly potent antimicrobials, some human pathogenic bacteria express specific ABC transporters that confer resistance and counteract their antimicrobial activity. Two distinct ABC transporter families are known to be involved in this process. These are the Cpr- and Bce-type ABC transporter families, named after their involvement in cationic peptide resistance in *Clostridium difficile*, and bacitracin efflux in *Bacillus subtilis*, respectively. Both resistance systems differentiate to each other in terms of the proteins involved. Here, we summarize the current knowledge and describe the divergence as well as the common features present in both the systems to confer lantibiotic resistance.

Keywords: lanthionine ring, lantibiotic, nisin, resistance, antimicrobial peptide, *L. lactis*

OPEN ACCESS

Edited by:
Richard J. Bingham,
Department of Biological Sciences,
University of Huddersfield,
United Kingdom

Reviewed by:
Anastassios C. Papageorgiou,
University of Turku, Finland
Christopher Cooper,
University of Huddersfield,
United Kingdom

****Correspondence:***
Sander H. J. Smits
sander.smits@hhu.de

Specialty section:
This article was submitted to Structural Biology, a section of the journal Frontiers in Molecular Biosciences

Received: *28 August 2017*
Accepted: *08 December 2017*
Published: *22 January 2018*

Citation:
Clemens R, Zaschke-Kriesche J, Khosa S and Smits SHJ (2018) Insight into Two ABC Transporter Families Involved in Lantibiotic Resistance. Front. Mol. Biosci. 4:91. doi: 10.3389/fmolb.2017.00091

INTRODUCTION

The urging need for novel antibiotics has put small antimicrobial peptides (AMPs) into a particular focus. Especially, a large group of peptides called bacteriocins have been extensively studied for an application purpose as novel antibiotics. Bacteriocins are small, ribosomally-synthesized peptides of which some display a high potent antimicrobial activity (Tagg et al., 1976; Cotter et al., 2005b) and have been already used since decades as food preservatives or as antibiotic alternatives in biomedical applications (Cleveland et al., 2001; Cotter et al., 2012).

A large group within the bacteriocin family, are ***lan***thionine containing *an**tibiotics*** termed lantibiotics. These lantibiotics are post-translationally modified peptides that contain dehydrated amino acids (Dehydrobutyrine and/or Dehydroalanine) and other unusual amino acid modifications (Jung, 1991; Willey and van der Donk, 2007; Bierbaum and Sahl, 2009; Alvarez-Sieiro et al., 2016). The Michael addition of a neighboring cysteine side chain residue to these dehydrated amino acids results in the formation of characteristic thioether bridges called lanthionine rings. These rings are primarily crucial for their high antimicrobial activity against mainly Gram-positive bacteria. The well-known lantibiotics nisin, gallidermin, and subtilin are highlighted in **Figure 1**. Lantibiotics are highly potent and nanomolar concentrations are already enough to fulfill their antimicrobial activity as observed for example for nisin produced by *Lactococcus lactis* species or subtilin produced by *Bacillus subtilis* (Delves-Broughton et al., 1996; Chatterjee et al., 2005).

In comparison to their high antimicrobial activity against Gram-positive bacteria, lantibiotics display a reduced effectiveness against Gram-negative bacteria. Many lantibiotics bind to lipid II or other peptidoglycan precursor inducing inhibition of cell wall synthesis. Some lantibiotics can subsequently form pores which lead to membrane leakage and rapid cell death (Héchard and Sahl, 2002; Bierbaum and Sahl, 2009). Due to their nanomolar activity, in combination with high stability

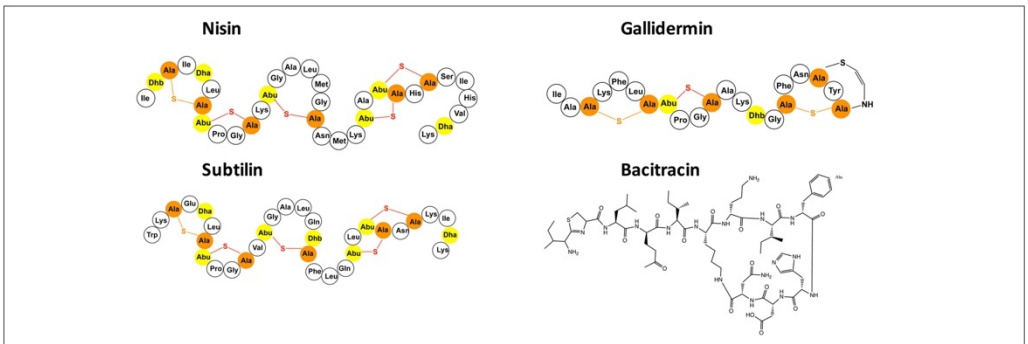

FIGURE 1 | Selected presentation of the lantibiotics nisin, gallidermin and subtilin as well as the bacteriocin bacitracin. The dehydrated amino acids and the cysteines of the lantibiotics are highlighted in yellow and orange. The (methyl-)lanthionine rings are visualized in orange and red.

against proteolytic digestion, lantibiotics are considered potential compounds for novel medical treatment.

A well-studied member of lantibiotics is nisin, which is produced by some *L. lactis* strains. It was shown that it is effective against the treatment of bacterial mastitis, methicillin-resistant *Staphylococcus aureus* (MRSA) and enterococcal infections (Brumfitt et al., 2002). Gallidermin and epidermin, produced by *Staphylococcus gallinarum* and *Staphylococcus epidermidis,* respectively, are some other examples of lantibiotics (Cotter et al., 2005a) and are associated with the treatment of acne, eczema, folliculitis, and impetigo.

The lantibiotic producer strains with a few exceptions, usually contain a single gene cluster, on which the structural genes for the lantibiotic itself, as well as for the modification and transport across the cellular membrane are located (Chatterjee et al., 2005; Willey and van der Donk, 2007; Alkhatib et al., 2012; Singh and Sareen, 2014). In many gene clusters, these genes are upregulated via a distinct two-component system (TCS) consisting of a histidine kinase (HK) and a response regulator (RR), which are located on the same gene cluster (Qiao et al., 1996). The upregulation is auto induced by its own lantibiotic (Kuipers et al., 1995).

Due to the high convergence of these gene clusters, it has been possible to detect potential lantibiotic gene clusters within newly sequenced genomes using *in silico* techniques (van Heel et al., 2013a). Such genome mining approaches have identified novel lantibiotic gene clusters in several species, such as the genes encoding for maddinglicin from *Clostridium maddingley*, agalacticin from *Streptococcus agalactiae*, bagelicin from *Streptococcus suis* and moraviensicin from *Enterococcus moraviensis* (van Heel et al., 2013b; Tracanna et al., 2017). These novel and mostly exotic lantibiotics can be expressed, modified and secreted by *L. lactis* using the well-characterized nisin biosynthetic machinery (van Heel et al., 2013b).

In order to prevent the activity of the secreted lantibiotic against their own membrane, the lantibiotic gene cluster contains additional genes (*lanI* and *lanFEG*), which form a lantibiotic (auto-)immunity system (Alkhatib et al., 2012). The *lanI* and *lanFEG* genes are conserved to a certain extent throughout the lantibiotic expressing bacteria (Alkhatib et al., 2012). Here LanI is a membrane-associated lipoprotein, which binds to the lantibiotic and thereby lowers the concentration of the lantibiotic reaching the membrane. Additionally, LanFEG forms an ABC transporter localized in the cellular membrane which effluxes the lantibiotic prior to pore formation (Stein et al., 2003, 2005; Draper et al., 2008, 2015).

Despite the odds, resistance against lantibiotics does exist and different resistance mechanisms have been unraveled so far. Resistance mechanisms comprise of modification in peptidoglycan or the cellular membrane (e.g., changes in phospholipid or fatty acid composition) as well as cell membrane modifications, such as lipopolysaccharides which are attached to the outer layer of the outer membrane of Gram-negative bacteria (Draper et al., 2015). Furthermore, some TCSs could be linked to lantibiotic resistance by upregulating the transcription of resistance-associated genes upon the presence of lantibiotic within the habitat of the bacteria. Other mechanisms resulting in resistance are the assembly of biofilms or the expression of resistance proteins such as the nisin resistance protein (NSR) found to be upregulated in nisin non-producing strains, inactivating nisin by specific proteolytic degradation (Sun et al., 2009). The lantibiotic resistance mechanisms have been nicely reviewed in detail in Draper et al. (2015).

Recently, several gene clusters were identified in various human pathogenic bacteria, which encode a lantibiotic resistance system based on the overexpression of membrane embedded proteins, that includes the presence of an ABC transporter (Khosa et al., 2013).

The expression of proteins within these gene clusters result in a detectable lantibiotic resistance. For example, resistance against nukacin ISK-I and lacticin 481 in *Streptococcus mutans* is mediated by the expression of *lcrSR-lctFEG* genes (Kawada-Matsuo et al., 2013a), while the expression of *cprABCK-R* operon in *Clostridium difficile* results in resistance against

different lantibiotics. Here, nisin, mutacin 1140, subtilin, and gallidermin were tested and resistance was observed (McBride and Sonenshein, 2011; Suárez et al., 2013). Furthermore, the proteins located on the *nsr* operon from *S. agalactiae* are together conferring resistance against nisin A, nisin H, and gallidermin (Khosa et al., 2016a,b; Reiners et al., 2017). All these resistance operons are characterized by the presence of a TCS consisting of a HK and a RR; as well as a membrane-embedded ATP-binding cassette (ABC) transporter (Gebhard, 2012; Khosa et al., 2013; Suárez et al., 2013). In some cases, an extra gene encoding a membrane-associated lipoprotein or a specific serine protease is present.

Upon examining these operons in detail, it was observed that the ABC transporters are responsible for lantibiotic resistance and can be divided into two groups: the CprABC-type and the BceAB-type ABC transporter family, both conferring resistance against lantibiotics and/or antimicrobial peptides in general.

Within this review, we will highlight these two lantibiotic resistance ABC transporter families and their corresponding gen clusters.

GENE CLUSTER ORGANIZATION OF ABC TRANSPORTERS INVOLVED IN LANTIBIOTIC RESISTANCE

The common feature of both operon types is the presence of a TCS, which upregulates the other genes by an external stimulus via binding of the lantibiotic. Furthermore, they both consist of an ABC transporter, which is thought to expel the lantibiotic once it has reached the bacterial membrane (**Figure 2**). In general, ABC transporter comprises of a transmembrane domain (TMD) and a nucleotide-binding domain (NBD). The NBD dimerizes upon binding of ATP, which is subsequently hydrolysed and the energy released is used to induce a conformational change within the TMD allowing substrate export or import. Furthermore, in some of these operons there is also the presence of either a lipoprotein or a membrane-associated specific protease.

CprABC-TYPE RESISTANCE OPERONS

Lantibiotic resistance operons belonging to the *Cpr* group contain three different genes encoding for an ABC transporter (one for the NBD and two different TMDs; highlighted in blue, **Figure 2**) and genes encoding a HK and RR, which build up the TCS. These transporters belong to the ABC-type 2 sub-family and on a genetic level closely resemble the immunity systems found in lantibiotic producing strains. This group is named after the most prominent member, the CprABC transporter from *C. difficile*, which confers resistance against nisin and gallidermin (McBride and Sonenshein, 2011; Suárez et al., 2013). Here, the NBD is encoded by *cprA* while *cprB* and *cprC* encode the two TMDs. CprB and CprC are of similar size and are predicted to contain six transmembrane helices each. Both CprB and CprC form a functional transporter together in the membrane as a heterodimer (**Figure 3**).

Other members of this group are *lcrSR-lctFEG* and *nsrFE$_1$E$_2$G-XRK*, both present in the genome of *S. mutans* (**Figure 2**). The encoded TMDs of this group contain six predicted transmembrane helices. They are upregulated via one promoter suggesting that they are expressed in equal stoichiometry. These ABC transporters, are closely related to the immunity ABC transporter LanFEG family, which consists of the NBD LanF and two TMDs LanE and LanG (as an example, the nisin immunity system called NisFEG is highlighted in **Figure 2**). These LanFEG ABC transporters are co-expressed in lantibiotic producer strains and have been shown to expel lantibiotics from the membrane preventing a suicidal effect (Stein et al., 2003, 2005; Alkhatib et al., 2012; AlKhatib et al., 2014b). The LanFEG genes are, in contrast to the Cpr group, encoded in a larger operon which also include genes for biosynthesis and transport machinery of the produced lantibiotic. Due to the operon similarity, one can assume that the *cpr* operons are evolutionary linked to the producing strains. Here however, only the genes for the resistance proteins are present and none of the biosynthetic machinery. Next to the ABC transporter genes, a TCS is present which consists of the HK and RR, which are distantly located on the chromosome (Suárez et al., 2013) (highlighted in green, **Figure 2**). These TCSs transfer the stimuli provided by the externally present lantibiotic into the cell and induce transcription of the genes.

BceAB RESISTANCE OPERON

Lantibiotic resistance operons belonging to the *Bce* group contain genes encoding for an ABC transporter, i.e., two different genes encoding one NBD and one large TMD (highlighted in blue, **Figure 2**). Additionally, a TCS is present consisting of a histidine kinase and response regulator. BceAB-type (ABC) transporters are putatively involved in antimicrobial peptide as well as lantibiotic removal from the lipid membrane (Gebhard and Mascher, 2011). They have been named after the transporter system from *B. subtilis*, which till date is the best characterized representative of ***B***acitracin ***e***fflux (Bce) transporters, conferring resistance against the antimicrobial peptide bacitracin (Ohki et al., 2003; Rietkötter et al., 2008).

Based on the Transport Classification Database (TCDB), BceAB-type transporters belong to the peptide 7 exporter family (Saier et al., 2009). The BceAB-type transporters are composed of two components, a NBD (BceA) and a single TMD (BceB) (**Figure 2**). The TMD consists of ten predicted transmembrane helices (TMHs) and contain a large, extracellular domain (ECD$_L$ where L stands for lantibiotic) between transmembrane helices VII and VIII (**Figure 3**). This extracellular domain appears to be the hallmark of BceAB-type transporters and consists of ~200–250 amino acids (Ohki et al., 2003; Rietkötter et al., 2008; Khosa et al., 2013; **Figure 3**).

Bioinformatically, ECD$_L$ are easy to detect and have been for example identified in the TMDs of the bacitracin resistance-associated ABC transporter BceAB in *Bacillus* species (Rietkötter et al., 2008), in the bacitracin and nisin resistance-associated ABC transporter VraDE in *S. aureus* (Hiron et al., 2011) and the nisin

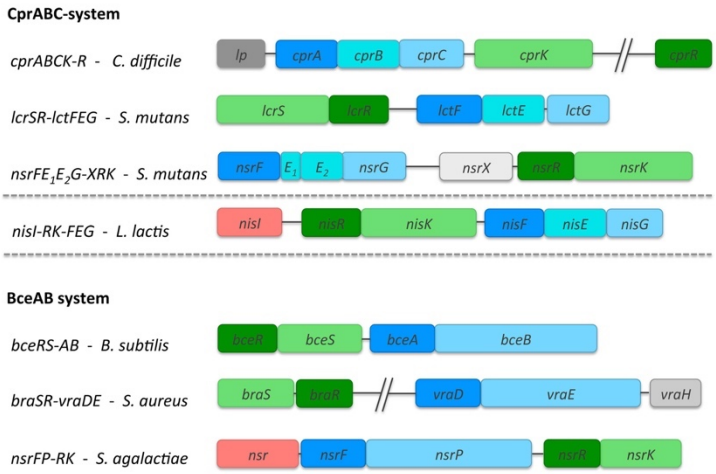

FIGURE 2 | Overview of the lantibiotic resistance operons belonging to the Cpr- and Bce- type systems. Three operon structures, each are highlighted as representatives for the Cpr and Bce group. For Cpr-type these are *cprABCK-R* from *C. difficile*, *nsrFE*$_1$*E*$_2$*G-XRK* and *lcrSR-lctFEG* from *S. mutans*. Additionally, the *nisRK-FEG* system from *L. lactis* involved in nisin immunity is also highlighted. For Bce-type, the three representatives comprise of *bceRS-AB* from *B. subtilis*, *braSR-vraDE* from *S. aureus* and the *nsrFP-RK* system from *S. agalactiae*. The size of the genes corresponds directly with the gene length as deposited in the NCBI database. The TCSs with RR (dark green) and HK (light green); and the ABC transporters are shown in different shades of blue. In the *bceAB* system, the NBD is dark blue while the TMD is shown in light blue. The additional TMD present in the *cprABC* systems is shown in cyan. The proteins, which are part of the operon but the function has not been determined so far are shown in gray. In case of the *nis* and *nsr* operons, an additional membrane-associated protein is present which is colored in red.

resistance-associated NsrFP in *S. agalactiae* (Khosa et al., 2013). These ECD$_L$ are found to be crucial for resistance determinants as they are supposed to recognize the lantibiotic extracellularly and subsequently induce the TCS-dependent signal transduction within the cell (Rietkötter et al., 2008; Hiron et al., 2011). Initial substrate binding usually occurs via these ECD$_L$, however, experimental evidence for this only has been indirectly proven via knockout studies (Falord et al., 2012).

In the Bce group, a BceRS-type TCS has co-evolved (Heijenoort, 1994; Dintner et al., 2011) composed of a response regulator (BceR) and a histidine kinase (BceS). The latter consists of two transmembrane helices with a short extracellular located loop of ~25 amino acids. Such a small loop is unusual for HKs, which normally consists of roughly 115–125 amino acids. This suggested that the TCS lacks an extracellular domain normally present to detect an external stimulus and is therefore, categorized as a member of the intramembrane-sensing histidine kinase family (Mascher et al., 2003; Mascher, 2006). Members of this family have been shown to be responsible for the upregulation of the corresponding ABC-transporter in the presence of its specific lantibiotic (Staron et al., 2011).

In summary, three CprABC-type as well as BceAB-type ABC transporters are mentioned in detail, which are all well studied so far in order to highlight both their functional properties and the differences between these two groups. Within the CprABC group, we have included the NisFEG ABC transporter, which confers immunity against nisin in the producer strains. General characteristics including protein sequence, size, and function of these systems are listed in **Tables 1**, **2**.

CprABC RESISTANCE SYSTEMS

The CprABCK-R System from *C. difficile*

The operon of the *cpr* (cationic antimicrobial peptide resistance) system from *C. difficile* consists of an ABC transporter and a TCS. The genetic organization of the Cpr system resembles the immunity system found in lantibiotic producing strains (see above).

The CprABC transporter from *C. difficile* is encoded by three different proteins: a nucleotide binding domain called CprA (26 kDa) and the two transmembrane domains called CprB and CprC (27 and 29 kDa, respectively; **Figure 3** and **Table 1**). Both of the TMDs have six predicted transmembrane helices and form a functional heterodimer (**Table 1**).

The TCS is composed of a RR *cprR* (CD3320) and a HK *cprK* (CD1352). The histidine kinase of the Cpr system contains an extracellular loop (113 aa) (**Table 1**), which has been proposed to be involved in sensing. Such a loop is a general feature of histidine kinases. The regulator does not directly belong to the *cpr* operon and is distantly located on the chromosome (McBride and Sonenshein, 2011; Suárez et al., 2013).

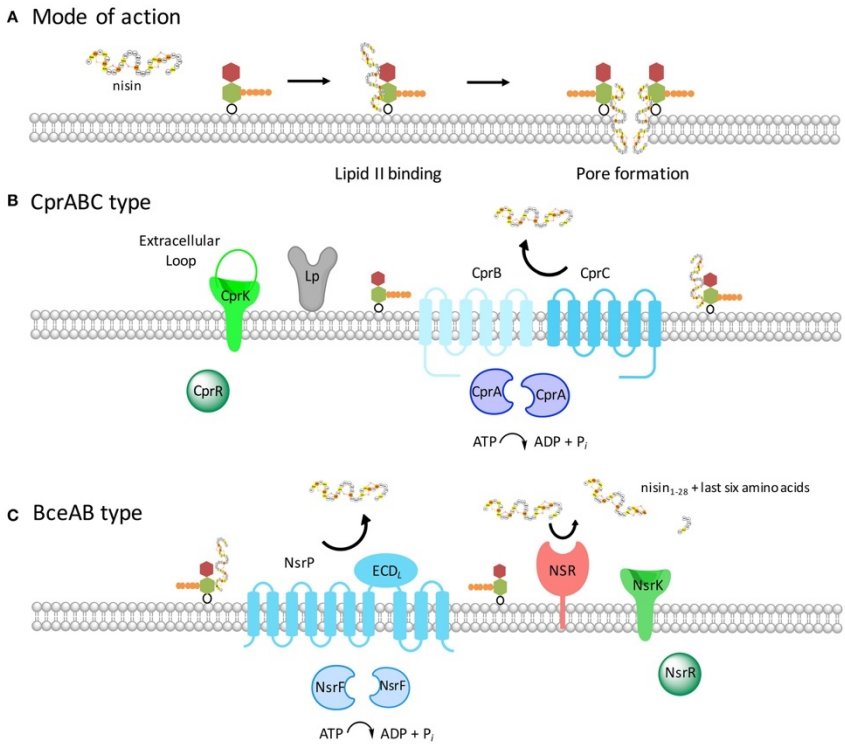

FIGURE 3 | Schematic representation of the two resistance systems of *C. difficile* and *S. agalactiae*. **(A)** The lantibiotic nisin A (see **Figure 1**) binds to the cell wall precursor lipid II, depicted with the N-acetyl glucosamine colored in red, the N-acetyl muramic acid shown in green and the pentapeptide presented in orange. The binding via the first two lanthionine rings of nisin to lipid II results growth inhibition and subsequently in pore formation. This results in rapid cell death already at nanomolar nisin concentrations. **(B)** The proteins encoded by the *cpr* operon are shown with the ABC transporter CprABC (depicted in blue) and the two-component system CprRK (depicted in green). The extracellular loop of the histidine kinase has also been shown. The lipoprotein adjacent to CprABC is depicted in gray. **(C)** The Nsr system of *S. agalactiae* is highlighted. The two-component system NsrRK and an efflux ABC transporter NsrFP are depicted in green and blue, respectively. The ECD_L present in the ABC transporter in between transmembrane helices seven and eight is indicated in cyan. Furthermore, an extra membrane-associated serine protease *Sa*NSR present in this system is shown in red. *Sa*NSR is a serine protease, which cleaves the last six amino acids of nisin off.

Within *C. difficile*, the *cpr* system has been shown to confer resistance against several lantibiotics such as nisin A, gallidermin, and subtilin. Although these lantibiotics are quite different in their amino acid composition, however the first two lanthionine rings are structurally conserved in their tertiary structure (Suárez et al., 2013), suggesting the importance of this region for the *cpr* genes to recognize lantibiotics. It was proposed that the lanthionine ring along with the proline and glycine residues form the sequence motif recognized by CprK resulting in signaling of the TCS CprK-CprR (Suárez et al., 2013).

The genes encoding the ABC transporter *cprABC* are regulated by *cprK-cprR* and are found adjacent to *cprK* in the genome. Insertional disruption of one of the transporter genes resulted in significant decrease in resistance against both nisin A and gallidermin. Hence, this TCS and ABC transporter pair contributes to the resistance of *C. difficile* toward many lantibiotics (Suárez et al., 2013). It has been shown that the addition of nisin induced the expression of CprABC, so it could be proven that the CprR is responsible for the upregulation (McBride and Sonenshein, 2011; Suárez et al., 2013).

Additionally, adjacent of the *cprABC* gene cluster, a lipoprotein is present (CD1348). Although, no involvement in lantibiotic resistance has been described so far, the genetic context resembles the BceAB system found in *S. agalactiae,* which contains the *Sa*NSR protein, a membrane associated resistance protein (see below). Interestingly, the lipoprotein is not upregulated by the presence of a lantibiotic or antimicrobial peptide and displays a basal expression level (Suárez et al., 2013).

TABLE 1 | Comparison of the different Cpr-type resistance systems with the TCS and the ABC transporter.

	CprABCK-R	*LcrSR-LctFEG*	*NsrFE$_1$E$_2$G-XRK*	*NisRK-FEG*
Organism	*C. difficile (Strain630)*	*S. mutans (UA159)*	*S. mutans (UA159)*	*L. lactis (NZ9700)*
Defense category	Resistance	Resistance	Resistance	Immunity
Resistance against	nisin A, subtilin, gallidermin, mutacin 1140, cinnamycin	lacticin 481, nukacin ISK-I	nisin A	nisin A
TMD [aa]	238 (B) 252 (C)	246 (E) 242 (G)	82 (E1) 171 (E2) 248 (G)	242 (E) 214 (G)
Oligomeric state	Dimer (B+C)	Dimer (E+G)	Trimer (G+E1+E2)	Dimer (E+G)
TMHs	6+6	6+6	6+2+4	6+6
NBD [aa]	235	255	234	225
Response regulator [aa]	219	229	219	229
Histidine kinase [aa]	462	437	460	447
Loop-cont. protein	Kinase	Kinase	Kinase	Kinase
Loop size [aa]	113	117	116	112

TABLE 2 | Comparison of the different Bce-type resistance machineries with the TCS and the ABC transporter.

	BceRS-AB	*BraSR-VraDE*	*NsrFP-RK*
Organism	*B. subtilis (Strain 168)*	*S. aureus (USA300)*	*S. agalactiae* (COH1)
Defense category	Resistance	Resistance	Resistance
Resistance against	bacitracin, actagardine, mersacidin	bacitracin, nisin A, daptomycin	nisin A, nisin H, gallidermin
TMD	646	626	651
Oligomeric state	Monomer	Monomer	Monomer
TMHs	10	10	10
NBD [aa]	253	252	250
Response regulator [aa]	231	221	222
Histidine kinase [aa]	334	295	262
ECD_L cont. protein	TMD	TMD	TMD
ECD_L size[aa]	216	195	220

The LcrSR-LctFEG and NsrFE$_1$E$_2$G-XRK Resistance Systems

S. mutans (UA159) has two resistance systems, namely, the LcrSR-LctFEG and NsrFE$_1$E$_2$G-XRK. Both consist of a TCS and an ABC transporter.

The LcrSR-LctFEG system confers resistance against lacticin 481 and nukacin ISK-I as determined with growth inhibition analyses (Kawada-Matsuo et al., 2013a,b).

Within this system, LcrR (26 kDa) is the RR and the LcrS (50 kDa) is the HK, which also contains an extracellular sensing loop (117aa) (**Table 1**). The ABC transporter consists of three different domains. The NBD LctF (29 kDa), which is important for the ATP binding and hydrolysis, and two transmembrane domains, LctE (28 kDa) and LctG (27 kDa), which each consist of six transmembrane helices each (Kawada-Matsuo et al., 2013b).

The NsrFE$_1$E$_2$G-XRK system contains a TCS NsrRK with the NsrR (25 kDa) as RR and the NsrK (53 kDa) as HK containing an extracellular loop of 116 amino acids. The ABC transporter system contains four proteins: the NBD NsrF (26 kDa) and the three TMDs NsrE$_1$E$_2$G. Here, the NsrG (28 kDa) has six transmembrane helices, the NsrE$_1$ (10 kDa) has two and NsrE$_2$ (20 kDa) has four transmembrane helices, so in total 12, which is similar to the other known ABC transporters. However, for NsrFE$_1$E$_2$G resistance against only nisin A was observed, which was examined using deletional mutants within the NsrRK system. For other tested lantibiotics like nukacin ISK-1, no resistance could be observed (Kawada-Matsuo et al., 2013b).

The NisFEG Immunity Transporter from *L. lactis*

In the self-immunity system of nisin producing strains, the cytoplasmic NisF (25 kDa) is composed of 225 amino (Siegers and Entian, 1995). Additionally, NisE (28 kDa) and NisG (24 kDa) are predominantly hydrophobic proteins, that form together an integral membrane part of the ABC transporter and are composed of six transmembrane helices each (Siegers and Entian, 1995). Using sequence similarity searches NisFEG likely exhibits a 2:1:1 stoichiometry to form a functional lantibiotic immunity LanFEG transporter (Siegers and Entian, 1995). Various gene knockout studies have shown that out of all the three genes of the ABC transporter, deletion of *nisE* gene has the most detrimental effect on immunity (Siegers and Entian, 1995).

The primarily function of NisFEG in providing immunity to the producer strain is the efflux of nisin molecules from the membrane before they can form pores (Stein et al., 2003; AlKhatib et al., 2014b). A similar function has been identified for the subtilin immunity ABC transporter SpaFEG, which is able to transport subtilin from the cytoplasmic membrane directly back into the exterior (Stein et al., 2005).

When expressed in the nisin sensitive *L. lactis* strain NZ9000, which does not carry the immunity genes *nisI* and *nisFEG* within its genome, NisFEG confers seven to eight fold of immunity when expressed alone (AlKhatib et al., 2014b).

The substrate specificity of NisFEG has been extensively studied. It has been shown that NisFEG recognizes the C-terminally located lanthionine ring and the last six amino acids of nisin as a reduction of 50% in the immunity provided by NisFEG was seen upon deletion of either of them (AlKhatib et al., 2014b).

THE Bce RESISTANCE SYSTEMS

BceRS-AB System from *B. subtilis*

The BceRS-AB system from *B. subtilis* consists of the ABC transporter, with NBD BceA (28 kDa) and TMD BceB (72 kDa), and the TCS with the response regulator BceR (27 kDa) and the histidine kinase BceS (39 kDa) (**Figure 3** and **Table 2**). Various

growth inhibition assays of strains expressing BceRS-AB and several deletion mutants have shown, that this system mediates resistance against actagardine, mersacidin, and bacitracin (Ohki et al., 2003; Staron et al., 2011).

For signal transduction purposes, both the BceAB ABC transporter as well as the TCS need to be present to confer a signal transduction inducing upregulation of the genes encoded on the operon. This is an unusual mode of signal transduction, as the HK cannot sense bacitracin alone, and needs the presence of the ABC transporter to sense the substrate in the surrounding. Furthermore, an ATP hydrolysis deficient transporter mutant highlighted that hydrolysis is required for this signaling process (Rietkötter et al., 2008). Based on random mutagenesis studies it was shown that the C-terminal part of the TMD BceB, specifically up to helix VIII is important for signaling and resistance of the BceAB-RS system in *B. subtilis* (Kallenberg et al., 2013).

The BceAB from *B. subtilis* has been to the best of our knowledge, the only system which has been purified and shown to form a multicomponent complex with its designated TCS BceRS upon binding of bacitracin (Dintner et al., 2014). These biochemical analyses of the BceAB and BceRS proteins showed that the TCS, more specifically the BceS module, and the transporter form a so-called sensory complex in the cytoplasmic membrane, where the kinase activity is relying on the BceAB transporter (Dintner et al., 2014). This further underlines the fact that the BceAB transporter from *B. subtilis* is directly involved in bacitracin sensing and consequently triggers the upregulation of its own gene by the TCS BceRS. This was further highlighted by mathematical modeling response dynamics of the Bce system, which suggested a direct correlation between the transport activity of BceAB, and the BceS kinase signaling activity (Fritz et al., 2015).

BceAB-like transporters are thought to recognize the target-peptide complex within the membrane and not the peptide as such (Bernard et al., 2007; Rietkötter et al., 2008). This idea is further strengthened by experiments suggesting that BceAB of *B. subtilis* does not export bacitracin, but instead acts as a flippase of the target molecule undecaprenyl pyrophosphate (UPP) to the cytoplasmic side of the membrane (Kingston et al., 2014), thereby removing the target of bacitracin. However, Surface Plasmon Resonance (SPR) spectroscopy studies of BceAB have shown that the TMD BceB binds bacitracin with a high affinity (K_D of 60 nM) in detergent solution and appears to be specific for the active bacitracin-Zn^{2+}-complexed form (Dintner et al., 2014). Although these results do not rule out that a bacitracin-UPP complex is recognized by BceAB, it suggests an effluxing mechanism for bacitracin. Random mutagenesis studies further highlighted, that the C-terminal part of the TMD BceB up to helix VIII is important for the signaling and the resistance of the BceRS-AB system in *B. subtilis* (Kallenberg et al., 2013).

The VraDE-BraRS from *S. aureus*

The VraDE-BraRS system of *S. aureus* is a system composed of the NBD VraD (28 kDa), the TMD VraE (70 kDa), the response regulator BraR (25 kDa), and the histidine kinase BraS (34 kDa). This system has been identified in *S. aureus* since only two of the 16 TCSs present have been linked to the Bce family. Here, the TCS GraRS (Meehl et al., 2007) and the VraDE-BraRS system, mediate cationic antimicrobial peptide resistance (Hiron et al., 2011).

The VraDE-BraRS system of *S. aureus* confers resistance against bacitracin, nisin A and daptomycin as determined via growth inhibition experiments of *S. aureus* (Hiron et al., 2011; Popella et al., 2016). Transcriptional fusions using the operon promoter revealed increased expression when induced with increasing sub-lethal bacitracin and nisin concentrations as previously observed for the BceRS/BceAB module of *B. subtilis* (Ohki et al., 2003; Hiron et al., 2011). The TCS BraRS activates transcription of the *BraDE* and *VraDE* operons, encoding two ABC transporters, which play distinct and original roles in bacitracin and nisin resistance. Here, VraDE is a specific detoxification system and is sufficient to confer resistance against bacitracin and nisin when expressed alone (Hiron et al., 2011) whereas BraDE and BraRS are involved in antibiotic sensing and signaling, respectively.

The ABC transporter VraDE is directly involved in bacitracin resistance. By using chimeric ABC transporter and domain-swapping variants, where the extracellular loop of VraD was exchanged by the one of VraE, it was observed that the extracellular domain of VraE is the determinant for bacitracin specificity (Hiron et al., 2011; Popella et al., 2016). Furthermore, it was shown that VraH, a small transmembrane protein, is further an essential component of the VraDE complex to form the functional VraDEH complex. VraH of *S. aureus* JE2 is a positively charged C-terminus containing a conserved YYKRREEKGK motif. The cytoplasmic VraD interacts with the transmembrane protein VraH. This complex however is formed only in the presence of VraE (Popella et al., 2016). Interestingly, VraH is only important for resistance against gallidermin. Nisin and bacitracin resistance appears to be independent of VraH. This is rather unexpected since gallidermin and nisin share the same structural and mechanistic features, whereas bacitracin is structurally unrelated. Additionally, gallidermin does not form pores in the membranes of most bacteria in contrast to nisin, indicating another mode of action (Popella et al., 2016).

The BraRS TCS has been shown to be specific for nisin and no upregulation occurred when using other antibiotics like vancomycin, fosfomycin, oxacillin, colistin, capreomycin, viomycin, or daptomycin (Hiron et al., 2011).

The NsrFP-RK System from *S. agalactiae*

The NsrFP-RK system from *S. agalactiae* is composed of the NBD NsrF (28 kDa), the TMD NsrP (74 kDa), the RR NsrR (25 kDa), and the HK NsrK (31 kDa) (characteristics of the proteins are listed in **Table 2**; Khosa et al., 2013). Further, the NsrFP-RK system includes an additional serine protease *Sa*NSR, which inactivates nisin by cleaving off the last six amino acids. *Sa*NSR is anchored in the membrane via a single transmembrane segment (Khosa et al., 2016a). This system confers resistance to multiple lantibiotics such as nisin A, nisin H, and gallidermin as determined with growth inhibition experiments in *L. lactis* (Khosa et al., 2013; Reiners et al., 2017). Furthermore, it was shown by SYTOX-green assay, that the resistance conferred

by the ABC transporter NsrFP is imparted by the inhibiting pore formation in the cell membrane and similar to the CprABC system (see above), it also recognizes specifically the N-terminal part of lantibiotics (Reiners et al., 2017), suggesting a common substrate specificity between these systems. For NsrFP, this was shown by a comprehensive mutational analysis of nisin and comparison of the fold of resistance (Reiners et al., 2017), thereby sensitively quantifying and comparing the growth inhibition studies between lantibiotics and their variants (AlKhatib et al., 2014a,b; Reiners et al., 2017). An advantage of the NsrFP system is their heterologous expression in *L. lactis*, which allows a mutational analysis, and holds true for the predominant substrate nisin A. Furthermore, the corresponding NsrR (RR) and NsrK (HK) are not present, which allowed the characterization of the NsrFP ABC transporter alone.

For NsrFP, an efflux transport activity has been reported (Reiners et al., 2017). Here, a peptide release assay revealed the transport direction of NsrFP. The efflux of nisin was shown by the amount of nisin present in the supernatant of the cell culture in comparison to a strain harboring an empty plasmid as well as a transport deficient mutant of NsrFP. Furthermore, NsrFP is the BceAB-type transporter that actually suggests an efflux transport direction using a peptide release assay. These results are similar to those previously obtained for the lantibiotic immunity transporters NisFEG and SpaFEG from *L. lactis* and *B. subtilis*, respectively, which have been shown to export their corresponding lantibiotics (Stein et al., 2003, 2005).

On the contrary, the TCS NsrRK of the Nsr system has been poorly described so far. Here, NsrR belongs to the large OmpR/PhoB subfamily of response regulators. The structure of the regulator NsrR has been solved by X-ray crystallography and a model in active dimeric DNA-bound state was postulated (Khosa et al., 2016b). This model revealed that the amino acids involved in phosphorylation, dimerization, as well as DNA-binding are conserved on sequence level throughout the family of regulators found in the BceAB resistance systems identified, so far. This suggests that other BceAB-type response regulators will probably have a similar tertiary structural arrangement.

An extra feature of the NsrFP-RK system is the presence of a membrane-associated serine protease in the operon called *Sa*NSR, which cleaves nisin at its C-terminus and the product $nisin_{1-28}$ has been shown to be 20–100 fold less effective against Gram-positive bacteria membranes (Sun et al., 2009; Khosa et al., 2016a).

The structure of *Sa*NSR was solved at 2.2 Å resolution and displays an N-terminal helical bundle, a protease cap and core domain. Within the latter, the highly conserved TASSAEM region is present. This region contains the active site and lies in a hydrophobic tunnel. Extensive computational modeling of the *Sa*NSR/nisin complex revealed that *Sa*NSR specifically recognizes the C-terminus of nisin, more specifically the last two lanthionine rings of nisin ensuring the exact coordination of the nisin cleavage site at the TASSAEM region (Khosa et al., 2016a). This clearly indicates that in contrast to the efflux mechanism of the ABC transporter NsrFP, *Sa*NSR is highly specific to confer resistance solely against nisin A.

FUTURE DIRECTIONS

Since (multi-) antibiotic resistant bacteria have rapidly evolved during the last decades, the urgent need for novel compounds is increasing. The secretion of antimicrobial peptides by microorganisms represent a giant pool of novel compounds, which can be used as initial lead structures to develop novel antibiotics.

Here, lantibiotics as small ribosomally-synthesized antimicrobial peptides became relevant and due to genome sequencing the number of identified lantibiotics is rapidly growing. Lantibiotics bind to the essential pyrophosphate-sugar moiety of the cell wall precursor lipid II. This is in contrast to well-known glycopeptide antibiotics vancomycin and teicoplanin, which bind to the D-Ala-D-alanyl group of lipid II (Draper et al., 2015). Due to this, it is believed that new resistance mechanisms against lantibiotics are hard to establish for bacteria.

However, inherent resistance against lantibiotics and antimicrobial peptides are already present and are mediated by ABC transporters, Cpr- and Bce-type transporter, which are present in most human pathogenic bacterial strains. This hampers a wide usage of lantibiotics against severe bacterial infections.

The Cpr ABC transporters resembles the known LanFEG transporter found in lantibiotic producer strains, involved in (auto-)immunity suggesting an evolutionary link. In contrast, the Bce-type ABC transporters appear to be a novel and unique transporter family, interacting directly with the TCS in the presence of the lantibiotic (Khosa et al., 2013; Dintner et al., 2014). Mechanistically, both families are not very well-understood. For the Cpr systems, it has been observed that they are able to expel the lantibiotic from the membrane back into the extracellular media. This would suggest that inhibiting the transporter would allow the lantibiotic to penetrate the membrane again. Therefore, a compound specifically targeting the Cpr transporters would be ideal to use as a lead compound ensuring the potent activity of the lantibiotic itself. To achieve this, more knowledge has to be gained about the exact mechanism of these transporters. Although studies have been performed *in vivo*, the understanding of binding affinities of the lantibiotic toward the transporter as well as some structural studies will clearly be needed in future. Structurally, the Cpr transporter appears to be a different class of ABC transporter since none of known ABC transporter structures seems to be an useful template for molecular modeling approaches using available computer tools, which suggest that structural studies will be needed.

The mechanism of the Bce-type transporters is poorly understood. Recently, for the NsrFP system from *S. agalactiae*, an export function was reported using a peptide release assay (Reiners et al., 2017). Nevertheless, also a flippase activity of the target molecule lipid II of the ABC transporters would fit to the published studies, since the amount of the lantibiotic in the supernatant would also increase, if the target of the lantibiotic is not present anymore. This hypothesis is also in line with the studies of the BceAB transporter of *B. subtilis* by Kingston et al. (2014). This flippase activity would also explain why these Bce-type transporters appear to have a large substrate

spectrum and are able to confer resistance against structurally different lantibiotics as well as some antimicrobial peptides. Here a special focus might be present for the uncharacterized ECD_L, the hallmark of BceAB transporters. The function of this ECD_L is unknown, the structure remains elusive so far and further it is not proven that it interacts with the lantibiotic. Therefore, studies revealing function of this ECD_L would likely give a starting point for studies toward the identification of an inhibitor. Remarkable is the complex formation of the BceAB transporter with the TCS. This unusual partnership within the membrane results in a macromolecular complex, which is induced by the presence of the lantibiotic. A pioneering study of the BceAB system from B. subtilis suggests that a bacitracin-UPP complex is recognized by BceAB, recognized by the C-terminal part of the TMD BceB up to helix VIII (Kallenberg et al., 2013). Also the complex with the TCS has been shown to be at least stabilized via the TMD. Therefore, studies on the exact function of the ECD_L, both biochemically and structurally, will be needed to gain a full understanding of the BceAB system.

Both transporters (BceAB and CprABC) have in common that they are upregulated by a specific TCS induced by the peptide in the medium. Inhibiting the histidine kinase would therefore, be an excellent target for novel drugs, which then in combination with lantibiotics would be a treatment procedure.

Since lantibiotics are active in the low nanomolar range against strains without resistance mechanisms, their potential is clearly demonstrated. If the resistance mechanisms of both transporter families are understood, the first step to inhibit these has been taken, lantibiotics and its variants thereof will be able to fulfill their whole antimicrobial potential.

With novel lantibiotics being identified in new sequenced genomes, the full potential of these antimicrobial peptides has likely not been explored. Probably, for every new lantibiotic discovered a specific resistance system may be present in some human pathogens. Since all lantibiotics target a similar molecule within the target membrane, it is plausible that these resistance mechanisms will be similar to the Cpr and Bce systems, therefore they serve as model systems for lantibiotic resistance.

AUTHOR CONTRIBUTIONS

RC, JZ-K, and SS wrote the manuscript. RC and SK prepared the figures. RC, JZ-K, SK, and SS finalized the manuscript.

FUNDING

We gratefully acknowledge funding of the graduate school 2158 (GRK2158) of the Deutsche Forschungsgesellschaft (DFG).

ACKNOWLEDGMENTS

The authors would like to thank Lutz Schmitt and the Institute of Biochemistry for fruitful discussions and their support. We would like to thank Till Harrar for database searches.

REFERENCES

Alkhatib, Z., Abts, A., Mavaro, A., Schmitt, L., and Smits, S. H. (2012). Lantibiotics: how do producers become self-protected? *J. Biotechnol.* 159, 145–154. doi: 10.1016/j.jbiotec.2012.01.032

AlKhatib, Z., Lagedroste, M., Fey, I., Kleinschrodt, D., Abts, A., and Smits, S. H. (2014a). Lantibiotic immunity: inhibition of nisin mediated pore formation by NisI. *PLoS ONE* 9:e102246. doi: 10.1371/journal.pone.0102246

AlKhatib, Z., Lagedroste, M., Zaschke, J., Wagner, M., Abts, A., Fey, I., et al. (2014b). The C-terminus of nisin is important for the ABC transporter NisFEG to confer immunity in *Lactococcus lactis*. *Microbiologyopen* 3, 752–763. doi: 10.1002/mbo3.205

Alvarez-Sieiro, P., Montalban-Lopez, M., Mu, D., and Kuipers, O. P. (2016). Bacteriocins of lactic acid bacteria: extending the family. *Appl. Microbiol. Biotechnol.* 100, 2939–2951. doi: 10.1007/s00253-016-7343-9

Bernard, R., Guiseppi, A., Chippaux, M., Foglino, M., and Denizot, F. (2007). Resistance to bacitracin in *Bacillus subtilis*: unexpected requirement of the BceAB ABC transporter in the control of expression of its own structural genes. *J. Bacteriol.* 189, 8636–8642. doi: 10.1128/JB.01132-07

Bierbaum, G., and Sahl, H. G. (2009). Lantibiotics: mode of action, biosynthesis and bioengineering. *Curr. Pharm. Biotechnol.* 10, 2–18. doi: 10.2174/138920109787048616

Brumfitt, W., Salton, M. R., and Hamilton-Miller, J. M. (2002). Nisin, alone and combined with peptidoglycan-modulating antibiotics: activity against methicillin-resistant *Staphylococcus aureus* and vancomycin-resistant enterococci. *J. Antimicrob. Chemother.* 50, 731–734. doi: 10.1093/jac/dkf190

Chatterjee, C., Paul, M., Xie, L., and van der Donk, W. A. (2005). Biosynthesis and mode of action of lantibiotics. *Chem. Rev.* 105, 633–684. doi: 10.1021/cr030105v

Cleveland, J., Montville, T. J., Nes, I. F., and Chikindas, M. L. (2001). Bacteriocins: safe, natural antimicrobials for food preservation. *Int. J. Food Microbiol.* 71, 1–20. doi: 10.1016/S0168-1605(01)00560-8

Cotter, P. D., Hill, C., and Ross, R. P. (2005a). Bacterial lantibiotics: strategies to improve therapeutic potential. *Curr. Protein Pept. Sci.* 6, 61–75. doi: 10.2174/1389203053027584

Cotter, P. D., Hill, C., and Ross, R. P. (2005b). Bacteriocins: developing innate immunity for food. *Nat. Rev. Microbiol.* 3, 777–788. doi: 10.1038/nrmicro1273

Cotter, P. D., Ross, R. P., and Hill, C. (2012). Bacteriocins—a viable alternative to antibiotics? *Nat. Rev. Microbiol.* 11, 95–105. doi: 10.1038/nrmicro2937

Delves-Broughton, J., Blackburn, P., Evans, R., and Hugenholtz, J. (1996). Applications of the bacteriocin, nisin. *Antonie Van Leeuwenhoek* 69, 193–202. doi: 10.1007/BF00399424

Dintner, S., Heermann, R., Fang, C., Jung, K., and Gebhard, S. (2014). A sensory complex consisting of an ATP-binding cassette transporter and a two-component regulatory system controls Bacitracin resistance in *Bacillus subtilis*. *J. Biol. Chem.* 289, 27899–27910. doi: 10.1074/jbc.M114.596221

Dintner, S., Staron, A., Berchtold, E., Petri, T., Mascher, T., and Gebhard, S. (2011). Coevolution of ABC transporters and two-component regulatory systems as resistance modules against antimicrobial peptides in Firmicutes Bacteria. *J. Bacteriol.* 193, 3851–3862. doi: 10.1128/JB.05175-11

Draper, L. A., Cotter, P. D., Hill, C., and Ross, R. P. (2015). Lantibiotic resistance. *Microbiol. Mol. Biol. Rev.* 79, 171–191. doi: 10.1128/MMBR.00051-14

Draper, L. A., Ross, R. P., Hill, C., and Cotter, P. D. (2008). Lantibiotic immunity. *Curr. Protein Pept. Sci.* 9, 39–49. doi: 10.2174/138920308783565750

Falord, M., Karimova, G., Hiron, A., and Msadek, T. (2012). GraXSR proteins interact with the VraFG ABC transporter to form a five-component system required for cationic antimicrobial peptide sensing and resistance in *Staphylococcus aureus*. *Antimicrob. Agents Chemother.* 56, 1047–1058. doi: 10.1128/AAC.05054-11

Fritz, G., Dintner, S., Treichel, N. S., Radeck, J., Gerland, U., Mascher, T., et al. (2015). A new way of sensing: need-based activation of antibiotic resistance by a flux-sensing mechanism. *mBio* 6:e00975. doi: 10.1128/mBio.00975-15

Gebhard, S. (2012). ABC transporters of antimicrobial peptides in Firmicutes bacteria–phylogeny, function and regulation. *Mol. Microbiol.* 86, 1295–1317. doi: 10.1111/mmi.12078

Gebhard, S., and Mascher, T. (2011). Antimicrobial peptide sensing and detoxification modules: unravelling the regulatory circuitry of *Staphylococcus aureus*. *Mol. Microbiol.* 81, 581–587. doi: 10.1111/j.1365-2958.2011.07747.x

Héchard, Y., and Sahl, H.-G. (2002). Mode of action of modified and unmodified bacteriocins from Gram-positive bacteria. *Biochimie* 84, 545–557. doi: 10.1016/S0300-9084(02)01417-7

Heijenoort, J. V. (1994). Biosynthesis of the bacterial peptidoglycan unit. *New Compr. Biochem.* 27, 39–54. doi: 10.1016/S0167-7306(08)60406-8

Hiron, A., Falord, M., Valle, J., Débarbouillé, M., and Msadek, T. (2011). Bacitracin and nisin resistance in *Staphylococcus aureus*: a novel pathway involving the BraS/BraR two-component system (SA2417/SA2418) and both the BraD/BraE and VraD/VraE ABC transporters. *Mol. Microbiol.* 81, 602–622. doi: 10.1111/j.1365-2958.2011.07735.x

Jung, G. (1991). Lantibiotics-ribosomally sythesized biologically acve polypeptides containing sulfide bridges and α,β-didehyroamino acids. *Angew. Chem. Int. Edn. English* 30, 1051–1068. doi: 10.1002/anie.199110513

Kallenberg, F., Dintner, S., Schmitz, R., and Gebhard, S. (2013). Identification of regions important for resistance and signalling within the antimicrobial peptide transporter BceAB of *Bacillus subtilis*. *J. Bacteriol.* 195, 3287–3297. doi: 10.1128/JB.00419-13

Kawada-Matsuo, M., Oogai, Y., Zendo, T., Nagao, J., Shibata, Y., Yamashita, Y., et al. (2013a). Involvement of the novel two-component NsrRS and LcrRS systems in distinct resistance pathways against Nisin A and Nukacin ISK-1 in *Streptococcus mutans*. *Appl. Environ. Microbiol.* 79, 4751–4755. doi: 10.1128/AEM.00780-13

Kawada-Matsuo, M., Yoshida, Y., Zendo, T., Nagao, J., Oogai, Y., Nakamura, Y., et al. (2013b). Three distinct two-component systems are involved in resistance to the class I bacteriocins, nukacin ISK-1 and nisin A, in *Staphylococcus aureus*. *PLoS ONE* 8:e69455. doi: 10.1371/journal.pone.0069455

Khosa, S., Alkhatib, Z., and Smits, S. H. (2013). NSR from *Streptococcus agalactiae* confers resistance against nisin and is encoded by a conserved nsr operon. *Biol. Chem.* 394, 1543–1549. doi: 10.1515/hsz-2013-0167

Khosa, S., Frieg, B., Mulnaes, D., Kleinschrodt, D., Hoeppner, A., Gohlke, H., et al. (2016a). Structural basis of lantibiotic recognition by the nisin resistance protein from *Streptococcus agalactiae*. *Sci. Rep.* 6:18679. doi: 10.1038/srep18679

Khosa, S., Hoeppner, A., Gohlke, H., Schmitt, L., and Smits, S. H. (2016b). Structure of the response regulator NsrR from *Streptococcus agalactiae*, which is involved in lantibiotic resistance. *PLoS ONE* 11:e0149903. doi: 10.1371/journal.pone.0149903

Kingston, A. W., Zhao, H., Cook, G. M., and Helmann, J. D. (2014). Accumulation of heptaprenyl diphosphate sensitizes *Bacillus subtilis* to bacitracin: implications for the mechanism of resistance mediated by the BceAB transporter. *Mol. Microbiol.* 93, 37–49. doi: 10.1111/mmi.12637

Kuipers, O. P., Beerthuyzen, M. M., de Ruyter, P. G., Luesink, E. J., and de Vos, W. M. (1995). Autoregulation of nisin biosynthesis in *Lactococcus lactis* by signal transduction. *J. Biol. Chem.* 270, 27299–27304. doi: 10.1074/jbc.270.45.27299

Mascher, T. (2006). Intramembrane-sensing histidine kinases: a new family of cell envelope stress sensors in Firmicutes bacteria. *FEMS Microbiol. Lett.* 264, 133–144. doi: 10.1111/j.1574-6968.2006.00444.x

Mascher, T., Margulis, N. G., Wang, T., Ye, R. W., and Helmann, J. D. (2003). Cell wall stress responses in *Bacillus subtilis*: the regulatory network of the bacitracin stimulon. *Mol. Microbiol.* 50, 1591–1604. doi: 10.1046/j.1365-2958.2003.03786.x

McBride, S. M., and Sonenshein, A. L. (2011). The dlt operon confers resistance to cationic antimicrobial peptides in *Clostridium difficile*. *Microbiology* 157, 1457–1465. doi: 10.1099/mic.0.045997-0

Meehl, M., Herbert, S., Götz, F., and Cheung, A. (2007). Interaction of the GraRS two-component system with the VraFG ABC transporter to support vancomycin-intermediate resistance in *Staphylococcus aureus*. *Antimicrob. Agents Chemother.* 51, 2679–2689. doi: 10.1128/AAC.00209-07

Ohki, R., Giyanto, Tateno, K., Masuyama, W., Moriya, S., Kobayashi, K., et al. (2003). The BceRS two-component regulatory system induces expression of the bacitracin transporter, BceAB, in *Bacillus subtilis*. *Mol. Microbiol.* 49, 1135–1144. doi: 10.1046/j.1365-2958.2003.03653.x

Popella, P., Krauss, S., Ebner, P., Nega, M., Deibert, J., and Gotz, F. (2016). VraH Is the third component of the *Staphylococcus aureus* VraDEH system involved in gallidermin and daptomycin resistance and pathogenicity. *Antimicrob. Agents Chemother.* 60, 2391–2401. doi: 10.1128/AAC.02865-15

Qiao, M., Ye, S., Koponen, O., Ra, R., Usabiaga, M., Immonen, T., et al. (1996). Regulation of the nisin operons in *Lactococcus lactis* N8. *J. Appl. Bacteriol.* 80, 626–634. doi: 10.1111/j.1365-2672.1996.tb03267.x

Reiners, J., Lagedroste, M., Ehlen, K., Leusch, S., Zaschke-Kriesche, J., and Smits, S. H. (2017). The N–terminal region of nisin is important for the BceAB-type ABC transporter NsrFP from *Streptococcus agalactiae* COH1. *Front. Microbiol.* 8:1643. doi: 10.3389/fmicb.2017.01643

Rietkötter, E., Hoyer, D., and Mascher, T. (2008). Bacitracin sensing in *Bacillus subtilis*. *Mol. Microbiol.* 68, 768–785. doi: 10.1111/j.1365-2958.2008.06194.x

Saier, M. H. Jr., Yen, M. R., Noto, K., Tamang, D. G., and Elkan, C. (2009). The transporter classification database: recent advances. *Nucleic Acids Res.* 37, D274–D278. doi: 10.1093/nar/gkn862

Siegers, K., and Entian, K. (1995). Genes involved in immunity to the lantibiotic nisin produced by *Lactococcus lactis* 6F3. *Appl. Environ. Microbiol.* 61, 1082–1089.

Singh, M., and Sareen, D. (2014). Novel LanT associated lantibiotic clusters identified by genome database mining. *PLoS ONE* 9:e91352. doi: 10.1371/journal.pone.0091352

Staron, A., Finkeisen, D. E., and Mascher, T. (2011). Peptide antibiotic sensing and detoxification modules of *Bacillus subtilis*. *Antimicrob. Agents Chemother.* 55, 515–525. doi: 10.1128/AAC.00352-10

Stein, T., Heinzmann, S., Düsterhus, S., Borchert, S., and Entian, K.-D. (2005). Expression and functional analysis of the subtilin immunity genes spaIFEG in the subtilin-sensitive host *Bacillus subtilis* MO1099. *J. Bacteriol.* 187, 822–828. doi: 10.1128/JB.187.3.822-828.2005

Stein, T., Heinzmann, S., Solovieva, I., and Entian, K.-D. (2003). Function of *Lactococcus lactis* nisin immunity genes nisI and nisFEG after coordinated expression in the surrogate host *Bacillus subtilis*. *J. Biol. Chem.* 278, 89–94. doi: 10.1074/jbc.M207237200

Suárez, J. M., Edwards, A. N., and McBride, S. M. (2013). The *Clostridium difficile* cpr locus is regulated by a noncontiguous two-component system in response to type A and B lantibiotics. *J. Bacteriol.* 195, 2621–2631. doi: 10.1128/JB.00166-13

Sun, Z., Zhong, J., Liang, X., Liu, J., Chen, X., and Huan, L. (2009). Novel mechanism for nisin resistance via proteolytic degradation of nisin by the nisin resistance protein NSR. *Antimicrob. Agents Chemother.* 53, 1964–1973. doi: 10.1128/AAC.01382-08

Tagg, J. R., Dajani, A. S., and Wannamaker, L. W. (1976). Bacteriocins of gram-positive bacteria. *Bacteriol. Rev.* 40, 722–756.

Tracanna, V., de Jong, A., Medema, M. H., and Kuipers, O. P. (2017). Mining prokaryotes for antimicrobial compounds: from diversity to function. *FEMS Microbiol. Rev.* 41, 417–429. doi: 10.1093/femsre/fux014

van Heel, A. J., de Jong, A., Montalban-Lopez, M., Kok, J., and Kuipers, O. P. (2013a). BAGEL3: automated identification of genes encoding bacteriocins and (non-)bactericidal posttranslationally modified peptides. *Nucleic Acids Res.* 41, W448–W453. doi: 10.1093/nar/gkt391

van Heel, A. J., Mu, D., Montalban-Lopez, M., Hendriks, D., and Kuipers, O. P. (2013b). Designing and producing modified, new-to-nature peptides with antimicrobial activity by use of a combination of various lantibiotic modification enzymes. *ACS Synth. Biol.* 2, 397–404. doi: 10.1021/sb3001084

Willey, J. M., and van der Donk, W. A. (2007). Lantibiotics: peptides of diverse structure and function. *Annu. Rev. Microbiol.* 61, 477–501. doi: 10.1146/annurev.micro.61.080706.093501

Conflict of Interest Statement: The authors declare that the research was conducted in the absence of any commercial or financial relationships that could be construed as a potential conflict of interest.

The reviewer CC and handling Editor declared their shared affiliation.

3.3. Chapter III - Bypassing the Nisin Resistance Protein

Published in: Bioorganic and Medicinal Chemistry

Impact factor: 2.80

Own Work: 40 %

Expression and Purification of the proteins
Performing biological and biochemical assays
Establishing and Performing of an cleavage efficiency assay
Preparation of the figures
Writing the manuscript

Bypassing lantibiotic resistance by an effective nisin derivative

Julia Zaschke-Kriesche, Lara V. Behrmann, Jens Reiners, Marcel Lagedroste and Sander H.J. Smits

Bioorganic & Medicinal Chemistry 27 (2019) 3454–3462

Contents lists available at ScienceDirect

Bioorganic & Medicinal Chemistry

journal homepage: www.elsevier.com/locate/bmc

Bypassing lantibiotic resistance by an effective nisin derivative

Julia Zaschke-Kriesche[a], Lara V. Behrmann[a], Jens Reiners[a], Marcel Lagedroste[a], Yvonne Gröner[b], Rainer Kalscheuer[b], Sander H.J. Smits[a,c,*]

[a] Institute of Biochemistry, Heinrich-Heine-University Duesseldorf, Universitaetsstrasse 1, 40225 Duesseldorf, Germany
[b] Institute of Pharmaceutical Biology and Biotechnology, Heinrich-Heine-University Düsseldorf, Universitaetsstrasse 1, 40225 Duesseldorf, Germany
[c] Center for Structural Studies, Heinrich-Heine-University Duesseldorf, Universitaetsstrasse 1, 40225 Duesseldorf, Germany

ARTICLE INFO

Keywords:
Lantibiotic
Nisin resistance protein
Activity

ABSTRACT

The need for new antibiotic compounds is rising and antimicrobial peptides are excellent candidates to fulfill this object. The bacteriocin subgroup lantibiotics, for example, are active in the nanomolar range and target the membranes of mainly Gram-positive bacteria. They bind to lipid II, inhibit cell growth and in some cases form pores within the bacterial membrane, inducing rapid cell death. Pharmaceutical usage of lantibiotics is however hampered by the presence of gene clusters in human pathogenic strains which, when expressed, confer resistance. The human pathogen *Streptococcus agalactiae* COH1, expresses several lantibiotic resistance proteins resulting in resistance against for example nisin.

This study presents a highly potent, pore forming nisin variant as an alternative lantibiotic which bypasses the *Sa*NSR protein. It is shown that this nisin derivate $nisin_{C28P}$ keeps its nanomolar antibacterial activity against *L. lactis* NZ9000 cells but is not recognized by the nisin resistance protein *Sa*NSR.

$Nisin_{C28P}$ is cleaved by *Sa*NSR *in vitro* with a highly decreased efficiency, as shown by an cleavage assay. Furthermore, we show that $nisin_{C28P}$ is still able to form pores in the membranes of *L. lactis* and is three times more efficient against *Sa*NSR-expressing *L. lactis* cells than wildtype nisin.

1. Introduction

Many efforts are currently taken to combat multi-drug resistant bacterial pathogens, which cause serious problems in hospital and health care settings. New antibiotics or new derivatives are required to fight against these bacteria. The difficulty in developing new antibiotics is that they have to bypass already known resistance systems in order to be highly active and to be considered for treatment. The family of antimicrobial peptides and here especially the subgroup of lantibiotics are very promising.

Lantibiotics are small antimicrobial peptides of 19–38 amino acids in size, ribosomally synthesized as prepeptides and mainly produced by Gram-positive bacteria.[1,2] They mature in the cytosol of these bacteria, where serine and threonine residues within the core peptide are specifically dehydrated and covalently linked with a neighbored cysteine side chain[3] forming so- called (methyl-)lanthionine rings. After maturation the modified prepeptide is secreted into the extracellular space and activated by cleaving off the leader peptide by a specific protease.[4,5] The family of lantibiotics is steadily increasing mainly due to the possibility to detect the encoding gene clusters by bioinformatical tools such as BAGEL4.[6] Most characterized lantibiotics are highly potent and display activities in the nM range,[7–12] and due to their low toxicity and high potency they are considered as potential novel antibiotics for the usage in the mammalian as well as veterinary medical treatment.[13,14] This is reflected by the fact that several lantibiotics like mutacin 1140, microbisporicin (also known as NAI-107) and actagardine have entered the state of clinical trials for the treatment of a variety of life-threatening diseases caused by human pathogenic bacteria.[15–17]

Importantly, lantibiotics are able to inhibit the growth of various multi-drug resistant pathogenic Gram-positive bacteria.[18,19] The mode of action of lantibiotics varies from binding to the bacterial cell wall precursor lipid II inducing growth inhibition to directing pore formation in the bacterial membrane, which leads to immediate cell death.[20–23]

The best characterized lantibiotic is nisin produced by several *Lactococcus lactis* (*L. lactis*) and *Streptococcus uberis* (*S. uberis*) strains and was discovered in 1928 by L. A. Rogers.[24–26] It has a broad antimicrobial spectrum against a wide range of Gram-positive bacteria including staphylococci, streptococci, bacilli and enterococci and has

* Corresponding author at: Institute of Biochemistry, Heinrich-Heine-University Duesseldorf, Universitaetsstrasse 1, 40225 Duesseldorf, Germany.
E-mail address: sander.smits@hhu.de (S.H.J. Smits).

https://doi.org/10.1016/j.bmc.2019.06.031
Received 12 March 2019; Received in revised form 29 May 2019; Accepted 18 June 2019
Available online 20 June 2019

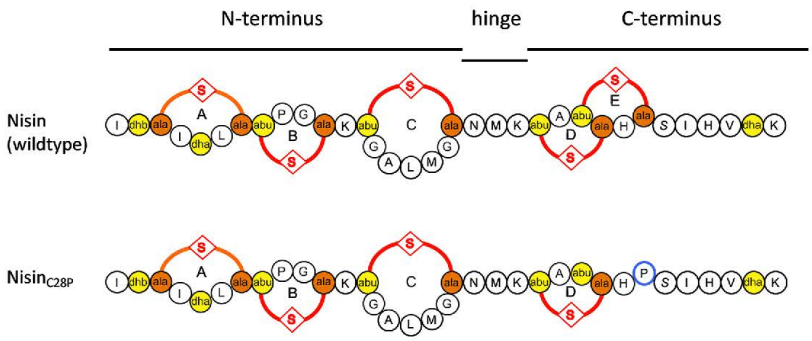

Fig. 1. Schematic view of nisin A wildtype and nisin$_{C28P}$. Introduced mutation at position 28 is highlighted in blue. The (methyl-)lanthionine rings, formed by a cysteine residue sidechain and a dehydrated amino acid residue are highlighted in orange and yellow (rings A, B, C, D and E) (adopted from Reiners et al.[42]).

therefore been used for food preservation for more than 60 years.[27] Nisin is composed of 34 amino acids and contains five (methyl-)lanthionine rings (ring A-E) (Fig. 1). With the *N*-terminal rings A and B it is able to bind to the pyrophosphate moiety of the cell wall precursor lipid II and thereby hampers the cell wall synthesis, which consequently inhibits cell growth.[20,28,29] By binding lipid II, the C-terminal part of nisin is able to flip into the membrane and to form pores composed of eight nisin and four lipid II molecules.[21,29,30] This induces the rapid diffusion of essential ions, causing a collapse of the vital ion gradients across the membrane, thereby leading to cell death.

The modification of the nisin precursor peptide in the cytosol has been very well understood, and numerous variants of nisin have been characterized with respect to their activity and the possibility to act against different species like Gram-negative bacteria.[31–33] Interestingly, although these lantibiotics use two simultaneous modes of action, some targeted bacteria escape the treatment by inducing changes in the cell wall composition, the induction of biofilm formation or by the expression of specific resistance proteins.[34]

In the case of nisin resistance, the latter is mediated by the so-called nisin resistance protein NSR encoded on the *nsr* gene cluster.[35] This gene was originally identified in *Streptococcus lactis* subsp. *diacetylactis* DRC3[36] and encodes a nisin resistance protein (NSR) which is membrane-associated *via* its strongly hydrophobic *N*-terminus.[36] NSR belongs to the S41 family of peptidases, specifically the C-terminal processing peptidases.[35]

An *nsr* gene has also been identified in *S. agalactiae* ATCC 13813, encoding a protein of 320 amino acids and a molecular weight of 36.2 kDa.[37] Heterologous expression of NSR from *S. agalactiae*, termed *Sa*NSR, in *L. lactis* NZ9000 was shown to confer a 20-fold increase in resistance against nisin. Genomic data and comparative sequence analysis using *nsr* from *S. agalactiae* as the query sequence revealed that *nsr* is found within an operon, which contains five different proteins and is very similar to the immunity system present in the producer strains.[38,39] The *nsr* operon consists of NSR and the ABC transporter NsrFP as well as a two-component system consisting of the response regulator NsrR and the histidine kinase NsrK. This operon was identified in different genera, more specifically in various strains of *Corynebacterium*, *Enterococcus*, *Leuconostoc*, *Staphylococcus* and *Streptococcus*.[35]

In vivo and *in vitro* studies have shown that *Sa*NSR proteolytically inactivates nisin by cleaving the peptide bond between MeLan28 and Ser29, i.e. cleaving off the last 6 amino acids of nisin. Sun et al. found that the resulting truncated nisin (nisin$_{1-28}$) displays reduced affinity for the cell membrane, a significantly diminished effectiveness in pore formation and a 100-fold reduction of bactericidal activity against *L. lactis* MG1363 compared to that of intact nisin.[40]

Many studies are known about nisin variants. However, in most cases they display a reduction of the activity and, more importantly, cannot bypass the NSR protein since they comprise modifications at the *N*-terminus of nisin. Recently, a nisin derivative was reported which bypasses the NSR protein by substituting the serine 29 at which cleavage takes place by a proline. However, the activity of this variant also dropped significantly.[41] We chose a different and rational approach for a mutation as we replaced the last cysteine residue by a proline, leading to a variant lacking the last lanthionine ring and thereby introducing a small ring-like structure which sterically is rather rigid (Fig. 1). We termed this variant nisin$_{C28P}$.

Interestingly, nisin$_{C28P}$ is highly active compared to wildtype nisin and is still able to induce pores in the membrane. The nisin resistance protein, however, is not able to cleave this variant efficiently. Altogether, this nisin variant appears to be a good candidate to bypass the known resistance systems while still displaying low nanomolar activity.

2. Material and Methods

2.1. Cloning and purification of the nisin variant nisin$_{C28P}$

Cloning of the nisin variant nisin$_{C28P}$ was performed as described in Reiners et al.[42] The plasmid pNZ-SV-nisA$_{C28P}$ was co-transformed into the *pIL3-BTC*-containing *L. lactis* NZ9000 strain[43] by electroporation as described by Holo and Nes.[44] Briefly, electrocompetent *L. lactis* NZ9000 pIL3-BTC cells were incubated for 30 min on ice with the plasmid pNZ-SV-nisA$_{C28P}$. The cells were exposed to a pulse setting of 1 kV, 25 µF, 200 Ω, for 4.5–5.0 ms and afterwards incubated with 950 µl of M17 medium with 0.5% glucose (GM17) for 3 h at 30 °C. Then cells were plated on SGM17-agar plates (M17 agar, 0.5% glucose, 0.5 M sucrose) with the appropriate antibiotics (5 µg/ml Cm/Erm), and a single colony was used for expression.

The prenisin variant nisin$_{C28P}$ was expressed and purified as described in Alkhatib et al.[45] though the expression time was changed from 24 h to 6 h. After harvesting the cells, lactic acid was added to the supernatant to a final concentration of 50 mM, and it was filtered with 0.45 µm filters. A cation exchange chromatography was performed, and nisin$_{C28P}$ was eluted by adding a buffer containing 1 M NaCl. The prenisin variant was activated by cleavage with purified NisP at 8 °C overnight as described by Abts et al.[46] For this, the endopeptidase NisP was expressed in *L. lactis* NZ9000 cells and purified from the supernatant by an immobilized metal affinity chromatography (IMAC). The pure protein was desalted and stored at −80 °C. The concentration of the active nisin variant was determined by RP-HPLC,[46] using a water/acetonitrile gradient (from 10% to 64% acetonitrile) acidified with 0.1% TFA and Tricine-SDS-PAGE.[47] The activated nisin$_{C28P}$ was directly

used for further assays.

Nisin was purified as previously described[12] with a cation exchange chromatography similar to the nisin$_{C28P}$ purification. The concentration was measured with RP-HPLC as described above and in Abts et al.[46]

The modification status of nisin$_{C28P}$ was analyzed using MALDI-TOF MS analysis, which was performed with an UltrafleXtreme, Bruker Daltonics, Software: Compass 1.4 in positive mode.[31]

2.2. Cloning and purification of the NSR protein

Cloning of the *nsr* gene from *Streptococcus agalactiae* COH1 was done as previously described[35] to obtain the plasmids pNZ-SV-*Sa*NSR and pNZ-SV-*Sa*NSR$_{S236A}$ for studies with recombinant *L. lactis* cells, as well as the plasmid pET-28b-*Sa*NSR30-N8His and pET-28b-*Sa*NSR30$_{S236A}$-N8His accordingly to Khosa et al. (2015) and Khosa et al. (2016) for *in vitro* studies.[37,48]

The plasmids pNZ-SV-*Sa*NSR and pNZ-SV-*Sa*NSR$_{S236A}$ were transformed into electrocompetent *L. lactis* NZ9000 by electroporating[44] the cells, using a pulse setting of 1 kV, 25 µF, 200 Ω, for 4.5–5.0 ms. After pulsing, 950 µl GM17 medium was added, the cells were incubated for 3 h at 30 °C and finally plated on SMGG-agar plates containing 5 µg/ml erythromycin.

The plasmids pET-28b-*Sa*NSR30-N8His and pET-28b-*Sa*NSR30$_{S236A}$-N8His were transformed into chemocompetent *E. coli* BL21 (DE3) cells for expression *via* a heat shock for 60 s at 42 °C. Afterwards 950 µl LB medium was added and the cells were incubated for one hour at 37 °C.

Expression and purification of *Sa*NSR30-N8His and *Sa*NSR30$_{S236A}$-N8His was performed like described in Khosa et al.[48] Briefly, the expression was induced with 1 mM IPTG at an OD$_{600}$ of 0.8–1.0 and grown at 18 °C with 160 rpm shaking overnight. After harvesting the cells and adding buffer containing 10% glycerol (50 mM TRIS, pH 8.0, 50 mM NaCl, 10% glycerol), the cells were disrupted with a homogenizer (Microfluidics) five times at 1.5 kbar. The cell suspension was centrifuged 45 min at 42,000 rpm, and the supernatant was loaded onto a HiTrap Chelating HP 5 ml column with immobilized nickel. The elution was performed with a 1–150 mM histidine gradient, and the concentrated protein fractions were further purified using a Superose 12 10/300 GL column for the size exclusion chromatography (SEC). The purified proteins were directly used for further assays since freezing of the protein resulted in a reduced activity. Further, the SEC buffer (25 mM MES, pH 6, 150 mM NaCl) was used for all *in vitro* assays unless stated otherwise.

2.3. Antimicrobial activity of nisin and nisin$_{C28P}$

The plasmids pNZ-SV-*Sa*NSR and pNZ-SV-*Sa*NSR$_{S236A}$ were transformed into *L. lactis* NZ9000 cells like described above. A plasmid named pNZ-SV-Erm, representing an empty vector, was also transformed into *L. lactis* NZ9000 and used as a control. In the following, these bacterial strains are referred to as NZ9000*Sa*NSR$_{S236A}$, NZ9000*Sa*NSR and NZ9000Erm. Growth inhibition assays with *L. lactis* NZ9000 pNZ-SV-Erm, *L. lactis* NZ9000 pNZ-SV-*Sa*NSR and *L. lactis* NZ9000 pNZ-SV-*Sa*NSR$_{S236A}$ were performed to determine the half maximal inhibitory concentration (IC$_{50}$) as previously described.[42] The nisin variant was diluted into a 96-well plate and the cells were added. After 5 h of incubation at 30 °C, the optical density was determined and the IC$_{50}$ values were calculated. The fold of resistance was obtained based on the IC$_{50}$ values according to Reiners et al.[42] There, the values from the NSR-expressing strains were compared to the values of the control strain (NZ9000Erm).

For the *in vitro* determination, the cleavage efficiency assay with freshly purified *Sa*NSR30-N8His, diluted in 25 mM MES, pH 6, 150 mM NaCl buffer was performed. The reaction was started by adding nisin or nisin$_{C28P}$, respectively.

The cleavage reaction was performed under varying conditions to obtain the best cleavage efficiency by *Sa*NSR30-N8His. The incubation time was varied from 5 to 30 min, the temperature from 20 °C to 40 °C. Further, the pH of the assay buffer was varied from 5.5 to 7.5.

For determination of the kinetics for the substrates nisin and nisin$_{C28P}$, the assay was performed for 10 min at 30 °C with 1 µM NSR30-N8His at pH 6 and 7.5, respectively.

The cleavage reaction was stopped by adding 0.2% trifluoroacetic acid (TFA) and analyzed by RP-HPLC as modified from Abts et al. (2013).[46] The measurement was performed with solvent A consisting of water/0.1% TFA (v/v) and solvent B acetonitrile/0.1% TFA (v/v). After the sample was injected into the LiChrospher RP-18 HPLC column (Merck), the elution was performed by a linear gradient over 60 min from 90% solvent A and 10% solvent B to 36% solvent A and 64% solvent B at a flow rate of 1 ml/min. The elution of the peptide was monitored by absorption at 205 nm. The cleavage efficiency of *Sa*NSR30-N8His was determined by integrating the peak of the cleaved last 6 amino acids.

Minimal inhibitory concentration (MIC) against nosocomial bacteria *S. aureus* ATCC 29213 and *E. faecalis* ATCC 29212 were determined according to the Clinical and Laboratory Standards Institute (CLSI) guidelines[49] in 96-well round bottom microtiter plates using Mueller Hinton broth. Briefly, precultured cells were seeded at a density of 5×10^4 colony forming units per well in a total volume of 100 µl containing twofold serial diluted compounds nisin or nisin$_{C28P}$, respectively. Protein buffer and Moxifloxacin were used as controls. Plates were incubated aerobically at 37 °C overnight. MIC values were determined macroscopically by identifying the concentration of tested compounds that led to complete inhibition of visual growth.

2.4. Pore formation of nisin and nisin$_{C28P}$

To visualize the pore formation mediated by nisin, the SYTOX green dye was used, which binds nucleic acid but is not membrane permeable.[37] The SYTOX Green Nucleic Acids Binding Assay was performed as described in Reiners et al.[37,42] We used *L. lactis* cells, with one of the described plasmids, at an OD$_{600}$ of 0.3 and added 1 µM SYTOX dye. The fluorescence signal was measured at an excitation and emission wavelength of 504 and 523 nm, respectively. During the whole assay the cell suspension was stirred and heated at 30 °C. After reaching a stable baseline the nisin variant was added and the changing fluorescence intensity could be observed.

3. Results

3.1. Expression and purification of nisin$_{C28P}$

We were interested in the ability to characterize a nisin variant which I) still is highly active like wildtype nisin, II) is able to form pores, and III) most importantly is not recognized by the nisin resistance protein. A nisin variant lacking the last ring (ring E) already showed that any adjustment leads to the result that the NSR protein from *S. agalactiae* is not able to cleave off the last six amino acids.[37] However, also the replacement of cysteine by alanine caused a 13-fold reduced activity. Whereas the IC$_{50}$ of wildtype nisin was determined to be 3.3 ± 0.1 nM, the nisin$_{C28A}$ variant displayed 42.2 ± 0.7 nM. Consequently, by introducing a proline residue, we designed a new variant termed nisin$_{C28P}$ which lacks the last lanthionine ring but still has a ring-like structure at this position.

The nisin variant nisin$_{C28P}$ was expressed in *L. lactis* NZ9000 containing a plasmid with the nisin modification and secretion system NisBTC as previously described for many other nisin variants.[31,37,50] We could express and purify nearly 6 mg nisin$_{C28P}$ per liter of cell culture similar to the yields described for wildtype prenisin expressed via the same procedure [31]. After purification *via* cation exchange chromatography, the prenisin leader peptide was cleaved by the purified leader peptidase NisP[31] resulting in active nisin$_{C28P}$ with a theoretical molecular weight of 3348 Da with eight dehydrations. The analysis of the

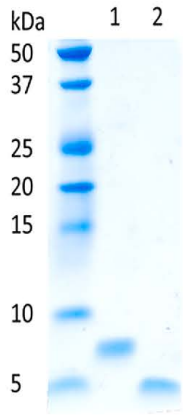

Fig. 2. Prenisin variant nisin$_{C28P}$ (1) and nisin variant nisin$_{C28P}$ (2) analyzed by a 16% Tricine-SDS gel with Precision Plus Protein Dual Xtra Standard (Bio-Rad) (left).

nisin variant with a 16% Tricine-SDS gel (Fig. 2) indicates the cleavage of the leader peptide with a mass difference of approximately 2 kDa. Since the peptidase NisP cleaves off the *N*-terminal leader sequence, no differences were observed in terms of cleavage efficiencies (92%) as determined by RP-HPLC analysis.

In addition, we tested the effect of the mutation on diffusion property *via* agar diffusion assay and could not detect a significant change for nisin$_{C28P}$ compared to wildtype nisin (data not shown).

The nisin$_{C28P}$ prenisin variant eluted between 18 and 21 min (Fig. 3a, blue trace). After cleavage the leader peptide eluted at 14–15 min (Fig. 3a, black trace) and the core peptide eluted between 22 and 24 min.

The nisin$_{C28P}$ core peptide is clearly visible and the concentration can be determined by peak integration using different insulin concentrations as a standard. We used the RP-HPLC measurements to analyze the purity and concentration of the nisin variant, however for further antimicrobial studies we used the total batch of nisin$_{C28P}$.

Furthermore, the nisin$_{C28P}$ core peptide was analyzed with MALDI-TOF MS to identify its modification status (Fig. 3b). Here, we observed that nisin$_{C28P}$ mainly exhibits 7–8 dehydrations as observed for wildtype nisin. Also, some nisin$_{C28P}$ species were present with nine dehydrations, which occurred due to the lack of the last lanthionine ring thereby allowing the dehydration of Ser29, which in the wildtype system is not possible due to sterical hindrance provoked by the lanthionine ring E (as previously described [51]).

3.2. Activity of nisin$_{C28P}$

The activity of nisin$_{C28P}$ was determined by IC$_{50}$ studies against three different recombinant strains derived from *L. lactis* NZ9000, which is intrinsically highly sensitive towards nisin. The NZ9000 strain was transformed with the empty pNZ-Erm vector control or with either the plasmid pNZ-*Sa*NSR or pNZ-*Sa*NSR$_{S236A}$, which, when induced, express the wildtype nisin resistance protein (*Sa*NSR) or an inactive variant (*Sa*NSR$_{S236A}$), respectively.[35] The only difference between the latter strains is therefore the presence or absence of an active *Sa*NSR protein.

The expression of both *Sa*NSR proteins was induced with a sublethal amount of nisin (0.3 nM), which has been shown to not interfere with the IC$_{50}$ determination.[37,42,45,52,53]

To determine the activity of nisin$_{C28P}$ against the NZ9000Erm, NZ9000*Sa*NSR and NZ9000*Sa*NSR$_{S236A}$ strains, cell growth was monitored at different nisin concentrations. From these experiments, growth inhibition of 50% of the cells was calculated, which is reflected in the IC$_{50}$ value.

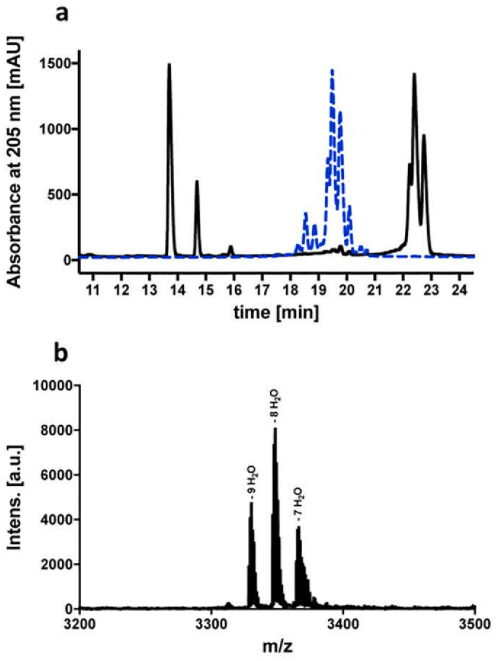

Fig. 3. RP-HPLC chromatogram and MALDI-TOF MS spectrum from nisin$_{C28P}$. RP-HPLC chromatogram of prenisin$_{C28P}$ (blue) and activated nisin variant nisin$_{C28P}$ (black) (a). MALDI-TOF spectrum from activated nisin$_{C28P}$ (b).

Nisin$_{C28P}$ was highly active as displayed by the IC$_{50}$ value against the NZ9000Erm strain of 5.5 ± 0.8 nM (Fig. 4 (black curve) and Table 1). This is comparable with the value obtained by wildtype nisin of 3.3 ± 0.1 nM. Against the *L. lactis* NZ9000*Sa*NSR (Fig. 4, green curve) and NZ9000*Sa*NSR$_{S236A}$ (Fig. 4, red curve) strains, an IC$_{50}$ value

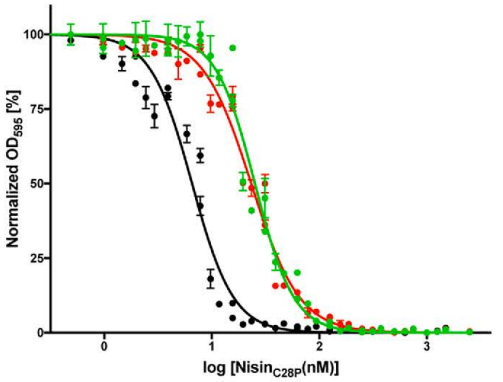

Fig. 4. Determination of the IC$_{50}$ values of nisin$_{C28P}$. The normalized measured OD$_{595}$ in percent against the logarithmic concentration of nisin$_{C28P}$. NZ9000Erm in black, NZ9000*Sa*NSR$_{S236A}$ in red and NZ9000*Sa*NSR in green.

Table 1
IC_{50} values of $nisin_{C28P}$ against NZ9000Erm, NZ9000*Sa*NSR, and NZ9000*Sa*NSR_{S236A} strains. By dividing the IC_{50} values of the NZ9000*Sa*NSR and NZ9000*Sa*NSR_{S236A} strains by the IC_{50} value obtained for the NZ9000Erm strain, the fold of resistance is obtained. *, Data for nisin taken from Khosa et al.[37]

	NZ9000Erm	NZ9000*Sa*NSR	NZ9000*Sa*NSR_{S236A}
IC_{50} $nisin_{C28P}$ [nM] (fold of resistance)	5.5 ± 0.8	22.5 ± 4.2 (3.5)	24.1 ± 2.3 (3.5)
IC_{50} nisin *[nM] (fold of resistance)	3.3 ± 0.1	66.4 ± 2.1 (20.1)	12.6 ± 0.7 (3.8)

Table 2
MIC values of nisin and $nisin_{C28P}$ against *S. aureus* ATCC 29213 and *E. faecalis* ATCC 29212. The MIC data are expressed as the mean (range) obtained from at least three independent repetitions for each strain.

	Nisin [μM]	$Nisin_{C28P}$ [μM]
S. aureus ATCC 29213	1.35 (0.937–1.875)	10.63 (9.375–12.5)
E. faecalis ATCC 29212	1.35 (0.937–1.875)	10.63 (9.375–12.5)

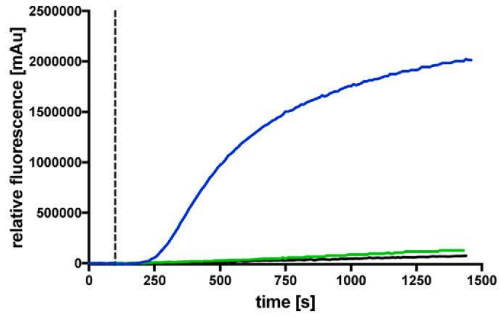

Fig. 5. Detection of pore formation. NZ9000*Sa*NSR strain with SYTOX green nucleic acid dye measured at 30 °C. Buffer (black), 30 nM nisin (green) and 30 nM $nisin_{C28P}$ (blue) added after 100 s (dashed line), respectively.

of 22.5 ± 4.2 nM and 24.1 ± 2.3 nM was determined, respectively.

These IC_{50} values indicate that *Sa*NSR *in vivo* does not properly cleave $nisin_{C28P}$; as a consequence, no resistance against $nisin_{C28P}$ is observed compared to *Sa*NSR_{S236A}. Wildtype nisin displays an IC_{50} value of 66.4 ± 2.1 nM against the NZ9000*Sa*NSR and 12.6 ± 0.7 nM against NZ9000*Sa*NSR_{S236A}.[37]

The fold of resistance values of wildtype nisin against the strains NZ9000*Sa*NSR_{S236A} and NZ9000*Sa*NSR were determined previously.[37] For the *L. lactis* strain NZ9000*Sa*NSR, a fold of resistance of 20 can be observed whereas for the *Sa*NSR_{S236A} mutant, unable to cleave nisin, the value for the fold of resistance is 3.8. Regarding the nisin derivate $nisin_{C28P}$, the fold of resistance value was determined to be 3.5 for both strains, the NZ9000*Sa*NSR and the mutant NZ9000*Sa*NSR_{S236A}, respectively (Table 1).

In addition the minimal inhibitory concentration (MIC) of nisin and $nisin_{C28P}$ were determined, according to the CLSI guidelines, against the nosocomial strains *S. aureus* and *E. faecalis* (Table 2). Wildtype nisin showed the same inhibitory activity (1.35 μM) against *S. aureus* and *E. faecalis* with a range of 0.937–1.875 μM. The assays with $nisin_{C28P}$ resulted in a MIC value of 10.63 μM (range from 9.375 μM to 12.5 μM) for *S. aureus* and *E. faecalis*, respectively, which is 7.8-fold decreased compared to wildtype.

3.3. Pore formation of the $nisin_{C28P}$ variant

Nisin is able to form pores in the membrane of Gram-positive bacteria by binding to lipid II and reorientation of the C-terminal part into the membrane.[21] This leads to membrane leakage, thus pore formation can be monitored using the SYTOX green nucleic acid dye.[54] If pores are formed, the dye is able to bind to the DNA and the fluorescence signal is increased. Since this is a rapid process, pore formation can be monitored in real time using fluorescence. We determined the pore formation capability of the nisin variant $nisin_{C28P}$ against the NZ9000*Sa*NSR strain.

The relative fluorescence is plotted against time and shown for different assay set ups (Fig. 5). First, the fluorescence is monitored until a stable baseline is reached (here 100 s) before $nisin_{C28P}$ was added, which is marked by the dashed line. We monitored the influence of 30 nM $nisin_{C28P}$ on the NZ9000*Sa*NSR strains (blue line). Here, it can be observed that the fluorescence highly increases after adding $nisin_{C28P}$, indicating that $nisin_{C28P}$ is able to form pores. This shows that *Sa*NSR is

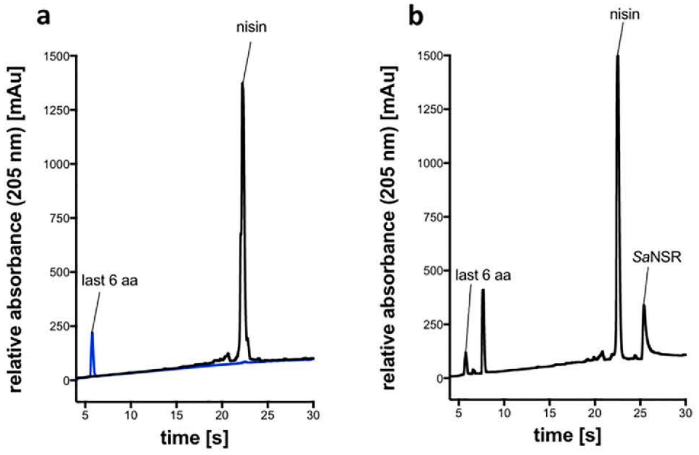

Fig. 6. Detection of nisin cleavage by *Sa*NSR. Analysis of *in vitro* samples *via* RP-HPLC. a) Relative absorbance spectrum of synthetic last 6 amino acids (blue) and pure nisin (black). b) spectrum of performed cleavage efficiency assay with *Sa*NSR and nisin in 1:10 ratio.

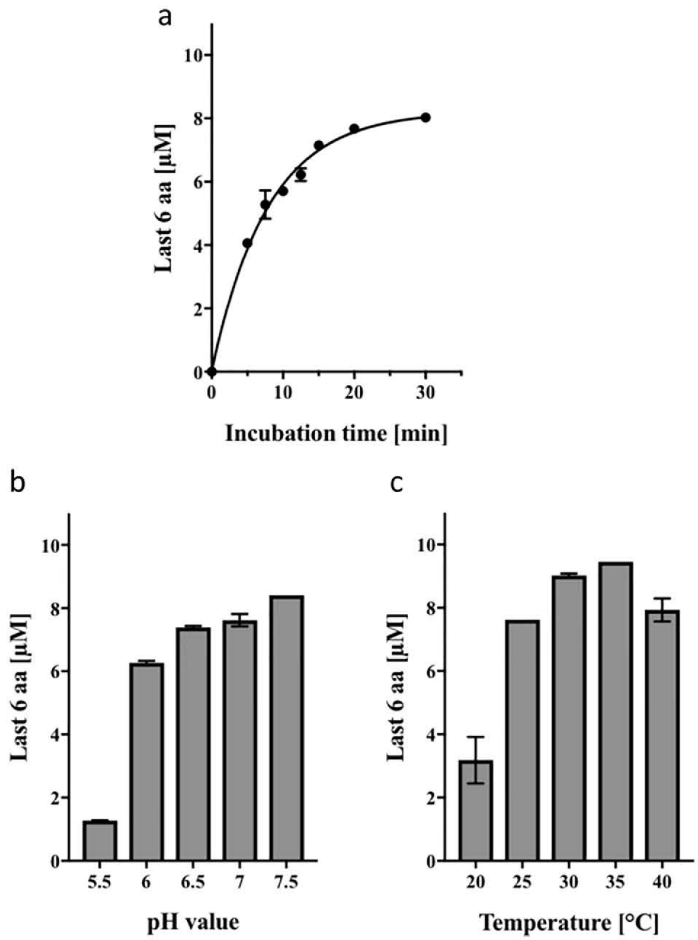

Fig. 7. In vitro characterization of *Sa*NSR. The amount of cleaved off last 6 amino acids of nisin is shown against different conditions. a) Varied incubation times between 5 and 30 min. b) Cleavage efficiency at different pH values from 5.5 to 7.5. c) Effect of different temperatures from 25 to 40 °C on cleavage efficiency (values were determined by at least three independent experiments).

not able to confer resistance and that nisin$_{C28P}$ bypasses the *Sa*NSR protein.

As a control, the assay was performed with buffer to ensure the buffer conditions did not influence the integrity of the *L. lactis* cells (Fig. 5, black line). No increase in fluorescence intensity was observed, indicating that no cells were permeabilized. Additionally, we checked for pore formation by adding 30 nM nisin, which is indicated by the green line. Since *Sa*NSR is able to confer resistance against nisin up to 60–70 nM, no pore formation was observed as previously reported.[55] Importantly, we used the same culture for these experiments so that the expression level of *Sa*NSR was the same, ensuring comparability of the experiments (see Section 2).

3.4. In vitro characterization of SaNSR30

Since we have observed that *Sa*NSR was not able to confer resistance against nisin$_{C28P}$ in recombinant *L. lactis*, we were wondering whether the cleavage of nisin$_{C28P}$ was inhibited and therefore tested *Sa*NSR's *in vitro* activity. To characterize the *Sa*NSR protein of *S. agalactiae,* it was heterologously expressed in *Escherichia coli* and purified *via* an *N*-terminal His-Tag using an immobilized ion metal affinity chromatography (IMAC) column followed by a size exclusion chromatography (SEC).[48] To monitor the cleavage efficiency of the purified protein towards nisin, an *in vitro* assay was performed and analyzed *via* RP-HPLC. Fig. 6 shows a representative chromatogram of the cleavage efficiency experiment.

A synthetic peptide composed of the C-terminal last 6 amino acids of nisin (Fig. 6a, blue spectrum) leads to an elution peak at 6 min, whereas the full-length nisin elutes as a broad peak at 22–23 min (Fig. 6a, black spectrum). The cleavage experiment shows a peak for the *Sa*NSR protein (26 min) as well as for nisin (22–23 min) and the C-terminally cleaved off 6 aa-peptide (6 min) (Fig. 6b). Additionally, two peaks with retention times of 7 and 8 min were detected in the chromatogram (Fig. 6b), those peaks were analyzed via mass spectrometry but could

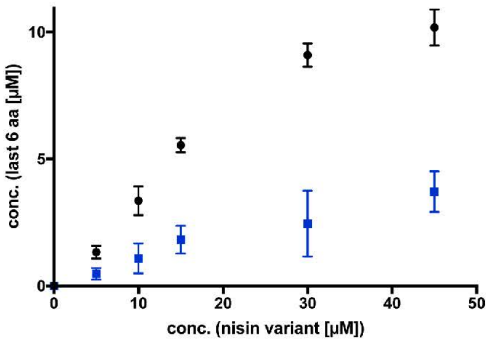

Fig. 8. *Sa*NSR cleavage of nisin and nisin$_{C28P}$. The cleaved off last six amino acids against the used amount of nisin (black) and nisin$_{C28P}$ (blue), respectively.

not be related to our protein or nisin, likely those peaks result from buffer conditions. The amount of the C-terminally cleaved off 6 aa-peptide of nisin was determined by integrating the peak and calculated based on a calibration with insulin.[46]

To establish the cleavage efficiency assay of *Sa*NSR, different conditions were tested. For all assays a protein-to-substrate ratio of 1:10 was used. The cleavage efficiency, indicated by the measured concentration of the cleaved off last 6 amino acids, was plotted against varying incubation times (pH 6, 30 °C) (Fig. 7a). There, the efficiency shows linearity between 10 and 15 min. Thus, for further studies an incubation time of 10 min was chosen to optimize the validity of the measurements. Next, the pH-dependency of nisin-cleavage by *Sa*NSR was investigated (Fig. 7b), using pH values from 5.5 to 7.5 at 30 °C with a 1:10 *Sa*NSR to nisin ratio. The optimal pH value for nisin cleavage seems to be 7.5. Higher pH values were not tested because nisin is unstable at basic pH. Instead of the optimal pH value of 7.5, the following assays were performed at pH 6 due to stability reasons of the substrate. Furthermore, different assay temperatures were tested to find the optimal temperature for the cleavage efficiency (1:10 ration, 30 °C, pH 6) (Fig. 7c). The temperature with the highest *Sa*NSR cleavage efficiency was found to be at 35 °C. The assays performed at 30 °C showed a similar cleavage efficiency. Due to protein stability (*Sa*NSR) the following assays were performed at 30 °C.

Considering these parameters, the cleavage of nisin and nisin$_{C28P}$ at different concentrations was examined. Fig. 8 shows an almost linear increase of cleaved product correlating with the amount of nisin variant. For nisin the highest detected amount of cleaved product is 10 µM (Fig. 8, black dots), for nisin$_{C28P}$ only an amount of 3 µM can be monitored (Fig. 8, blue squares). Further, it can be observed that the slope of the nisin assay is 3 times higher than the one of the nisin$_{C28P}$ assay.

4. Discussion

Antibiotics are essential for the prevention, control and treatment of infectious diseases in humans and animals. However, antibiotic resistance has increased drastically, so that it became crucial to find alternatives.[56] One alternative could be the treatment with lantibiotics, which exhibit antimicrobial activity against different human pathogenic bacteria.[57] Nevertheless, some human pathogens are resistant against lantibiotics, such as *Streptococcus agalactiae*, which expresses two resistance proteins. One is the BceAB-type transporter NsrFP[58] and the other is the nisin resistance protein NSR.[35]

We focused on a rational approach to design a nisin variant which bypasses the latter resistance protein.

The growth inhibition studies with the nisin variant nisin$_{C28P}$ revealed an IC$_{50}$ of 22.5 nM for the NZ9000*Sa*NSR strain, which is almost similar to the IC$_{50}$ value for the mutant NZ9000*Sa*NSR$_{S236A}$ (24.1 nM) (Fig. 4, Table 1).

In comparison to the values for nisin from Khosa et al.[55] (Table 1), the nisin$_{C28P}$ fold of resistance of NZ9000*Sa*NSR as well as of NZ9000*Sa*NSR$_{S236A}$ against the sensitive strain are similar to the nisin fold of resistance of the NZ9000*Sa*NSR$_{S236A}$. Considering that the *Sa*NSR$_{S236A}$ mutant is able to bind nisin but not to cleave off the last six amino acids, it is suggested that *Sa*NSR is also still able to bind the nisin variant *in vivo* but is not able to cleave it. This fits to the molecular dynamic studies which showed the interactions between the catalytic domain in *Sa*NSR and the rings D and E of nisin.[37]

The determination of the minimal inhibitory concentration (MIC) for nisin$_{C28P}$ revealed in a 7.8-fold decreased antimicrobial activity when compared to nisin for both tested strains, *S.aureus* and *E. faecalis* (Table 2).

The nosocomial strain *S. aureus* was found to hold a gene encoding for the BceAB-type transporter VraDE.[59] Besides bacitracin this transporter confers resistance against nisin A.[59,60] One could conclude that the variant nisin$_{C28P}$ is a more efficient identified substrate of VraDE, which would explain the decreased MIC value compared to nisin. Additional to the ABC transporter a small transmembrane protein VraH of *S. aureus* forms a complex with VraD, in the presence of VraE.[60]

The resistance against nisin and bacitracin appears to be independent of VraH, however, gallidermin resistance is based on VraH.[60] As gallidermin and nisin have a structural similar *N*-terminus and only differ at the C-terminal part, it is very likely that nisin$_{C28P}$, with the mutation at the C-terminus, is recognized by the transmembrane protein VraH, whereas wildtype nisin remains unaffected, which would result in a higher MIC value for the nisin variant.

Similar MIC results were obtained for *E. faecalis*, which is bacitracin resistant due to the BcrAB-type transporter BcrAB.[61,62] Till date not

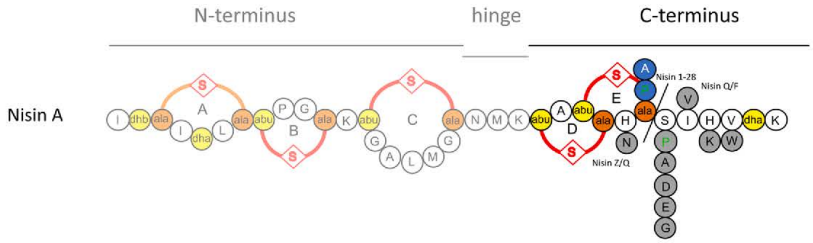

Fig. 9. Schematic view of nisin A with C-terminal variants and mutations. Highlighted view of the C-terminus of nisin A with natural variants and single mutations (grey) as well as ring disrupting mutations (blue). Mutations which result in a diminished *Sa*NSR resistance are highlighted as green letters. The (methyl-)lanthionine rings, formed by a cysteine residue side chain and a dehydrated amino acid residue are highlighted in orange and yellow (rings A, B, C, D and E) (41, 42, 45, 65–69).

much is known about this type of resistance ABC-transporters,[63] nevertheless for bacteriocin resistance associated transporters it is common, that they confer resistance against several bacteriocins.[34,58] Supposable the BcrAB transporter of *E. faecalis* confers resistance against nisin and, in a greater extent, to the nisin variant investigated in this study. Former studies also reported a nisinase activity connected to *E. faecalis*, which is supposed to reduce the C-terminal dehydroalanyl-lysine of nisin.[34,64] This part of nisin could be more accessible for the enzyme in nisin$_{C28P}$ due to the smaller ring-like structure at the C-terminus.

Summarized for both investigated nosocomial strains knock-out mutants for every potential target protein must be examined to elucidate the reason for different antimicrobial effectiveness of nisin$_{C28P}$ compared to nisin. However, the nisin variant is active against *S. aureus* and *E, faecalis*, although 7.8-fold decreased, leading to the assumption that the modification of the last ring in nisin conserves the overall antimicrobial activity but specifically influences the recognition by *Sa*NSR.

Further, we demonstrated that the nisin variant nisin$_{C28P}$ is still able to form pores in the *L. lactis* cells, even at concentrations (30 nM) were nisin does not affect the *Sa*NSR-expressing cells. In addition, we observed that the increase of fluorescence intensity appears with a delay of about 100 s after addition of nisin$_{C28P}$, indicating that pore formation starts slowly. This result is in line with studies showing that the rings D and E of nisin are, together with the hinge region, responsible for the flipping inside the membrane to form the pores.[21]

The nisin cleavage assay showed a decreased efficiency by *Sa*NSR to cleave the variant nisin$_{C28P}$ compared to nisin (Fig. 8). This cleavage is likely possible since this nisin variant is still able to bind to the *Sa*NSR protein. Although ring E is a major determinant for stable *Sa*NSR binding and cleavage the proline in this variant will allow more flexibility within the binding site, thereby adopting slightly different orientations. Since the exact orientation is needed for cleavage this will ultimately result in less cleavage efficiency.

Previous nisin variant studies showed diverse outcomes of mutations at the C-terminus. On the one hand, mutations of ring E, where the last cysteine residue was substituted by an alanine, resulted in a lack of the last ring E. This led to a clear drop of the activity compared to the wildtype nisin A.[42,45] On the other hand, a mutation within the last ring E from Asn27 to Lys resulted in no change of the activity of nisin.[65] Latter is comparable to the natural nisin variants A and Z, which differ in the position 27 with a histidine residue and an asparagine residue, respectively, and have similar activities as well.[66,67]

The natural variant nisin Q also possesses an asparagine residue at position 27, like nisin Z, and additionally the isoleucine at position 30 is substituted by a valine residue, which leads to a drop of the activity against *L. lactis* cells.[67] Surprisingly, nisin F, another natural nisin variant which differs to nisin A only in position 30 with a valine residue similar to nisin Q, has an activity against *L. lactis* similar to nisin A[67] (Fig. 9).

Previous studies showed that mutations in Ser29, the amino acid directly after ring E, result in activities against *L. lactis* strains that are comparable to nisin A wildtype.[41,68] Interestingly, the substitution of this serine by a proline led to an increased activity of the lantibiotic against the nisin resistance protein NSR.[41] Contradictory, further mutations within the last 6 amino acids after ring E, like His31 and Val32, and the complete deletion of these last 6 amino acids of nisin caused diminished antibacterial activity[42,45,65,69] (Fig. 9).

Comparing those previous results, the only known mutations leading to a decreased resistance of the NSR protein against a nisin variant are the Ser29Pro mutations by Field et al.[41] and the results of the nisin$_{C28P}$ variant depicted here (Fig. 9, green letters).

This study presents a highly potent, pore forming nisin variant as an alternative lantibiotic to bypass the nisin resistance protein of *S. agalactiae*. We showed that *Sa*NSR indeed displayed a decreased cleavage efficiency *in vitro* but conferred no resistance against nisin$_{C28P}$ *in vivo*. Compared to the *Sa*NSR mutant and the previous data for nisin, it can be assumed that *Sa*NSR is still able to bind nisin$_{C28P}$ *in vivo*, which however revealed in low IC_{50} values. In summary, we detected a lantibiotic with a three times higher activity against *Sa*NSR-expressing *L. lactis* cells than nisin.

Funding

This work has been funded by the Deutsche Forschungsgemeinschaft (DFG, German Research Foundation) – Project number 270650915 (Research Training Group GRK2158, TP4a to S.S. and TP2a to R.K.).

Acknowledgments

We thank all members of the Institute of Biochemistry for fruitful discussions. J.Z.-K. and S.S. would like to thank Peter Proksch for his enthusiasm as well as continuous interest in our project.

Appendix A. Supplementary data

Supplementary data to this article can be found online at https://doi.org/10.1016/j.bmc.2019.06.031.

References

1. Sahl HG, Bierbaum G. Lantibiotics: biosynthesis and biological activities of uniquely modified peptides from gram-positive bacteria. *Annu Rev Microbiol*. 1998;52:41–79.
2. Klaenhammer TR. Genetics of bacteriocins produced by lactic acid bacteria. *FEMS Microbiol Rev*. 1993;12(1–3):39–85.
3. Chatterjee C, Paul M, Xie L, van der Donk WA. Biosynthesis and mode of action of lantibiotics. *Chem Rev*. 2005;105(2):633–684.
4. Lagedroste M, Smits SHJ, Schmitt L. Substrate specificity of the secreted nisin leader peptidase NisP. *Biochem*. 2017;56(30):4005–4014.
5. Montalban-Lopez M, Deng J, van Heel AJ, Kuipers OP. Specificity and application of the lantibiotic protease NisP. *Front Microbiol*. 2018;9:160.
6. van Heel AJ, de Jong A, Song C, Viel JH, Kok J, Kuipers OP. BAGEL4: a user-friendly web server to thoroughly mine RiPPs and bacteriocins. *Nucleic Acids Res*. 2018;46(W1):W278–W281.
7. Birri DJ, Brede DA, Nes IF. Salivaricin D, a novel intrinsically trypsin-resistant lantibiotic from *Streptococcus salivarius* 5M6c isolated from a healthy infant. *Appl Environ Microbiol*. 2012;78(2):402–410.
8. Draper LA, Cotter PD, Hill C, Ross RP. The two peptide lantibiotic lacticin 3147 acts synergistically with polymyxin to inhibit Gram negative bacteria. *BMC Microbiol*. 2013;13:212.
9. Brotz H, Bierbaum G, Leopold K, Reynolds PE, Sahl HG. The lantibiotic mersacidin inhibits peptidoglycan synthesis by targeting lipid II. *Antimicrob Agents Chemother*. 1998;42(1):154–160.
10. Ghobrial OG, Derendorf H, Hillman JD. Pharmacodynamic activity of the lantibiotic MU1140. *Int J Antimicrob Agents*. 2009;33(1):70–74.
11. Xin B, Zheng J, Liu H, et al. Thusin, a novel two-component lantibiotic with potent antimicrobial activity against several Gram-positive pathogens. *Front Microbiol*. 2016;7:1115.
12. Abts A, Mavaro A, Stindt J, et al. Easy and rapid purification of highly active nisin. *Int J Pept*. 2011;2011:175145.
13. Cotter PD. Bioengineering: a bacteriocin perspective.F54. *Bioengineered*. 2012;3(6):313–319.
14. Knerr PJ, van der Donk WA. Discovery, biosynthesis, and engineering of lantipeptides. *Annu Rev Biochem*. 2012;81:479–505.
15. Dawson MJ, Scott RW. New horizons for host defense peptides and lantibiotics. *Curr Opin Pharmacol*. 2012;12(5):545–550.
16. Sandiford SK. Current developments in lantibiotic discovery for treating *Clostridium difficile* infection. *Expert Opin Drug Discov*. 2019;14(1):71–79.
17. Ongey EL, Yassi H, Pflugmacher S, Neubauer P. Pharmacological and pharmacokinetic properties of lanthipeptides undergoing clinical studies. *Biotechnol Lett*. 2017;39(4):473–482.
18. Dischinger J, Chipalu SB, Bierbaum G. Lantibiotics: promising candidates for future applications in health care. *Int J Med Microbiol*. 2014;304(1):51–62.
19. Mota-Meira M, Lapointe G, Lacroix C, Lavoie MC. MICs of mutacin B-Ny266, nisin A, vancomycin, and oxacillin against bacterial pathogens. *Antimicrob Agents Chemother*. 2000;44(1):24–29.
20. Brötz H, Josten M, Wiedemann I, et al. Role of lipid-bound peptidoglycan precursors in the formation of pores by nisin, epidermin and other lantibiotics. *Mol Microbiol*. 1998;30(2):317–327.
21. Hasper HE, de Kruijff B, Breukink E. Assembly and stability of nisin-lipid II pores. *Biochem*. 2004;43(36):11567–11575.
22. Hasper HE, Kramer NE, Smith JL, et al. An alternative bactericidal mechanism of action for lantibiotic peptides that target lipid II. *Science*. 2006;313(5793):1636–1637.

23. Roy U, Islam MR, Nagao J, et al. Bactericidal activity of nukacin ISK-1: an alternative mode of action. *Biosci Biotechnol Biochem*. 2014;78(7):1270–1273.
24. Rogers LA. The inhibiting effect of *Streptococcus lactis* on *Lactobacillus bulgaricus*. *J Bacteriol*. 1928;16(5):321–325.
25. Rogers LA, Whittier EO. Limiting factors in the lactic fermentation. *J Bacteriol*. 1928;16(4):211–229.
26. Wirawan RE, Klesse NA, Jack RW, Tagg JR. Molecular and genetic characterization of a novel nisin variant produced by *Streptococcus uberis*. *Appl Environ Microbiol*. 2006;72(2):1148–1156.
27. Delves-Broughton J, Blackburn P, Evans RJ, Hugenholtz J. Applications of the bacteriocin, nisin. *Antonie Van Leeuwenhoek*. 1996;69(2):193–202.
28. Breukink E, Wiedemann I, van Kraaij C, Kuipers OP, Sahl HG, de Kruijff B. Use of the cell wall precursor lipid II by a pore-forming peptide antibiotic. *Science*. 1999;286(5448):2361–2364.
29. Medeiros-Silva J, Jekhmane S, Paioni AL, et al. High-resolution NMR studies of antibiotics in cellular membranes. *Nat Commun*. 2018;9(1):3963.
30. Breukink E, van Heusden HE, Vollmerhaus PJ, et al. Lipid II is an intrinsic component of the pore induced by nisin in bacterial membranes. *J Biol Chem*. 2003;278(22):19898–19903.
31. Lagedroste M, Reiners J, Smits SHJ, Schmitt L. Systematic characterization of position one variants within the lantibiotic nisin. *Sci Rep*. 2019;9(1):935.
32. Li Q, Montalban-Lopez M, Kuipers OP. Increasing the antimicrobial activity of nisin-based lantibiotics against Gram-negative pathogens. *Appl Environ Microbiol*. 2018;84(12).
33. Zhou L, van Heel AJ, Montalban-Lopez M, Kuipers OP. Potentiating the activity of nisin against *Escherichia coli*. *Front Cell Dev Biol*. 2016;4:7.
34. Draper LA, Cotter PD, Hill C, Ross RP. Lantibiotic resistance. *Microbiol Mol Biol Rev*. 2015;79(2):171–191.
35. Khosa S, Alkhatib Z, Smits SH. NSR from *Streptococcus agalactiae* confers resistance against nisin and is encoded by a conserved nsr operon. *J Biol Chem*. 2013;394(11):1543–1549.
36. Froseth BR, McKay LL. Molecular characterization of the nisin resistance region of *Lactococcus lactis subsp. lactis* biovar diacetylactis DRC3. *Appl Environ Microbiol*. 1991;57(3):804–811.
37. Khosa S, Frieg B, Mulnaes D, et al. Structural basis of lantibiotic recognition by the nisin resistance protein from *Streptococcus agalactiae*. *Sci Rep*. 2016;6:18679.
38. Kuipers OP, Beerthuyzen MM, Siezen RJ, De Vos WM. Characterization of the nisin gene cluster nisABTCIPR of *Lactococcus lactis*. Requirement of expression of the nisA and nisI genes for development of immunity. *Eur J Biochem*. 1993;216(1):281–291.
39. Siegers K, Entian KD. Genes involved in immunity to the lantibiotic nisin produced by *Lactococcus lactis* 6F3. *Appl Environ Microbiol*. 1995;61(3):1082–1089.
40. Sun Z, Zhong J, Liang X, Liu J, Chen X, Huan L. Novel mechanism for nisin resistance via proteolytic degradation of nisin by the nisin resistance protein NSR. *Antimicrob Agents Chemother*. 2009;53(5):1964–1973.
41. Field D, Blake T, Mathur H, et al. Bioengineering nisin to overcome the nisin resistance protein. *Mol Microbiol*. 2018.
42. Reiners J, Lagedroste M, Ehlen K, Leusch S, Zaschke-Kriesche J, Smits SHJ. The N-terminal region of nisin is important for the BceAB-Type ABC transporter NsrFP from *Streptococcus agalactiae* COH1. *Front Microbiol*. 2017;8:1643.
43. Rink R, Kuipers A, de Boef E, et al. Lantibiotic structures as guidelines for the design of peptides that can be modified by lantibiotic enzymes. *Biochem*. 2005;44(24):8873–8882.
44. Holo H, Nes IF. High-Frequency Transformation, by electroporation, of *Lactococcus lactis subsp. cremoris* grown with glycine in osmotically stabilized media. *Appl Environ Microbiol*. 1989;55(12):3119–3123.
45. AlKhatib Z, Lagedroste M, Zaschke J, et al. The C-terminus of nisin is important for the ABC transporter NisFEG to confer immunity in *Lactococcus lactis*. *MicrobiologyOpen*. 2014;3(5):752–763.
46. Abts A, Montalban-Lopez M, Kuipers OP, Smits SH, Schmitt L. NisC binds the FxLx motif of the nisin leader peptide. *Biochem*. 2013;52(32):5387–5395.
47. Tricine-SDS-PAGE Schägger H. *Nat Protoc*. 2006;1(1):16–22.
48. Khosa S, Hoeppner A, Kleinschrodt D, Smits SH. Overexpression, purification, crystallization and preliminary X-ray diffraction of the nisin resistance protein from *Streptococcus agalactiae*. *Acta Crystallogr F Struct Biol Commun*. 2015;71(Pt 6):671–675.
49. CLSI. *Methods for Dilution Antimicrobial Susceptibility Tests for Bacteria That Grow Aerobically: Approved Standard*. CLSI; 2012:9.
50. Khusainov R, Kuipers OP. The presence of modifiable residues in the core peptide part of precursor nisin is not crucial for precursor nisin interactions with NisB- and NisC. *PLoS ONE*. 2013;8(9):e74890.
51. Lubelski J, Khusainov R, Kuipers OP. Directionality and coordination of dehydration and ring formation during biosynthesis of the lantibiotic nisin. *J Biol Chem*. 2009;284(38):25962–25972.
52. Plat A, Kluskens LD, Kuipers A, Rink R, Moll GN. Requirements of the engineered leader peptide of nisin for inducing modification, export, and cleavage. *Appl Environ Microbiol*. 2011;77(2):604–611.
53. Kuipers A, de Boef E, Rink R, et al. NisT, the transporter of the lantibiotic nisin, can transport fully modified, dehydrated, and unmodified prenisin and fusions of the leader peptide with non-lantibiotic peptides. *J Biol Chem*. 2004;279(21):22176–22182.
54. Roth BL, Poot M, Yue ST, Millard PJ. Bacterial viability and antibiotic susceptibility testing with SYTOX green nucleic acid stain. *Appl Environ Microbiol*. 1997;63(6):2421–2431.
55. Khosa S, Lagedroste M, Smits SH. Protein Defense Systems against the Lantibiotic Nisin: Function of the Immunity Protein NisI and the Resistance Protein NSR. *Front Microbiol*. 2016;7:504.
56. Cheng G, Hao H, Xie S, et al. Antibiotic alternatives: the substitution of antibiotics in animal husbandry? *Front Microbiol*. 2014;5:217.
57. Piper C, Cotter PD, Ross RP, Hill C. Discovery of medically significant lantibiotics. *Curr Drug Discov Technol*. 2009;6(1):1–18.
58. Clemens R, Zaschke-Kriesche J, Khosa S, Smits SHJ. Insight into Two ABC Transporter Families Involved in Lantibiotic Resistance. *Front Mol Biosci*. 2017;4:91.
59. Hiron A, Falord M, Valle J, Debarbouille M, Msadek T. Bacitracin and nisin resistance in *Staphylococcus aureus*: a novel pathway involving the BraS/BraR two-component system (SA2417/SA2418) and both the BraD/BraE and VraD/VraE ABC transporters. *Mol Microbiol*. 2011;81(3):602–622.
60. Popella P, Krauss S, Ebner P, Nega M, Deibert J, Gotz F. VraH Is the Third Component of the *Staphylococcus aureus* VraDEH System Involved in Gallidermin and Daptomycin Resistance and Pathogenicity. *Antimicrob Agents Chemother*. 2016;60(4):2391–2401.
61. Manson JM, Keis S, Smith JM, Cook GM. Acquired bacitracin resistance in *Enterococcus faecalis* is mediated by an ABC transporter and a novel regulatory protein. *BcrR Antimicrob Agents Chemother*. 2004;48(10):3743–3748.
62. Fang C, Stiegeler E, Cook GM, Mascher T, Gebhard S. *Bacillus subtilis* as a platform for molecular characterisation of regulatory mechanisms of *Enterococcus faecalis* resistance against cell wall antibiotics. *PLoS ONE*. 2014;9(3):e93169.
63. Gebhard S. ABC transporters of antimicrobial peptides in Firmicutes bacteria-phylogeny, function and regulation. *Mol Microb*. 2012;86(6):1295–1317.
64. Jarvis B. Enzymic reduction of the C-terminal dehydroalanyl-lysine sequence in nisin. *Biochem J*. 1970;119(5):56P.
65. Rollema HS, Kuipers OP, Both P, de Vos WM, Siezen RJ. Improvement of solubility and stability of the antimicrobial peptide nisin by protein engineering. *Appl Environ Microbiol*. 1995;61(8):2873–2878.
66. de Vos WM, Mulders JW, Siezen RJ, Hugenholtz J, Kuipers OP. Properties of nisin Z and distribution of its gene, nisZ. *Lactococcus lactis Appl Environ Microbiol*. Jan 1993;59(1):213–218.
67. Piper C, Hill C, Cotter PD, Ross RP. Bioengineering of a Nisin A-producing *Lactococcus lactis* to create isogenic strains producing the natural variants Nisin F. *Q and Z Microb Biotechnol*. 2011;4(3):375–382.
68. Field D, Begley M, O'Connor PM, et al. Bioengineered nisin A derivatives with enhanced activity against both Gram positive and Gram negative pathogens. *PLoS ONE*. 2012;7(10):e46884.
69. Breukink E, van Kraaij C, van Dalen A, et al. The orientation of nisin in membranes. *J Biochem*. 1998;37(22):8153–8162.

3.4. Chapter IV – Lantibiotic immunity and resistance proteins

Published in: Bioorganic and Medicinal Chemistry

Impact factor: 2.80

Own Work: 40 %

Expression and Purification of the proteins
Performing biological and biochemical assays
Preparation of the figures
Writing the manuscript

Influence of nisin hinge-region variants on antibiotic immunity and resistance proteins

Julia Zaschke-Kriesche, Jens Reiners, Marcel Lagedroste and Sander H.J. Smits

Bioorganic & Medicinal Chemistry 27 (2019) 3947–3953

Contents lists available at ScienceDirect

Bioorganic & Medicinal Chemistry

journal homepage: www.elsevier.com/locate/bmc

Influence of nisin hinge-region variants on lantibiotic immunity and resistance proteins

Julia Zaschke-Kriesche, Jens Reiners, Marcel Lagedroste, Sander H.J. Smits*

Institute of Biochemistry, Heinrich-Heine-University Duesseldorf, Universitaetsstrasse 1, 40225 Duesseldorf, Germany

ARTICLE INFO

Keywords:
Lantibiotic
Nisin immunity
Nisin resistance protein
Antimicrobial activity

ABSTRACT

The rising existence of antimicrobial resistance, confirms the urgent need for new antimicrobial compounds. Lantibiotics are active in a low nanomolar range and represent good compound candidates. The lantibiotic nisin is well studied, thus it is a perfect origin for exploring novel lantibiotics via mutagenesis studies. However, some human pathogens like *Streptococcus agalactiae COH1* already express resistance proteins against lantibiotics like nisin.

This study presents three nisin variants with mutations in the hinge-region and determine their influence on both the growth inhibition as well as the pore-forming activity. Furthermore, we analyzed the effect of these mutants on the nisin immunity proteins NisI and NisFEG from *Lactococcus lactis,* as well as the nisin resistance proteins *Sa*NSR and *Sa*NsrFP from *Streptococcus agalactiae COH1*.

We identified the nisin variant $_{20}$NMKIV$_{24}$ with an extended hinge-region, to be an excellent candidate for further studies to eventually overcome the lantibiotic resistance in human pathogens, since these proteins do not recognize this variant well.

1. Introduction

Antimicrobial resistance (AMR) is a severe danger to human health across the world. Many compounds, which were blockbuster in pharmaceutical sales, are nearly ineffective due to AMR.

Therefore, it is of fundamental importance to explore the wide biological landscape for new compounds, that exploit new antimicrobial mechanism, or to re-design existing compounds such that resistance mechanisms are bypassed. To achieve the latter, an understanding of the exact mode of action of the compound is the first priority, as well as the resistance mechanism, which was developed by the threated bacteria.

One large class of potentially antimicrobial compounds are antimicrobial peptides (AMPs), secreted by bacteria for quorum sensing and surviving purpose. There, one extensively studied class of AMPs are lantibiotics, which are classified in different classes (class I-IV).[1–3] They are expressed and secreted by numerous bacteria and can be discovered in genome sequences by new genome mining tools like for example BAGEL4.[4] Lantibiotics are expressed as a precursor peptide inside the cell and are post-translationally modified by specific enzymes, which are all localized on a single operon.[5–9] The modifications are installed in the core peptide by the modification enzymes LanB and LanC (lantibiotics class I). LanB dehydrates specifically serine and threonine residues, whereas LanC catalyzes the crosslink of cysteine residues to the dehydrated amino acids, to subsequently form (methyl-)lanthionine rings.[10–16] These rings are characteristic for lantibiotics and cause high heat stability, resistance to proteolytic cleavage and are most importantly crucial for their high antimicrobial potency.[17–22]

Nisin is one of the best studied lantibiotics, produced by *Lactococcus lactis* and is considered as a model system for lantibiotics as well as the modification and secretion of lantibiotics. The whole nisin biosynthesis is well understood and the modification enzymes NisB and NisC have been successfully employed to install (methyl-)lanthionine rings in unrelated targets like angiotensin and several unrelated lantibiotics.[23–25]

Nisin consists of 34 amino acids and five (methyl-)lanthionine rings (Fig. 1), which can be subdivided in three parts. An *N*-terminal part harboring ring A, B and C, where it was shown that ring A and B bind to the cell wall precursor lipid II[26] and results in cell growth inhibition.[27] Next is a flexible hinge-region, consisting of three amino acids (NMK), which allow the third part (C-terminal) to reorient after lipid II binding and penetrate into the target cell membrane.[28–30] Once four lipid II molecules and eight nisin molecules come together, the C-terminal part of the nisin molecules form a stable pore in the membrane. This pore induces leakage and efflux of vital ions, vitamins and other substances of the cell, which subsequently leads to rapid cell death.[29,31] There,

* Corresponding author.
E-mail address: sander.smits@hhu.de (S.H.J. Smits).

https://doi.org/10.1016/j.bmc.2019.07.014
Received 2 May 2019; Received in revised form 6 July 2019; Accepted 9 July 2019
Available online 10 July 2019

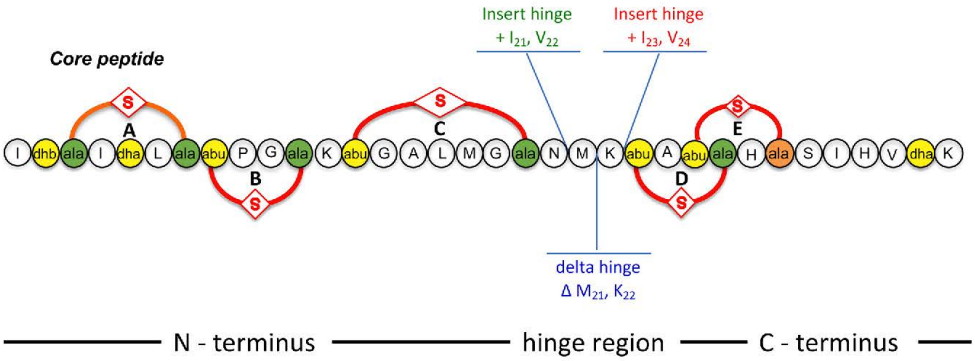

Fig. 1. Schematic representation of nisin. The (methyl-)lanthionine rings, formed by a cysteine residue side chain and a dehydrated amino acid residue are highlighted in yellow and green. The (methyl-)lanthionine rings A, B, C, D and E are depicted in red (adopted from (49)). Introduced mutations are indicated in green (extension inside hinge-region), red (extension after hinge-region) and blue (partially deletion of the hinge-region).

pore formation is a very rapid process and cell lysis occurs already within seconds after addition of nanomolar concentration of nisin to a cell culture.[31,32]

Although impressive progress has been made in to use of lantibiotics as medical treatment compounds there are some drawbacks.[33–35] Lantibiotics are used for decades as food-preservatives (e.g. nisin[36]) and bacterial resistance seldom occurred. Nevertheless, some mechanisms are described, which mainly involve proteins conferring resistance against lantibiotics.[37] First of all, the lantibiotic producing strains express two proteins LanI and LanFEG, which prevent a suicidal effect.[37,38] Secondly, some human pathogenic strains that do not produce lantibiotics express proteins, causing resistance to lantibiotics. This resistance is often conferred by a membrane-anchored peptidase and an ABC transporter belonging to the BceAB-type superfamily.[39,40] Both systems are able to confer resistance even up to high nanomolar concentration.[32,39,41]

Several variants of nisin have been made and characterized.[42–47] Here, we focus on the hinge-region of nisin and made three variants. First a partially deletion in the hinge-region ($\Delta_{21}MK_{22}$) and two extended hinge-regions by introducing extra amino acids either at the C-terminus of the hinge-region, or within the hinge-region, and named them after their sequence ($_{20}NMKIV_{24}$ and $_{20}NIVMK_{24}$). It was shown that the hinge-region of nisin is predicted to be a pharmaceutical hotspot. Some variants of this region were characterized and showed improved activity against used indicator strains.[30,47,48] We characterize these variants with respect to their growth inhibition ability, as well as for their pore forming efficiency.

Furthermore, we extended this study on these variants by analyzing whether the immunity proteins NisI and NisFEG from *L. lactis*, as well as the resistance protein *Sa*NSR and *Sa*NsrFP from *Streptococcus agalactiae COH1* are still able to confer resistance.

2. Material and methods

2.1. Cloning and purification of the nisin hinge-region variants

The insertion of the amino acids IV and the deletion of the amino acids MK were achieved by PCR, using the primer pairs (forward:5′ ATTGTTATGAAAACAGCAACTTGTCATTGTAG3′, reverse 5′GTTACAA CCCATCAGAGCTCC3′) for the hinge-region sequence $_{20}NIVMK_{24}$, the primer pairs (forward: 5′ATTGTTACAGCAACTTGTCATTGTAG3′, reverse 5′TTTCATGTTACAACCCATCAG3′) for the insert $_{20}NMKIV_{24}$ and the primer pairs (forward: 5′ACAGCAACTTGTCATTGTAG3′, reverse 5′ GTTACAACCCATCAGAGC3′) for the partially deleted hinge-region variant, named delta hinge ($\Delta_{21}MK_{22}$). Therefore, oligonucleotides were 5′ phosphorylated. After successful PCR-reaction the template pNZ-SV-nisA was digested with *Dpn*I. The amplified PCR products were gel-extracted, ligated and transformed into *E. coli* DH5α. Sequence analysis verified the new plasmids.

The hinge-region variants were expressed and purified as previously described.[32,50,51] After harvesting the cells, 50 mM lactic acid was added to the supernatant before filtering through 0.45 µm filters. An ion-exchange chromatography was performed and by adding a buffer containing 1 M NaCl the hinge-region variants were eluted. The prenisin variants were activated using purified NisP at 8 °C overnight to cleave off the leader peptide, as described.[52] Therefore, the endopeptidase NisP was expressed in *L. lactis* cells and purified by an immobilized metal-ion affinity chromatography (IMAC). After desalting the pure NisP protein was stored at −80 °C upon further usage. The concentration of the active hinge-region variant was determined by RP-HPLC, using a gradient from 90% water and 10% acetonitrile containing 0.1% TFA to 36% water and 64% acetonitrile.[52] The activated variants were directly used for further analysis.

Wild-type nisin was purified as previously described,[53] using an ion-exchange chromatography step. The concentration was measured with RP-HPLC as described above.

The modification state of the nisin hinge-region variants were analyzed using MALDI-TOF analysis, which were performed as described elsewhere.[54]

2.2. Expression of resistance and immunity proteins

The used *L. lactis* strains were previously described.[32,41,49,55] The strains containing the plasmid for the nisin resistance protein (*Sa*NSR) is termed NZ9000NSR, for the ABC transporter NisFEG the strain is called NZ9000NisFEG. The strain containing the lipoprotein NisI is termed NZ9000NisI and with the Bce-AB-type transporter *Sa*NsrFP is called NZ9000NsrFP. A nisin sensitive control strain NZ9000 without any resistance proteins, called NZ9000Cm, is however transformed with an empty plasmid and threatened the same as the other strains used.

2.3. Pore formation of nisin hinge-region variants

The SYTOX Green dye was used to visualize pore formation mediated by wild-type nisin or the variants. This dye binds nucleic acid without crossing intact membranes of living cells.[56] The SYTOX Green Nucleic Acids Binding Assay was performed as described.[32,41,49] Here, we used *L. lactis* cells, containing the described empty plasmid, at an

OD_{600} of 0.3 and added 1 μM SYTOX dye. The fluorescence signal was detected at an excitation and emission wavelength of 504 and 523 nm, respectively. The cell suspension was stirred and heated at 30 °C during the whole assay. After reaching a stable baseline, the nisin variants were added (final concentration was three times the determined IC_{50} value) and the change of fluorescence intensity was monitored online.

2.4. Activity of hinge-region variants against sensitive and resistant strains

As described in Reiners et al. (2017)[49] growth inhibition assays were performed to determine the half-maximal inhibitory concentration (IC_{50}). In a 96-well plate the nisin variants were diluted and the different *L. lactis* NZ9000 cells were added. The plate was incubated at 30 °C for 5 h and afterwards the OD_{595} was measured to finally determine the IC_{50} values.

3. Results

3.1. Expression and purification of nisin hinge-region variants

Here, we cloned and expressed three different variants of nisin inside the hinge-region. We extended the hinge-region (in wild-type nisin the amino acids are NMK) by the amino acids isoleucine and valine in the beginning ($_{20}$NIVMK$_{24}$) and at the end of the hinge-region ($_{20}$NMKIV$_{24}$). Furthermore, we created a mutant where the hinge-region was partially deleted (Δ_{21}MK$_{22}$). These nisin variants were expressed using the *L. lactis* NZ9000 strain transformed with a plasmid with the nisin modification and secretion system NisBTC,[57] as well as the plasmid with the modified nisin gene. As a control we used the same system expressing the wild-type nisin. We could express and purify nearly 4.4 mg of all three nisin variants per liter of cell culture, which is 70% of the yield described for wild-type prenisin plasmid based expression system (Fig. 2D).[54] After purification, the prenisin leader peptide was cleaved off by the purified peptidase NisP[54] resulting in activation of the nisin variants. Although the peptidase NisP cleaves off the *N*-terminal leader peptide sequence, some differences were observed in terms of cleavage efficiencies as determined by RP-HPLC analysis. The core peptide for all three variants was clearly visible and by peak integration the concentration was determined using different insulin (chain B) or nisin concentrations as a standard.[54] Whereas under these experimental conditions the efficiency of wild-type prenisin was nearly 94%,[54] the cleavage efficiency for the $_{20}$NIVMK$_{24}$, $_{20}$NMKIV$_{24}$ and Δ_{21}MK$_{22}$ variants were determined to be 81.2 ± 4.9 %, 74.3 ± 3.8 % and 48.1 ± 3.5 %, respectively (Fig. 2A–C). This indicates that the flexibility of the hinge-region influences the binding to or the cleavage by NisP.

Table 1
Nisin variants with percentage of cleavage by NisP, detected dehydrations with MS, installed lanthionine rings and protein yield per liter culture. Main species found in MS analysis are marked in bold.

Nisin variant	Cleavage [%]	Dehydrations	Lanthionine rings	Yield [mg/L culture]
wild-type nisin	94.0 ± 1.8	**8**; 7	5	6.04 ± 0.26
$_{20}$NIVMK$_{24}$	81.2 ± 4. 9	9; **8**; 7; 6; 5; 4	5; 4; 3	4.38 ± 0.66
$_{20}$NMKIV$_{24}$	74.3 ± 3.8	9; **8**; 7; 6; 5	5; 4	4.42 ± 0.45
Δ_{21}MK$_{22}$	48.1 ± 3.5	9; **8**; 7; 6; 5; 4; 1; 0	5; 4; 3; 2; 1; 0	4.34 ± 0.56

Furthermore, the core peptides of the $_{20}$NIVMK$_{24}$, $_{20}$NMKIV$_{24}$ and Δ_{21}MK$_{22}$ variants were analyzed with MALDI-TOF MS to determine their modification state. Here, we observed that the variants exhibit a wider spectrum of dehydrations then observed for wild-type nisin (Table 1). Whereas wild-type nisin exhibits seven to eight dehydrations and five installed lanthionine rings, the amount of dehydrations found in the nisin variant $_{20}$NIVMK$_{24}$ ranges from four to nine. Similarly, the number of free thiol-groups from cysteine residues, which are not involved in (methyl-) lanthionine rings vary from three to five. In the nisin variant $_{20}$NMKIV$_{24}$ the number of dehydrations is five to nine with

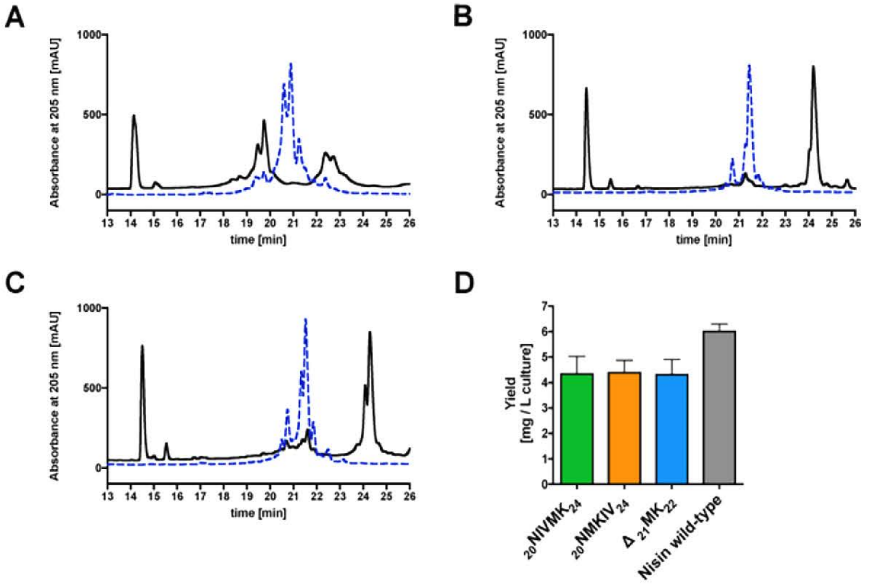

Fig. 2. RP-HPLC chromatogram of the nisin variants. Shown are the elution profiles of the prenisin variants (blue) and the nisin variants after cleavage by NisP (black) A) Δ_{21}MK$_{22}$ B) $_{20}$NIVMK$_{24}$ C) $_{20}$NMKIV$_{24}$. D) Yield of the prenisin variants as determined by HPLC analyses using an insulin chain B standard.

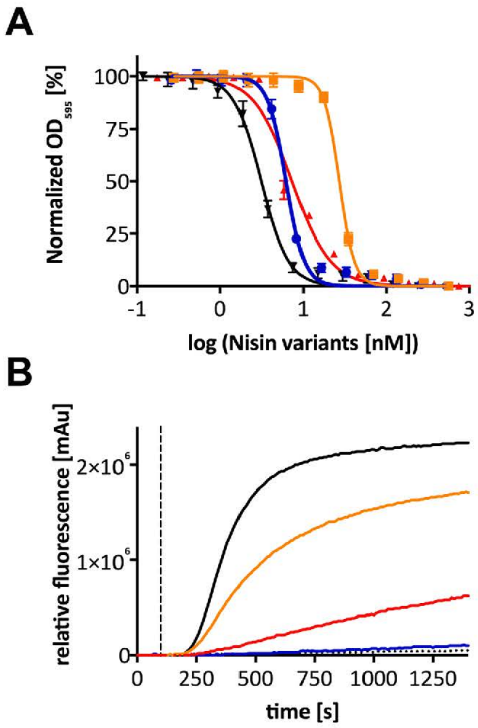

Fig. 3. IC_{50} measurements and SYTOX green assay A) Determination of the IC_{50} values of nisin and the nisin variants. The normalized OD_{595} in percentage was plotted against the logarithmic concentration of nisin variants. The measurements were performed using the sensitive *L. lactis* NZ9000Cm strain. B) NZ9000Cm strain with SYTOX green nucleic acid dye measured at 30 °C. The nisin variants, were added at a final concentration of three times the determined IC_{50} value. The addition of nisin is indicated by the vertical dotted line. Shown are the curves for wild-type nisin (black) $\Delta_{21}MK_{22}$ (blue) $_{20}NIVMK_{24}$ (red) and $_{20}NMKIV_{24}$ (orange) and buffer (black dots).

four to five installed (methyl-) lanthionine rings. The variant $\Delta_{21}MK_{22}$ has zero to eight dehydrations with zero to five installed (methyl-) lanthionine rings. However, the main species contained eight dehydrations, with five installed (methyl-) lanthionine rings. In summary, one can observe that the hinge-region influences the modification machinery, resulting in less dehydrated species. Clearly, the main species in all variants were fully modified (Table 1).

3.2. Activity of nisin hinge-region variants

We tested the activity of the different nisin variants using a growth inhibition assay, resulting in an IC_{50} value against the *L. lactis* NZ9000Cm strain, which is highly sensitive to nisin.[49] As a control we used freshly purified wild-type nisin, which was purified similarly to the nisin variants. Here, wild-type nisin displayed an IC_{50} value of 7.13 ± 0.35 nM, which is in-line with previous studies.[32,41,49,58] The variants displayed a lower antimicrobial activity, which was also observed previously.[47] Here, the variant $\Delta_{21}MK_{22}$ displayed an IC_{50} value of 43.44 ± 13.98 nM (Fig. 3a and Table 2), which leads to a six-fold increase compared to wild-type nisin. The activity of the variant $_{20}NIVMK_{24}$ was the same as wild-type nisin within experimental error and resulted in an IC_{50} value of 8.17 ± 1.23 nM (Fig. 3A and Table 2). This is in contrast to Zhou et al. (2015), where a four-fold decreased antimicrobial activity was determined for this variant.[47] The nisin variant $_{20}NMKIV_{24}$ showed a medium antimicrobial activity with an IC_{50} value of 22.26 ± 5.93 nM, which implies a three-fold reduction (Fig. 3A and Table 2). Summarized, the mutation of the hinge-region influences the antimicrobial activity. Especially, deletions of amino acids in the hinge-region lead to significantly drop in antimicrobial activity.[47]

Further, we tested whether the nisin variants are still able to form pores in the membranes of bacterial cells using the well-established SYTOX Green assay.[32,41,49] Here, we used the *L. lactis* NZ9000Cm strain, where the addition of three times the measured IC_{50} value of wild-type nisin resulted in an almost immediate increase of the fluorescence signal. This indicates a rapid pore formation within the membrane (Fig. 3B black line). As a control, we added buffer to the cells, which resulted in no fluorescence increase over the measured time interval.

For the hinge-region variants, we also used a final concentration of three times the previously determined IC_{50} value. The variant $_{20}NMKIV_{24}$ still displayed the ability to form pores in the membrane of *L. lactis*, nevertheless the pore formation is slower in comparison to wild-type nisin as depicted by a less steep increase of the fluorescence signal (Fig. 3B orange line). For the variant $_{20}NIVMK_{24}$ an even slower pore formation and only 15% of the fluorescence signal increase were observed (Fig. 3B red line).

Interestingly, the variant $\Delta_{21}MK_{22}$ displayed no pore formation under this experimental setup (Fig. 3B blue line), indicating that the flexible hinge-region indeed is crucial for the insertion of nisin into the lipid bilayer as previously shown.[30] The results of the SYTOX green assay in combination with the determined antimicrobial activities (IC_{50} values of the variants) allow the connection of a decreased activity with an altered pore forming ability of the nisin variants.

3.3. Activity against immunity and resistance proteins

LanI and LanFEG are the immunity proteins expressed in some lantibiotic producers, to circumvent a suicidal effect of lantibiotic. For the nisin producer *L. lactis* these proteins are NisI and NisFEG. Whereas NisI seems to recognize the full nisin molecule, the ABC transporter NisFEG recognizes the C-terminus.[41] We tested whether the hinge-region variants effect the immunity system of *L. lactis* by expressing each protein using a plasmid-based system,[32,41] where the strains are termed NZ9000NisI and NZ9000NisFEG. By determining the IC_{50} value and comparison of the IC_{50} with the sensitive strain a fold of resistance (FR) can be calculated. The FR value of wild-type nisin for NZ9000NisI is 6.91 ± 0.65 and 7.43 ± 0.74 for NZ9000NisFEG (Table 2, Figs. 4A and 5).

For the variant $_{20}NIVMK_{24}$ the determined IC_{50} values were 77.35 ± 3.82 nM and 106.73 ± 2.37 nM against NZ9000NisI and NZ9000NisFEG, respectively. This corresponds to FR values of 9.46 ± 0.98 for NZ9000NisI and 13.06 ± 1.72 for NZ9000NisFEG reflecting a better recognition of this variant by the immunity proteins.

For the variant $_{20}NMKIV_{24}$ the IC_{50} values were determined to be 73.16 ± 7.71 nM and 36.89 ± 7.17 against NZ9000NisI and NZ9000NisFEG, respectively. This resulted in FR values of 3.29 ± 0.57 for NZ9000NisI and of 1.66 ± 0.13 for NZ9000NisFEG, which represent a decreased immunity potency against this variant. Thus, this nisin variant, although slightly lower in antimicrobial activity is not recognized by the immunity proteins anymore.

The variant $\Delta_{21}MK_{22}$ displayed IC_{50} values of 108.70 ± 5.77 and 72.11 ± 2.57 against the NZ9000NisI and NZ9000NisFEG, respectively. This results in a reduction of the FR value to 2.50 ± 0.75 for NZ9000NisI and 1.66 ± 0.53 for NZ9000NisFEG. This suggests that the flexible linker needs to be present for the recognition of nisin by the immunity protein (Table 2, Figs. 4B and 5).

Table 2
IC_{50} values of nisin wild-type and hinge-region variants as well as calculated fold of resistance (FR) values for the strains NZ9000Cm, NZ9000NisI, NZ9000NisFEG, NZ9000NSR and NZ9000NsrFP.

Nisin variant	NZ9000Cm	NZ9000NisI		NZ9000NisFEG		NZ9000NSR		NZ9000NsrFP	
	IC50 (nM)	IC50 (nM)	FR	IC50 (nM)	FR	IC50 (nM)	FR	IC50 (nM)	FR
Wild-type nisin	7.13 ± 0.35	49.32 ± 7.02	6.91 ± 0.65	53.03 ± 7.84	7.43 ± 0.74	76.04 ± 5.75	10.66 ± 0.28	82.29 ± 5.11	11.54 ± 0.15
$_{20}$NIVMK$_{24}$	8.17 ± 1.23	77.35 ± 3.82	9.46 ± 0.98	106.73 ± 2.37	13.06 ± 1.72	101.80 ± 1.67	12.45 ± 1.71	121.43 ± 3.06	14.85 ± 1.91
$_{20}$NMKIV$_{24}$	22.26 ± 5.93	73.16 ± 7.71	3.29 ± 0.57	36.89 ± 7.17	1.66 ± 0.13	64.76 ± 3.10	2.91 ± 0.68	44.35 ± 2.15	1.99 ± 0.47
Δ_{21}MK$_{22}$	43.44 ± 13.98	108.70 ± 5.77	2.50 ± 0.75	72.11 ± 2.57	1.66 ± 0.53	221.13 ± 10.95	5.09 ± 1.55	212.80 ± 11.26	4.90 ± 1.47

We also tested the nisin hinge-region variants against strains of *L. lactis*, which are transformed with a plasmid encoding *Sa*NSR and *Sa*NsrFP, respectively. Both proteins originate from an operon in the human pathogen *S. agalactiae* and it has been shown that they confer resistance against nisin when expressed in *L. lactis*.[49,58] The variant Δ_{21}MK$_{22}$ displayed an IC_{50} value of 221.1 ± 10.95 nM and 212.80 ± 11.26 nM against NZ9000NSR and NZ9000NsrFP, respectively. This represents a lower FR value of 5.09 ± 1.55 for NZ9000NSR and 4.90 ± 1.47 for NZ9000NsrFP when compared to wild-type nisin (see Table 2).

The variant $_{20}$NIVMK$_{24}$ is in contrast similarly recognized by the resistance proteins as observed by the IC_{50} values of 101.80 ± 1.67 nM (FR of 12.45 ± 1.71) and 121.43 ± 3.06 (FR of 14.85 ± 1.91) for the NZ9000NSR and NZ9000NsrFP strains, respectively (Table 2, Figs. 4C and 5).

However, the highest decrease of FR mediated by the resistance proteins was observed for the variant $_{20}$NMKIV$_{24}$, which displayed low IC_{50} values. Here, the IC_{50} values were 64.76 ± 3.10 nM (FR of 2.91 ± 0.68) against NZ9000NSR and 44.35 ± 2.15 nM (FR of 1.99 ± 0.47) against NZ9000NsrFP bypasses the resistance mechanism and might be a less suitable substrate for the resistance proteins (Table 2, Figs. 4C and 5).

4. Discussion

In this study, we focused on three nisin hinge-region variants including their property in expression and activation along with investigating their effect on antimicrobial activity. Here, we especially focused on their impact to immunity and resistance proteins compared to wild-type nisin. The two variants $_{20}$NIVMK$_{24}$ and $_{\Delta 21}$MK$_{22}$ were previously partly characterized[47] and we extended these studies by the immunity and resistance proteins.

The nisin variant $_{20}$NIVMK$_{24}$ showed four to nine dehydrations, which leads to the assumption that the dehydratase NisB either has a reduced recognition of this variant or the variant itself somehow hinders the dehydration reaction sterically. The cleavage efficiency of NisP

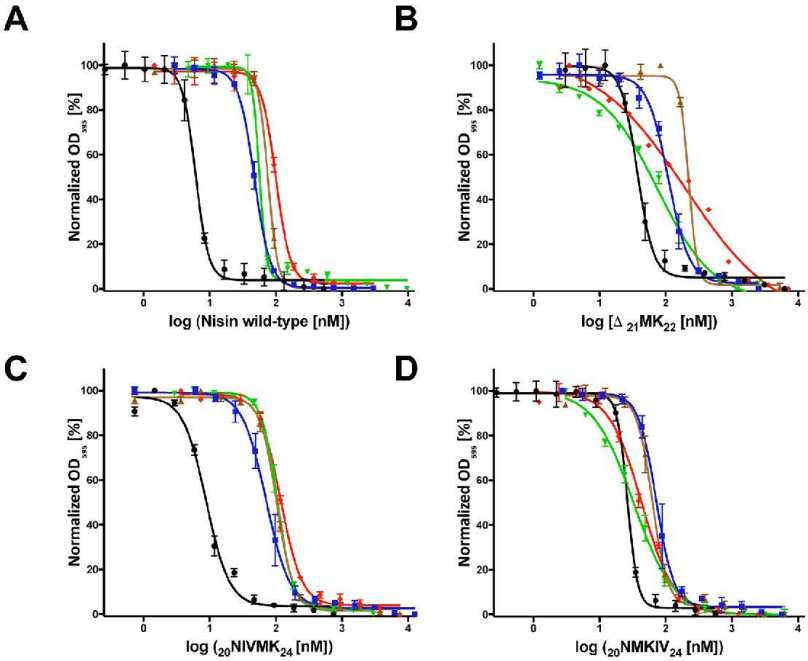

Fig. 4. IC_{50} measurements of the nisin variants against the *L. lactis* NZ9000 strain expressing the immunity and resistance protein respectively. A) nisin wild-type B) nisin Δ_{21}MK$_{22}$ C) nisin $_{20}$NIVMK$_{24}$ and D) nisin $_{20}$NMKIV$_{24}$. L. lactis NZ9000Cm (black), NZ9000NisI (blue), NZ9000NisFEG (green), NZ9000NSR (brown) and NZ9000NsrFP (red).

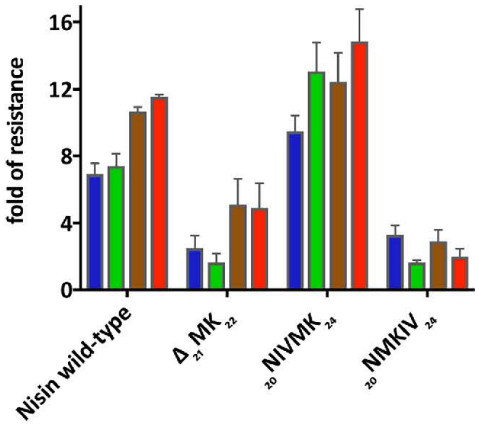

Fig. 5. Calculated fold of resistance values against of NZ9000NisI (blue), NZ9000NisFEG (green), NZ9000NSR (brown) and NZ9000NsrFP (red) against NZ9000Cm for nisin wild-type, nisin $\Delta_{21}MK_{22}$, nisin $_{20}NIVMK_{24}$ and nisin $_{20}NMKIV_{24}$.

for $_{20}NIVMK_{24}$ (81.2 ± 4.9 %) is slightly reduced compared to wild-type nisin, suggesting a reduced binding affinity of NisP. Nevertheless, the extended hinge-region influences the antimicrobial activity against *L. lactis* NZ9000Cm marginal, but strongly inhibits the pore-forming activity. This is in contrast to previous studies, where the same variant showed an highly decreased activity compared to nisin wild-type against *L. lactis*[47].

Higher folds of resistance of $_{20}NIVMK_{24}$ for the immunity proteins NisI (9.46 ± 0.98) and NisFEG (13.06 ± 1.72) compared to wild-type nisin (6.91 ± 0.65 for NisI and 7.43 ± 0.74 for NisFEG) indicate an increased recognition of the nisin variant by the nisin immunity proteins. There, the mutation inside the hinge-region seems not to influence the recognition or affinity of the resistance proteins *Sa*NSR and *Sa*NsrFP. Furthermore, due to the extended flexible hinge-region of the nisin variant $_{20}NIVMK_{24}$ the binding of lipid II seems not influenced but the insertion into the cell membrane and thereby pore formation is malfunctioning.

The nisin variant $_{20}NMKIV_{24}$ has two additional amino acids at the end of the hinge-region, which shows five to nine dehydrations and a cleavage efficiency of NisP of 74%, leading to the assumption that also for this variant the NisB and NisP recognition might be affected.

In view of the antimicrobial activity against NZ9000Cm a drop is observed (22.26 ± 5.93 nM), whereas the fold of resistance for the immunity transporter NisFEG and the resistance transporter *Sa*NsrFP remains very low (Table 2). Besides, the FR values for NisI and *Sa*NSR are reduced, compared to wild-type nisin.

Furthermore, this nisin variant showed an almost similar increase of the fluorescence signal in the SYTOX assay, suggesting it is still able to form pores.

This nisin variant with an extended hinge-region seems not to be recognized by the resistance and immunity proteins, although it exhibits a slightly lower antimicrobial activity. The antimicrobial activity is slightly decreased by this mutation, which can be explained by a broadened dehydration pattern. The pore forming ability seems not to be influenced, compared to the decreased recognition of immunity as well as resistance proteins this implies an improved flexibility of nisin $_{20}NMKIV_{24}$.

Thus, it appears that this variant might be a less suitable substrate for the resistance proteins. This characteristic could be utilized as a new starting point to discover a new lantibiotic derivative, to overcome the nisin resistance in human pathogens such as *S. agalactiae*.

Nisin variant $\Delta_{21}MK_{22}$ with a radical shortened hinge-region shows an extended dehydration pattern and surprisingly a drastically reduced cleavage efficiency (49.6 ± 3.57 %). Additionally, the formation of the lanthionine rings was hindered, resulting in less amount of active nisin variant. Hence, this indicates that the flexibility of the hinge-region not only influences the binding to the dehydratase NisB and the protease NisP but also might hinder the effectiveness of the cyclase NisC. Continuative the antimicrobial activity of nisin $\Delta_{21}MK_{22}$ is six times reduced compared to wild-type nisin, which is in-line with the results of Zhou *et al.* (2015)[47]. This observation is confirmed by the SYTOX assay, which reveals almost no pore formation for the shortened nisin variant.

However, the fold of resistance of the immunity proteins against nisin $\Delta_{21}MK_{22}$ suggests that the flexible linker needs to be present for the recognition of nisin by them. Additionally, the resistance proteins also showed a decreased FR value compared to wild-type nisin, indicating the limited flexibility influences the recognition by *Sa*NSR and *Sa*NsrFP.

The immunity protein NisFEG, as well as the resistance protein *Sa*NSR recognize the C-terminal part of nisin, whereas NisI and *Sa*NsrFP seem to perceive nisin *N*-terminus[27,41,49,58] leading to the assumption, that not a sterically hindrance of the accessibility of one of the termini is responsible for a loss of recognition by the immunity proteins but the restricted flexibility.

Comparing the results for the three nisin hinge-region variants it can be combined that not the extension of the hinge-region in nisin variant $_{20}NIVMK_{24}$ is responsible for the decrease in pore-forming activity but the interruption of the wild-type hinge-region due to the fact that the mutation of nisin variant $_{20}NMKIV_{24}$ does not influence the pore forming process, whereas the nisin variant $_{20}NIVMK_{24}$ showed drastically reduced pore formation.

Moreover, it can be assumed that the wild-type hinge-region of nisin is essential for the recognition by the immunity protein NisI, but especially by NisFEG, as we see a drop in immunity when reducing the length of the hinge-region as well as extending it.

Although, preceding mutagenesis studies showed an enhanced activity of nisin hinge-region variants against *S. agalactiae*[46], this study exhibits a promising nisin variant ($_{20}NMKIV_{24}$), bypassing this lantibiotic resistance of the human pathogen, while showing just a slight decrease of antimicrobial and pore forming activity. These results can be used as a basis for further investigations on the recognition mechanism of the nisin modification enzymes and immunity proteins as well as for profound studies of the nisin resistance proteins of *S. agalactiae*.

Funding

This work has been funded by the Deutsche Forschungsgemeinschaft (DFG, German Research Foundation) – Project number 270,650,915/GRK2158 TP4a to S.S.

Acknowledgment

We thank all members of the Institute of Biochemistry for fruitful discussions.

Appendix A. Supplementary data

Supplementary data to this article can be found online at https://doi.org/10.1016/j.bmc.2019.07.014.

References

1. Kellner R, Jung G, Horner T, et al. Gallidermin: a new lanthionine-containing polypeptide antibiotic. *Eur J Biochem*. 1988;177(1):53–59.
2. Willey JM, van der Donk WA. Lantibiotics: peptides of diverse structure and function.

Annu Rev Microbiol. 2007;61:477–501.
3. Arnison PG, Bibb MJ, Bierbaum G, et al. Ribosomally synthesized and post-translationally modified peptide natural products: overview and recommendations for a universal nomenclature. *Nat Prod Rep.* 2013;30(1):108–160.
4. van Heel AJ, de Jong A, Song C, Viel JH, Kok J, Kuipers OP. BAGEL4: a user-friendly web server to thoroughly mine RiPPs and bacteriocins. *Nucleic Acids Res.* 2018;46(W1):W278–W281.
5. Schnell N, Entian KD, Schneider U, et al. Prepeptide sequence of epidermin, a ribosomally synthesized antibiotic with four sulphide-rings. *Nature.* 1988;333(6170):276–278.
6. Banerjee S, Hansen JN. Structure and expression of a gene encoding the precursor of subtilin, a small protein antibiotic. *J Biol Chem.* 1988;263(19):9508–9514.
7. Buchman GW, Banerjee S, Hansen JN. Structure, expression, and evolution of a gene encoding the precursor of nisin, a small protein antibiotic. *J Biol Chem.* 1988;263(31):16260–16266.
8. Kaletta C, Entian KD. Nisin, a peptide antibiotic: cloning and sequencing of the nisA gene and posttranslational processing of its peptide product. *J Bacteriol.* 1989;171(3):1597–1601.
9. Dodd HM, Horn N, Gasson MJ. Analysis of the genetic determinant for production of the peptide antibiotic nisin. *J Gen Microbiol.* 1990;136(3):555–566.
10. Karakas Sen A, Narbad A, Horn N, et al. Post-translational modification of nisin. The involvement of NisB in the dehydration process. *Eur J Biochem.* 1999;261(2):524–532.
11. Koponen O, Tolonen M, Qiao M, Wahlström G, Helin J, Saris PE. NisB is required for the dehydration and NisC for the lanthionine formation in the post-translational modification of nisin. *Microbiology.* 2002;148(Pt 11):3561–3568.
12. Kluskens LD, Kuipers A, Rink R, et al. Post-translational modification of therapeutic peptides by NisB, the dehydratase of the lantibiotic nisin. *Biochemistry.* 2005;44(38):12827–12834.
13. Weil HP, Beck-Sickinger AG, Metzger J, et al. Biosynthesis of the lantibiotic Pep5. Isolation and characterization of a prepeptide containing dehydroamino acids. *Eur J Biochem.* 1990;194(1):217–223.
14. Gutowski-Eckel Z, Klein C, Siegers K, Bohm K, Hammelmann M, Entian KD. Growth phase-dependent regulation and membrane localization of SpaB, a protein involved in biosynthesis of the lantibiotic subtilin. *Appl Environ Microbiol.* 1994;60(1):1–11.
15. Okeley NM, Paul M, Stasser JP, Blackburn N, van der Donk WA. SpaC and NisC, the cyclases involved in subtilin and nisin biosynthesis, are zinc proteins. *Biochemistry.* 2003;42(46):13613–13624.
16. Rink R, Kluskens LD, Kuipers A, Driessen AJ, Kuipers OP, Moll GN. NisC, the cyclase of the lantibiotic nisin, can catalyze cyclization of designed nonlantibiotic peptides. *Biochemistry.* 2007;46(45):13179–13189.
17. Rollema HS, Kuipers OP, Both P, de Vos WM, Siezen RJ. Improvement of solubility and stability of the antimicrobial peptide nisin by protein engineering. *Appl Environ Microbiol.* 1995;61(8):2873–2878.
18. Lu Y, Jiang L, Chen M, Huan L, Zhong J. Improving heat and pH stability of nisin by site-directed mutagenesis. *Wei Sheng Wu Xue Bao.* 2010;50(11):1481–1487.
19. Rink R, Arkema-Meter A, Baudoin I, et al. To protect peptide pharmaceuticals against peptidases. *J Pharmacol Toxicol Methods.* 2010;61(2):210–218.
20. Gross E, Morell JL. The presence of dehydroalanine in the antibiotic nisin and its relationship to activity. *J Am Chem Soc.* 1967;89(11):2791–2792.
21. Chan WC, Leyland M, Clark J, et al. Structure-activity relationships in the peptide antibiotic nisin: antibacterial activity of fragments of nisin. *FEBS Lett.* 1996;390(2):129–132.
22. Jung G. Lantibiotics—ribosomally synthesized biologically active polypeptides containing sulfide bridges and α,β-didehydroamino acids. *Angew. Chem., Int. Ed.* 1991;30(9):1051–1068.
23. Kuipers A, de Boef E, Rink R, et al. NisT, the transporter of the lantibiotic nisin, can transport fully modified, dehydrated, and unmodified prenisin and fusions of the leader peptide with non-lantibiotic peptides. *J Biol Chem.* 2004;279(21):22176–22182.
24. van Heel AJ, Kloosterman TG, Montalban-Lopez M, et al. Discovery, production and modification of five novel lantibiotics using the promiscuous nisin modification machinery. *ACS Synth Biol.* 2016;5(10):1146–1154.
25. Montalbán-López M, van Heel AJ, Kuipers OP. Employing the promiscuity of lantibiotic biosynthetic machineries to produce novel antimicrobials. *FEMS Microbiol Rev.* 2017;41(1):5–18.
26. Hsu ST, Breukink E, Tischenko E, et al. The nisin-lipid II complex reveals a pyrophosphate cage that provides a blueprint for novel antibiotics. *Nat Struct Mol Biol.* 2004;11(10):963–967.
27. Wiedemann I, Breukink E, van Kraaij C, et al. Specific binding of nisin to the peptidoglycan precursor lipid II combines pore formation and inhibition of cell wall biosynthesis for potent antibiotic activity. *J Biol Chem.* 2001;276(3):1772–1779.
28. van Heusden HE, de Kruijff B, Breukink E. Lipid II induces a transmembrane orientation of the pore-forming peptide lantibiotic nisin. *Biochemistry.* 2002;41(40):12171–12178.
29. Hasper HE, de Kruijff B, Breukink E. Assembly and stability of nisin-lipid II pores. *Biochemistry.* 2004;43(36):11567–11575.
30. Medeiros-Silva J, Jekhmane S, Paioni AL, et al. High-resolution NMR studies of antibiotics in cellular membranes. *Nat Commun.* 2018;9(1):3963.
31. Wiedemann I, Benz R, Sahl HG. Lipid II-mediated pore formation by the peptide antibiotic nisin: a black lipid membrane study. *J Bacteriol.* 2004;186(10):3259–3261.
32. AlKhatib Z, Lagedroste M, Fey I, Kleinschrodt D, Abts A, Smits SH. Lantibiotic immunity: inhibition of nisin mediated pore formation by NisI. *PLoS ONE.* 2014;9(7) e102246.
33. Dischinger J, Basi Chipalu S, Bierbaum G. Lantibiotics: promising candidates for future applications in health care. *Int J Med Microbiol.* 2014;304(1):51–62.
34. Gomes KM, Duarte RS, de Freire Bastos MD. Lantibiotics produced by *Actinobacteria* and their potential applications (a review). *Microbiology.* 2017;163(2):109–121.
35. Sandiford SK. Current developments in lantibiotic discovery for treating *Clostridium difficile* infection. *Expert Opin Drug Discov.* 2019;14(1):71–79.
36. Delves-Broughton J, Blackburn P, Evans RJ, Hugenholtz J. Applications of the bacteriocin, nisin. *Antonie Van Leeuwenhoek.* 1996;69(2):193–202.
37. Draper LA, Cotter PD, Hill C, Ross RP. Lantibiotic resistance. *Microbiol Mol Biol Rev.* 2015;79(2):171–191.
38. Alkhatib Z, Abts A, Mavaro A, Schmitt L, Smits SH. Lantibiotics: how do producers become self-protected? *J Biotechnol.* 2012;159(3):145–154.
39. Khosa S, AlKhatib Z, Smits SH. NSR from *Streptococcus agalactiae* confers resistance against nisin and is encoded by a conserved nsr operon. *Biol Chem.* 2013;394(11):1543–1549.
40. Clemens R, Zaschke-Kriesche J, Khosa S, Smits SHJ. Insight into Two ABC Transporter Families Involved in Lantibiotic Resistance. *Front Mol Biosci.* 2017;4:91.
41. AlKhatib Z, Lagedroste M, Zaschke J, et al. The C-terminus of nisin is important for the ABC transporter NisFEG to confer immunity in *Lactococcus lactis*. *Microbiologyopen.* 2014;3(5):752–763.
42. Plat A, Kuipers A, G De Lange J, N Moll G, Rink R. Activity and Export of Engineered Nisin-(1-22) Analogs; 2011.
43. Rink R, Wierenga J, Kuipers A, et al. Dissection and modulation of the four distinct activities of nisin by mutagenesis of rings A and B and by C-terminal truncation. *Appl Environ Microbiol.* 2007;73(18):5809–5816.
44. Molloy EM, Field D, O' Connor PM, Cotter PD, Hill C, Ross RP. Saturation mutagenesis of lysine 12 leads to the identification of derivatives of nisin A with enhanced antimicrobial activity. *PLoS One.* 2013;8(3) e58530.
45. Zhou L, Shao J, Li Q, et al. Incorporation of tryptophan analogues into the lantibiotic nisin. *Amino Acids.* 2016;48(5):1309–1318.
46. Healy B, Field D, O'Connor PM, Hill C, Cotter PD, Ross RP. Intensive mutagenesis of the nisin hinge leads to the rational design of enhanced derivatives. *PLoS ONE.* 2013;8(11) e79563.
47. Zhou L, van Heel AJ, Kuipers OP. The length of a lantibiotic hinge region has profound influence on antimicrobial activity and host specificity. *Front Microbiol.* 2015;6:11.
48. Piper C, Cotter PD, Ross RP, Hill C. Discovery of medically significant lantibiotics. *Curr Drug Discov Technol.* 2009;6(1):1–18.
49. Reiners J, Lagedroste M, Ehlen K, Leusch S, Zaschke-Kriesche J, Smits SHJ. The N-terminal region of nisin is important for the BceAB-type ABC transporter NsrFP from *Streptococcus agalactiae* COH1. *Front Microbiol.* 2017;8:1643.
50. Mavaro A, Abts A, Bakkes PJ, et al. Substrate recognition and specificity of the NisB protein, the lantibiotic dehydratase involved in nisin biosynthesis. *J Biol Chem.* 2011;286(35):30552–30560.
51. Lubelski J, Overkamp W, Kluskens LD, Moll GN, Kuipers OP. Influence of shifting positions of Ser, Thr, and Cys residues in prenisin on the efficiency of modification reactions and on the antimicrobial activities of the modified prepeptides. *Appl Environ Microbiol.* 2008;74(15):4680–4685.
52. Abts A, Montalban-Lopez M, Kuipers OP, Smits SH, Schmitt L. NisC binds the FxLx motif of the nisin leader peptide. *Biochemistry.* 2013;52(32):5387–5395.
53. Abts A, Mavaro A, Stindt J, et al. Easy and rapid purification of highly active nisin. *Int J Pept.* 2011;2011 175145.
54. Lagedroste M, Reiners J, Smits SHJ, Schmitt L. Systematic characterization of position one variants within the lantibiotic nisin. *Sci Rep.* 2019;9(1):935.
55. Khosa S, Lagedroste M, Smits SH. Protein defense systems against the lantibiotic nisin: function of the immunity protein NisI and the resistance protein NSR. *Front Microbiol.* 2016;7:504.
56. Roth BL, Poot M, Yue ST, Millard PJ. Bacterial viability and antibiotic susceptibility testing with SYTOX green nucleic acid stain. *Appl Environ Microbiol.* 1997;63(6):2421–2431.
57. Rink R, Kuipers A, de Boef E, et al. Lantibiotic structures as guidelines for the design of peptides that can be modified by lantibiotic enzymes. *Biochemistry.* 2005;44(24):8873–8882.
58. Khosa S, Frieg B, Mulnaes D, et al. Structural basis of lantibiotic recognition by the nisin resistance protein from *Streptococcus agalactiae*. *Sci Rep.* 2016;6:18679.

3.5. Chapter V – Bypassing the nisin resistance of the SaNSR protein

Published in: Bioorganic and Medicinal Chemistry

Impact factor: 2.80

Own Work: 15 %

Expression and Purification of the proteins
Performing biological and biochemical assays
Preparation of the figures
Writing the manuscript

Small-molecule inhibitors of nisin resistance protein NSR from the human pathogen *Streptococcus agalactiae*

Nicola Porta, **Julia Zaschke-Kriesche,** Benedikt Frieg, Mohanraj Gopalswamy, Aleksandra Zivkovic, Manuel Etzkorn, Holger Stark, Sander Smits, Holger Gohlke

Bioorganic & Medicinal Chemistry 27 (2019) 115079

Contents lists available at ScienceDirect

Bioorganic & Medicinal Chemistry

journal homepage: www.elsevier.com/locate/bmc

Small-molecule inhibitors of nisin resistance protein NSR from the human pathogen *Streptococcus agalactiae*

Nicola Porta[a,h], Julia Zaschke-Kriesche[b], Benedikt Frieg[c,d,i], Mohanraj Gopalswamy[a], Aleksandra Zivkovic[a], Manuel Etzkorn[d,e,f], Holger Stark[a], Sander H.J. Smits[b,g], Holger Gohlke[a,c,d,j,*]

[a] Institute for Pharmaceutical and Medicinal Chemistry, Heinrich-Heine-Universität Düsseldorf, Universitätsstrasse 1, 40225 Düsseldorf, Germany
[b] Institute of Biochemistry, Heinrich-Heine-Universität Düsseldorf, Universitätsstrasse 1, 40225 Düsseldorf, Germany
[c] John von Neumann Institute for Computing (NIC), Jülich Supercomputing Centre (JSC), Forschungszentrum Jülich GmbH, Wilhelm-Johnen-Straße, 52425 Jülich, Germany
[d] Institute of Complex Systems – Structural Biochemistry (ICS-6), Forschungszentrum Jülich GmbH, Wilhelm-Johnen-Straße, 52425 Jülich, Germany
[e] Institute of Physical Biology, Heinrich-Heine-Universität Düsseldorf, Universitätsstrasse 1, 40225 Düsseldorf, Germany
[f] JuStruct: Jülich Center for Structural Biology, Forschungszentrum Jülich, GmbH, Wilhelm-Johnen-Straße, 52425 Jülich, Germany
[g] Center for Structural Studies, Heinrich-Heine-Universität Düsseldorf, Universitätsstrasse 1, 40225 Düsseldorf, Germany

ARTICLE INFO

Keywords:
Antibiotic resistance
Lantibiotics
Nisin
Screening
Small-molecule inhibitors

ABSTRACT

Lantibiotics are antimicrobial peptides produced by Gram-positive bacteria and active in the nanomolar range. Nisin is the most intensely studied and used lantibiotic, with applications as food preservative and recognized potential for clinical usage. However, different bacteria that are pathogenic for humans and do not produce nisin, including *Streptococcus agalactiae*, show an innate resistance that has been related to the nisin resistance protein (NSR), a membrane-associated protease. Here, we report the first-in-class small-molecule inhibitors of *Sa*NSR identified by virtual screening based on a previously derived structural model of the nisin/NSR complex. The inhibitors belong to three different chemotypes, of which the halogenated phenyl-urea derivative NPG9 is the most potent one. Co-administration of NPG9 with nisin yields increased potency compared to nisin alone in *Sa*NSR-expressing bacteria. The binding mode of NPG9, predicted with molecular docking and validated by extensive molecular dynamics simulations, confirms a structure-activity relationship derived from the *in vivo* data. Saturation transfer difference-NMR experiments demonstrate direct binding of NPG9 to *Sa*NSR and agree with the predicted binding mode. Our results demonstrate the potential to overcome *Sa*NSR-related lantibiotic resistance by small molecules.

1. Introduction

Without doubt, antibiotic resistance is one of the greatest health threats of our time. Misuse and overuse of antibiotics have accelerated the evolutionary selection process, which led to resistance against essentially all approved antibiotics.[1] Hence, there is an urgent need for antimicrobial compounds that can be used as alternatives to the classical antibiotic treatment. In this context, lantibiotics, a class of antimicrobial peptides, are attractive candidates due to their high activity against a wide range of Gram-positive human pathogenic bacteria.[2,3] Peculiar post-translational modifications are contributing to the high thermostability and general stability against proteolytic degradation. Specifically, the enzymatic dehydration of Ser and Thr results in the formation of 2,3-dehydroalanine (Dha) and 2,3-dehydrobutyrine (Dhb) residues. Nucleophilic addition of the thiol group of a neighboring Cys residue then yields distinctive lanthionine (Lan from Dha) and methyllanthionine (MeLan from Dhb) rings, the presence of which is essential for the high antimicrobial potency.[4]

Nisin is the most-studied lantibiotic and produced by a group of Gram-positive bacteria belonging to *Lactococcus* and *Streptococcus* species.[5] This 34 amino acids long cationic peptide is constituted of five lanthionine rings named A to E successively from the N- to the C-

* Corresponding author at: Universitätsstr. 1, 40225 Düsseldorf, Germany.
E-mail address: gohlke@uni-duesseldorf.de (H. Gohlke).
[h] ORCID: 0000-0002-6005-4372.
[i] ORCID: 0000-0002-7877-0262.
[j] ORCID: 0000-0001-8613-1447.

https://doi.org/10.1016/j.bmc.2019.115079
Received 8 May 2019; Received in revised form 31 July 2019; Accepted 25 August 2019
Available online 26 August 2019

terminus. Since it was discovered in 1928,[6] it is one of the oldest known antibacterial agents. Nisin has been used widely as a food preservative, and initial therapeutic applications include human ulcer therapy and mastitis control in cattle.[7] Studies have reported that nisin can prevent the growth of drug-resistant bacterial strains, such as methicillin-resistant *Staphylococcus aureus* and *Clostridium difficile*. Increasing evidence indicates that nisin can also exhibit selective cytotoxicity towards cancer cells (for more details see review[5]). Its modes of action are related to the interaction with cellular membranes: for example specific binding of lipid II,[8] thus inhibition of cell wall synthesis by interrupting peptidoglycan production,[9] and formation of pores within the cell membrane that are made up of lipid II and nisin molecules.[9,10]

Due to their multiple modes of action, hardly any resistance against lantibiotics has developed over the past decades. However, different bacteria that are pathogenic for humans and do not produce nisin, including *Streptococcus agalactiae*, show an innate resistance that has been related to the nisin resistance protein (NSR), a membrane-associated protease.[11,12] Specifically, NSR is a C-terminal processing protease belonging to the S41 family, as classified by MEROPS, the peptidase database.[13] The resistance mechanism involves enzymatic inactivation of nisin by cleavage of the last six residues. The resulting nisin fragment displays a up to 100-fold lower antibacterial efficacy and reduced affinity towards cellular membranes.[14]

The crystal structure of NSR from *Streptococcus agalactiae* (*Sa*NSR) was solved.[15] It contains an *N*-terminal helical bundle, and protease cap and core domains. The latter displays a region with the highly conserved TASSAEM sequence, with the previously identified catalytically active Ser236.[11] The other residue constituting the catalytic dyad is His98, located between the helical bundle and the cap domain. Overall, the three domains constitute a hydrophobic tunnel of ~10 Å width, and the protease cap forms a lid-like structure above it. By integrative modeling and mutagenesis studies a structural model of a nisin/*Sa*NSR complex was generated that reveals that *Sa*NSR recognizes the last C-terminal lanthionine ring of nisin, ring E.[15] This recognition determines the substrate specificity of *Sa*NSR and ensures the exact coordination of the nisin cleavage site (peptide bond between MeLan28 in ring E and Ser29).

The identification of small-molecule inhibitors that interfere with *Sa*NSR function is of utmost importance for making a therapy with nisin most effective. Here, we identified, by repetitive rounds of ligand- and structure-based virtual screening (Fig. 1A), analogs search, and *in vivo* testing, inhibitors of *Sa*NSR with different chemotypes. In order to prioritize molecules that resemble the recognition fragment of nisin and can inhibit *Sa*NSR function, both shape matching and molecular docking were performed. *In vivo* validation of selected compounds revealed a selective functional inhibition towards *Sa*NSR-expressing bacteria. To investigate NPG9 binding to *Sa*NSR at the atomistic level, and further validate its binding mode, extensive molecular dynamics (MD) simulations of free ligand diffusion (fldMD) were performed. Finally, saturation transfer difference (STD) NMR experiments on NPG9 provide an additional validation of the binding mode from the biophysical point of view.

2. Materials and methods

2.1. Preparation of nisin and SaNSR structures

The structures of nisin (extracted from PDB ID: 1WCO[10]) and *Sa*NSR (PDB ID: 4Y68[15]) were used for this study. In nisin, Asn27 was substituted by His to obtain a suitable nisin A structure from the crystallized nisin Z variant. *Sa*NSR is a monomer in solution,[15] therefore, only chain A was considered for further steps. Both structures were preprocessed with the Protein Preparation Wizard[16] of Schrödinger's Maestro Suite. Bond orders as well as missing hydrogen atoms were assigned, and the H-bond network was optimized. Finally, the systems were energy-minimized using the OPLS 2005 force field,[17] resulting in a root mean square deviation (RMSD) of 0.3 Å with respect to the initial structure.

2.2. Query generation

To screen for molecules with similar shape properties as the recognition region of nisin, we built a query for ligand-based virtual screening. To do so and to consider structural mobility, the nisin structure was subjected to all-atom MD simulations in explicit solvent, as reported previously,[15] using Amber 16.[18] Three independent trajectories of 500 ns length were analyzed with the cpptraj software.[19] To extract relevant conformations explored by nisin in solution, the MD-derived structural ensemble was clustered applying a hierarchical agglomerative approach. Prior to the clustering, conformations extracted every 5 ns were fit on the D ring region, using the first frame as reference, in order to remove global translation and rotation. As distance metric, the RMSD of backbone atoms was used, with a cutoff value for forming clusters of 4.5 Å. From the representative structures of the five most populated clusters, three different multi-conformation queries were built (Fig. 1B) using ROCS[20]: I) based on rings DE, Ser29 and Ile30; II) based on rings DE only; III) based on ring E, Ser29 and Ile30.

2.3. Virtual screening

A general workflow of the protocol used is reported in Fig. 1A. Compounds were collected from ZINC15[21] and eMolecules (https://www.emolecules.com) databases, which together contain over 20 million molecules. For database preparation, including filtering and generation of up to 200 conformations per ligand, Omega[22] was used. In order to filter out compounds with unwanted pharmacokinetics, a drug-like filter was applied, and only compounds with logP < 6 and molecular weight (MW) between 200 and 600 Da were retained. A shape-based similarity search was then performed with the three shape queries generated above. Only the best fitting conformation for each compound was saved. The top 500 molecules for each query (1500 in total) were then docked into the *Sa*NSR pocket using Glide[23] implemented in the Schrödinger's Maestro Suite 2017-1 (LLC, New York, NY, USA). A cubic grid of length 20 Å was centered on the catalytic residues His98 and Ser236. Compounds were first docked using Glide-SP (standard precision) protocol, and the 50% best-ranked were subsequently re-docked using Glide-XP (extra precision) protocol, which does more extensive sampling and uses a more sophisticated scoring function than the Glide-SP protocol. The best-ranked 750 compounds were then clustered with Canvas[24] based on 2D similarity (Tanimoto index calculated on MACCS keys fingerprint) and visually inspected, in order to select compounds with high diversity. At the end of this run, 11 compounds were purchased and tested.

The same protocol was applied a second time with additional filtering steps, in order to filter out structures with high complexity and those exhibiting non-lead-like properties: the first filter excluded compounds with more than five rings (RNG) and more than one chiral center (STER); the second is based on molecular descriptors related to lead structures,[25] namely ≤10 rotatable bonds (RTB) and a MW ≤ 460 Da. This resulted in 23 compounds being purchased and tested.

Finally, considering preliminary *in vivo* data, a third group of compounds was selected based on the similarity with NPG9. An analogs search was performed focusing mainly on bioisosteric replacements of halogen atoms or variations of the two hydroxyl groups, resulting in the acquisition and testing of 12 derivatives.

2.4. Molecular dynamics simulations

In order to investigate the recognition process and validate the predicted binding mode of inhibitors with *Sa*NSR, a set of MD simulations was performed considering NPG9 as model inhibitor. NPG9 was

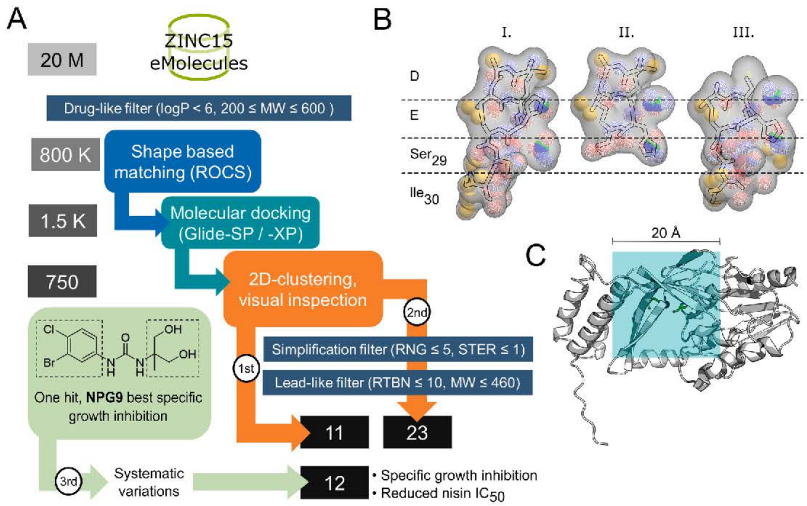

Fig. 1. Virtual screening for *Sa*NSR inhibitors. (A) Workflow for compound selection applied in this study. Shape-based matching followed by molecular docking and 2D clustering plus visual inspection led to the selection of in total 46 compounds for testing, 11 in the first round, additional 23 in the second round applying further filter criteria, and 12 more based on similarity to NPG9. These compounds were tested for growth inhibition in *Sa*NSR-expressing cells and/or reduced nisin IC_{50}. On the left, the number of compounds considered in each step is indicated (K: indicates thousands; M: indicates millions). (B) Three queries generated for shape matching, based on varying nisin fragments including rings D and E, Ser29, and Ile30. For reasons of clarity, just one out of the five representative structures each is overlaid as sticks. The molecular shape is represented as a grey surface, while the chemical features are shown as spheres: H-bond acceptors as red grid, H-bond donors as blue grid, hydrophobic centers in yellow, rings and cations in green and blue, respectively. (C) Representation of the *Sa*NSR structure used for docking (PDB ID: 4Y68) and the cubic grid centered on the catalytic dyad His98 and Ser236 (green sticks). (For interpretation of the references to color in this figure legend, the reader is referred to the web version of this article.)

optimized with Gaussian[26] at the Hartree-Fock level with the 6-31G* basis set. Partial charges for each atom were derived with the RESP procedure,[27] as implemented in Antechamber,[28] by fitting to electrostatic potential grids generated by Gaussian. Different simulation systems of *Sa*NSR and NPG9 were prepared for MD simulations with the LEaP program.[29] In particular, both the docking pose (P0, later referred to as "bound simulations") and ten random configurations of NPG9 relative to *Sa*NSR (P1-P10, later referred to as "free ligand diffusion simulations", fldMD) were considered. In the first case, the structural stability of the complex and the diffusion of the ligand within the tunnel were analyzed. In the latter cases, the diffusion of the ligand was investigated aiming for reconstructing of the binding pathway of the *Sa*NSR inhibitor. The ten random configurations were generated with packmol[30] with a minimum distance between NPG9 and *Sa*NSR of 15 Å. Sodium counter ions were added to establish charge neutrality. Each system was placed in a truncated octahedral box of TIP3P water[31] with a minimum distance to the border of the box of 11 Å, resulting in a NPG9 concentration of ~1.4 mM. Structural relaxation, thermalization, and production runs of MD simulations were conducted with pmemd.cuda[32] of Amber 16[18] using the ff14SB force field[33] for the protein, GAFF force field[34] for the ligand, and Joung-Chetham parameters for ions.[35] For each starting complex five independent replica of 500 ns length each were performed, resulting in a total of 50 simulations with a cumulative simulation time of 25 µs. Additionally, we performed MD simulations starting from the docked binding mode of NPG9 bound to *Sa*NSR. Again, five independent replicas of 500 ns length each were performed. In order to set up independent replicas and obtain slightly different starting structures, the target temperature was set to different values during thermalization (299.8 K, 299.9 K, 300.0 K, 300.1 K, 300.2 K and 300.3 K). A description of the thermalization protocol can be found elsewhere.[36]

The analysis of the MD trajectories was carried out with cpptraj[19] on snapshots extracted every 1 ns. To measure structural mobility, we computed the residue-wise root mean square fluctuations (RMSF) of backbone atoms of *Sa*NSR relative to the starting structure. To evaluate opening and closing of the cap domain, the distance between the centers of mass of the β-hairpin (262-TVNETFMLYDGARLALTTGIV-282) and the short loop regions of the protease core facing the tunnel (133-ISKL-136 and 135-TGGN-171) was computed. To investigate the molecular recognition of NPG9, the all-atom RMSD with respect to the ligand docking pose ($RMSD_d$) or the previous frame ($RMSD_p$) were computed. Cutoff values of $RMSD_d \leq 2.5$ Å and $RMSD_p \leq 2.5$ Å were used respectively to define binding on the protein surface (unspecific) and within the *Sa*NSR tunnel (specific). Bound conformations were then clustered applying a hierarchical agglomerative approach and an RMSD cutoff value of 1.5 Å. Prior to the clustering, conformations were fit on the 10% least mobile residues of *Sa*NSR, located in the protease core domain.

2.5. Compound acquisition

The 46 selected compounds were either custom-synthetized or purchased from different suppliers as powder (Table S1). To ensure that there was no degradation of the compounds during the study, purity was re-assessed in a semi-quantitative way with LC-MS (exemplary cases are shown in Figs. S4–S8; see also next chapter).

2.6. Purity assessment with LC-MS

The compounds' stock solutions (~1 mg/ml in DMSO) were diluted with methanol hypergrade to concentrations of ~0.1–0.2 mg/ml. A volume of 2 µl was injected for each measurement. Relative purity of the compounds was determined as ratio of the area under the curve. LC system: Elute SP LC System (Bruker Daltonics, Bremen, Germany) with

vacuum degasser, binary pump, autosampler, column oven. Column: Intensity Solo 2 C18 (100 mm * 2.1 mm); Temperature: 50° C; Mobile phase: A. water hypergrade with 0.1% formic acid (v/v) (Merck); B. Acetonitrile hypergrade (Merck); Flow Rate: 0.2 ml/min. Method 1: 0–4 min 95% A, 4–16 min gradient 95% to 5% A, 16–17 min gradient 5% to 0% A, reconditioning: 17–18 min gradient 0% to 95% A, 18–21 min 95% A. Method 2: 0–4 min 98% A, 4–5 min gradient 98% to 95% A, 5–9 min 95% A, 9–16 min gradient 95% to 5% A, 16–17 min gradient 5% to 0% A, reconditioning: 17–18 min gradient 0% to 98% A, 18–21 min 98% A. MS-System: amaZon speed ETD ion Trap LC/MSn System (Bruker Daltonics, Bremen, Germany); Ionisation: electronspray; Polarity: positive; Alternating ion-polarity: on; Scan range: *m/z*: 80–1200; Nebulizer: Nitrogen, 15 Psi; Dry Gas: Nitrogen, 8 l/min, 200 °C; Massrange mode: UltraScan.

2.7. Cloning of the SaNSR protein

For studies in recombinant *Lactococcus lactis* cells, the plasmid pNZ-SV-*Sa*NSR was obtained by cloning the gene nsr from *S. agalactiae* as previously described.[11] The plasmid was transformed using electrocompetent *L. lactis* NZ9000 cells. Therefore, a pulse setting of 1 kV, 25 µF, 200 Ω, for 4.5–5.0 ms was used to electroporate the cells.[37] Afterwards, 950 µl GM17 media was added, and the cells were incubated for 3 h at 30 °C. At last, the cells were plated on SMGG-agar plates containing 5 µg/ml erythromycin. For STD-NMR studies, the plasmid pET-28b-*Sa*NSR30-N8His was cloned as reported previously[38] and transformed into chemocompetent *E. coli* BL21 (DE3) cells using a 42 °C heat shock for 60 s. After 1 h incubation at 37 °C, the cells were finally plated on LB-agar plates containing 30 µg/ml kanamycin.

2.8. Expression and purification of the SaNSR protein

*Sa*NSR30-N8His was expressed and purified as previously described.[38] Therefore, in *E. coli* BL21 (DE3) pET-28b-*Sa*NSR30-N8His at an OD_{600} of = 0.8–1.0, the expression was induced with 1 mM IPTG and the cells were incubated overnight at 18 °C with 160 rpm shaking. Subsequently, the cells were harvested and homogenized five times using 1.5 kbar (Microfluidics Homogenizer). After harvesting the cell debris at 42,000 rpm for 45 min the supernatant was used for an ion metal affinity chromatography, using a HiTrap Chelating HP 5 ml column and an elution buffer containing 150 mM histidine. The eluted protein was further purified with a Superose 12 10/300 GL column, 25 mM MES pH 6 buffer with 150 mM NaCl.

2.9. Purification of nisin

Nisin was purified with cation exchange chromatography as previously described.[39] To determine the concentration, the peptide was analyzed with RP-HPLC as previously described.[40]

2.10. Growth inhibition assay

In vivo validation of selected compounds was performed to test their ability to specifically inhibit the growth of *Sa*NSR-expressing strains. To do so, *L. lactis* cells grown in GM17 medium with 5 µg/ml erythromycin and 1 ng/ml nisin overnight. The cells were diluted in fresh media to an OD_{595} of 0.1 and incubated for 30 min at 30 °C. In a 96 well plate, 50 µl of the selected compounds and the DMSO control (20%) were added. 150 µl of *L. lactis* NZ9000 pNZ-SV-Erm and *L. lactis* NZ9000 pNZ-SV-*Sa*NSR cells supplemented with 30 nM nisin, respectively, were added. After 5 h at 30 °C the optical density was measured, and the relative growth inhibition was calculated by comparing the normalized values for *L. lactis* NZ9000 pNZ-SV-*Sa*NSR.

2.11. Measurement of reduced nisin IC_{50} values

In order to evaluate the inhibitory effect of the compounds, the reduced nisin IC_{50} was measured as previously described.[41] In 96 well plates, a serial dilution of nisin was mixed with 150 µl of preincubated cells (OD_{595} 0.1) containing 120 µM or 300 µM compound. The optical density was measured after 5 h incubation at 30 °C and the IC_{50} values were calculated. Reduced nisin IC_{50} values were determined based on IC_{50} values of the *Sa*NSR-expressing strain (*L. lactis* NZ9000 pNZ-SV-*Sa*NSR) with inhibitory compound compared to the same strain without compound and expressed as ratio of the two IC_{50} values given in percent.

2.12. Saturation transfer difference (STD) NMR experiments

As a biophysical validation of direct binding, STD NMR measurements were performed for the model inhibitor NPG9. This method allows identifying the binding of small ligands to macromolecules with dissociation constants K_D in the nM to mM range and characterizing the binding epitopes on the ligands.[42,43] NMR experiments were recorded on a Bruker Avance III HD^+ 600 MHz spectrometer at 298 K in 100 mM sodium phosphate, 150 mM sodium chloride, 5% (v/v) DMSO, and 10% (v/v) D_2O. Trimethylsilyl propionate (TSP) was used as an internal standard. STD NMR was performed with on-resonance protein saturation at 0.9 ppm using 2 s saturation time. Subtraction of the 1D STD spectrum was performed internally via phase cycling after every scan to minimize artefacts arising from temperature and magnet instability.[42,43] The STD NMR experiment was carried out using 18 µM of *Sa*NSR protein and 1.8 mM of NPG9 compound. All NMR spectra were processed and analyzed with TOPSPIN 3.2 (Bruker).

3. Results and discussion

3.1. Compounds selection

A hierarchical virtual screening protocol was applied to find small-molecules that inhibit *Sa*NSR (Fig. 1). Starting from a subset of drug-like molecules, using the free databases of commercially available compounds ZINC15 and eMolecules, 1500 compounds were selected based on shape similarity with nisin fragments involved in *Sa*NSR recognition. In order to do so, rapid overlay of chemical structures (ROCS)[20] was applied for the calculation of 3D shape and chemical similarity. We built three queries, considering rings D and E as well as residues Ser29 and Ile30 (query I), rings D and E alone (query II), and ring E, Ser29 and Ile30 (query III) (Fig. 1B). The selections were motivated by the fact that rings D and E form the recognition element of nisin at *Sa*NSR and Ser29 and Ile 30 are in close proximity to the cleavage site (peptide bond between MeLan28 in ring E and Ser29).[15] The best fitting compounds were submitted to molecular docking with Glide[23] in order to predict their configuration within the *Sa*NSR binding site and to rank them according to the potential molecular interactions, as expressed by the docking score. The 750 molecules with the best docking scores were clustered and visually inspected, leading to the selection of 11 drug-like compounds for testing (NPG8 – NPG19, Table S1). In a second virtual screening run, two additional filtering steps were considered. The first filter excluded compounds with more than five rings (RNG) and more than one chiral center (STER). The second filter is based on molecular descriptors related to lead structures,[25] namely ≤10 rotatable bonds (RTB) and a molecular weight (MW) ≤ 460 Da. After this run, 23 compounds were purchased and tested (NPG20 – NPG42, Table S1).

3.2. Biological activity

For experimental validation of the two groups of in total 34 compounds, a specific growth inhibition *in vivo* assay was performed, in

Table 1
Subset of compounds that showed *Sa*NSR inhibitory activity.[a]

Internal ID, structure	Selection run	Specific growth inhibition[b]	Reduced Nisin IC_{50}[b]	
		150 μM[c]	120 μM[c]	300 μM[c]
NPG9 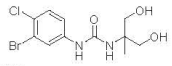	1st	57.91 ± 1.72	50.5 ± 1.5	n.d.
NPG13 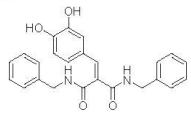	1st	16.89 ± 3.61	–	32.2 ± 5.0
NPG24 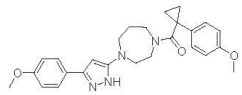	2nd	20.66 ± 4.56	–	20.5 ± 12.1
NPG46 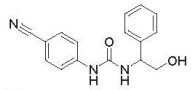	3rd	–	8.1 ± 7.0	13.5 ± 6.4
NPG51 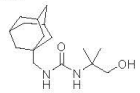	3rd	–	4.0 ± 4.4	8.5 ± 5.8

[a] The full list of 46 tested compounds is shown in Table S1. Values were determined by at least three independent experiments. Measurements not performed are reported as "–". In cases where the compound was inhibiting the cell growth even without nisin, the measurement was marked as not determinable, "n.d.". Unless compounds are reported with explicit stereochemistry notation, the mixture of stereoisomers with undefined configurations was tested.
[b] In %.
[c] Used compound concentration.

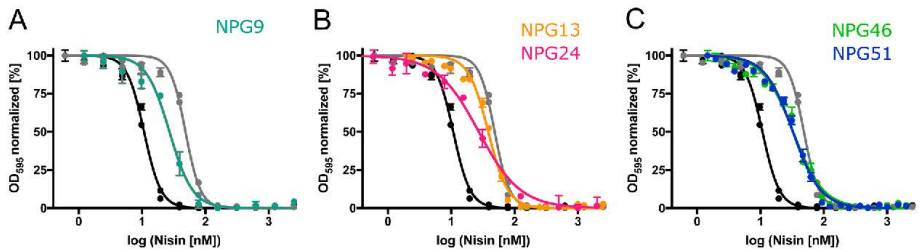

Fig. 2. Determination of IC_{50} values of nisin in the presence or absence of a *Sa*NSR inhibitor. Dose-response curves for *Sa*NSR-expressing strain NZ9000*Sa*NSR (in grey) and for the control strain NZ9000Erm (in black) are reported in comparison to *Sa*NSR-expressing strain NZ9000*Sa*NSR (A) with 120 μM of NPG9 (in cyan), (B) with 300 μM of NPG13 (in orange) and 300 μM of NPG24 (in magenta), and (C) with 300 μM of NPG46 (in green) and 300 μM of NPG51 (in blue). The normalized measured OD_{595} is shown in percentage against the logarithmic concentration of nisin. Values were determined by at least three independent experiments. (For interpretation of the references to color in this figure legend, the reader is referred to the web version of this article.)

which the selective inhibition towards *Sa*NSR-expressing *L. lactis* cells over *L. lactis NZ9000 pNZ-SV-Erm* containing an empty plasmid as control is probed utilizing a specific nisin concentration (30 nM). Specific growth inhibition is calculated as ratio between measured optical densities for the two strains and expressed as percentage. This assay was performed as a screening method, because *Sa*NSR-expressing bacteria are resistant against the nisin concentration used and growth is compared to the control strain; hence, only compounds inhibiting *Sa*NSR activity and making the bacteria more susceptible to nisin are identified.

Among the 34 compounds, three compounds showed a relevant inhibitory effect on *Sa*NSR at the tested concentration of 150 μM (Tables 1 and S1). In particular, NPG9 inhibits bacterial growth by ~58% in the presence of nisin as compared to control bacteria lacking *Sa*NSR. Based on this, a third group of compounds was searched that are similar to NPG9 with respect to molecular recognition properties. For this, an analogs search was performed focusing on the following substitutions: bioisosteric replacement of halogen atoms with electron-withdrawing groups (e.g., cyano or trifluoromethyl groups[44]), substitution of the phenyl group with bulky hydrophobic moieties, or

variations of the two hydroxyl groups. This step resulted in the selection of 12 derivatives (NPG43 – NPG55, Table S1; NPG53 was excluded from the study due to chemical stability issues). On this subset, as well as on NPG9 for comparison, *in vivo* validation was performed measuring reduced nisin IC_{50} values. The reduced nisin IC_{50} values denote nisin's potency from dose-response curves for the *Sa*NSR-expressing strain in the presence of a fixed concentration of inhibitor, compared to the same strain without inhibitor; reduced nisin IC_{50} values are expressed as the ratio between these two IC_{50} values and given in percent. Hence, a strongly shifted dose-response curve towards the control strain NZ9000Erm, which is sensitive to nisin, indicates a higher inhibitory potency of the compound (Fig. 2). To determine the inhibitory effect of the compounds, 120 µM and 300 µM were added to the assay with the *Sa*NSR-expressing strain. Some compounds (e.g., NPG9) had a *Sa*NSR-independent inhibitory effect on cell growth and could not be investigated at the higher concentration of 300 µM. Nisin IC_{50} values are reduced by ~50% if NPG9 is used at 120 µM concentration (Table 1, Fig. 2A), and by ~9 to 32% for NPG13, NPG24, NPG46 and NPG51 if these compounds are used at 300 µM concentration (Table 1, Fig. 2B-C).

3.3. Structure activity relationship (SAR) study

Most of the active molecules are linear, with one (e.g., NPG9) or two (e.g., NPG46) hydrophobic parts separated by an amide or urea linker. The presence of amide-like groups is not surprising because we searched for analogs of the peptide nisin. NPG13 displays a branching with an additional aromatic moiety (catechol) resulting in a *T*-shaped geometry.NPG24 is structurally different from the others, with pyrazolyl, 1,4-diazepanyl, amide and cyclopropyl groups arranged in a linear fashion between two methoxyphenyl moieties. It displays weak growth inhibition and a moderately reduced nisin IC_{50}, similarly to NPG13. Finally, NPG46 and NPG51, structural analogs of NPG9, display only very little reduced nisin IC_{50} values (Tables 1, S1 and Fig. 2). From the current data, a limited structure–activity relationship (SAR) can be derived (Fig. 3): the minimal requirement for activity are a linear molecular shape and one or two hydrophobic regions separated by an amide-like group.[45] In nisin, MeLan and Ile residues represent these hydrophobic regions. Additionally, a hydroxyl group (e.g., NPG9) or an aromatic polar group (e.g., NPG13), matching respectively with Ser29 and His28 of nisin, can be present.

3.4. Binding mode prediction

This SAR derived from experimental data can be rationalized in terms of binding modes generated by molecular docking (Fig. 4). In general, the binding mode of the compounds is consistent with the nisin/*Sa*NSR model previously reported[15] in terms of location and orientation of the ligand within the *Sa*NSR tunnel. As the binding mode prediction was done by molecular docking and, thus, independently from the ligand-based virtual screening, these findings implicitly validate the generated queries (Fig. 1B). Additionally, the amide bond (or amide-like group[45]) is placed in-between the catalytic dyad, as found for the cleavage site of nisin.[15] More specifically, the hydrophobic regions of the ligands are consistently located in proximity of two hydrophobic patches within the tunnel, one formed by Val264, Tyr192, Ile202, Phe190, Met240 and Met173 in the upper region, and the other by Tyr261 and Ala235 close to the catalytic dyad. In both regions, most of the ligands (NPG9, NPG13, NPG24, NPG46) can perform favorable interactions with the π-electron systems of Phe190 and Tyr261 residues (also termed π-π stacking). In the central portion of the tunnel, hydrophilic residues are prevalent instead, matching with the properties of the amide-like linker of the ligands: the linkers are involved in H-bond interactions with Gln100, Asn265, His98, Arg275, and Thr267 of the protease cap domain and Ser236, Ser237, Ser135, Thr169, and Gly171 of the core domain. Interestingly, in most of the compounds the amide-like group performs stabilizing interactions with the catalytic dyad of *Sa*NSR. However, for NPG51 with a bulkier adamantyl substituent, there are no such favorable interactions, and π-π stacking interactions are not possible either. Thus, sterically less demanding groups in the region mimicking the DE rings of nisin are apparently more favorable.

In order to investigate the recognition process and validate the predicted binding mode of *Sa*NSR inhibitors, a set of MD simulations was performed, considering NPG9 as model inhibitor. In general, all-atom MD simulations are more detailed than molecular docking in that they allow to take into account protein mobility and to describe explicitly water molecules and ions. To ensure robustness of our results, multiple independent replica MD simulations were performed, for which NPG9 initially was either placed inside the protein binding site in the docked pose (five bound MD simulations starting from P0) or at ten randomly chosen positions in the solvent surrounding *Sa*NSR (50 fldMD simulations, five replicas from each position P1-P10). In fldMD simulations, protein and ligand molecules interact in an unbiased manner, allowing to investigate in atomistic detail association and dissociation processes.

Analysis of *Sa*NSR motions reveals for fldMD simulations that the *N*-terminus, helical bundle, and cap domain are most mobile, while the core domain and C-terminus are rather immobile (Fig. S1A). As the cap domain constitutes part of the *Sa*NSR tunnel, its movements lead to *Sa*NSR exploring both open and closed states (Fig. S1D). Still, even for fldMD simulations, the closed state is present in less than 1/6 of the cases (Fig. S1-D, two replicas with > 75% and six with 75–50% closed frames). Thus, even when starting from unbound *Sa*NSR, the tunnel is frequently accessible for the ligand.

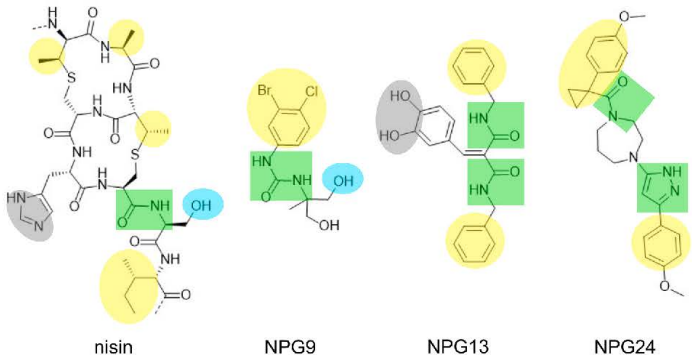

Fig. 3. Chemical structures of the recognition region of nisin to *Sa*NSR and compounds with *Sa*NSR inhibitory activity. Fragments with similar properties are highlighted, with the nisin cleavage site (or amide-like groups) in green, hydrophobic moieties in yellow, hydroxyl groups in blue, and polar-aromatic groups in grey. (For interpretation of the references to color in this figure legend, the reader is referred to the web version of this article.)

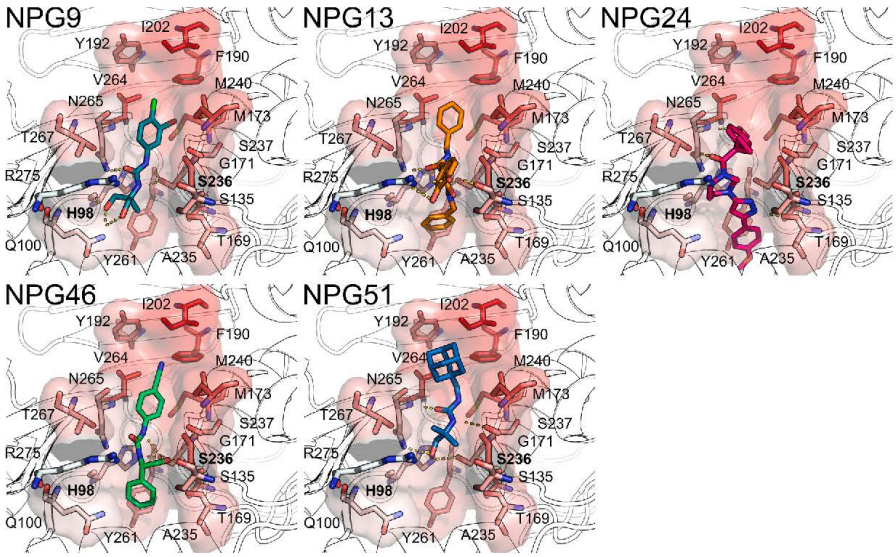

Fig. 4. Binding modes generated by molecular docking of the subset of compounds that show *Sa*NSR inhibitory activity (Table 1). Residues located at a distance ≤ 4 Å to the ligand are represented as surface-stick model, and the color scale from white to red represents increasing hydrophobicity of the residue (Eisenberg hydrophobicity scale[46]). The catalytically active His98 and Ser236 are highlighted in bold. H-bonds are shown as dashed lines. In the case of NPG46, only the *S*-stereoisomer with more favorable docking score is shown. (For interpretation of the references to color in this figure legend, the reader is referred to the web version of this article.)

To quantify ligand binding, as done previously,[47] the RMSD, as measure of the average distance between atoms of different configurations, was calculated (Figs. 5 and S2A). Each frame was therefore compared with the docked ligand pose (giving a $RMSD_d$ value) and with the previous frame in the trajectory (giving a $RMSD_p$ value) (Fig. S2A). The first measure indicates (specific) binding to the tunnel (applying an $RMSD_d \leq 2.5$ Å, meaning high similarity with the docked ligand pose); if this is not given, the second measure indicates unspecific binding to the protein surface (applying an $RMSD_p \leq 2.5$ Å, meaning low variability in ligand's coordinates over time). MD simulations originating from the NPG9 docked pose revealed in general a stable binding mode, except in two cases where the ligand diffuses in the direction of a hydrophobic region formed by Tyr192, Ile202, and Phe190, which may be linked to a weak binding affinity; still, the ligand does not leave completely the tunnel (Fig. S2B-C). During the 50 fldMD simulations, the ligand is in contact with the protein in ~75% of the frames (unspecific binding; Fig. S3 and Table S2). Yet, clusters C3 and C6, which contain together 18% of the frames, represent NPG9 conformations that are in very good agreement with the docked NPG9 pose (Fig. S3), as indicated by $RMSD_d \leq 2.5$ Å of the cluster representatives. Analysis of the time series of $RMSD_d$ values along all 50 fldMD simulations furthermore shows that such binding events occur across 11 different trajectories (Fig. S2D): in three of them bound frames represent 10–50% of the total ones, and in one replica even > 50% (Fig. 5). In some trajectories, the bound pose (configurations with $RMSD_d \leq 2.5$ Å) is reached in ~100 ns of simulation time (Fig. 5, P2-II and P6-II), while in others it is reached after more than 400 ns (Fig. 5, P4-II and P8-III). In both cases, the ligand stays bound for the remainder of the simulation time. Finally, in three out of the four cases, the ligand enters the tunnel from the entrance closer to the catalytic dyad (Fig. 5, P2-II, P4-II and P6-II), suggesting that this may be the preferential access pathway. Overall, the fldMD simulations thus confirm the docked binding pose in an independent manner, which lends support to the above structure-based rationalization of the SAR.

3.5. Biophysical validation

Finally, for NPG9, STD NMR experiments were performed (Fig. 6). The most intense STD NMR signals are observed for aromatic protons, and weaker signals for one NH proton and the aliphatic CH_2 protons are detected. Due to an experimental artefact, CH_3 protons were not considered.[48] These results demonstrate that the ligand is binding to *Sa*NSR and are consistent with our binding mode model according to which the phenyl ring of NPG9 make interactions with *Sa*NSR (Fig. 4).

4. Conclusions

In conclusion, we identified the first-in-class small-molecule inhibitors of *Sa*NSR, belonging to three different chemotypes, of which the halogenated phenyl-urea derivative NPG9 is the most potent one. So far, no other biological activities have been reported for these compounds.[49] Co-administration with nisin yields increased potency compared to nisin alone in *in vivo* experiments with *Sa*NSR-expressing bacteria. The minimal requirement for activity are a linear molecular shape and one or two hydrophobic regions separated by an amide-like group. STD NMR experiments demonstrate direct binding of NPG9 to *Sa*NSR and are in accordance with a predicted binding mode. Together, these findings make these compounds interesting for further investigations, towards generating more potent inhibitors to overcome *Sa*NSR-related lantibiotic resistance by small molecules.

Declaration of Competing Interest

The authors declare that they have no known competing financial interests or personal relationships that could have appeared to influence the work reported in this paper.

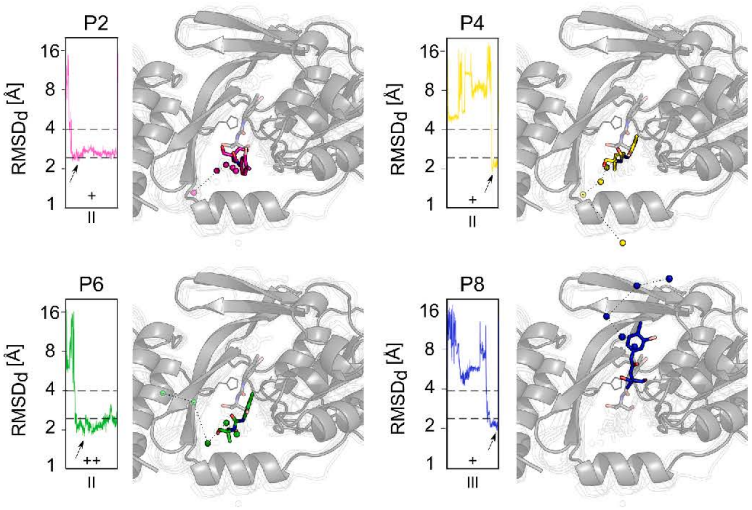

Fig. 5. Analysis of NPG9 binding events for selected replicas of MD simulations. $RMSD_d$ time evolution of NPG9 during the fldMD simulations replicas with 10–50% and > 50% bound frames ($RMSD_d \leq 2.5$ Å), marked with "+" and "++", respectively. Dashed lines representing the cutoff values for binding (2.5 Å, in black) and for pre-bound states within the tunnel (4 Å, in grey) are given. Each box with roman numbers represents a replica of 500 ns length; P2, 4, 6, and 8 denote the random starting position of the ligand. The arrow highlights the frame with lowest $RMSD_d$, whose configuration is depicted (in color) and overlaid to the docking pose (in grey) within the *Sa*NSR binding site. The positions of the ligand in previous frames are also reported in terms of the centers of mass (spheres) in order to show the path leading to a bound state. Fig. S2D shows the binding events for all the replicas of MD simulations performed.

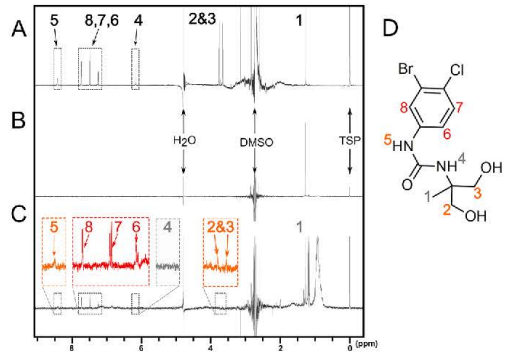

Fig. 6. STD NMR of compound NPG9 in complex with *Sa*NSR. (A) Reference 1D ^{1}H NMR (STD-off) spectrum and STD spectrum of a sample containing 1.8 mM of NPG9 compound (B) without and (C) with 18 µM of *Sa*NSR protein. Assignment of the individual peaks for NPG9 is indicated by numbers from 1 to 8, color-coded according to the relative intensity of the STD signal from NPG9 protons. Strong signals (red) for aromatic (positions 6, 7, and 8) and weak signals (orange) for one NH (position 5) and aliphatic CH_2 protons (positions 2 and 3) were detected, which correlate with the proximity to *Sa*NSR. Methyl protons (position 1) are affected by irradiation power spillover (as visible by strong signal in the absence of *Sa*NSR protein in panel B), and one NH signal is not visible (position 4) (both grey colored). (For interpretation of the references to color in this figure legend, the reader is referred to the web version of this article.)

Acknowledgements

This study was funded by the Deutsche Forschungsgemeinschaft (DFG, German Research Foundation) – 270650915 (Research Training Group GRK 2158, TP4a to HG and SS, TP1d to HS and an Emmy Noether grant ET 102/2-1 to ME). We are grateful for computational support by the "Zentrum für Informations und Medientechnologie" at the Heinrich-Heine-Universität Düsseldorf and the computing time provided by the John von Neumann Institute for Computing (NIC) to HG and BF on the supercomputer JURECA at Jülich Supercomputing Centre (JSC) (user ID: HKF7). Funding by Deutsche Forschungsgemeinschaft (DFG) (INST 208/704-1 FUGG) to purchase the hybrid computer cluster used in this study is gratefully acknowledged. The authors acknowledge access to the Jülich-Düsseldorf Biomolecular NMR Center that is jointly run by Forschungszentrum Jülich and Heinrich-Heine-Universität Düsseldorf. The Center for Structural Studies is funded by the Deutsche Forschungsgemeinschaft (DFG Grant number 417919780).

Author contribution

HG and SS conceived and supervised the study; NP and BF performed *in silico* screening; JZK performed *in vivo* assays; MG performed and analyzed STD NMR measurements, and ME contributed to the analysis; AZ performed LC-MS purity assessment; NP performed MD simulations; NP and HG wrote the manuscript; JZK, SS, and HS contributed to the writing.

Appendix A. Supplementary data

Supplementary data to this article can be found online at https://doi.org/10.1016/j.bmc.2019.115079.

References

1. Chen L, et al. Notes from the field: pan-resistant New Delhi Metallo-Beta-Lactamase-producing Klebsiella pneumoniae – Washoe County, Nevada, 2016. *MMWR Morb Mortal Wkly Rep*. 2017;66(1):33.
2. Sahl HG, Bierbaum G. Lantibiotics: biosynthesis and biological activities of uniquely modified peptides from gram-positive bacteria. *Annu Rev Microbiol*. 1998;52:41–79.
3. Dischinger J, Basi Chipalu S, Bierbaum G. Lantibiotics: promising candidates for future applications in health care. *Int J Med Microbiol*. 2014;304(1):51–62.
4. Oppedijk SF, Martin NI, Breukink E. Hit 'em where it hurts: the growing and structurally diverse family of peptides that target lipid-II. *BBA Biomemb*. 2016;1858(5):947–957.
5. Shin JM, et al. Biomedical applications of nisin. *J Appl Microbiol*. 2016;120(6):1449–1465.
6. Rogers LA, Whittier EO. Limiting factors in the lactic fermentation. *J Bacteriol*. 1928;16(4):211–229.
7. Delves-Broughton J, et al. Applications of the bacteriocin, nisin. *Antonie Van Leeuwenhoek*. 1996;69(2):193–202.
8. Hasper HE, et al. An alternative bactericidal mechanism of action for lantibiotic peptides that target lipid II. *Science*. 2006;313(5793):1636–1637.
9. Wiedemann I, et al. Specific binding of nisin to the peptidoglycan precursor lipid II

combines pore formation and inhibition of cell wall biosynthesis for potent antibiotic activity. *J Biol Chem*. 2001;276(3):1772–1779.
10. Hsu ST, et al. The nisin-lipid II complex reveals a pyrophosphate cage that provides a blueprint for novel antibiotics. *Nat Struct Mol Biol*. 2004;11(10):963–967.
11. Khosa S, Alkhatib Z, Smits SH. NSR from Streptococcus agalactiae confers resistance against nisin and is encoded by a conserved nsr operon. *Biol Chem*. 2013;394(11):1543–1549.
12. Froseth BR, McKay LL. Molecular characterization of the nisin resistance region of Lactococcus lactis subsp. lactis biovar diacetylactis DRC3. *Appl Environ Microbiol*. 1991;57(3):804–811.
13. Rawlings ND, et al. The MEROPS database of proteolytic enzymes, their substrates and inhibitors in 2017 and a comparison with peptidases in the PANTHER database. *Nucleic Acids Res*. 2018;46(D1):D624–D632.
14. Sun Z, et al. Novel mechanism for nisin resistance via proteolytic degradation of nisin by the nisin resistance protein NSR. *Antimicrob Agents Chemother*. 2009;53(5):1964–1973.
15. Khosa S, et al. Structural basis of lantibiotic recognition by the nisin resistance protein from Streptococcus agalactiae. *Sci Rep*. 2016:6.
16. Schrödinger Release 2017-1: Schrödinger Suite 2017-1 Protein Preparation Wizard, Schrödinger, LLC, New York, NY, 2017.
17. Banks JL, et al. Integrated modeling program, applied chemical theory (IMPACT). *J Comput Chem*. 2005;26(16):1752–1780.
18. Case DA, et al. *AMBER 2016*. San Francisco: University of California; 2016.
19. Roe DR, Cheatham 3rd TE. PTRAJ and CPPTRAJ: software for processing and analysis of molecular dynamics trajectory data. *J Chem Theory Comput*. 2013;9(7):3084–3095.
20. Hawkins PC, Skillman AG, Nicholls A. Comparison of shape-matching and docking as virtual screening tools. *J Med Chem*. 2007;50(1):74–82.
21. Sterling T, Irwin JJ. ZINC 15–ligand discovery for everyone. *J Chem Inf Model*. 2015;55(11):2324–2337.
22. Hawkins PC, et al. Conformer generation with OMEGA: algorithm and validation using high quality structures from the Protein Databank and Cambridge Structural Database. *J Chem Inf Model*. 2010;50(4):572–584.
23. Schrödinger Release 2017-1: Schrödinger Suite 2017-1 Glide, Schrödinger, LLC, New York, NY, 2017.
24. Schrödinger Release 2017-1: Schrödinger Suite 2017-1 Canvas, S., LLC, New York, NY, 2017.
25. Oprea TI, et al. Is there a difference between leads and drugs? A historical perspective. *J Chem Inf Comput Sci*. 2001;41(5):1308–1315.
26. Frisch MJ, et al. *Gaussian 16, Revision B.01*. Wallingford CT: Gaussian Inc; 2016.
27. Bayly CI, et al. A well-behaved electrostatic potential based method using charge restraints for deriving atomic charges – the resp model. *J Phys Chem*. 1993;97(40):10269–10280.
28. Wang J, et al. Automatic atom type and bond type perception in molecular mechanical calculations. *J Mol Graph Model*. 2006;25(2):247–260.
29. Schafmeister CEAF, Ross WS, Romanovski V. *LEaP*. San Francisco: University of California; 1995.
30. Martinez L, et al. PACKMOL: a package for building initial configurations for molecular dynamics simulations. *J Comput Chem*. 2009;30(13):2157–2164.
31. Jorgensen WL, et al. Comparison of simple potential functions for simulating liquid water. *J Chem Phys*. 1983;79(2):926–935.
32. Salomon-Ferrer R, et al. Routine Microsecond Molecular Dynamics Simulations with AMBER on GPUs. 2. Explicit Solvent Particle Mesh. *Ewald. J Chem Theory Comput*. 2013;9(9):3878–3888.
33. Maier JA, et al. ff14SB: improving the accuracy of protein side chain and backbone parameters from ff99SB. *J Chem Theory Comput*. 2015;11(8):3696–3713.
34. Wang J, et al. Development and testing of a general amber force field. *J Comput Chem*. 2004;25(9):1157–1174.
35. Joung IS, Cheatham 3rd TE. Determination of alkali and halide monovalent ion parameters for use in explicitly solvated biomolecular simulations. *J Phys Chem B*. 2008;112(30):9020–9041.
36. Frieg B, et al. Molecular mechanisms of glutamine synthetase mutations that lead to clinically relevant pathologies. *PLoS Comput Biol*. 2016;12(2):e1004693.
37. Holo H, Nes IF. High-frequency transformation, by electroporation, of lactococcus lactis subsp. cremoris grown with glycine in osmotically stabilized media. *Appl Environ Microbiol*. 1989;55(12):3119–3123.
38. Khosa S, et al. Overexpression, purification, crystallization and preliminary X-ray diffraction of the nisin resistance protein from Streptococcus agalactiae. *Acta Crystallogr F Struct Biol Commun*. 2015;71(Pt 6):671–675.
39. Abts A, et al. Easy and rapid purification of highly active nisin. *Int J Pept*. 2011;2011:175145.
40. Abts A, et al. NisC binds the FxLx motif of the nisin leader peptide. *Biochemistry*. 2013;52(32):5387–5395.
41. Reiners J, et al. The N-terminal region of nisin is important for the BceAB-type ABC transporter NsrFP from Streptococcus agalactiae COH1. *Front Microbiol*. 2017;8:1643.
42. Mayer M, Meyer B. Group epitope mapping by saturation transfer difference NMR to identify segments of a ligand in direct contact with a protein receptor. *J Am Chem Soc*. 2001;123(25):6108–6117.
43. Mayer M, Meyer B. Characterization of ligand binding by saturation transfer difference NMR spectroscopy. *Angew Chem Int Ed Engl*. 1999;38(12):1784–1788.
44. Patani GA, LaVoie EJ. Bioisosterism: a rational approach in drug design. *Chem Rev*. 1996;96(8):3147–3176.
45. Graham TH, et al. Pyrazoles as non-classical bioisosteres in prolylcarboxypeptidase (PrCP) inhibitors. *Bioorg Med Chem Lett*. 2014;24(7):1657–1660.
46. Eisenberg D, Weiss RM, Terwilliger TC. The hydrophobic moment detects periodicity in protein hydrophobicity. *Proc Natl Acad Sci U S A*. 1984;81(1):140–144.
47. Buch I, Giorgino T, De Fabritiis G. Complete reconstruction of an enzyme-inhibitor binding process by molecular dynamics simulations. *Proc Natl Acad Sci U S A*. 2011;108(25):10184–10189.
48. Xia Y, et al. Clean STD-NMR spectrum for improved detection of ligand-protein interactions at low concentration of protein. *Magn Reson Chem*. 2010;48(12):918–924.
49. ChEMBL database (accessed on April 23rd 2019).

SUPPORTING INFORMATION

Small-molecule inhibitors of nisin resistance protein NSR from the human pathogen *Streptococcus agalactiae*

Nicola Porta[a], Julia Zaschke-Kriesche[b], Benedikt Frieg[c,d], Mohanraj Gopalswamy[a], Aleksandra Zivkovic[a], Manuel Etzkorn[d,e,f], Holger Stark[a], Sander H. J. Smits[b,g], Holger Gohlke[a,c,d*]

[a]Institute for Pharmaceutical and Medicinal Chemistry, Heinrich-Heine-Universität Düsseldorf, Universitätsstrasse 1, 40225 Düsseldorf, Germany.

[b]Institute of Biochemistry, Heinrich-Heine-Universität Düsseldorf, Universitätsstrasse 1, 40225 Düsseldorf, Germany.

[c]John von Neumann Institute for Computing (NIC), Jülich Supercomputing Centre (JSC), Forschungszentrum Jülich GmbH, Wilhelm-Johnen-Straße, 52425 Jülich, Germany.

[d]Institute of Complex Systems – Structural Biochemistry (ICS-6), Forschungszentrum Jülich GmbH, Wilhelm-Johnen-Straße, 52425 Jülich, Germany

[e]Institute of Physical Biology, Heinrich-Heine-Universität Düsseldorf, Universitätsstrasse 1, 40225 Düsseldorf, Germany

[f]JuStruct: Jülich Center for Structural Biology, Forschungszentrum Jülich, GmbH, Wilhelm-Johnen-Straße, 52425 Jülich, Germany

[g]Center for Structural Studies, Heinrich-Heine-Universität Düsseldorf, Universitätsstrasse 1, 40225 Düsseldorf, Germany.

Author ORCID
Nicola Porta: 0000-0002-6005-4372
Benedikt Frieg: 0000-0002-7877-0262
Holger Gohlke: 0000-0001-8613-1447

Keywords: antibiotic resistance, lantibiotics, nisin, screening, small-molecule inhibitors

[*]Corresponding author.

Address: Universitätsstr. 1, 40225 Düsseldorf, Germany.

Phone: (+49) 211 81 13662; Fax: (+49) 211 81 13847

E-mail: gohlke@uni-duesseldorf.de.

Supplementary Tables

Table S1. Details of all the compounds tested for *Sa*NSR inhibitory activity[a].

Internal ID, structure	SMILES, ZINC15 ID	Supplier ID	Selection run	Specific growth inhibition[b]	Reduced Nisin IC_{50}[b]	
				150 µM[c]	120 µM[c]	300 µM[c]
NPG8 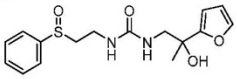	CC(CNC(=O)NCCS(=O)C1=CC=CC=C1)(C2=CC=CO2)O **ZINC78942111**	Enamine Z1283395717	1st	13.37 ± 1.42	-	-
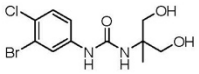	CC(CO)(CO)NC(=O)NC1=CC(=C(C=C1)Cl)Br **ZINC92822447**	Enamine Z1578208899	1st	57.91 ± 1.72	50.5 ± 1.5	n.d.
NPG11 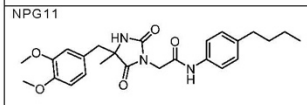	CCCCC1=CC=C(C=C1)NC(=O)CN2C(=O)C(NC2=O)(C)CC3=CC(=C(C=C3)OC)OC **ZINC8724100**	Enamine Z16204276	1st	14.09 ± 4.61	-	-
NPG12 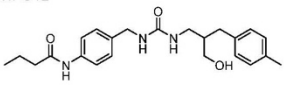	CCCC(=O)NC1=CC=C(C=C1)CNC(=O)NCC(C2=CC=C(C=C2)C)CO **ZINC252486134**	Enamine Z1828067648	1st	19.56 ± 3.30	-	-

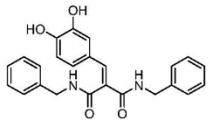	O=C(NCC1=CC=CC=C1)C(=CC1=CC=C(O)C(O)=C1)C(=O)NCC1=CC=CC=C1 **ZINC6628261**	Enamine Z46085255	1st	16.89 ± 3.61	-	32.2 ± 5.0
NPG14 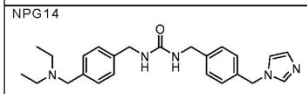	CCN(CC)CC1=CC=C(C=C1)CNC(=O)NCC2=CC=C(C=C2)CN3C=CN=C3 **ZINC45606131**	Enamine Z484300464	1st	< 1	-	-
NPG15 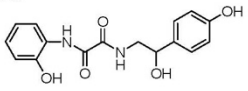	C1=CC=C(C(=C1)NC(=O)C(=O)NCC(C2=CC=C(C=C2)O)O)O **ZINC44890675**	Vitas STK929988	1st	13.55 ± 2.08	-	-
NPG16 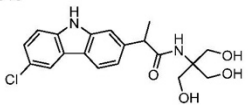	CC(C1=CC2=C(C=C1)C3=C(N2)C=CC(=C3)Cl)C(=O)NC(CO)(CO)CO **ZINC8990409**	Vitas STK622987	1st	8.21 ± 6.99	-	-

NPG17 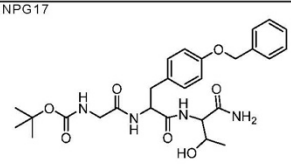	CC(C(C(=O)N)NC(=O)C(CC1=CC=C(C=C1)OCC2=CC=CC=C2)NC(=O)CNC(=O)OC(C)(C)C)O **ZINC4016472**	Vitas STK368270	1st	17.51 ± 1.80	-	-
NPG18 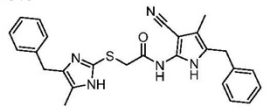	CC1=C(NC(=C1C#N)NC(=O)CSC2=NC(=C(N2)C)C3=CC=CC=C3)CC4=CC=CC=C4 **ZINC12372029**	Vitas STK510666	1st	15.32 ± 6.07	-	-
NPG19 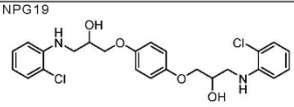	C1=CC=C(C(=C1)NCC(COC2=CC=C(C=C2)OCC(CNC3=CC=CC=C3Cl)O)O)Cl **ZINC1514727**	Vitas STL337299	1st	< 1	-	-
NPG20 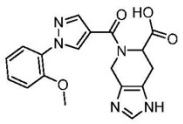	COC1=C(C=CC=C1)[N]2C=C(C=N2)C(=O)N3CC4=C(CC3C(O)=O)[NH]C=N4 **ZINC95530407**	ChemBridge Corporation 96091890 (MolPort-028-743-236)	2nd	10.75 ± 7.79	-	-

NPG21 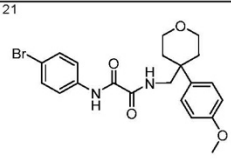	COC1=CC=C(C=C1)C2(CCOCC2)CNC(=O)C(=O)NC3=CC=C(Br)C=C3 **ZINC16856861**	ChemDiv, Inc. D176-0033 (MolPort-001-779-206)	2nd	< 1	-	-
NPG22 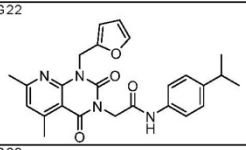	CC(C)C1=CC=C(NC(=O)CN2C(=O)N(CC3=CC=CO3)C4=NC(=CC(=C4C2=O)C)C)C=C1 **ZINC12446300**	ChemDiv, Inc. J026-0296 (MolPort-006-387-850)	2nd	< 1	-	-
NPG23 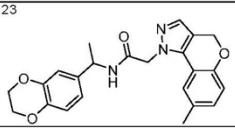	CC(NC(=O)C[N]1N=CC2=C1C3=CC(=CC=C3OC2)C)C4=CC5=C(OCCO5)C=C4 **ZINC6819698**	ChemDiv, Inc. C762-0210 (MolPort-007-666-849)	2nd	< 1	-	-
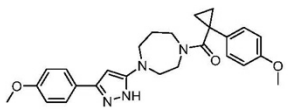	COC1=CC=C(C=C1)C2=N[NH]C(=C2)N3CCCN(CC3)C(=O)C4(CC4)C5=CC=C(OC)C=C5 **ZINC169753176**	ChemDiv, Inc. P803-1933 (MolPort-039-020-386)	2nd	20.66 ± 4.56	-	20.5 ± 12.1

NPG25 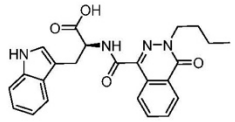	CCCCN1N=C(C(=O)N[C@@H](CC2=C[NH]C3=CC=CC=C23)C(O)=O)C4=C(C=CC=C4)C1=O **ZINC13117738**	ENAMINE Ltd. Z98653619 (MolPort-003-325-779)	2nd	3.21 ± 3.91	-	-
NPG26 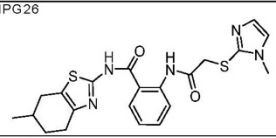	CC1CCC2=C(C1)SC(=N2)NC(=O)C3=C(NC(=O)CSC4=NC=C[N]4C)C=CC=C3 **ZINC9245226**	ENAMINE Ltd. Z70812187 (MolPort-005-510-624)	2nd	1.38 ± 3.28	-	-
NPG27 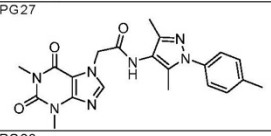	CN1C(=O)N(C)C2=C([N](CC(=O)NC3=C(C)[N](N=C3C)C4=CC=C(C)C=C4)C=N2)C1=O **ZINC5117887**	ENAMINE Ltd. Z112210324 (MolPort-009-388-359)	2nd	14.20 ± 3.49	-	-
NPG28 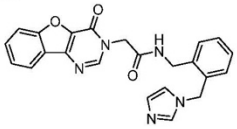	O=C(CN1C=NC2=C(OC3=CC=CC=C23)C1=O)NCC4=CC=CC=C4C[N]5C=CN=C5 **ZINC32860056**	ENAMINE Ltd. Z203879860 (MolPort-009-426-367)	2nd	< 1	-	-

NPG29 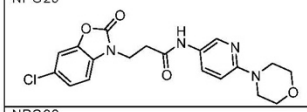	ClC1=CC=C2N(CCC(=O)NC3=CN=C(C=C3)N4CCOCC4)C(=O)OC2=C1 **ZINC32873596**	ENAMINE Ltd. Z220578738 (MolPort-009-435-905)	2nd	18.98 ± 2.43	-	-
NPG30 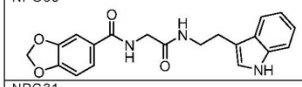	O=C(CNC(=O)C1=CC=C2OCOC2=C1)NCCC3=C[NH]C4=CC=CC=C34 **ZINC13002934**	ENAMINE Ltd. Z32439864 (MolPort-009-511-291)	2nd	< 1	-	-
NPG31 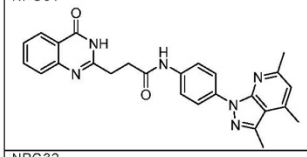	CC1=NC2=C(C(=C1)C)C(=N[N]2C3=CC=C(NC(=O)CCC4=NC5=CC=CC=C5C(=O)N4)C=C3)C **ZINC32925584**	ENAMINE Ltd. Z414857148 (MolPort-009-641-465)	2nd	< 1	-	1.9 ± 4.5
NPG32 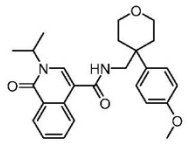	COC1=CC=C(C=C1)C2(CCOCC2)CNC(=O)C3=CN(C(C)C)C(=O)C4=CC=CC=C34 **ZINC72324948**	Eximed EiM08-24723 (MolPort-019-950-482)	2nd	4.86 ± 5.53	-	-

NPG33 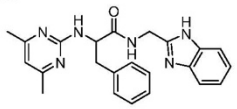	CC1=NC(=NC(=C1)C)NC(CC2=CC=CC=C2)C(=O)NCC3=NC4=C([NH]3)C=CC=C4 **ZINC218333282**	Eximed EiM08-37860 (MolPort-035-704-400)	2nd	< 1	-	n.d.
NPG34 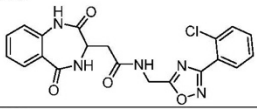	ClC1=CC=CC=C1C2=NOC(=N2)CNC(=O)CC3NC(=O)C4=CC=CC=C4NC3=O **ZINC253411316**	Eximed EiM08-40467 (MolPort-039-347-548)	2nd	< 1	-	-
NPG35 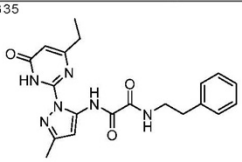	CCC1=CC(=O)NC(=N1)[N]2N=C(C)C=C2NC(=O)C(=O)NCCC3=CC=CC=C3 **ZINC9037777**	Life Chemicals Inc. F2353-0133 (MolPort-003-119-349)	2nd	< 1	-	-
NPG36 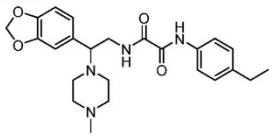	CCC1=CC=C(NC(=O)C(=O)NCC(N2CCN(C)CC2)C2=CC3=C(OCO3)C=C2)C=C1 **ZINC20614320**	Life Chemicals Inc. F2573-0077 (MolPort-003-137-918)	2nd	6.03 ± 8.68	-	-

8

NPG37 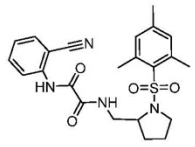	CC1=CC(C)=C(C(C)=C1)S(=O)(=O)N1CCCC1CNC(=O)C(=O)NC1=C(C=CC=C1)C#N **ZINC9806342**	Life Chemicals Inc. F2574-0245 (MolPort-003-138-270)	2nd	< 1	-	-
NPG38 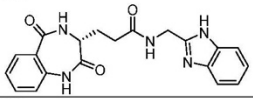	O=C(CC[C@H]1NC(=O)C2=C(NC1=O)C=CC=C2)NCC3=NC4=C([NH]3)C=CC=C4 **ZINC206231654**	Otava, Ltd. 11182550 (MolPort-039-347-724)	2nd	9.95 ± 2.76	-	-
NPG39 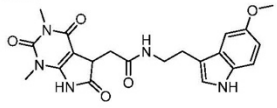	COC1=CC2=C([NH]C=C2CCNC(=O)CC3C(=O)NC4=C3C(=O)N(C)C(=O)N4C)C=C1 **ZINC8764885**	Pharmeks, Ltd. PHAR270111 (MolPort-002-536-737)	2nd	11.32 ± 2.45	-	-
NPG40 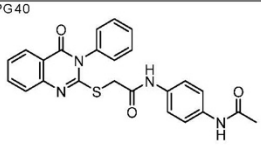	CC(=O)NC1=CC=C(NC(=O)CSC2=NC3=C(C=CC=C3)C(=O)N2C4=CC=CC=C4)C=C1 **ZINC9375995**	UkrOrgSynthesis Ltd. Stock PB19471594 (MolPort-003-349-336)	2nd	7.58 ± 1.95	-	-

9

NPG41 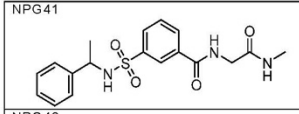	CNC(=O)CNC(=O)C1=CC(=CC=C1)[S](=O)(=O)NC(C)C2=CC=CC=C2 **ZINC14014863**	UkrOrgSynthesis Ltd. Stock PB52410938 (MolPort-004-553-563)	2nd	7.92 ± 2.12	-	-
NPG42 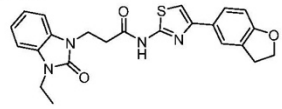	CCN1C(=O)N(CCC(=O)NC2=NC(=CS2)C3=CC4=C(OCC4)C=C3)C5=CC=CC=C15 **ZINC32869020**	UkrOrgSynthesis Ltd. Stock PB218366878 (MolPort-009-621-062)	2nd	< 1	-	-
NPG43 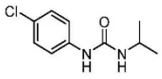	CC(C)NC(=O)NC1=CC=C(Cl)C=C1	ENAMINE Ltd Z44580876 (MolPort-001-837-585)	3rd	-	-	< 1
NPG44 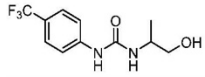	CC(CO)NC(=O)NC1=CC=C(C=C1)C(F)(F)F	ENAMINE Ltd Z409949780 (MolPort-009-050-473)	3rd	-	-	< 1
NPG45 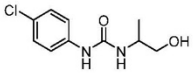	CC(CO)NC(=O)NC1=CC=C(Cl)C=C1	ENAMINE Ltd Z332430512 (MolPort-009-268-177)	3rd	-	-	< 1

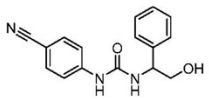	OCC(NC(=O)NC1=CC=C(C=C1)C#N)C2=CC=CC=C2	ENAMINE Ltd Z500741592 (MolPort-011-908-152)	3rd	-	8.1 ± 7.0	13.5 ± 6.4
NPG47 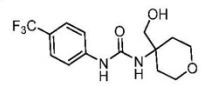	OCC1(CCOCC1)NC(=O)NC2=CC=C(C=C2)C(F)(F)F	ENAMINE Ltd Z1127202114 (MolPort-019-685-112)	3rd	-	< 1	< 1
NPG48 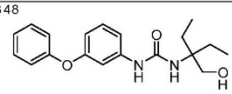	CCC(CC)(CO)NC(=O)NC1=CC(=CC=C1)OC2=CC=CC=C2	ENAMINE Ltd Z1341324083 (MolPort-023-183-503)	3rd	-	-	< 1
NPG49 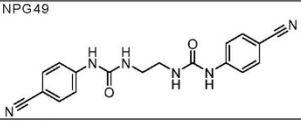	O=C(NCCNC(=O)NC1=CC=C(C=C1)C#N)NC2=CC=C(C=C2)C#N	ENAMINE Ltd Z1004228850 (MolPort-023-230-374)	3rd	-	-	< 1
NPG50 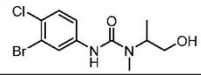	CC(CO)N(C)C(=O)NC1=CC(=C(Cl)C=C1)Br	ENAMINE Ltd Z1620605386 (MolPort-029-931-250)	3rd	-	-	n.d.

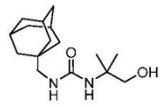	CC(C)(CO)NC(=O)NC C12CC3CC(CC(C3)C1)C2	Life Chemicals Inc F1130-0104 (MolPort-002-237-133)	3rd	-	4.0 ± 4.4	8.5 ± 5.8
NPG52 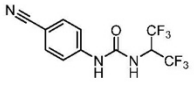	FC(F)(F)C(NC(=O)NC1 =CC=C(C=C1)C#N)C(F)(F)F	Specs AK-968/40332480 (MolPort-002-791-780)	3rd	-	-	n.d.
NPG54 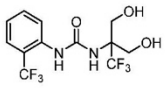	OCC(CO)(NC(=O)NC1 =C(C=CC=C1)C(F)(F)F)C(F)(F)F	UkrOrgSynthesis Ltd. Stock PB2683130118 (MolPort-044-379-453)	3rd	-	< 1	< 1
NPG55 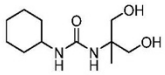	CC(CO)(CO)NC(=O)N C1CCCCC1	Vitas-M Laboratory, Ltd. (Premium) STK149406 (MolPort-001-537-543)	3rd	-	-	< 1

[a]Values were determined by at least three independent experiments. Measurements not performed are reported as "-". Specific growth inhibition or reduced nisin IC_{50} values lower than 1% are marked as "< 1". In cases where the solubility of the compound was not compatible with the concentration required in the assay, leading to precipitation, or where the compound was inhibiting the cell growth even without nisin, the measurement was marked as not determinable, "n.d.". If not reported with explicit stereochemistry notation, the undefined stereochemical mixture was tested.

[b]In %.

[c]Used compound concentration.

Table S2. Cluster summary of unspecific binding events.

Cluster	Frac[a]	AvgDist[b] [Å]	StDev[c] [Å]	AvgCDist[d] [Å]	C0 Ratio[e]
C0	0.19	0.54	0.19	1.78	1.00
C1	0.17	0.51	0.19	1.79	0.92
C2	0.14	0.51	0.19	1.80	0.77
C3	0.10	0.45	0.17	1.79	0.53
C4	0.10	0.50	0.18	1.78	0.52
C5	0.09	0.54	0.22	1.87	0.46
C6	0.08	0.52	0.18	1.75	0.40
C7	0.07	0.54	0.20	1.83	0.39
C8	0.05	0.52	0.20	1.76	0.24

[a]Cluster size as fraction of total frames where $RMSD_p \leq 2.5$ Å.

[b]Average distance between points in the cluster.

[c]Standard deviation of points in the cluster.

[d]Average distance of this cluster to every other cluster.

[e]C0 ratio represents the fold difference with the most populated cluster.

Supplementary Figures

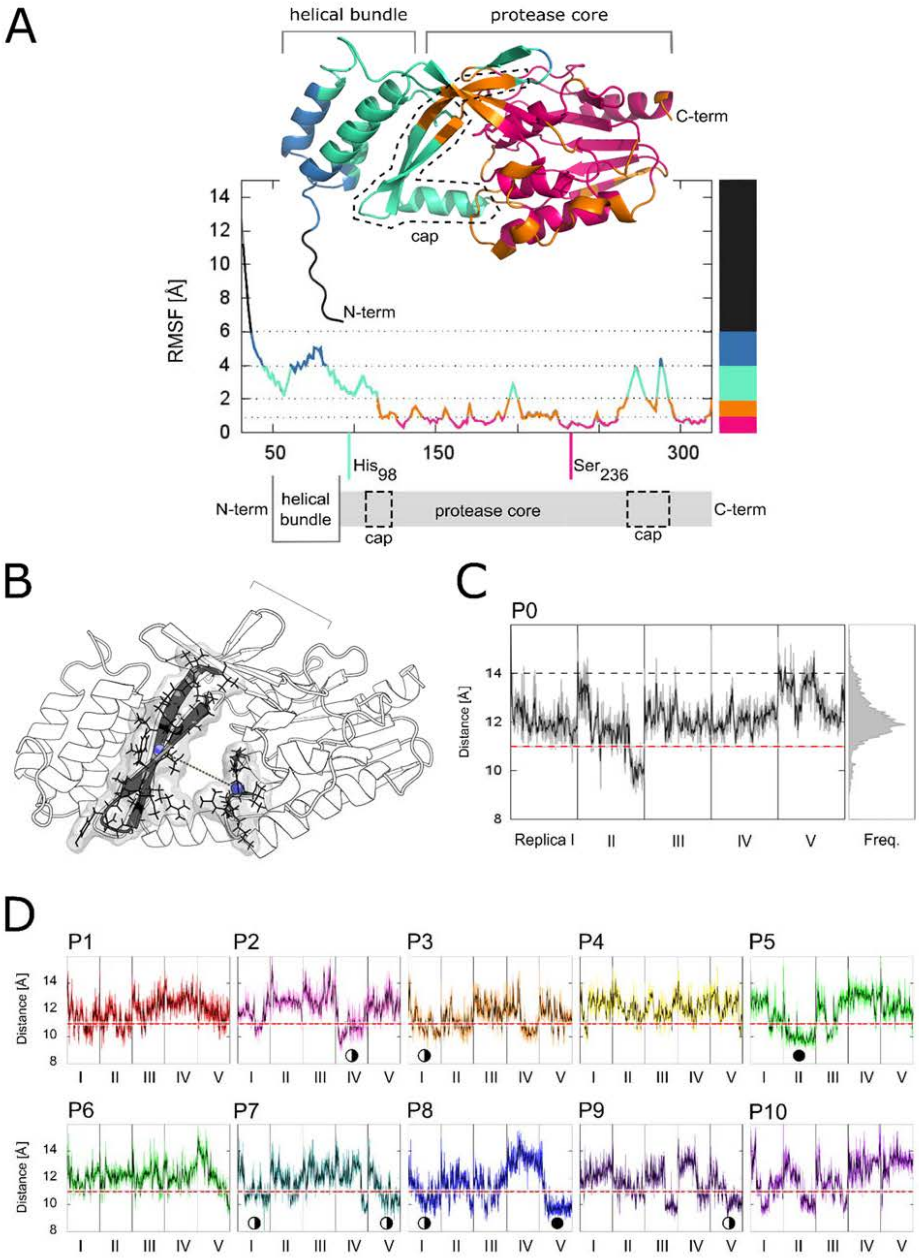

14

Figure S1. Mobility of the cap domain. (A) *Sa*NSR mobility expressed as RMSF of C_α atoms after fitting on the 10% least mobile residues, averaged over 50 fldMD simulations; in addition to the line plot, the values are mapped onto the cartoon representation according to the color scale. The helical bundle, cap, and protease core domains are highlighted, as are the residues of the catalytic dyad. **(B)** Distance between the center of mass of the β-hairpin (263-TVNETFMLYDGARLALTTGIV-283) and the short loop regions of the protease core facing the tunnel (134-ISKL-137 and 169-TGGN-172). This distance was considered to evaluate the opening (when > 11 Å) and closing (when ≤ 11 Å) of the cap domain. The β-hairpin and the two loop regions are highlighted in grey, and their centers of mass are shown in blue. **(C)** Opening and closing of the cap domain for five bound MD simulations, started from the docking pose (P0). The distance in the crystal structure (~ 14 Å) and the cutoff considered (11 Å) are shown as grey and red dotted lines, respectively. (**D)** Opening and closing of the cap domain for 50 fldMD simulations, started from 10 random positions (P1 to P10). Replicas where the cap domain is closed in > 75 % or 50-75 % of the frames are highlighted with full- or half-colored circles, respectively. Each box with a roman number represents a replica of 500 ns length.

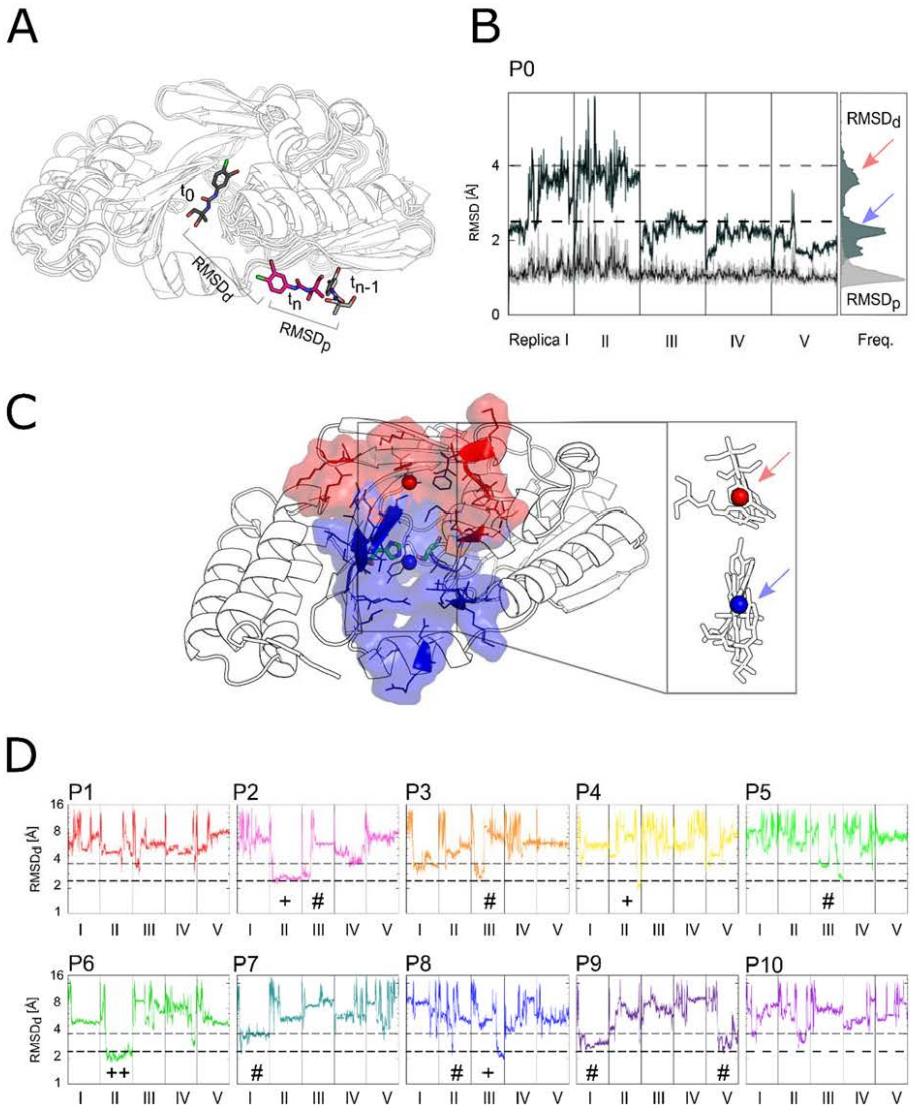

Figure S2. Analysis of NPG9 binding events. (A) Illustrative representation of RMSD measurement of NPG9 with respect to the docking pose ($RMSD_d$) and to the previous frame ($RMSD_p$). Conformations with $RMSD_p \leq 2.5$ Å are considered bound to the protein (unspecific binding), while with the ones with $RMSD_d \leq 2.5$ Å are considered stably bound to the pocket (specific binding). **(B)** RMSD time evolution of NPG9 during five bound MD simulations, started from the docking pose (P0). **(C)** *Sa*NSR depiction showing two groups of representative ligand conformations inside the tunnel. Conformations of the five bound MD simulations were clustered using 1.5 Å as cutoff. The centers of mass of the ligand are shown as blue and red spheres, and residues at a distance ≤ 4 Å are depicted as surface. Residues of the catalytic dyad are shown as green sticks. **(D)** $RMSD_d$ time evolution of NPG9 during 50 fldMD simulations, started from 10 random positions (P1 to P10). Replicas where the bound frames ($RMSD_d \leq 2.5$ Å) represent > 0 %, > 10 % and > 50% of the total are marked with "#", "+" and "++", respectively. Dashed lines representing the cutoff values for binding (2.5 Å, in black) and for pre-bound states within the tunnel (4 Å, in grey) are given. Each box with roman numbers represents a replica of 500 ns length.

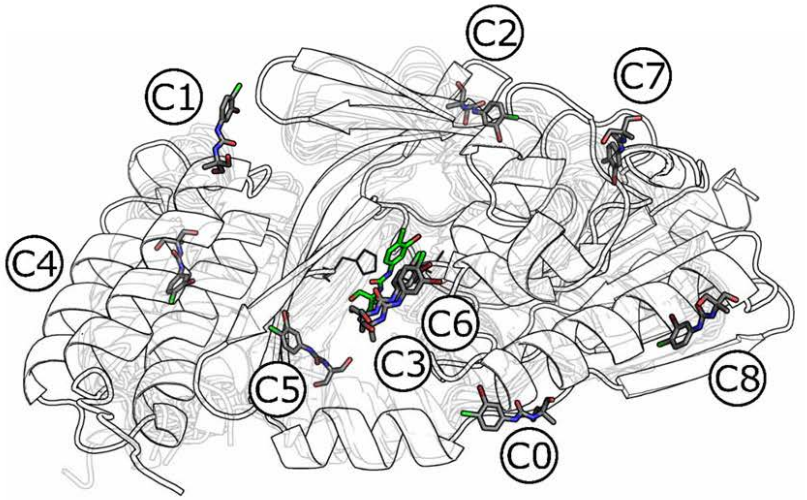

Figure S3. Unspecific binding events. Unspecific binding events of NPG9 during 50 fldMD simulations, defined as conformations with $RMSD_p \leq 2.5$ Å. The docking pose is also reported as green sticks. Conformations were clustered using a cutoff value for forming clusters of 1.5 Å (see also Table S2). Clusters containing less than 5% of the structures were ignored. The nine most populated clusters relate to 97.5% of all conformations.

A

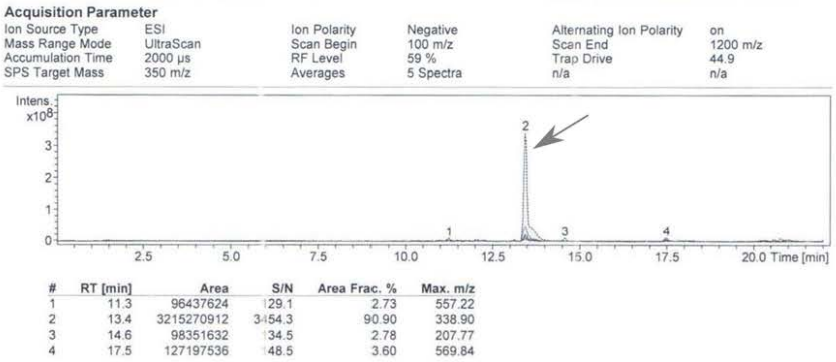

#	RT [min]	Area	S/N	Area Frac. %	Max. m/z
1	11.3	96437624	129.1	2.73	557.22
2	13.4	3215270912	3454.3	90.90	338.90
3	14.6	98351632	34.5	2.78	207.77
4	17.5	127197536	48.5	3.60	569.84

B

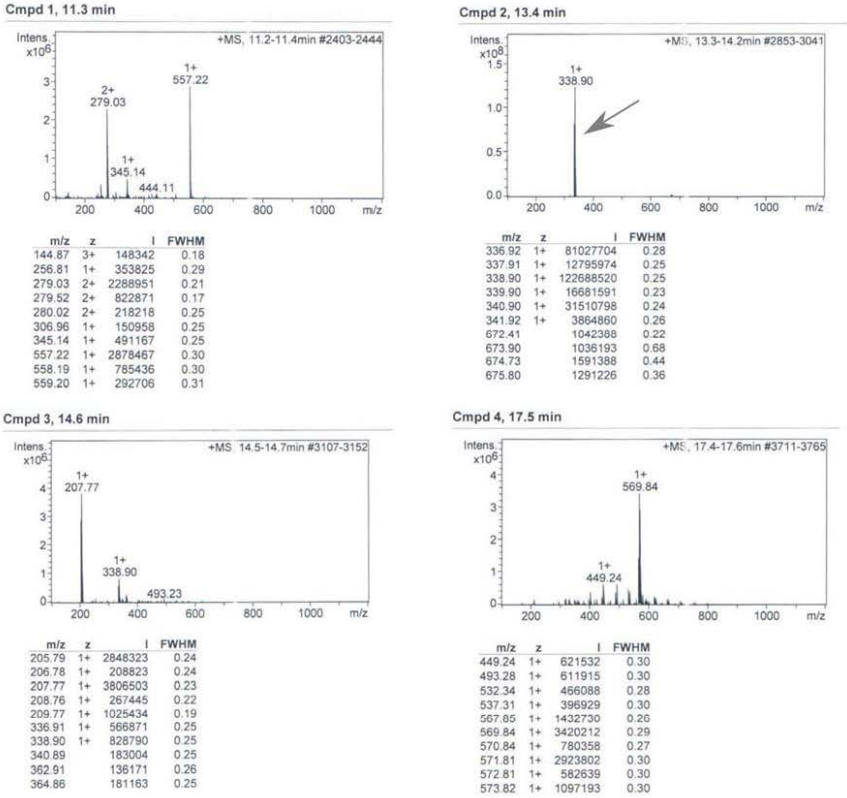

m/z	z	I	FWHM
144.87	3+	148342	0.18
256.81	1+	353825	0.29
279.03	2+	2288951	0.21
279.52	2+	822871	0.17
280.02	2+	218218	0.25
306.96	1+	150958	0.25
345.14	1+	491167	0.25
557.22	1+	2878467	0.30
558.19	1+	785436	0.30
559.20	1+	292706	0.31

m/z	z	I	FWHM
336.92	1+	81027704	0.28
337.91	1+	12795974	0.25
338.90	1+	122688520	0.25
339.90	1+	16681591	0.23
340.90	1+	31510798	0.24
341.92	1+	3864860	0.26
672.41		1042388	0.22
673.90		1036193	0.68
674.73		1591388	0.44
675.80		1291226	0.36

m/z	z	I	FWHM
205.79	1+	2848323	0.24
206.78	1+	208823	0.24
207.77	1+	3806503	0.23
208.76	1+	267445	0.22
209.77	1+	1025434	0.19
336.91	1+	566871	0.25
338.90	1+	828790	0.25
340.89		183004	0.25
362.91		136171	0.26
364.86		181163	0.25

m/z	z	I	FWHM
449.24	1+	621532	0.30
493.28	1+	611915	0.30
532.34	1+	466088	0.28
537.31	1+	396929	0.30
567.85	1+	1432730	0.26
569.84	1+	3420212	0.29
570.84	1+	780358	0.27
571.81	1+	2923802	0.30
572.81	1+	582639	0.30
573.82	1+	1097193	0.30

Figure S4. LC-MS spectra of compound NPG9 (M = 337.60 Da). (A) LC chromatogram. The relative purity equals 90.90%. (B) MS spectrum, the peaks corresponding to NPG9 (M+1) are highlighted with an arrow. Method 1 was used.

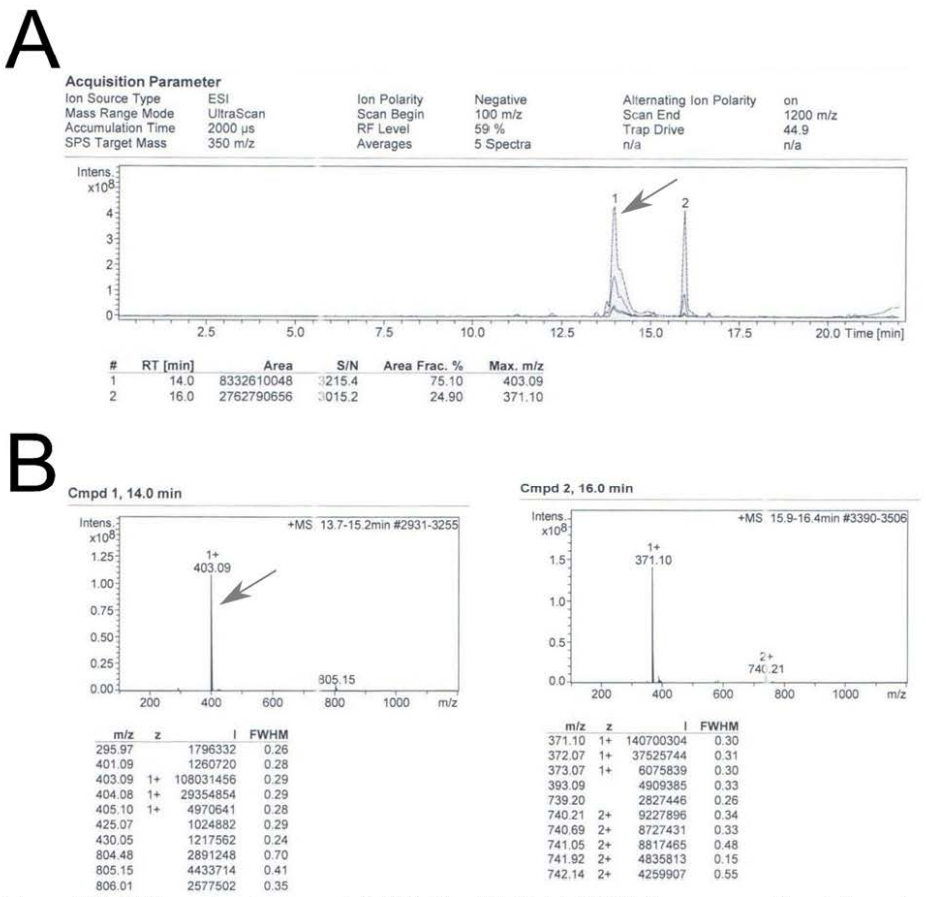

Figure S5. LC-MS spectra of compound NPG13 (M = 402.16 Da). (A) LC chromatogram. The relative purity equals 75.10%, the main peak of the impurity corresponds to a derivative without hydroxyls (M=370.17 Da). (B) MS spectrum, the peaks corresponding to NPG13 (M+1) are highlighted with an arrow. Method 1 was used.

A

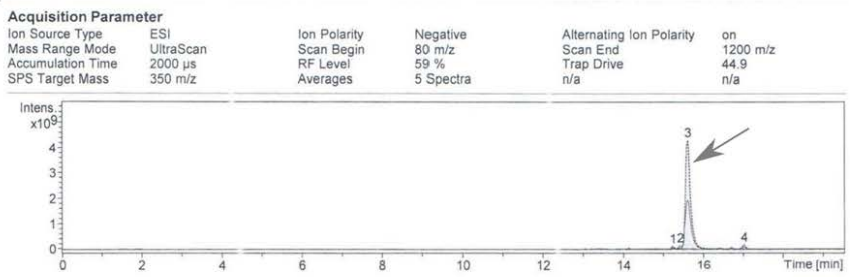

Acquisition Parameter

Ion Source Type	ESI	Ion Polarity	Negative	Alternating Ion Polarity	on
Mass Range Mode	UltraScan	Scan Begin	80 m/z	Scan End	1200 m/z
Accumulation Time	2000 µs	RF Level	59 %	Trap Drive	44.9
SPS Target Mass	350 m/z	Averages	5 Spectra	n/a	n/a

B

#	RT [min]	Area	S/N	Area Frac. %	Max. m/z
1	15.2	507817696	980.1	1.21	389.18
2	15.4	495698176	1042.6	1.18	330.13
3	15.6	39341142016	40577.5	93.51	447.21
4	17.0	1726738560	2094.3	4.10	445.21

Cmpd 1, 15.2 min

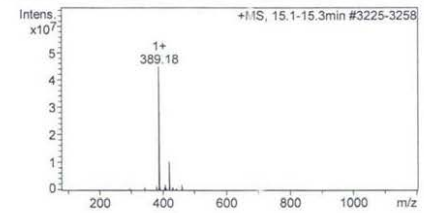

m/z	z	I	FWHM
381.60		877096	0.22
389.18	1+	44850652	0.29
390.15	1+	11662986	0.28
391.17	1+	1887424	0.26
410.13	2+	2269866	0.16
410.64	2+	917598	0.16
421.17	1+	10454289	0.28
422.17	1+	2984156	0.29
433.20		955477	0.30
461.18		1145122	0.26

Cmpd 2, 15.4 min

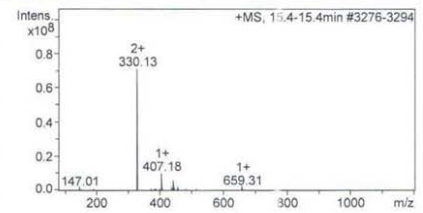

m/z	z	I	FWHM
147.01		1540652	0.19
330.13	2+	71004056	0.19
330.58	2+	29798656	0.21
331.08	2+	5742719	0.26
407.18	1+	10178943	0.30
408.18	1+	2736588	0.31
439.04		1819120	0.23
445.18	1+	6110586	0.31
446.17	1+	2030738	0.26
659.31	1+	1860640	0.31

Cmpd 3, 15.6 min

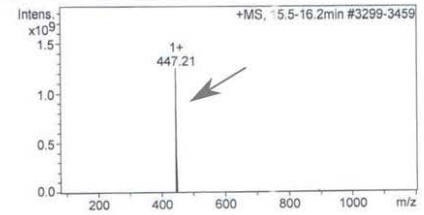

m/z	z	I	FWHM
447.21	1+	1247200000	0.30
448.17	1+	370809888	0.30
449.20	1+	65276212	0.29
450.20	1+	7247452	0.26
892.25		3313241	0.13
892.53		5996038	0.24
893.12		12632767	0.58
893.31		13947635	0.56
894.38		6065583	0.54
895.35		3901530	0.20

Cmpd 4, 17.0 min

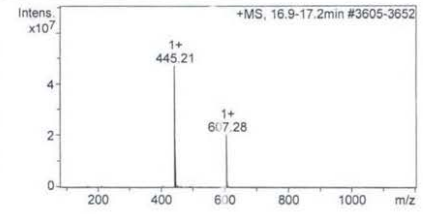

m/z	z	I	FWHM
212.08		585871	0.26
445.21	1+	47235160	0.30
446.18	1+	13304784	0.29
447.18	1+	4071773	0.29
448.18	1+	742434	0.30
449.21		600744	0.27
453.20		716972	0.26
607.28	1+	20478030	0.27
608.26	1+	7681689	0.32
609.27	1+	1535233	0.34

Figure S6. LC-MS spectra of compound NPG24 (M = 446.55 Da). (A) LC chromatogram. The relative purity equals 93.51%. (B) MS spectrum, the peaks corresponding to NPG24 (M+1) are highlighted with an arrow. Method 2 was used.

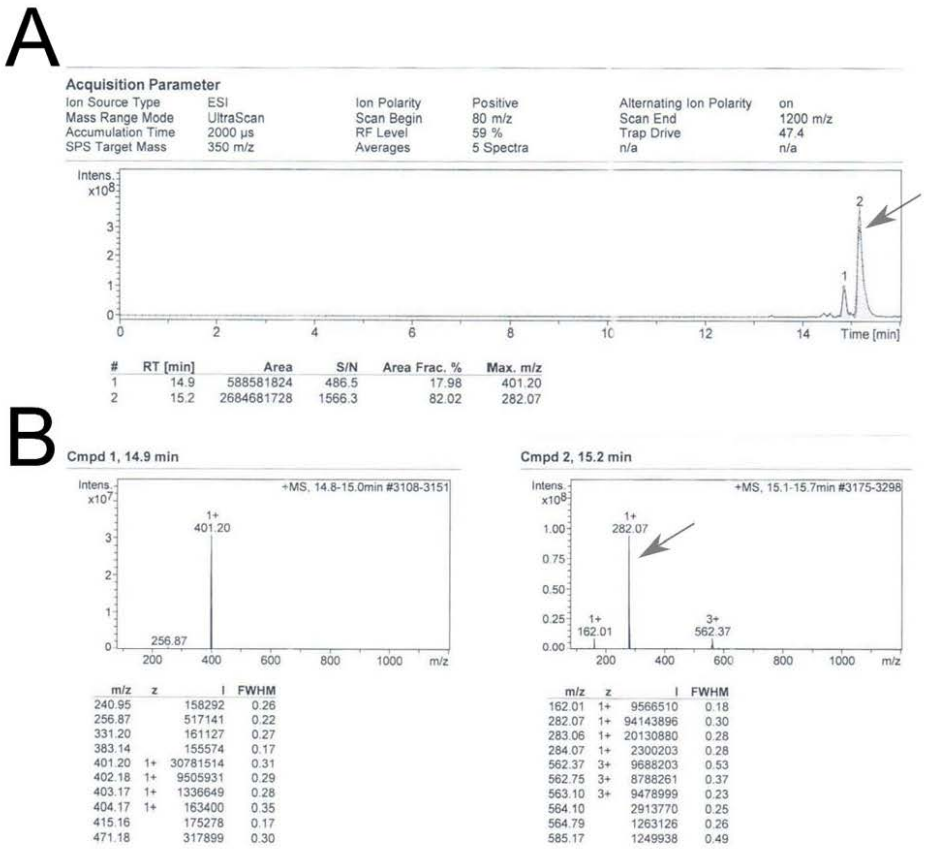

Figure S7. LC-MS spectra of compound NPG46 (M = 281.32 Da). (A) LC chromatogram. The relative purity equals 82.02%. (B) MS spectrum, the peaks corresponding to NPG46 (M+1) are highlighted with an arrow. Method 2 was used.

A

Acquisition Parameter

Ion Source Type	ESI	Ion Polarity	Negative	Alternating Ion Polarity	on
Mass Range Mode	UltraScan	Scan Begin	80 m/z	Scan End	1200 m/z
Accumulation Time	2000 µs	RF Level	59 %	Trap Drive	44.9
SPS Target Mass	350 m/z	Averages	5 Spectra	n/a	n/a

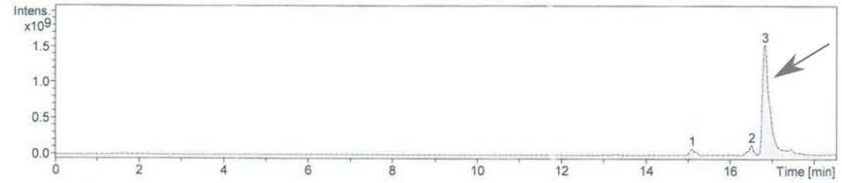

#	RT [min]	Area	S/N	Area Frac. %	Max. m/z
1	15.1	2304874752	1491.5	9.27	425.31
2	16.5	1299167360	1501.6	5.22	315.16
3	16.8	21265432576	15496.7	85.51	281.17

B

Cmpd 1, 15.1 min

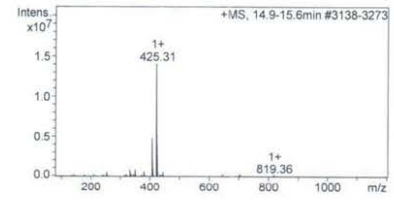

m/z	z	I	FWHM
256.89		608871	0.26
336.20	1+	854016	0.29
352.67	2+	823742	0.25
381.65		633303	0.17
410.19	2+	4818470	0.26
410.65	2+	2848737	0.17
411.15	2+	1086942	0.19
425.31	1+	14071638	0.30
426.27	1+	4272831	0.26
427.27	1+	751775	0.22

Cmpd 2, 16.5 min

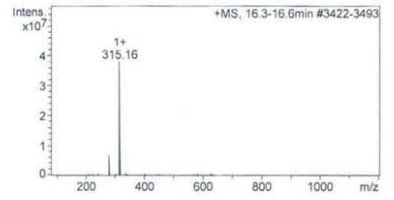

m/z	z	I	FWHM
212.09		415561	0.28
225.11		460054	0.25
281.17	1+	6901984	0.28
282.16	1+	1442877	0.26
315.16	1+	38107964	0.27
316.14	1+	7444280	0.25
317.14	1+	13890192	0.25
318.15	1+	2771121	0.21
319.18	1+	342364	0.26
337.11		529844	0.22

Cmpd 3, 16.8 min

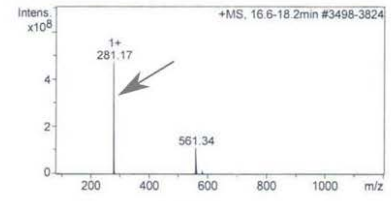

m/z	z	I	FWHM
90.19		4531992	0.29
281.17	1+	472549696	0.28
282.16	1+	94754040	0.27
283.17	1+	12545662	0.23
559.07		5369372	0.16
561.34		111358696	0.96
562.30	1+	35077892	0.56
563.33	1+	9491555	0.37
583.39		9191644	0.27
584.38		3307603	0.40

Figure S8. LC-MS spectra of compound NPG51 (M = 280.41 Da). (A) LC chromatogram. The relative purity equals 85.51%. (B) MS spectrum, the peaks corresponding to NPG51 (M+1) are highlighted with an arrow. Method 2 was used.

3.6. Chapter VI – Mechanism of the ABC Transporter NsrFP

Published in: in preparation

Impact factor:

Own Work: 35 %

Expression and Purification of the proteins

Performing biological and biochemical assays

Preparation of the figures

Writing the manuscript

Mechanism of the BceAB-type transporter NsrFP from *Streptococcus agalactiae*

Julia Zaschke-Kriesche, Sandra Unsleber, Irina Voitsekhovskaia, Andreas Kulik, Nina Overbeck, Jelle Postma, Stefanie Weidtkamp-Peters, Kai Stühler, Evi Stegmann and Sander H.J. Smits

Mechanism of the BceAB-type transporter NsrFP from *Streptococcus agalactiae*

Julia Zaschke-Kriesche[a], Sandra Unsleber[b], Irina Voitsekhovskaia[b], Andreas Kulik[b], Nina Overbeck[c], Jelle Postma[d], Stefanie Weidtkamp-Peters[d], Kai Stühler[c], Evi Stegmann[b] and Sander H.J. Smits[a,e*]

[a] *Institute of Biochemistry, Heinrich-Heine-University Duesseldorf, Universitaetsstrasse 1, 40225 Duesseldorf, Germany.*

[b] *Interfaculty Institute of Microbiology and Infection Medicin, Eberhard Karls University, Auf der Morgenstelle 28, 72076 Tübingen, Germany.*

[c] *Molecular Proteomics Laboratory, Heinrich-Heine-University Duesseldorf, Universitaetsstrasse 1, 40225 Duesseldorf, Germany.*

[d] *Center for Advanced Imaging, Heinrich-Heine-University Duesseldorf, Universitaetsstrasse 1, 40225 Duesseldorf, Germany.*

[e] *Center of Structural Studies Heinrich-Heine-University Duesseldorf, Universitaetsstrasse 1, 40225 Duesseldorf, Germany.*

*Corresponding author: Sander.Smits@hhu.de

Keywords: BceAB-type, antibiotic resistance, nisin, bacitracin, lipid II

Abstract

Treatment of bacterial infections are the great challenge of our era due to the evolved resistance mechanisms against antibiotics. Here we elucidate the mechanism of the BceAB-type transporer NsrFP from *Streptococcus agalactiae* COH1, which is encoded on one operon with a two-component system NsrRK and the nisin resistance protein (NSR).

This study shows an expanded substrate specificity of *Sa*NsrFP not only against lantibiotics, like nisin and gallidermin, but also against several other antimicrobial compounds suggesting a general transport mechanism. Interestingly, a remarkable high fold of resistance was detected for bacitracin. Investigation on the growth behavior, the cell wall composition as well as proteome analysis pointed to the same mechanism of *Sa*NsrFP, acting as a model system for all BceAB-type transporter. In this study we elucidate this overall mechanism and demonstrate that *Sa*NsrFP confers resistance due to a flipping of the cell wall precursor lipid II into the cytosol.

Introduction

Bacterial infection cause over 150,000 death every year and are the major threat for humans (1-4). Treatments have been possible by the development of antibiotics which have been around since 1917 starting with penicillin (5). In recent years however antibiotic resistance has become a great challenge, and targeted bacteria evolved several different resistance mechanisms (6). The Achilles' heel of bacteria was shown to be the essential cell wall precursor lipid II (7). Besides lipid II itself also its biosynthesis and recycling pathway, are potent targets for new antibiotic compounds (8). The bacterial cell wall is composed of peptidoglycan, a polymer of N-acetylmuramic acid (MurNAc) and N-acetylglucosamine (GlcNAc) cross-linked by a pentapeptide (9). Briefly, lipid I is built in the cytoplasm by MraY attaching UDP-MurNAc-pentapeptide to the lipid carrier undecaprenyl phosphate (UP), sequentially UDP-GlcNAc is attached through MurG resulting in lipid II. The peptidoglycan precursor is afterwards flipped to the extracellular space (or periplasm in Gram-negative bacteria), still anchored to the membrane *via* undecaprenyl. Subsequently, the GlcNAc-MurNAc-pentapeptide subunit is incorporated into the peptidoglycan (PGN), leaving undecaprenyl pyrophosphate (UPP) residing in the membrane. This UPP is then dephosphorylated to undecaprenyl phosphate (UP), which is flipped back into the cytoplasm, and implemented into a new peptidoglycan synthesis cycle (10). Interrupting this cycle effectively results in inhibition of bacteria growth leading to cell death (7, 8). Further when lipid II is targeted the lipid carrier UP is not recycled, conclusively no new lipid II can be synthesized within the cytosol.

This lipid II cycle has been the target of numerous natural and chemically derived antimicrobial compounds, for example binding to different moieties of lipid II like the pyrophosphate moiety (Lantibiotics like nisin and gallidermin) or the pentapeptide (Glycopeptides like vancomycin) or in the case of bacitracin the target is UPP. One specific class are small antimicrobial peptides (AMPs), specifically binding to lipid II called bacteriocins (11). They target lipid II like acylcyclodepsipeptides, lipoglycodepsipeptides and glycopeptide antibiotics. A member of the acylcyclodepsipeptides is lysobactin, also known as katanosin B, first isolated from a *Lysobacter species* (12, 13). Lysobactin inhibits the peptidoglycan synthesis by binding lipid II in a 1:1 ratio (14), further it is shown to bind to the reducing end of lipid-linked cell wall precursors (14) (Figure 1A).

Ramoplanin is a lipoglycodepsipeptide antibiotic, produced by *Actinoplanes sp.* ATCC 33076 (15, 16). Ramoplanin was shown to bind the pyrophosphate and the muramic acid moiety of lipid II however and in contrast to others it acts as a dimer (8, 17, 18) (Figure 1A).

The glycopeptide antibiotic vancomycin, produced by *Streptomyces orientalis* (19) binds to the D-Ala-D-Ala sequence of the pentapeptide of lipid II (20-22) (Figure 1A). All three display an highly potent activity in the nanomolar range.

In 2015 a novel depsipeptide antibiotic named teixobactin was discovered, which is produced by Gram-negative *Eleftheria terrae* and was shown to bind to the phosphate moiety and the MurNAc of lipid II. Teixobactin shows antimicrobial activity against human pathogens like *M. tuberculosis,* methicillin resistance *S. aureus* and vancomycin resistant *Enterococci* (23).

In addition to antibiotics specifically binding lipid II also other parts of the peptidoglycan synthesis cycle have been proven to be antimicrobial targets. For example, the cyclic peptide bacitracin. Produced by some *Bacillus* species bacitracin has been successfully used in medical treatments against bacterial infections since decades (24-27). The target of bacitracin was shown to be undecaprenyl-pyrophosphate (UPP) thereby preventing the recycling of the lipid carrier resulting in an interrupted peptidoglycan synthesis (28, 29) (Figure 1B).

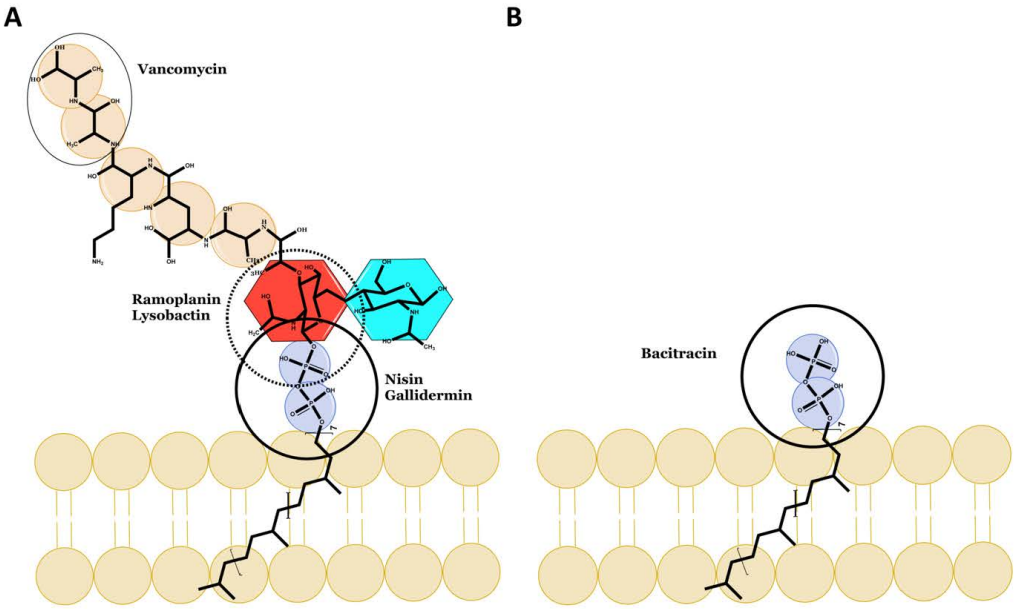

Figure 1: Schematic representation of antibiotics targeting lipid II and UPP. A) Schematic view of lipid II, anchored to the membrane (yellow) with its undecaprenyl-pyrophosphate (blue), N-acetyl muramic acid (red), N-acetyl glucosamine (turquoise) and the pentapeptide Ala-Glu-Lys-(Asn)-Ala-Ala (orange). Highlighted are the target regions of nisin and gallidermin (bold), ramoplanin and lysobactin (dashed) and vancomycin (plain). **B)** Schematic view of undecaprenyl-pyrophoshphate with its phosphates (blue), anchored to the membrane (yellow) and highlighted target region of bacitracin (bold).

3

Lantibiotics represent a subclass of bacteriocins and are ribosomally synthesized and posttranslational modified peptides (30-32). The best studied lantibiotic is nisin, produced by some *Lactococcus lactis* and *Streptococcus uberis* strains (30, 31), which has a potent antimicrobial effect against several Gram-positive bacteria due to multiple modes of action (33-35). First the N-terminal part of nisin binds the pyrophosphate moiety of lipid II (Figure 1A), thereby inhibiting the peptidoglycan synthesis cycle (11, 35). Secondly, nisin is also able to form pores into the membrane with its C-terminus which leads to rapid cell death due to the efflux of nutrients and ions (36). By genome mining approaches the family of lantibiotics is raising and till date over 150 lanthipeptides have been identified in the genomes of bacteria, , like virgicin from a *Virgibacillus* species, tikitericin from *Thermogemmatispora* T81 and Z-geobacillin from *Geobaccilus* species (37-42).

Hampering the usage of antibiotic bacteriocins as well as lantibiotics in medical treatment is the presence of resistance mechanisms found in human pathogenic bacteria.

A rather novel family of ABC transporter, the **Ba**c**e**itracin **e**fflux (Bce) type transporter have been identified to confer high resistance against bacitracin as well as against lantibiotics like nisin and gallidermin in *Bacillus subtilis, Staphylococcus aureus* and *Streptococcus agalactiae*, respectively (43-49). The homo-dimeric BceAB-type transporter, which were first discovered in *B. subtilis* (50) are encoded on one operon with the BceRS-like TCS. All BceAB-type transporter share a common architecture of a nucleotide binding domain (NBD) and a transmembrane domain (TMD) (51). In the latter a large, characteristic extracellular domain (ECD) between helices VII and VIII (43, 45, 50, 51) is found, which however is not conserved on a sequence level. Interestingly the kinase encoded on the same operon lacks an extracellular sensing domain (43, 45, 50), suggesting a dual function of the transporter, which putatively on the one hand acts as a sensor and on the other hand mediates the resistance against AMPs (52). Several putative mechanisms have been assumed for BceAB-type transporter ranging from antimicrobial peptide removal from the membrane (53), operating as an exporter (46) or flipping undecaprenyl pyrophosphate, a sub-product of the lipid II cycle (54). Although BceAB-type transporters have been intensely studied in the last years and were found in several human pathogenic bacteria the resistance mechanism of the ABC-transporter family remains unsolved.

Here, we focus on the BceAB-type transporter NsrFP from *Streptococcus agalactiae* COH1 (*Sa*NsrFP) which is encoded on an single operon together with a two-component system (TCS) composed of a histidine kinase NsrK and a response regulator NsrR.

Additionally, the nisin resistance protein (NSR), a serine protease specifically cleaving the last 6 amino acid of nisin, is encoded on this *nsr* operon of *S. agalactiae* (45). Recently, it was postulated SaNsrFP is an exporter expelling the lantibiotic once it reached the membrane(46).

In this study we use *Sa*NsrFP as a model system to elucidate the mechanism of the resistance transporter.

4

Material and Methods

Cloning and Expression

Cloning of *nsrFP* from *S. agalactiae* COH1 was performed liked described in Alkhatib et al. (2014) (55) and Reiners et al. (2017) (46) to gain the plasmids pIL-SV *Sa*NsrFP and pIL-SV *Sa*NsrF$_{H202A}$P, latter containing a point mutation in the H-loop which is known to be important for the ATP-hydrolysis (56). These plasmids as well as an empty vector pIL-SVCm were transformed into electrocompetent *L. lactis* NZ9000 cells (57) and the generated strains are termed NZ9000NsrFP, NZ9000NsrF$_{H202A}$P and NZ9000Cm.

The *L. lactis* strains NZ9000NsrFP, NZ9000NsrF$_{H202A}$P were grown in GM17 medium containing 5 µg/ml chloramphenicol. The expression was induced by adding 0.3 nM nisin, cultures were grown at 30°C.
For analyzing the expression, cultures were grown for 5 h and afterwards harvested using a centrifugation step 30 minutes at 5000 x g. The pellets were resuspended with resuspension buffer (50 mM HEPES pH 8.0, 150 mM NaCl, 10 % glycerol) to an OD_{600} of 200 and 1/3 (w/v) 0.5 mm glass beads were added. The cells were lysed and the supernatant was separated by harvesting cell debris as well as glass beads with a 10,000 x g centrifugation step. The membranes were harvested from the supernatant by 100,000 x g centrifugation step. Membrane fractions were prepared with SDS-loading dye (0.2 M Tris–HCl, pH 6.8, 10% (w/v) SDS, 40% (v/v) glycerol, 0.02% (w/v) bromophenol and β-mercaptoethanol). These samples were used for SDS-PAGE and western blot analysis and expressed *Sa*NsrFP proteins detected with a polyclonal antibody against the large extracellular domain of *Sa*NsrP (Davids Biotechnologie, Regensburg, Germany).

Biological assays

Purification of Nisin

Nisin was purified with an ion-exchange chromatography as previously described (58) and the concentration determined with RP-HPLC according to Abts et al. (2013) (59).

Determination of the half-maximal inhibitory concentration (IC_{50})

The half maximal inhibitory concentration was determined according to Abts et al. (2011) (58). Briefly, *L. lactis* NZ9000Cm, *L. lactis* NZ9000NsrFP and *L. lactis* NZ9000NsrF$_{H202A}$P cells were grown in GM17 medium containing 5 µg/ml chloramphenicol and 0.3 nM nisin at 30°C overnight. Fresh GM17Cm medium with sublethal amount of nisin (0.3 nM) was inoculated with overnight cultures to an OD_{600} of 0.1. A 96-well plate

5

was prepared with a serial dilution of examined antibiotics and subsequent the cell culture was added and plates were incubated at 30°C for 5h. Afterwards the optical density was measured and the IC_{50} values for each strain and antibiotic were calculated (46).To make those values more comparable the fold of resistance was determined by dividing the IC_{50} values of *L. lactis* NZ9000NsrFP and *L. lactis* NZ9000NsrF_{H202A}P with the corresponding value for *L. lactis* NZ9000Cm.

Growth curve

To detect the growth behavior of the different strains precultures of *L. lactis* NZ9000Cm, *L. lactis* NZ9000NsrFP and *L. lactis* NZ9000NsrF_{H202A}P cells were grown in GM17 medium with 5 µg/ml chloramphenicol and 0.3 nM nisin at 30 °C overnight. Freshly prepared GM17Cm medium with 0.3 nM nisin was inoculated with overnight cultures to an OD_{600} of 0.1 and grown to an OD_{600} of 0.4 - 0.5 at 30 °C. These steps were repeated and afterwards the cells were diluted to an OD_{600} of 0.05 in GM17Cm medium containing 0.3 nM nisin. Cells were prepared with additional nisin (1 nM - 40 nM) and bacitracin (0.1 µM - 100 µM) concentrations, respectively. Growth was detected at OD_{584} every 10 minutes with a FLUOstar OPTIMA (BMG Lab technology).

Proteom analysis

Sample preparation

The *L. lactis* strains NZ9000NsrFP, NZ9000NsrF_{H202A}P were grown at 30 °C in GM17 medium containing 5 µg/ml chloramphenicol and 0.3 nM nisin. Precultures were inoculated to an OD_{600} of 0.1 and grown to the exponential growth phase before a main culture was inoculated to an OD_{600} of 0.1. The cells were harvested after 5 h at 5000 x g and the pellet was resuspended in phosphate buffer pH 7 to an OD_{600} of 200 and 1/3 (w/v) 0.5 mm glass beads were added. The cells were lysed and the supernatant was separated by a centrifugation of 10,000 x g.
Protein concentration was determined by means of Pierce 660 nm Protein Assay (Fischer Scientific, Schwerte, Germany) and 10 µg protein per sample were loaded on an SDS-PAGE for in-gel-digestion. The isolated gel pieces were reduced, alkylated and underwent afterwards tryptic digestion. The peptides were resolved in 0.1 % trifluoracetic acid and subjected to liquid chromatography.

LC-MS analysis

For the LC-MS analysis a QExactive plus (Thermo Scientific, Bremen, Germany) connected with an Ultimate 3000 Rapid Separation liquid chromatography system (Dionex / Thermo Scientific, Idstein, Germany) equipped with an Acclaim PepMap 100 C18 column (75 µm inner diameter, 25 cm length, 2 mm particle size from Thermo Scientific, Bremen, Germany) was applied. The length of the LC gradient was 120 minutes. The mass spectrometer was operating in positive mode and coupled with a nano electrospray ionization source. Capillary temperature was set to 250°C and source voltage to 1.4 kV. In the QExactive plus mass spectrometer for the survey scans a mass range from 200 to 2000 m/z at a resolution of 70,000 was used. The automatic gain control was set to 3,000,000 and the maximum fill time was 50 ms. The 10 most intensive peptide ions were isolated and fragmented by high-energy collision dissociation (HCD).

Computational mass spectrometric data analysis

Proteome Discoverer (version 2.1.0.81, Thermo Fisher Scientific, Bremen, Germany) was applied for peptide/protein identification applying Mascot (version 2.4, Matrix Science, London, UK) as search engine employing the EnsemblBacteria database (*Lactococcus lactis* subsp. Cremoris NZ900; date 03-11-2019). A false discovery rate of 1% ($p \leq 0.01$) on peptide level was set as identification threshold. Proteins were quantified with Progenesis QI for Proteomics (Version 2.0, Nonlinear Dynamics, Waters Corporation, Newcastle upon Tyne, UK). Only proteins containing at least two unique peptides were taken into consideration. For the calculation of enriched proteins in the groups a 5 % false discovery rate and a minimum fold change of two was used.

Peptidoglycan analysis

Isolation of peptidoglycan

600 ml main culture of *L. lactis* NZ9000Cm, *L. lactis* NZ9000NsrFP and *L. lactis* NZ9000NsrF_{H202A}P were inoculated to an OD_{600} of 0.1 with an overnight culture and grown at 30 °C. After the cells reached the late exponential growth phase (OD 0.8-0.9) cells were harvested and stored at -20°C. To isolate the peptidoglycan the cells were thawed on ice and resuspended in 15 ml of 50 mM Tris/HCl pH 7.0 buffer. Cell suspension was added dropwise to 60 ml of boiling, stirred 4 % SDS solution. After additional 15 minutes of boiling suspension was cooled to room temperature and centrifuged 10 minutes at 13,000 x g. The pellet was washed two times with 1 M NaCl and afterwards with water unless no SDS was detectable in the supernatant

7

(60). Pellet was resuspended in 1 ml water and 1/3 volume glas beads (∅ 0.5 mm) were added. Cells were lysed and glass beads were harvested at 2,000 x g for 5 minutes. The supernatant was centrifuged 15 minutes at 25,000 x g and the cell walls resuspended in 100 mM Tris/HCl pH 8.5 buffer including 20 mM $MgSO_4$. After adding 10 µg/ml DNase I and 50 µg/ml RNase the samples were incubated at 37 °C with 180 rpm for 2 hours. An 18 hours incubation occurred at the same conditions after addition of 10 mM $CaCl_2$ and 100 µg/ml trypsin. Enzymes were stopped by adding 1 % SDS and incubation at 80 °C for 15 minutes. The suspension was diluted to 20 ml with water and centrifuged at 25,000 x g for 30 minutes the pellet was resuspended and incubated at 37 °C for 15 minutes with 10 ml 8 M LiCl and 10 ml 100 mM EDTA pH7, respectively. The peptidoglycan pellet was washed with water, acetone and water before it was lyophilized and stored at -20°C.

The samples were treated with mutanolysin in an enzymatic buffer as follows: 150 µL of resuspended peptidoglycan was mixed with 60 µL of mQ water and added with 75 µL of TES buffer (200 mM TES, 4mM $MgCl_2$, pH 7.0 with final concentration in the sample: 150 mM TES, 3 mM $MgCl_2$, pH 7.0) and 15 µL (75U) of mutanolysin (Sigma-Aldrich, 5 kU/mL, dissolved in mQ water). Samples were incubated at 37 °C overnight and afterwards centrifuged with 14000 rpm for 5 min.

HPLC-MS analysis

90 µl of the sample were injected into a Reprosil-Gold 300 C_{18} column (5 µm by 250 mm by 4.6 mm internal diameter) by use of an HPLC-MS instrument (XCT 6330 LC/MSD Ultra Trap system; Agilent Technologies). The HPLC parameters were as follows: holding with 5% of solvent B (methanol + 0.06% HCOOH) over 5 min and then start with linear gradient from 30% solvent B against 70% solvent A (water + 0.1% HCOOH) for 150 min with additional holding with 30% solvent B over 30 min with a flow rate of 500 µL/min. The MS measurement was performed alternated ionization between positive and negative, with a capillary voltage of 3.5 kV at 350 °C.

Cell wall precursor analysis

Growth condition and sample preparation

Cells were grown in M17 medium supplemented with 0.5 % glucose and 0.3 nM nisin overnight at 30°C without shaking. At next day 100 ml with 0.5 % glucose and 0.3 nM nisin were inoculated with overnight cultures to on OD_{600} = 0.1. When OD_{600} = 1.2 100 µg/ml bacitracin was added to the cultures to enrich cell wall precursors and cultures were incubated for further 30 min at 30°C. This step was repeated once. (As

8

control a second culture each was harvested before bacitracin was added at an OD_{600}=1.2 and cell pellets were stored at -20 °C) After incubation with bacitracin the cells were harvested and the cell pellets were stored at -20 °C. At the next day the cell pellets were resuspended in 25 ml water and cooked for 60 min in boiling water. Cell debris were removed by centrifugation (15 min, 500 x g, 4 °C). The supernatant, containing the cell wall precursors, was lyophilisized overnight. Cell pellets were resuspended in 150 µl water and used for LC/MS analysis.

LC/MS analysis of cell wall fragments

5 µl of each sample was injected into XCT6330 LC/MSD ultra trap system (Agilent Technologies) equipped with a Nucleosil 100 C18 column (3 µm x 100 mm × 2 mm internal diameter, Dr. Maisch GmbH). The column was used at 40°C. A linear gradient was performed from 0 % up to 10 % eluent B (0.06 % formic acid in acetonitrile) over 25 min with a flow rate of 400 µl/min. The column was re-equilibrated for 10 min with 100 % buffer A (0,1 % formic acid in water). Ionization alternated between positive and negative ion mode with a capillary voltage of 3.5 kV at 350 °C. Extracted ion chromatograms (EIC) in negative ion mode for UDP-MurNAc-Ala-Glu-Lys-Ala-Ala (m/z^{-1} 1148.34 +/-0.1) and UDP-MurNAc-Ala-Glu-Lys-Asp-Ala-Ala (m/z^{-1} 1263.37 +/- 0.1) were analyzed with Data Analysis (Bruker), exported as .xy files and presented with GraphPad Prism 6.0.

Analysis of NsrFP with BODIPY™ FL Vancomycin

L. lactis NZ9000Cm, NZ9000NsrFP and NZ9000$NsrF_{H202A}$P cells were inoculated to an OD_{600} of 0.1 in fresh GM17 media supplemented 5 µg/ml chloramphenicol and 0.3 nM nisin. Cells were grown at 30°C to an OD_{600} of 0.3 to 0.4 again inoculated to an OD_{600} of 0.1. Cells grown again at 30°C and used for further assays at an OD_{600} of 0.3 to 0.4.

The relative fluorescence was measured with a FluoroLog (Horiba) at an excitation wavelength of 480 nm and an emission wavelength of 514 nm. The cell suspension was stirred at 30°C during the assay. After a stable baseline was reached BODIPY™ FL Vancomycin was added and the fluorescence intensity observed.

9

Results

Recently, we showed that different lantibiotics were recognized by *Sa*NsrFP (46). These were however structurally related antimicrobial compounds e.g. peptides and we extended this to a structurally divers rather unrelated group, including ramoplanin, vancomycin and lysobactin as known lipid II binders, as well as bacitracin which binds to the lipid carrier UPP.
Although some resistance was observed for the lipid II binders (2-6-fold), a striking resistance was observed for bacitracin (see Figure 2A, SI Figure 1 and Table 1). Here an almost 350-fold of resistance against bacitracin was observed suggesting that *Sa*NsrFP is not recognizing the lipid II binders itself (SI Figure 2). It is rather likely that a different target is recognized by SaNsrFP, which is then transported into the cytoplasm, for example lipid II, UPP or UP which are present at the bacterial membrane exterior. Since the first group of substrates are all lipid II binders and bacitracin is an UPP binder, which is the product of lipid II after incorporation of the GlcNAc-MurNAc-pentapeptide subunit into the PGN, this high resistance observed suggests that *Sa*NsrFP is actively involved somewhere in the step of the recycling of lipid II.

To verify whether the observed resistance occurs from active transport mediated by the *Sa*NsrFP BceAB-type transporter we also expressed a dead mutant *Sa*NsrF$_{H202A}$P which displayed similar values as the sensitive *L. lactis* strain indicating no resistance. Both, the wildtype and dead mutant *Sa*NsrFP are expressed at the same level as observed by western blot analysis of the membranes (Figure 2B shows for the *Sa*NsrFP expressing strain as well as for the dead mutant expressing strain bands with a height of approximately 50 kDa. Both proteins were expressed at the same level, whereas the control cells (NZ9000Cm) show no expression).

To verify whether *Sa*NsrFP is modulating the cell wall synthesis we investigated the components of the cell wall. Here we observed components out of the amino sugars and the pentapeptide with an aspartate cross linking bridge for the sensitive strain and the dead mutant (Figure 2C, highlighted in green), which differ from the *Sa*NsrFP expressing strain in the cross linking bridge composed of two alanine residues (Figure 2 C, highlighted in yellow). Interestingly, the *Sa*NsrF$_{H202A}$P expressing strain also showed some of the double-alanine PGN species, suggesting that the active transporter somehow causes a modulation of the cell wall components (Figure 2C, SI Figure 3).

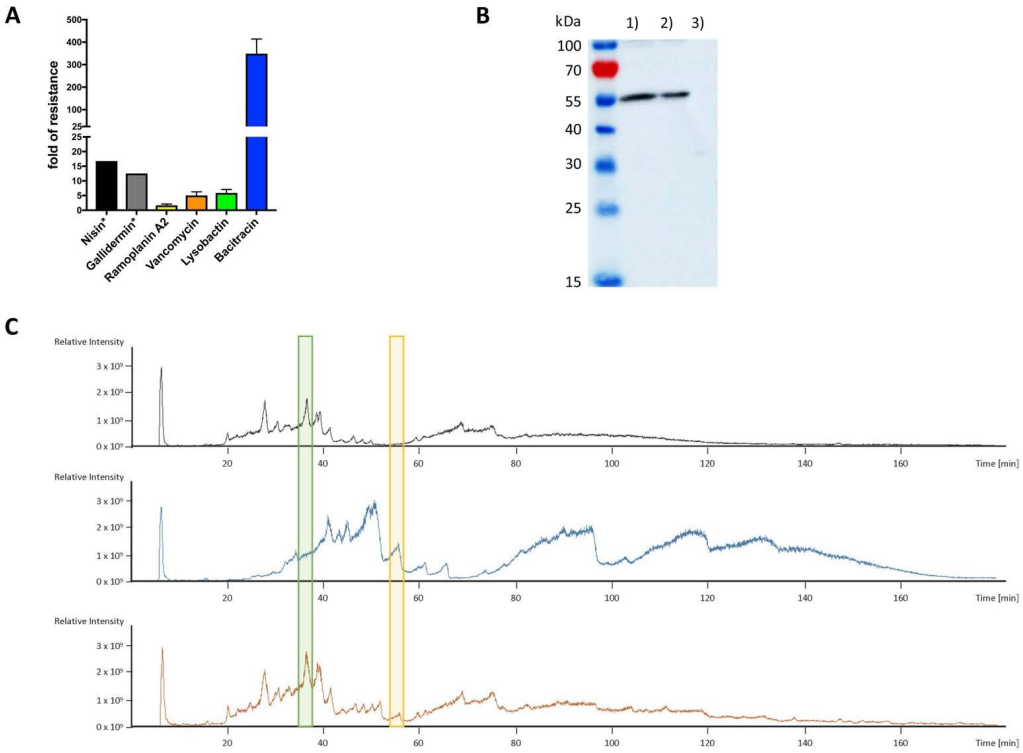

Figure 2: A) Fold of resistance of *L. lactis* NZ9000NsrFP against *L. lactis* NZ9000Cm calculated with determined IC_{50} of ramoplanin A2 (yellow), vancomycin (orange), lysobactin (green) and bacitracin (blue). Values for nisin and gallidermin were taken from Reiners et al. (2017) (46) and marked with an asterisk. Values were calculated from at least 5 independent measurements. **B) Expression of *Sa*NsrFP (1) and *Sa*NsrF$_{H202A}$P (2)** in *L. lactis* NZ9000 as well as the empty vector pIL-SV in *L. lactis* NZ9000 monitored *via* western blot with a polyclonal antibody against the extracellular domain of *Sa*NsrP**. C) HPLC Chromatogram** purified peptidoglycan from *L. lactis* NZ9000Cm (black), *L. lactis* NZ9000NsrFP (blue) and *L. lactis* NZ9000NsrF$_{H202A}$P (orange). Marked peaks could be related to the mass of GlcNAc-MurNAc-Ala-iGlu-Lys-(Asp)-Ala-Ala (green) and GlcNAc-MurNAc-Ala-iGlu-Lys-(Ala-Ala)-Ala-Ala (yellow).

Binding of bacitracin to UPP causes inhibition of the lipid II recycling, resulting in accumulation of the intra cellular cell wall precursors (28, 29, 61). We tested whether this accumulation is occurring when *Sa*NsrFP is expressed in *L. lactis*. As a control we used the non-expressing strain, carrying an empty plasmid, as well as a strain expressing the *Sa*NsrFP dead mutant. Here we observed the characteristic accumulation of the cell wall precursors UDP-MurNAc-Ala-Glu-Lys-Ala-Ala (1148.4 m/z^{-1}) and UDP-MurNAc-Ala-Glu-Lys-(Asn)-Ala-Ala (1263.4 m/z^{-1}) in the NZ9000Cm strain (SI Figure 4). Intriguingly, in the *Sa*NsrFP expressing strain no accumulation was observed indicating that the expression of *Sa*NsrFP results in a bypass of this accumulation, untimely bacitracin cannot bind to UPP. This is underlined with the results that

NZ9000NsrF$_{H202A}$P shows a slightly reduced cell wall precursor accumulation when compared to sensitive cells, mediated by bacitracin, as expected for an inactive mutant (SI Figure 4).

This suggests that lipid II recycling is still occurring in the SaNsrFP strain however taking a different route. Since bacitracin does not inhibit the cell growth anymore only two points in the lipid II recycling might be the substrate for *Sa*NsrFP, either lipid II itself or UPP prior to bacitracin binding. UPP normally is not flipped back and introduced into a new lipid II synthesis cycle. Rather it is dephosphorylated prior to flipping at the cytosolic site. Both possibilities however require an adjustment of the cells with respect to the availability of the enzymes involved in lipid II synthesis.

To investigate this, we examined a whole proteome analysis of NZ9000NsrFP, NZ9000Cm and NZ9000NsrF$_{H202A}$P *L. lactis* strains grown under identical conditions. The proteomes of these were analyzed by mass spectrometry leading to the quantification of 894 proteins (identified by at least two unique peptides in each strain). The comparison between NZ9000Cm and NZ9000NsrFP revealed 315 differential proteins (Figure 3A). 339 proteins show differential abundances between NZ9000NsrF$_{H202A}$P and NZ9000NsrFP (Figure 3B). This implicated that the *Sa*NsrFP expressing strain need to react significantly to counter act the transport mediated by the BceAB transporter. Further analysis displayed that proteins involved in cell wall synthesis are downregulated in the proteome resulting from the NZ9000NsrFP strain (Figure 3A & B and SI Figure 5). Downregulated proteins in *Sa*NsrFP expressing cells include the phosphoenolpyruvate-protein phosphotransferase MurA (ADJ59149), UDP-N-acetylmuramate-L-alanine ligase MurC (ADJ61283), UDP-N-acetylmuramoyl-L-alanyl-D-glutamate synthetase MurD (ADJ59924), UDP-N-acetylmuramoylalanyl-D-glutamate-2, 6-diaminopimelate ligase MurE (ADJ60966), UDP-N-acetylmuramoylalanyl-D-glutamyl-2,6-diaminopimelate--D-alanyl-D-alanine ligase MurF (ADJ59382) and N-acetylmuramic acid-6-phosphate etherase MurQ (ADJ60417). Further several proteins involved in the synthesis of single components of the lipid II synthesis, like UDP or the amino sugars are down regulated in NZ9000NsrFP as well (SI Figure 5).

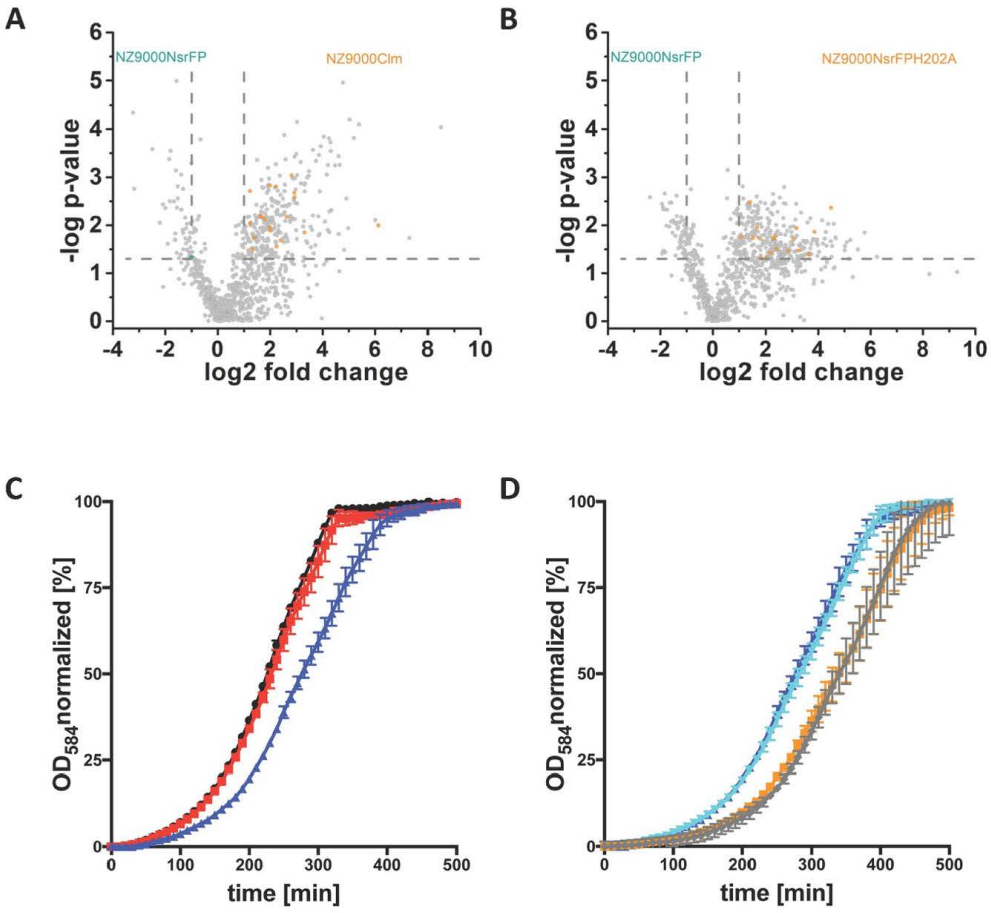

Figure 3: A) Volcano plot of the proteome analysis of **NZ9000NsrFP against NZ9000Cm** and **B) NZ9000NsrFP against NZ9000NsrF$_{H202A}$P.** Proteins involved in the cell wall synthesis are highlighted in orange if upregulated in NZ9000Cm (A) and NZ9000NsrF$_{H202A}$P (B) as well as highlighted in blue if upregulated in NZ9000NsrFP. **C) Growth curve** of *L. lactis* NZ9000NsrFP (blue), *L. lactis* NZ9000NsrF$_{H202A}$P (red) and *L. lactis* NZ9000Cm (black) induced with 0.3 nM nisin. **D) Growth curve** of *L. lactis* NZ9000NsrFP (blue) induced with 0.3 nM nisin and *L. lactis* NZ9000NsrFP (turquoise), *L. lactis* NZ9000NsrF$_{H202A}$P (orange) and *L. lactis* NZ9000Cm (grey) induced with 0.3 nM nisin and additionall 100 nM bacitracin. Our initial IC_{50} analysis showed that the *Sa*NsrFP strain was still growing under treatment of bacitracin. A drawback of this analysis is that the OD was measured after a couple of hours by which the initial growth rate and behavior was not detected.

13

Since the major lipid II cell wall synthesis proteins are down regulated in NZ9000NsrFP and the transporter confers a high resistance against a cell wall precursor preventing bacteriocins we were interested whether expression of the transporter also influences the growth behavior of the cells.

After preparing the cells the growth of NZ9000Cm, NZ9000NsrFP and NZ9000NsrF_{H202A}P was observed over 500 minutes (Figure 3C). All strains were inoculated at an OD_{600} of 0.05 and induced with 0.3 nM nisin. Here the NZ9000NsrFP (blue) displayed a reduced growth in the early stage which appears to be arising from an adjustment of the cell due to the expression of *Sa*NsrFP. Interestingly this behavior is not observed for the NZ9000NsrF_{H202A}P (Figure 3C red), which displayed the same growth behavior as the NZ9000Cm strain (Figure 3C black).

We repeated these experiments with an additional 100 nM bacitracin. Here a reduction of the growth can be observed in the NZ9000Cm strain which can be explained by the results found in the IC_{50} value. 100 nM is below the IC_{50} of bacitracin which still allows the cells to grow but a reduction is present due to the binding of UPP by bacitracin. Not surprising is that the NZ9000NsrF_{H202A}P strain shows a similar behavior and displayed a reduced growth. Intriguingly is the observation that the NZ9000NsrFP strain shows no reduced growth (Figure 3D). Meaning that it grows faster under similar conditions. Interestingly the growth curve is similar to the curve observed for the same strain without bacitracin. This implicates that *Sa*NsrFP is resistant towards bacitracin. Importantly, the growth curve observed for *Sa*NsrFP is reduced when compared to the sensitive and the dead mutant of *Sa*NsrFP expressing cells, suggesting that the established recycling of lipid II is bypassed. The new route however required some adjustment within the cells, which explains the delay in cell growth in the beginning of the curve.

So far all results point to a cell wall precursor related mechanism for the ABC-transporter *Sa*NsrFP. Since all antibiotics *Sa*NsrFP confers resistance to are either binding the cell wall precursor lipid II or target another cell wall synthesis step a lipid II binding fluorophore BODIPY™ FL Vancomycin was used to investigate on the functional mechanism of *Sa*NsrFP.

At first the cells were monitored with an excitation and emission wavelength from 480 and 514 nm and the relative fluorescence was observed over the measuring time. For all concentrations and strains after adding the dye an fast increase of the fluorescence signal is detectable which than decreases over time till it reaches an equilibrium. Interestingly this equilibrium is at a lower relative fluorescence intensity for NZ9000NsrFP with the concentration 1000 nM and 2000 nM of BODIPY™ FL Vancomycin compared to NZ9000NsrF_{H202A}P and NZ9000Cm (SI Figure 6). This indicates an effect on lipid II mediated by the expression of *Sa*NsrFP.

Discussion

Previous studies showed that the BceAB type ABC transporter *Sa*NsrFP confers resistance against the lantibiotic nisin and gallidermin (46), both binding to the pyrophosphate of the cell wall precursor lipid II (11, 35, 62). As both tested lantibiotics target the same moiety of the cell wall precursor in this study we addressed the substrate specificity in a brouder context.

It has been determined that *Sa*NsrFP confers a minor resistance against Ramoplanin A2 whereas the transporter mutant, unable to hydrolyze ATP, showed an almost similar value (Table Y, Figure XB). By contrast *Sa*NsrFP showed resistance against lysobactin. This results seemed to be inconsistent as both bacteriocins share the N-acetyl muramic acid (MurNAc) and the pyrophosphate of lipid II as a target, but it was shown that ramoplanin A2 binds lipid II as a dimer whereas lysobactin targets monomeric (8, 14, 17, 18). This results raised the assumption that the mechanism of *Sa*NsrFP is rather lipid II related than that the antibiotics itself are affected. To proof this assumption we also tested vancomycin, which in contrast does not bind to the sugar or phosphate moiety but to the D-Ala-D-Ala sequence of the pentapeptide of lipid II (20-22). The results for vancomycin show resistance mediated by the expression of *Sa*NsrFP. This let us to the expectation *Sa*NsrFP flips lipid II back into the cytoplasm, resulting in a lower accessibility of the target for the tested antibiotics.

As a control the cyclopeptide bacitracin, which binds to the pyrophosphate of UPP, was tested (28, 29). UPP arises as an interstage product in the peptidoglycan cycle. Bacitracin interrupts this cycle by binding to UPP and therefore preventing the dephosphorylation and translocation. Our investigations with bacitracin resulted in surprisingly high fold of resistance of 349.15 ± 64.9 for *L. lactis* NZ9000NsrFP and a 25 fold less value of 13.70 ± 9.1 for *L. lactis* NZ9000NsrF$_{H202A}$P. Contemplating the proposed *Sa*NsrFP mechanism this results could arise if lipid II is flipped back into the cytoplasm. The peptidoglycan synthesis cycle would be cut short at this step so UPP would not be present in the extracellular space and bacitracin lacks a target.

Interestingly also other BceAB-type ABC-transporter confer a high resistance against bacitracin. In *Listeria monocytogenes* the transporter AnrAB was detected, which was first thought to confer resistance against nisin. AnrAB was tested against other AMPs and showed resistance also against the lantibiotic gallidermin and the highest resistance, of all tested substances, against bacitracin (49). The ABC-transporter BceAB of *B. subtilis* showed, besides resistance against nisin and gallidermin, the highest resistance against bacitracin as well (44). Also studies with VraDE of *S. aureus* showed resistance against nisin and gallidermin and also against bacitracin mediated by this transporter (47, 48). As all mentioned transporter confer resistance against the lantibiotic nisin and the cyclic peptide bacitracin, while those share neither structural nor target

similarities, it can be assumed that the transporters must share a mechanism involving the lipid II recycling process.

However, we were concerned about the fact that the dead mutant variant still shows higher IC_{50} values than the control strain with an empty plasmid, nevertheless this observation can be explained. On the one hand it was shown for several ABC-transporter that variants with mutations of the H-loop still show some rest activity (e.g. (63, 64)). On the other hand the transmembrane domain *Sa*NsrP is not affected by the NBD mutation so it is supposable *Sa*NsrP still binds to lipid II but is unable to flip it into the cytoplasm due to the lack of energy.

As a control we checked the peptidoglycan composition of all strains which is altered in the *Sa*NsrFP expressing strain. Here we could observe a double-alanine cross linking bridge instead of an aspartate in the sensitive strain. It might be possible that *Sa*NsrFP decarboxylases the aspartate residue by flipping lipid II inside of the cell. The resulting, altered lipid II cross linking bridge is subsequently rather extended by a second alanine residue than carboxylated back to an aspartate.

A disturbance of the peptidoglycan synthesis due to flipping of lipid II should result in an altered growth behavior of the cells so we detected growth curves of *L. lactis* NZ9000NsrFP and the control strains. Untreated cells which were only induced with a sublethal amount of nisin showed a decelerated growth of *L. lactis* NZ9000NsrFP compared to *L. lactis* NZ9000NsrF_{H202A}P and *L. lactis* NZ9000Cm (Figure XC). Further we treated the cells with 100 nM bacitracin which results in a breakdown of the growth of the control cells but did not influence the growth of *L. lactis* NZ9000NsrFP (Figure XD). Those results support our hypothesis since less provided lipid II results in a slower peptidoglycan synthesis and subsequently in a slower growth and further treatment with bacitracin does not influence the growth of *Sa*NsrFP expressing cells if the target is absent.
Based on this it was of major interest to check the proteome of the cells. The cell extract was analyzed and displayed that proteins involved in cell wall synthesis are downregulated in NZ9000NsrFP proteome. This result can be explained if lipid II is flipped into the cytoplasm by *Sa*NsrFP, subsequently less lipid II has to be synthesized which would result in less expression rate of the involved proteins.

Studies with BODIPY™ FL Vancomycin showed a decreased relative fluorescence intensity for NZ9000NsrFP cells than for the control cells. For fluorophores like BODIPY™ it is known they are quenched concentration dependent due to a Förster-type inductive resonance transfer (65-67) . A more decreased relative fluorescence signal would therefore indicate more bound BODIPY™ FL Vancomycin, which could on the one

16

hand results from more produced lipid II in NZ9000NsrFP cells, which is very unlikely due to the downregulated proteins of the lipid II synthesis. On the other hand, which is more likely, we found out that peptidoglycan cross linking bridges in *Sa*NsrFP expressing cells are altered to Ala-Ala, which is the binding motif of vancomycin. Hence, we have plenty much binding sites for the fluorophore coupled compound which subsequently results in more Förster-type inductive resonance transfer and consequently to a higher fluorophore quenching.

Since we postulated a lipid II flippase mechanism the original flippase in the lipid II synthesis MurJ should be considered, which transports the cell wall precursor from the cytosol to the extracellular space. Recently the mechanism of this protein and its conformations were elucidated (68, 69). MurJ belongs to the multidrug/oligosaccharidyl-lipid/polysaccharide (MOP) superfamily, composed of 14 TMHs, which are distinct into the N-lobe (TMH 1-6), the C-lobe (TMH 7-12) and the TMHs 13 and 14, which do not belong to the core transport domain. It is postulated, that a loop between TMH 6 and 7 has an effect on the inner- and outward-facing conformation (68). Compared to the BceAB-type transporters no large transmembrane loop is existent, but a large extracellular domain between TMH 7 and 8, whose function is still unknown. As this extracellular domain (ECD) is very specific for this kind of transporters it is very likely that it fulfills an important function, which could be the change of the conformation of the transporter to enable the transport of lipid II from the extracellular space into the cytoplasm. Further it is thought that this ECD could act as a sensor since the extracellular sensing domain in BceAB-type transporter related histidine kinases is absent.

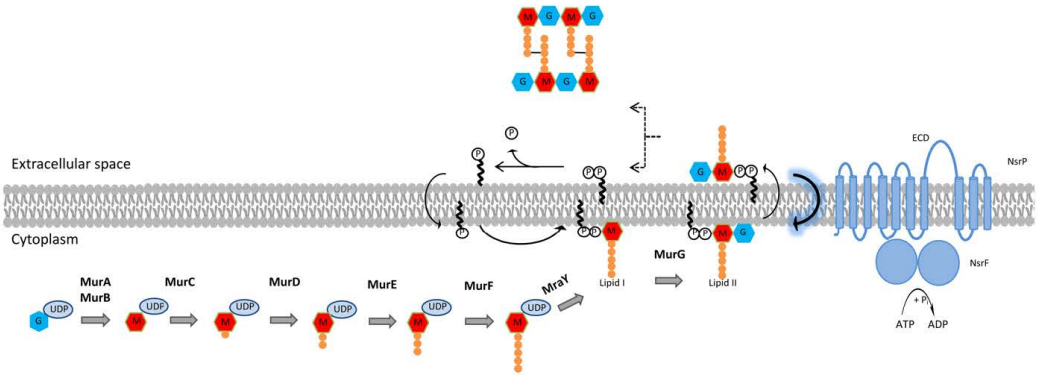

Figure 4: Postulated mechanism of *Sa*NsrFP. Schematic view of peptidoglycan synthesis. Phosphates are marked with an P, undecaprenyl as a black curved line, uridine phosphate (UDP) in light blue, GlcNAc in blue, MurNAc in red and aminoacids of the pentapeptide in orange. The transporter *Sa*NsrFP is demonstrated in blue with a highlighted arrow for the postulated flippase mechanism of lipid II inside of the cytoplasm.

17

In Figure 4 the postulated mechanism of *Sa*NsrFP is demonstrated. Based on all results from this study a flippase activity of the transporter is very likely to prevent the cells from lipid II targeting antibiotics and especially from bacitracin. Prior studies postulated an export mechanism of *Sa*NsrFP, based on a peptide release assay, which results in more nisin in the supernatant of *Sa*NsrFP expressing cells compared to the control cells (46). Related to the flippase mechanism, this results can also be explained by removing the target molecule lipid II from the extracellular space. Subsequently less nisin is able to bind and more nisin can be detected in the supernatant. This also explains further assumptions of the removal from AMPs from the membrane (53). A study about the BceAB transporter from *B. subtilis* postulates a flipping of undecaprenyl pyrophosphate (UPP) in order to remove the bacitracin target and therefore confers resistance against bacitracin (54). Other studies about the same transport showed additionally resistance against nisin and gallidermin, mediated by BceAB, which could not be explained by a UPP flippase mechanism (44). It is more likely that this type of transporters relocate the cell wall precursor lipid II and thereby suppress the formation of UPP, which subsequently results in the bacitracin resistance (Figure 4).

Acknowledgement

This work was funded by the Deutsche Forschungsgemeinschaft (DFG, German Research Foundation) – 270650915/GRK 2158.

Bibliography

1. Li B, Webster TJ. Bacteria antibiotic resistance: New challenges and opportunities for implant-associated orthopedic infections. J Orthop Res. 2018;36(1):22-32.
2. ECDC/EMEA. The Bacterial Challenge: Time to React. . Joint Technical Report2009.
3. Laxminarayan R, Duse A, Wattal C, Zaidi AK, Wertheim HF, Sumpradit N, et al. Antibiotic resistance-the need for global solutions. Lancet Infect Dis. 2013;13(12):1057-98.
4. Pumart P, Phodha T, Thamlikitkul V, Riewpaiboon A, Prakongsai P, Limwattananon S. Health and economic impacts of antimicrobial resistance in Thailand. . Journal of Health Services Research & Policy2012. p. 352-60.
5. Flemming A. On the antibacterial action of cultures of a penicillium, with special reference to their use in the isolation of *B. influenza*. *British journal of experimental pathology* 1929. p. 226–36.
6. Dever LA, Dermody TS. Mechanisms of bacterial resistance to antibiotics. Arch Intern Med. 1991;151(5):886-95.
7. Muller A, Klockner A, Schneider T. Targeting a cell wall biosynthesis hot spot. Nat Prod Rep. 2017;34(7):909-32.
8. Breukink E, de Kruijff B. Lipid II as a target for antibiotics. Nat Rev Drug Discov. 2006;5(4):321-32.

9. Beeby M, Gumbart JC, Roux B, Jensen GJ. Architecture and assembly of the Gram-positive cell wall. Mol Microbiol. 2013;88(4):664-72.
10. Lovering AL, Safadi SS, Strynadka NC. Structural perspective of peptidoglycan biosynthesis and assembly. Annu Rev Biochem. 2012;81:451-78.
11. Wiedemann I, Breukink E, Van Kraaij C, Kuipers OP, Bierbaum G, De Kruijff B, et al. Specific Binding of Nisin to the Peptidoglycan Precursor Lipid II Combines Pore Formation and Inhibition of Cell Wall Biosynthesis for Potent Antibiotic Activity. Journal of Biological Chemistry. 2001;276(3):1772-9.
12. O'Sullivan J, McCullough JE, Tymiak AA, Kirsch DR, Trejo WH, Principe PA. Lysobactin, a novel antibacterial agent produced by Lysobacter sp. I. Taxonomy, isolation and partial characterization. J Antibiot (Tokyo). 1988;41(12):1740-4.
13. Bonner DP, O'Sullivan J, Tanaka SK, Clark JM, Whitney RR. Lysobactin, a novel antibacterial agent produced by Lysobacter sp. II. Biological properties. J Antibiot (Tokyo). 1988;41(12):1745-51.
14. Lee W, Schaefer K, Qiao Y, Srisuknimit V, Steinmetz H, Müller R, et al. The Mechanism of Action of Lysobactin. J Am Chem Soc. 2016;138(1):100-3.
15. Montecalvo MA. Ramoplanin: a novel antimicrobial agent with the potential to prevent vancomycin-resistant enterococcal infection in high-risk patients. J Antimicrob Chemother. 2003;51 Suppl 3:iii31-5.
16. Cavalleri B, Pagani H, Volpe G, Selva E, Parenti F. A-16686, a new antibiotic from Actinoplanes. I. Fermentation, isolation and preliminary physico-chemical characteristics. J Antibiot (Tokyo). 1984;37(4):309-17.
17. Hu Y, Helm JS, Chen L, Ye XY, Walker S. Ramoplanin inhibits bacterial transglycosylases by binding as a dimer to lipid II. J Am Chem Soc. 2003;125(29):8736-7.
18. Hamburger JB, Hoertz AJ, Lee A, Senturia RJ, McCafferty DG, Loll PJ. A crystal structure of a dimer of the antibiotic ramoplanin illustrates membrane positioning and a potential Lipid II docking interface. Proc Natl Acad Sci U S A. 2009;106(33):13759-64.
19. JORDAN DC, INNISS WE. Selective inhibition of ribonucleic acid synthesis in *Staphylococcus aureus* by vancomycin. Nature. 1959;184(Suppl 24):1894-5.
20. ANDERSON JS, MATSUHASHI M, HASKIN MA, STROMINGER JL. LIPID-PHOSPHOACETYLMURAMYL-PENTAPEPTIDE AND LIPID-PHOSPHODISACCHARIDE-PENTAPEPTIDE: PRESUMED MEMBRANE TRANSPORT INTERMEDIATES IN CELL WALL SYNTHESIS. Proc Natl Acad Sci U S A. 1965;53:881-9.
21. Perkins HR. Specificity of combination between mucopeptide precursors and vancomycin or ristocetin. Biochem J. 1969;111(2):195-205.
22. Chatterjee AN, Perkins HR. Compounds formed between nucleotides related to the biosynthesis of bacterial cell wall and vancomycin. Biochem Biophys Res Commun. 1966;24(3):489-94.
23. Ling LL, Schneider T, Peoples AJ, Spoering AL, Engels I, Conlon BP, et al. A new antibiotic kills pathogens without detectable resistance. Nature. 2015;517(7535):455-9.
24. Konz D, Klens A, Schörgendorfer K, Marahiel MA. The bacitracin biosynthesis operon of *Bacillus licheniformis* ATCC 10716: molecular characterization of three multi-modular peptide synthetases. Chem Biol. 1997;4(12):927-37.
25. Nakano MM, Zuber P. Molecular biology of antibiotic production in *Bacillus*. Crit Rev Biotechnol. 1990;10(3):223-40.
26. Johnson BA, Anker H, Meleney FL. BACITRACIN: A NEW ANTIBIOTIC PRODUCED BY A MEMBER OF THE *B. SUBTILIS* GROUP. Science. 1945;102(2650):376-7.
27. MELENEY FL, JOHNSON B. Bacitracin therapy; the first hundred cases of surgical infections treated locally with the antibiotic. J Am Med Assoc. 1947;133(10):675-80.
28. Storm DR, Strominger JL. Complex formation between bacitracin peptides and isoprenyl pyrophosphates. The specificity of lipid-peptide interactions. J Biol Chem. 1973;248(11):3940-5.
29. Economou NJ, Cocklin S, Loll PJ. High-resolution crystal structure reveals molecular details of target recognition by bacitracin. Proc Natl Acad Sci U S A. 2013;110(35):14207-12.
30. Chatterjee C, Paul M, Xie L, van der Donk WA. Biosynthesis and mode of action of lantibiotics. Chemical Reviews. 2005;105(2):633-84.

31. Klaenhammer TR. Genetics of bacteriocins produced by lactic acid bacteria. FEMS Microbiol Rev. 1993;12(1-3):39-85.
32. Sahl HG, Bierbaum G. Lantibiotics: biosynthesis and biological activities of uniquely modified peptides from gram-positive bacteria. Annu Rev Microbiol. 1998;52:41-79.
33. Brötz H, Josten M, Wiedemann I, Schneider U, Götz F, Bierbaum G, et al. Role of lipid-bound peptidoglycan precursors in the formation of pores by nisin, epidermin and other lantibiotics. Molecular Microbiology. 1998;30(2):317-27.
34. Hasper HE, Kramer NE, Smith JL, Hillman JD, Zachariah C, Kuipers OP, et al. An alternative bactericidal mechanism of action for lantibiotic peptides that target lipid II. Science. 2006;313(5793):1636-7.
35. Hsu ST, Breukink E, Tischenko E, Lutters MA, de Kruijff B, Kaptein R, et al. The nisin-lipid II complex reveals a pyrophosphate cage that provides a blueprint for novel antibiotics. Nat Struct Mol Biol. 2004;11(10):963-7.
36. Hasper HE, de Kruijff B, Breukink E. Assembly and stability of nisin-lipid II pores. Biochemistry. 2004;43(36):11567-75.
37. van Heel AJ, de Jong A, Song C, Viel JH, Kok J, Kuipers OP. BAGEL4: a user-friendly web server to thoroughly mine RiPPs and bacteriocins. Nucleic Acids Res. 2018;46(W1):W278-W81.
38. Baindara P, Nayudu N, Korpole S. Whole genome mining reveals a diverse repertoire of lanthionine synthetases and lanthipeptides among the genus Paenibacillus. J Appl Microbiol. 2019.
39. Huo L, Zhao X, Acedo JZ, Estrada P, Nair SK, van der Donk WA. Characterization of a dehydratase and methyltransferase in the biosynthesis of a ribosomally-synthesized and post-translationally modified peptide in Lachnospiraceae. Chembiochem. 2019.
40. Gupta V, Singh SS, Sidhu C, Grover V, Pinnaka AK, Korpole S. Virgicin, a novel lanthipeptide from Virgibacillus sp. strain AK90 exhibits inhibitory activity against Gram-positive bacteria. World J Microbiol Biotechnol. 2019;35(9):133.
41. Xu B, Aitken EJ, Baker BP, Turner CA, Harvey JE, Stott MB, et al. Genome mining, isolation, chemical synthesis and biological evaluation of a novel lanthipeptide, tikitericin, from the extremophilic microorganism. Chem Sci. 2018;9(37):7311-7.
42. Alkhalili RN, Canbäck B. Identification of Putative Novel Class-I Lanthipeptides in Firmicutes: A Combinatorial. Int J Mol Sci. 2018;19(9).
43. Ohki R, Giyanto, Tateno K, Masuyama W, Moriya S, Kobayashi K, et al. The BceRS two-component regulatory system induces expression of the bacitracin transporter, BceAB, in Bacillus subtilis. Molecular Microbiology. 2003;49(4):1135-44.
44. Staron A, Finkeisen DE, Mascher T. Peptide antibiotic sensing and detoxification modules of Bacillus subtilis. Antimicrob Agents Chemother. 2011;55(2):515-25.
45. Khosa S, AlKhatib Z, Smits SH. NSR from *Streptococcus agalactiae* confers resistance against nisin and is encoded by a conserved nsr operon. Biol Chem. 2013;394(11):1543-9.
46. Reiners J, Lagedroste M, Ehlen K, Leusch S, Zaschke-Kriesche J, Smits SHJ. The N-terminal Region of Nisin Is Important for the BceAB-Type ABC Transporter NsrFP from *Streptococcus agalactiae* COH1. Front Microbiol. 2017;8:1643.
47. Hiron A, Falord M, Valle J, Debarbouille M, Msadek T. Bacitracin and nisin resistance in *Staphylococcus aureus:* a novel pathway involving the BraS/BraR two-component system (SA2417/SA2418) and both the BraD/BraE and VraD/VraE ABC transporters. Mol Microbiol. 2011;81(3):602-22.
48. Popella P, Krauss S, Ebner P, Nega M, Deibert J, Gotz F. VraH Is the Third Component of the *Staphylococcus aureus* VraDEH System Involved in Gallidermin and Daptomycin Resistance and Pathogenicity. Antimicrob Agents Chemother. 2016;60(4):2391-401.
49. Collins B, Curtis N, Cotter PD, Hill C, Ross RP. The ABC transporter AnrAB contributes to the innate resistance of *Listeria monocytogenes* to nisin, bacitracin, and various beta-lactam antibiotics. Antimicrob Agents Chemother. 2010;54(10):4416-23.
50. Rietkötter E, Hoyer D, Mascher T. Bacitracin sensing in *Bacillus subtilis*. Molecular microbiology. 2008;68(3):768-85.

51. Clemens R, Zaschke-Kriesche J, Khosa S, Smits SHJ. Insight into Two ABC Transporter Families Involved in Lantibiotic Resistance. Front Mol Biosci. 2017;4:91.
52. Fritz G, Dintner S, Treichel NS, Radeck J, Gerland U, Mascher T, et al. A New Way of Sensing: Need-Based Activation of Antibiotic Resistance by a Flux-Sensing Mechanism. MBio. 2015;6(4):e00975.
53. Susanne Gebhard TM. Antimicrobial peptide sensing and detoxification modules:unravelling the regulatory circuitry of *Staphylococcus aureus*. Molecular Microbiology. 2011;81:581-7.
54. Kingston AW, Zhao H, Cook GM, Helmann JD. Accumulation of heptaprenyl diphosphate sensitizes *Bacillus subtilis* to bacitracin: implications for the mechanism of resistance mediated by the BceAB transporter. Mol Microbiol. 2014;93(1):37-49.
55. AlKhatib Z, Lagedroste M, Zaschke J, Wagner M, Abts A, Fey I, et al. The C-terminus of nisin is important for the ABC transporter NisFEG to confer immunity in *Lactococcus lactis*. Microbiologyopen. 2014;3(5):752-63.
56. Zaitseva J, Jenewein S, Jumpertz T, Holland IB, Schmitt L. H662 is the linchpin of ATP hydrolysis in the nucleotide-binding domain of the ABC transporter HlyB. EMBO J. 2005;24(11):1901-10.
57. Holo H, Nes IF. High-Frequency Transformation, by Electroporation, of *Lactococcus lactis* subsp. cremoris Grown with Glycine in Osmotically Stabilized Media. Appl Environ Microbiol. 1989;55(12):3119-23.
58. Abts A, Mavaro A, Stindt J, Bakkes PJ, Metzger S, Driessen AJ, et al. Easy and rapid purification of highly active nisin. Int J Pept. 2011;2011:175145.
59. Abts A, Montalban-Lopez M, Kuipers OP, Smits SH, Schmitt L. NisC binds the FxLx motif of the nisin leader peptide. Biochemistry. 2013;52(32):5387-95.
60. Hayashi K. A rapid determination of sodium dodecyl sulfate with methylene blue. Anal Biochem. 1975;67(2):503-6.
61. Siewert G, Strominger JL. Bacitracin: an inhibitor of the dephosphorylation of lipid pyrophosphate, an intermediate in the biosynthesis of the peptidoglycan of bacterial cell walls. Proc Natl Acad Sci U S A. 1967;57(3):767-73.
62. Bonelli RR, Schneider T, Sahl HG, Wiedemann I. Insights into in vivo activities of lantibiotics from gallidermin and epidermin mode-of-action studies. Antimicrob Agents Chemother. 2006;50(4):1449-57.
63. Schultz KM, Merten JA, Klug CS. Characterization of the E506Q and H537A dysfunctional mutants in the E. coli ABC transporter MsbA. Biochemistry. 2011;50(18):3599-608.
64. Ernst R, Kueppers P, Klein CM, Schwarzmueller T, Kuchler K, Schmitt L. A mutation of the H-loop selectively affects rhodamine transport by the yeast multidrug ABC transporter Pdr5. Proc Natl Acad Sci U S A. 2008;105(13):5069-74.
65. Knoester J. On the theory of concentration self-quenching by statistical traps. In: van Himbeeren JE, editor. The Journal of Chemical Physics1986. p. 3571-6.
66. Prlj A. Fluorescence Quenching in BODIPY Dyes: The Role of Intramolecular Interactions and Charge Transfer. In: Vannay L, Corminboeuf C, editors. Helvetica Chimica Acta2017.
67. Beddard GS. Concentration quenching in chlorophyll. In: Porter G, editor. Nature Letter1976. p. 366-7.
68. Kuk ACY, Hao A, Guan Z, Lee SY. Visualizing conformation transitions of the Lipid II flippase MurJ. Nat Commun. 2019;10(1):1736.
69. Kuk AC, Mashalidis EH, Lee SY. Crystal structure of the MOP flippase MurJ in an inward-facing conformation. Nat Struct Mol Biol. 2017;24(2):171-6.

Supporting Information

Mechanism of the BceAB-type transporter NsrFP from *Streptococcus agalactiae*

Julia Zaschke-Kriesche[a], Sandra Unsleber[b], Irina Voitsekhovskaia[b], Andreas Kulik[b], Nina Overbeck[c], Jelle Postma[d], Stefanie Weidtkamp-Peters[d], Kai Stühler[c], Evi Stegmann[b] and Sander H.J. Smits[a,e*]

[a] *Institute of Biochemistry, Heinrich-Heine-University Duesseldorf, Universitaetsstrasse 1, 40225 Duesseldorf, Germany.*

[b] *Interfaculty Institute of Microbiology and Infection Medicin, Eberhard Karls University, Auf der Morgenstelle 28, 72076 Tübingen, Germany.*

[c] *Molecular Proteomics Laboratory, Heinrich-Heine-University Duesseldorf, Universitaetsstrasse 1, 40225 Duesseldorf, Germany.*

[d] *Center for Advanced Imaging, Heinrich-Heine-University Duesseldorf, Universitaetsstrasse 1, 40225 Duesseldorf, Germany.*

[e] *Center of Structural Studies Heinrich-Heine-University Duesseldorf, Universitaetsstrasse 1, 40225 Duesseldorf, Germany.*

*Corresponding author: Sander.Smits@hhu.de

Keywords: BceAB-type, antibiotic resistance, nisin, bacitracin, lipid II

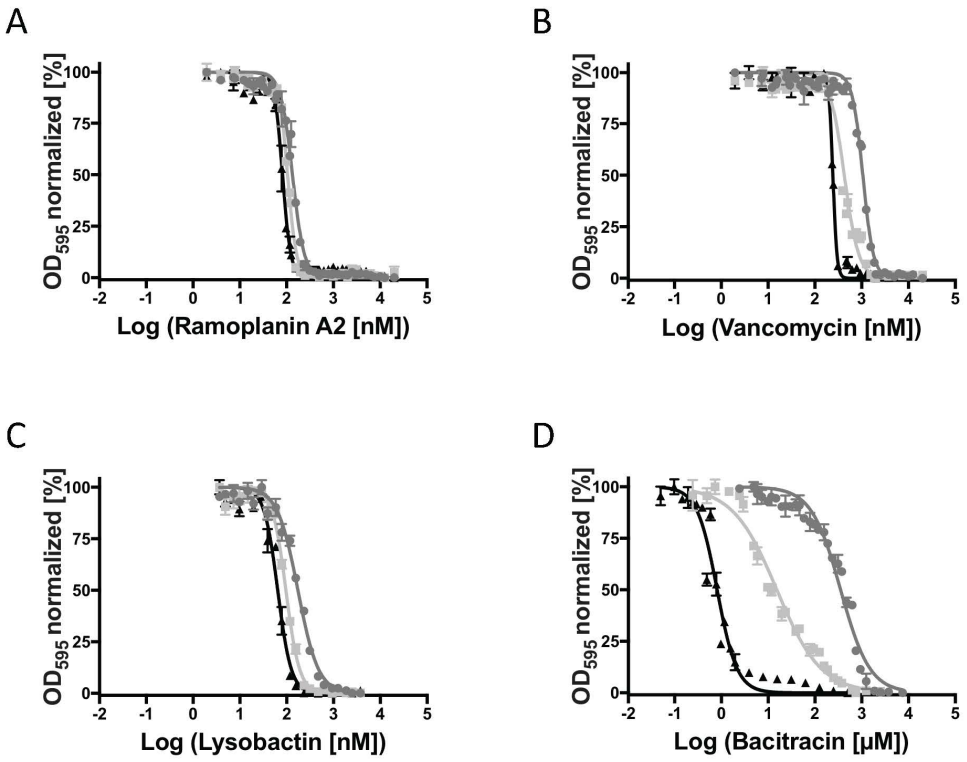

SI Figure 1: Representative inhibitional growth curves of **A) Ramoplanin A2**, **B) Vancomycin**, **C) Lysobactin** and **D) Bacitracin.** Normalized OD_{595} is plotted against the logarithmic concentration of the antibiotic. NZ9000Cm is demonstrated in black, NZ9000NsrF$_{H202A}$P in light grey and NZ9000NsrFP in grey.

SI Table 1: Measured IC_{50} values and calculated fold of resistance for the antibiotics Ramoplanin A2, Vancomycin, Lysobactin and Bacitracin and for the strains NZ9000Cm , NZ9000NsrF_{H202A}P and NZ9000NsrFP.

Antibiotic	*L. lactis* NZ9000Cm IC_{50} [nM]	*L. lactis* NZ9000NsrFP IC_{50} [nM]	*L. lactis* NZ9000NsrFP Fold of resistance	*L. lactis* NZ9000NsrF_{H202A}P IC_{50} [nM]	*L. lactis* NZ9000NsrF_{H202A}P Fold of resistance
Ramoplanin A2	73.00 ± 18.2	120.52 ± 34.2	1.65 ± 0.5	91.67 ± 20.5	1.26 ± 0.3
Vancomycin	213.57 ± 27.0	1077.92 ± 263.5	5.05 ± 1.2	325.38 ± 117.1	1.52 ± 0.5
Lysobactin	30.77 ± 16.8	181.68 ± 36.5	5.91 ± 1.2	101.80 ± 52.2	3.31 ± 1.8
Bacitracin	937.64 ± 93.9	327500.00 ± 60883.9	349.15 ± 64.9	12854.8 ± 8517.2	13.70 ± 9.1

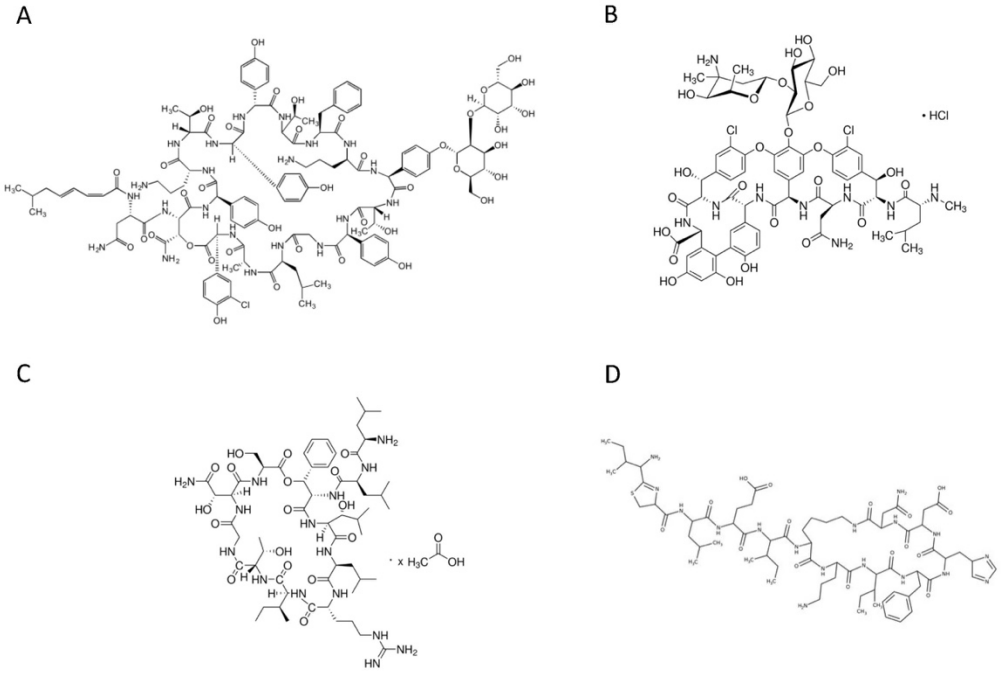

SI Figure 2: Structures of A) Ramoplanin A2 from AdipoGen life sciences, **B) Vancomycin** from Fluka Analytical, **C) Lysobactin** from Sigma life sciences and **D) Bacitracin** from Fisher BioReagents.

2

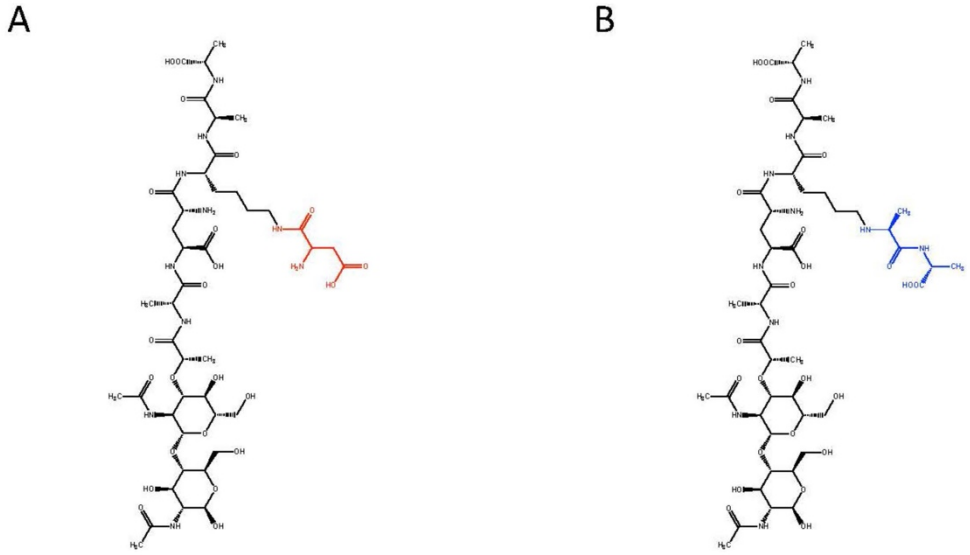

SI Figure 3: A) Structure of GlcNAc-MurNAc-Ala-iGlu-Lys-(Asp)-Ala-Ala with aspartate bridge in red found in *L. lactis* NZ9000Cm and *L. lactis* NZ9000NsrF$_{H202A}$P **B) Structure of GlcNAc-MurNAc-Ala-iGlu-Lys-(Ala-Ala)-Ala-Ala** with alanine bridge in blue found in *L. lactis* NZ9000NsrF$_{H202A}$P and *L. lactis* NZ9000NsrFP.

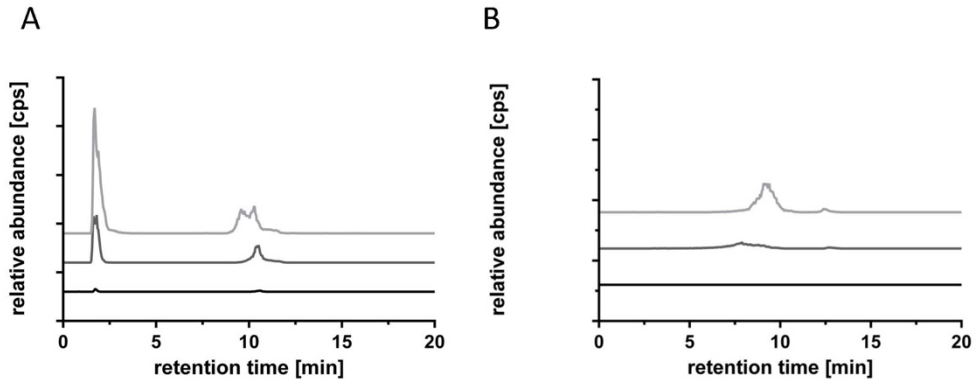

SI Figure 4: Relative abundance in cps against retention time in min of precursor accumulation after treatment with bacitracin. A) Spectrum for 1148.4 m/z^{-1} and **B)** Spectrum for 1263.4 m/z^{-1} of the strains NZ9000Cm (light grey), NZ9000NsrF$_{H202A}$P (grey) and NZ9000NsrFP (black).

3

ADJ60406

ADJ60417

ADJ60503

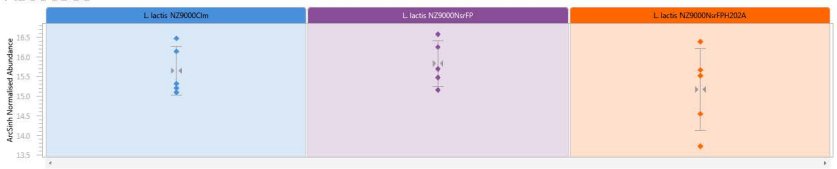

ADJ60765

ADJ60806

ADJ60966

4

ADJ59149

ADJ59249

ADJ59347

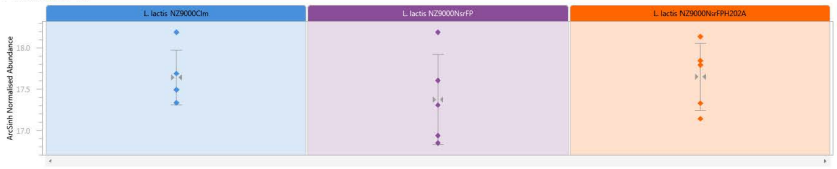

ADJ59379

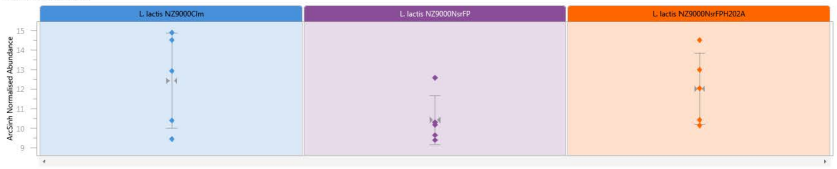

ADJ59381

ADJ59382

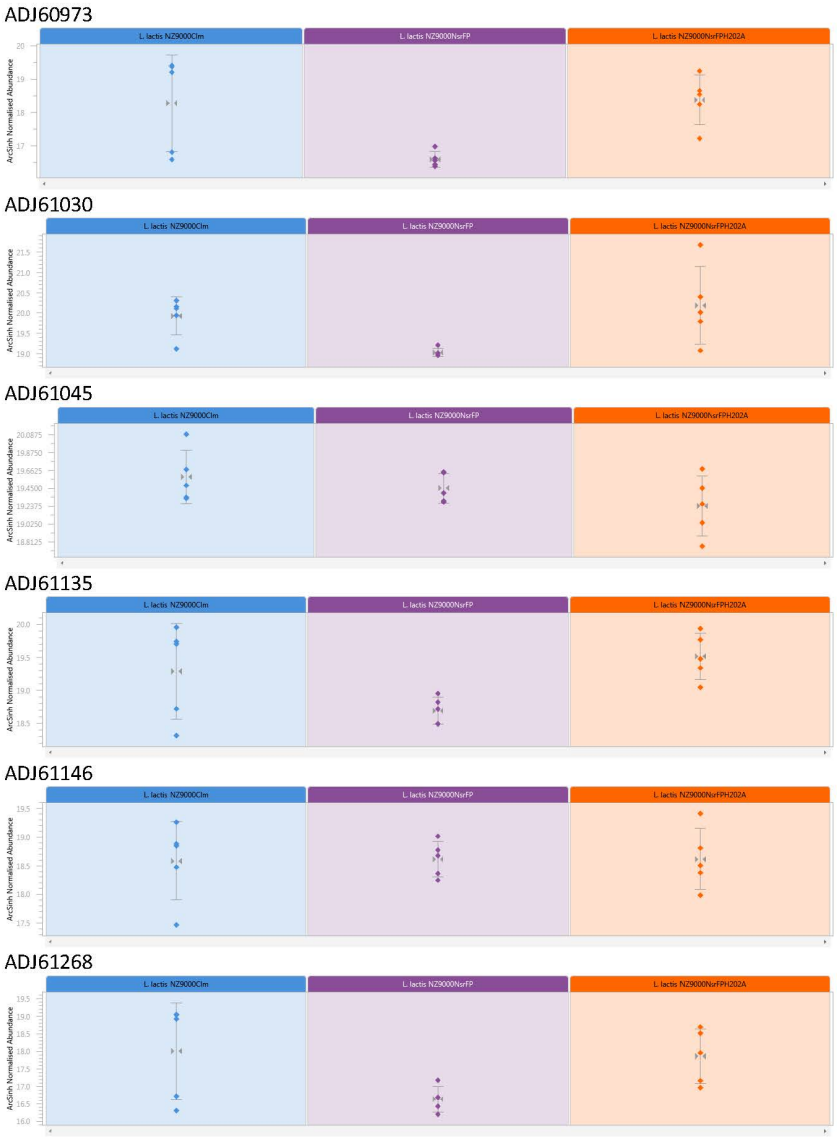
ADJ60973
L. lactis NZ9000Clm
L. lactis NZ9000NsrFP
L. lactis NZ9000NsrFPH202A
ArcSinh Normalised Abundance
ADJ61030
ADJ61045
ADJ61135
ADJ61146
ADJ61268

b

ADJ61283

ADJ61304

ADJ61321

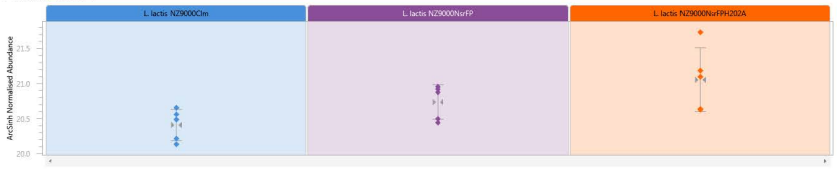

ADJ61415

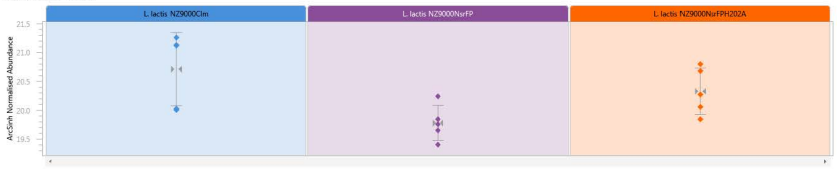

ADJ61465

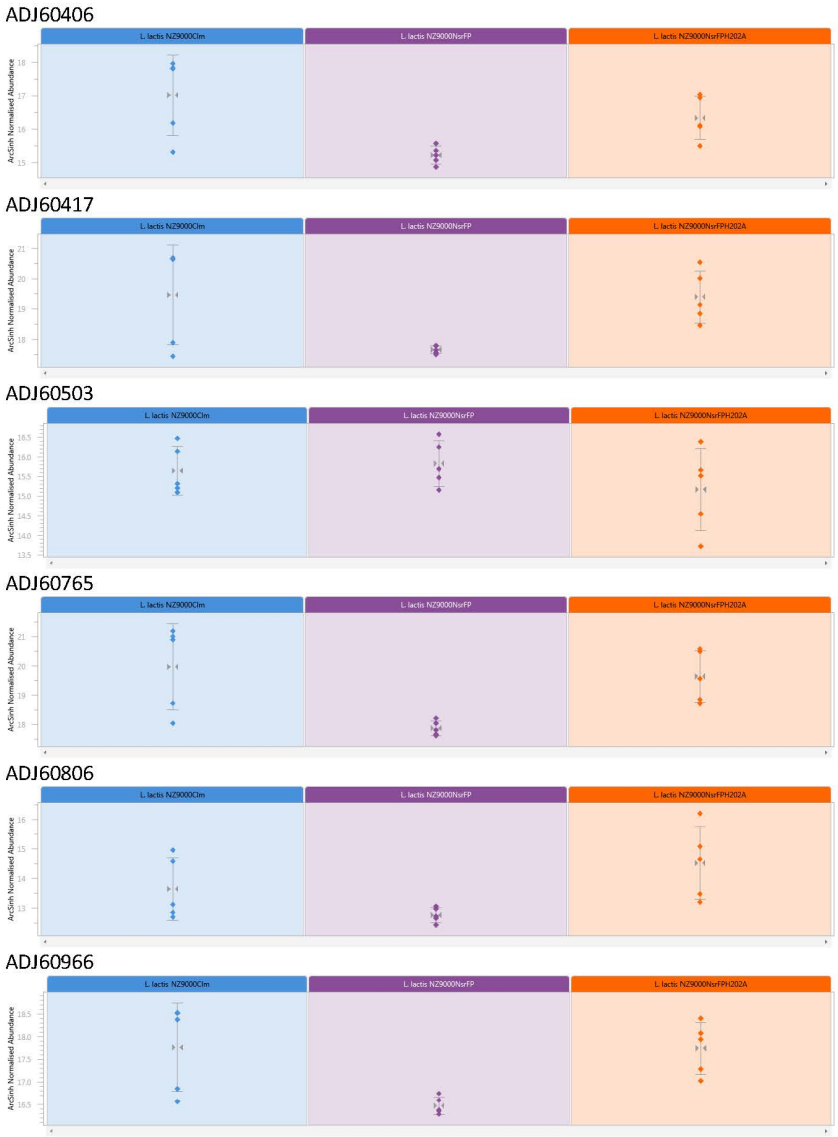

SI Figure 5: Normalized abundance of several proteins of the proteome analysis of *L. lactis* NZ9000Cm (blue), NZ9000NsrFP (violette) and NZ9000NsrF$_{H202A}$P (orange).

8

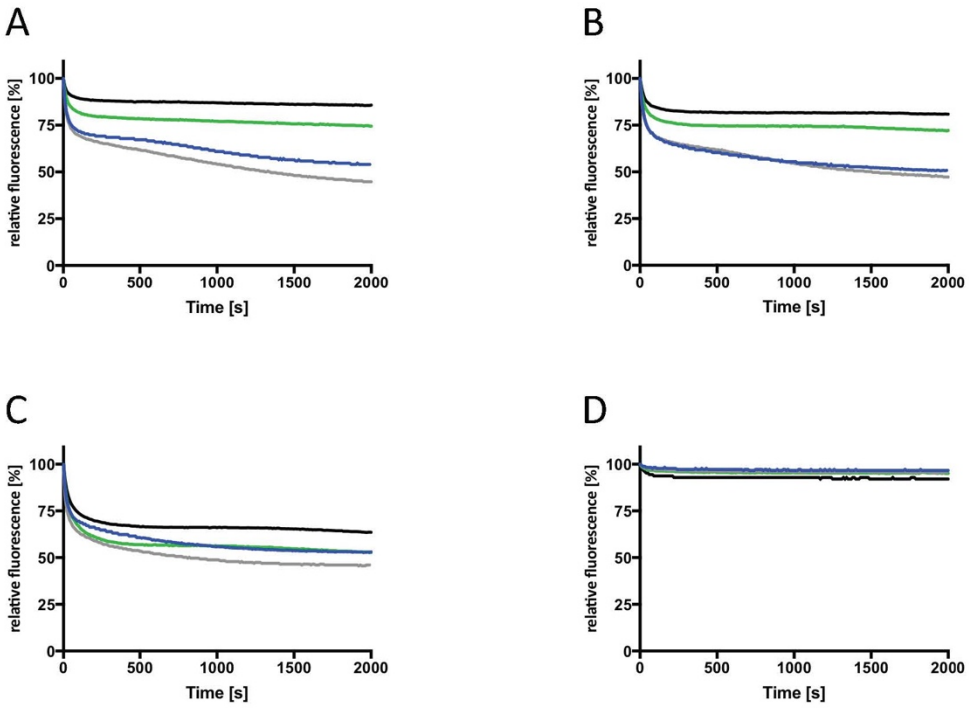

SI Figure 6: Relative fluorescence of BODIPY™ FL Vancomycin at different concentration of 250 nM (blue), 500 nM (grey), 1000 nM (green) and 2000 nM (black) for the strains A) NZ9000Cm, B) NZ9000NsrF$_{H202A}$P and C) NZ9000NsrFP as well as a control measurement without bacteria (D).

3.7. Chapter VII – Natural compounds against nisin resistance

Published in: in preparation

Impact factor:

Own Work: 60 %

Expression of the proteins

Performing biological assays

Preparation of the figures

Writing the manuscript

Natural compounds against nisin resistance

Julia Zaschke-Kriesche, Peter Proksch and Sander H.J. Smits

Natural compounds against nisin resistance

Julia Zaschke-Kriesche[a], Peter Proksch[b] and Sander H. J. Smits [a,c]

[a] *Institute of Biochemistry, Heinrich-Heine-University Duesseldorf, Universitaetsstrasse 1, 40225 Duesseldorf, Germany.*
[b] *Insitute for Pharmaceutical Biology and Biotechnology,Heinrich-Heine-University Duesseldorf, Universitaetsstrasse 1, 40225 Duesseldorf, Germany.*

Abstract

For pharmaceutical research it is a great goal to elucidate and overcome resistance mechanisms present in human pathogenic bacteria. In this study natural compounds were screened on their ability to inhibit the growth of cells expressing the nisin resistance proteins *Sa*NSR and *Sa*NsrFP of the human pathogen *Streptococcus agalactiae*. Here we show an assay to elucidate whether natural compounds specifically inhibit resistance proteins and present some promising candidates, including cyclic peptides, diterpenes and ceramides, which cause inhibition of the nisin resistance ABC-transporter *Sa*NsrFP.

Introduction

Elucidating and overcoming resistance mechanisms of human pathogenic bacteria is the main goal of pharmaceutical companies. One strategy to reach this goal is the application of natural compounds, as potential antimicrobial agents. One group of natural compounds are lantibiotics, produced by mainly Gram-positive bacteria (1, 2). They are produced as prepeptides and mature in the cytosol of the bacteria, thereby forming lanthionine rings which are necessary for their stability and activity (3-5). The best studied lantibiotic is nisin, produced by *Lactococcus lactis* and *Streptococcus uberis* strains (6, 7). Nisin has a dual mode of action. First the N-terminal part of nisin binds to the pyrophosphate moiety of the cell wall precursor lipid II, thereby inhibiting peptidoglycan synthesis (8, 9). Secondly, nisin forms pores out of eight nisin and four lipid II molecules into the bacterial membrane which leads to rapid cell death due to the efflux of nutrients and ions and subsequently to a collapse of the membrane potential (10). Pharmaceutical usage of nisin and other lantibiotics like subtilin from *B. subtilis* and gallidermin from *S. gallinarium* are hampered by the presence of resistance mechanisms in human pathogenic bacteria (11-15). For example, mediated by the nsr operon in the human pathogenic strain *Streptococcus agalactiae* (16, 17). The nisin resistance protein operon (nsr operon) of *S. agalactiae* is composed of genes encoding a serine protease NSR, an ABC-transporter NsrFP and a two-component system NsrRK (16).

*Sa*NSR belongs to the S41 peptidase family and has a specific catalytic dyad mechanism consisting of a serine and a histidine residue (18, 19). NSR confers resistance against nisin by degrading the lantibiotic *via* cleavage between MeLan28 and Ser29 of nisin (17), thereby reducing the antimicrobial activity 100 fold (17, 20). If

*Sa*NSR is expressed in a nisin sensitive *L. lactis* strain a 18-20-fold resistance against nisin can be observed (16).

The ABC-transporter NsrFP from *S. agalactiae* consists of a nucleotide binding domain NsrF and a transmembrane domain NsrP and belongs to the BceAB-type transporter (16). If expressed in a nisin sensitive *L. lactis* strain *Sa*NsrFP confers 16-fold of resistance against nisin and 12-fold of resistance against the lantibiotic gallidermin. As nisin and gallidermin are similar in the N-terminal part it was assumed that NsrFP also recognizes the N-terminal part of nisin. Further it was shown that *Sa*NsrFP prevents the cells from pore formation mediated by nisin and an efflux mechanism of the transporter was postulated based on an peptide release assay (21). Despite this the mechanism and the structure of NsrFP from *S. agalactiae* remains unknown.

In this study we present a screening of compounds and derivatives from natural source like fungi and marine organisms on their effect on the nisin resistance proteins *Sa*NSR and *Sa*NsrFP from *S. agalactiae.*

Material and Methods

Cloning of nisin resistance proteins

For studies in recombinant *L. lactis* cells the plasmid pNZ-SV-*Sa*NSR was obtained by cloning the gene nsr from *S. agalactiae* COH1 as previously described (16). Cloning of *nsrFP* from *S. agalactiae* COH1 was performed liked described in Alkhatib et al. (2014) (22) and Reiners et al. (2017) (21) to gain the plasmid pIL-SV *Sa*NsrFP. Briefly, the plasmid was transformed using electrocompetent *L. lactis NZ9000* cells and a pulse setting of 1 kV, 25 µF, 200 Ω, for 4.5-5.0 ms to electroporate the cells (23). Afterwards 950 µl GM17 media was added and the cells incubated for 3h at 30 °C. At last the cells were plated on SMGG-agar plates containing 5 µg/ml erythromycin and chloramphenicol, respectively.

Purification of nisin

Nisin was purified as previously described using a cation exchange chromatography (24). To obtain the concentration the peptide was analyzed with RP-HPLC as described previously (25). Briefly a water/acetonitrile gradient, acidified with 0.1 % TFA, was used from 10 % acetonitrile to 64 % acetonitrile.

Growth inhibition assay

To verify the nisin concentration used for the specific growth inhibition an assay similar to the previously described IC_{50} assay was performed (21). Briefly nisin was diluted in a 96-well plate and the strains *L. lactis*

2

NZ9000, *L. lactis* NZ9000NSR and *L. lactis* NZ9000NsrFP were added. After incubation at 30°C for 5 hours the OD_{595} was measured and normalized.

Specific growth inhibition assay

To screen the natural compounds on their ability to specifically inhibit the growth of *Sa*NSR or *Sa*NsrFP expressing strains the cells were grown in GM17 medium with 5 µg/ml erythromycin or chloramphenicol and 1 ng/ml nisin overnight. The cells were diluted in fresh media to an OD_{595} of 0.1 and incubated for 30 min at 30 °C. In a 96 well plate 50 µl of the natural substances and the DMSO control were added. 150 µl *L. lactis* cells were added to natural substances. Each resistance protein expressing strain, *L. lactis* NZ9000 pNZ-SV-*Sa*NSR and *L. lactis* NZ9000 pIL-SV-*Sa*NsrFP was sublemented with 30 nM nisin and compared to the corresponding sensitive strain, *L. lactis* NZ9000 pNZ-SV-Erm and *L. lactis* NZ9000 pIL-SV-Clm. Cells were grown at 30°C for 5 hours and OD_{595} was measured.

Natural compounds

The natural compounds were obtained from Prof. Dr. Proksch, Insitute for pharmaceutical biology and biotechnology of the Heinrich-Heine-University Düsseldorf. They are dissolved in DMSO at a concentration of 10 mM and stored at -20 °C until further usage. For the specific growth inhibition assay the compounds were diluted with water. A list with all compounds is found in the appendix of this chapter.

Results

Conditions for the screening of natural compounds

To verify if a compound specifically inhibits the resistance proteins all compounds were used at the same concentration of 100 µM for the control strain and the resistance strain. Hence it can be visualized whether a compound has an unspecific inhibition effect, which would result in an decreased optical density for both strains. Further the nisin concentration depending growth for all strains was determined (Figure 1). For the resistance strains *L. lactis* NZ9000NSR (blue) and *L. lactis* NZ9000NsrFP (red) the growth curve is shifted to higher nisin concentrations than for *L. lactis* NZ9000 (black). The dotted line marks a nisin concentration of 30 nM (log = 1.48), here the growth for the resistant strains is still 100 % whereas the sensitive cells are dead. This concentration of 30 nM nisin was used for the further assays to see whether the compounds specifically inhibit the resistance protein, which would result in a drop of the growth of *L. lactis* NZ9000NSR and *L. lactis* NZ9000NsrFP, respectively.

3

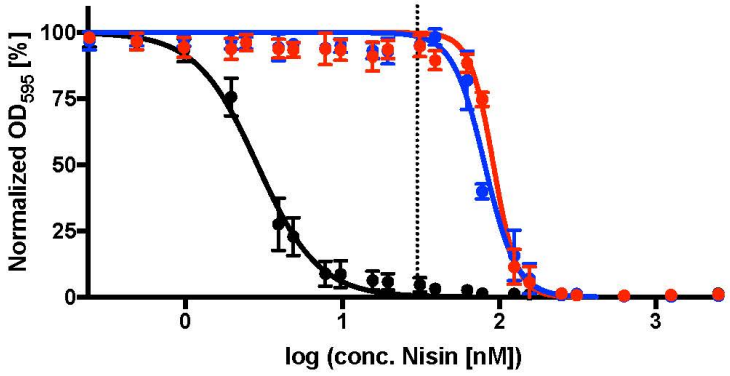

Figure 1: Growth curves in the presence of nisin. Normalized OD_{595} against logarithmic nisin concentrations [nM] for the strains *L. lactis* NZ9000 (black), *L. lactis* NZ9000NSR (blue) and *L. lactis* NZ9000NsrFP (red). The dotted line at log 1.48 demonstrates a nisin concentration of 30 nM, which is used in further assays.

Screening of natural compounds against Sa*NSR and* Sa*NsrFP*

120 natural compounds provided by the research group of Prof. Dr. Proksch, Insitute for pharmaceutical biology and biotechnology of the Heinrich-Heine-University Düsseldorf were screened on their ability of specific growth inhibition against *Sa*NSR and *Sa*NsrFP expressing cells. Therefore, the OD_{595} was measured in presence of 100 µM compound and normalized against the DMSO control. Further the normalized ODs for the resistance protein expressing strains were divided by the normalized ODs for the sensitive strains and subtracted from 100 % to gain the specific growth inhibition of *L. lactis* NZ9000 pNZ-SV-*Sa*NSR and *L. lactis* NZ9000 pIL-SV-*Sa*NsrFP. The threshold was set to 40 % specific growth inhibition since 100 µM compound were used and lower inhibition than 40 % is rather due to random binding or weak affinity than due to a specific inhibition of the resistance protein. Figure 2 and 3 show the results for all natural compounds screened for *Sa*NSR and Figure 4 and 5 for *Sa*NsrFP.

For the *Sa*NSR expressing strain some compounds like dibromhemibastadin-1, W493 B and homosekikaic acid showed a slightly growth inhibition but did not reach the threshold of 40 %.

For *L. lactis* NZ9000 pNZ-SV-*Sa*NSR no specific inhibitor was recognized by the screening of 120 compounds (Figure 2 and 3).

For the ABC-transporter expressing strain some compounds showed a high inhibitory effect over 40 % and were further analyzed. Those compounds were bakuchiol, sekikaic acid, Cerebroside C, callyaerin G, callyaerin E, g114 and alterporriol E (Figure 4 and 5).

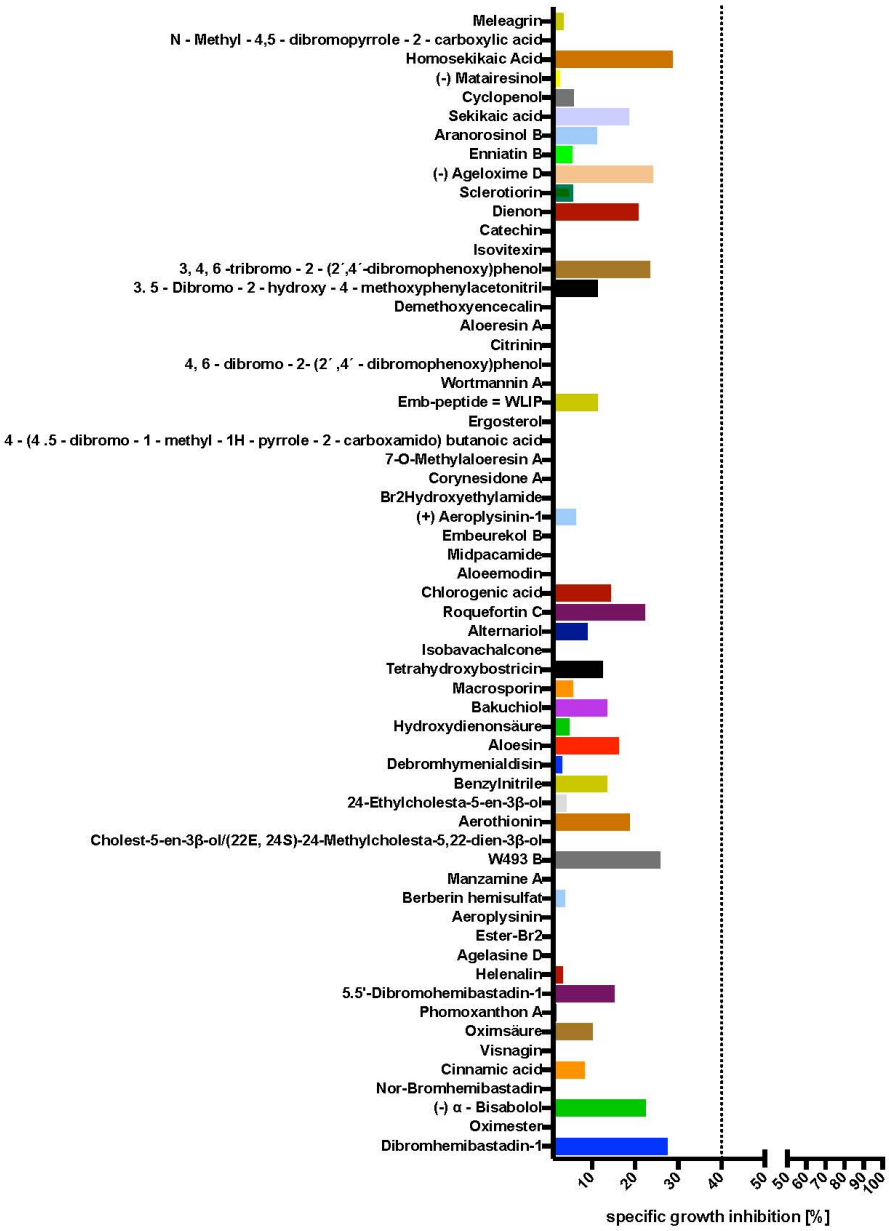

Figure 2: Natural compound screen on *L. lactis* NZ9000 pNZ-SV-*Sa*NSR. First set of 60 compounds [100 µM] screened on their ability to specifically inhibit the growth of *L. lactis* NZ9000 pNZ-SV-*Sa*NSR in the presence of 30 nM nisin. Line at 40 % specific growth inhibition shows threshold for further studies. Compounds with no inhibitional effect are shown with no bar.

5

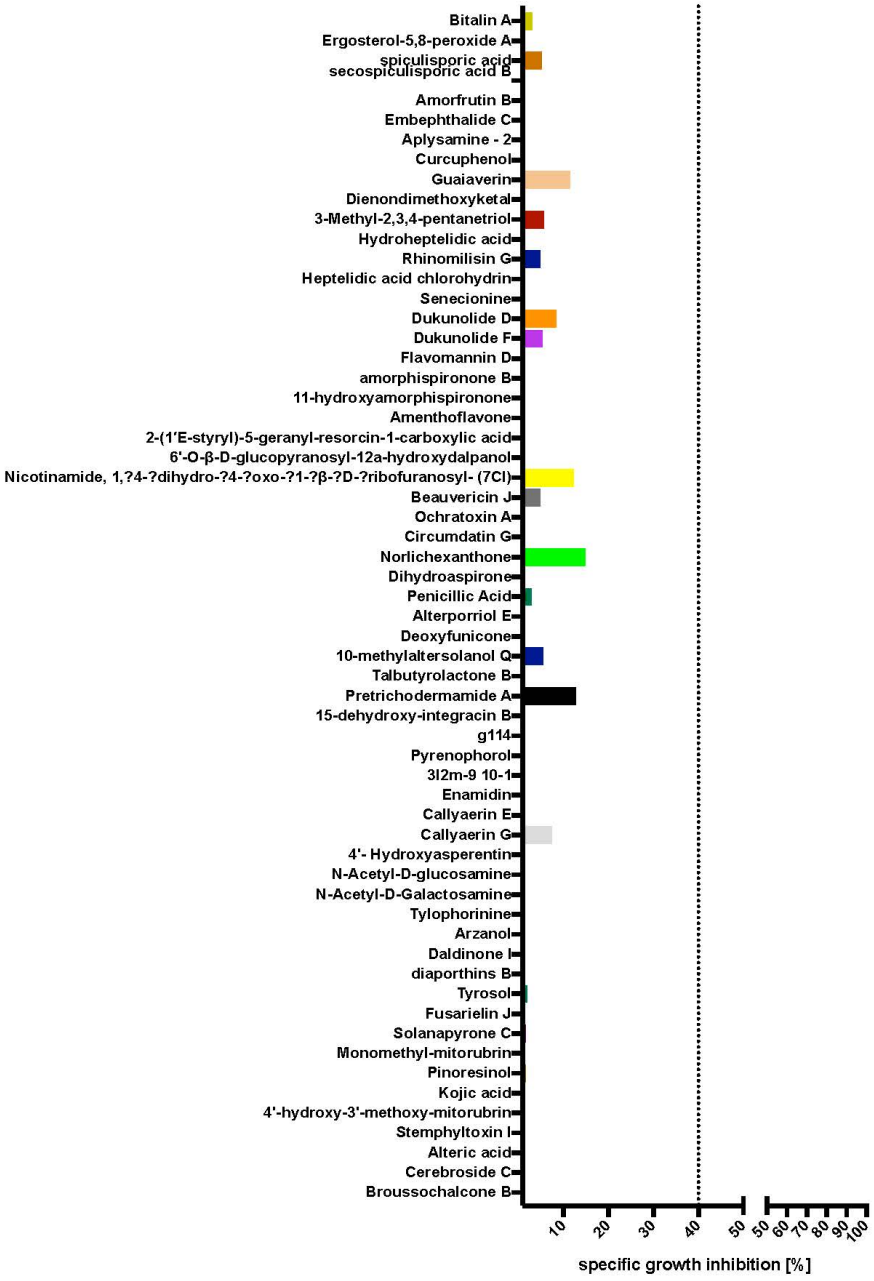

Figure 3: Natural compound screen on *L. lactis* NZ9000 pNZ-SV-*Sa*NSR. Second set of 60 compounds [100 µM] screened on their ability to specifically inhibit the growth of *L. lactis* NZ9000 pNZ-SV-*Sa*NSR in the presence of 30 nM nisin. Line at 40 % specific growth inhibition shows threshold for further studies. Compounds with no inhibitional effect are shown with no bar.

6

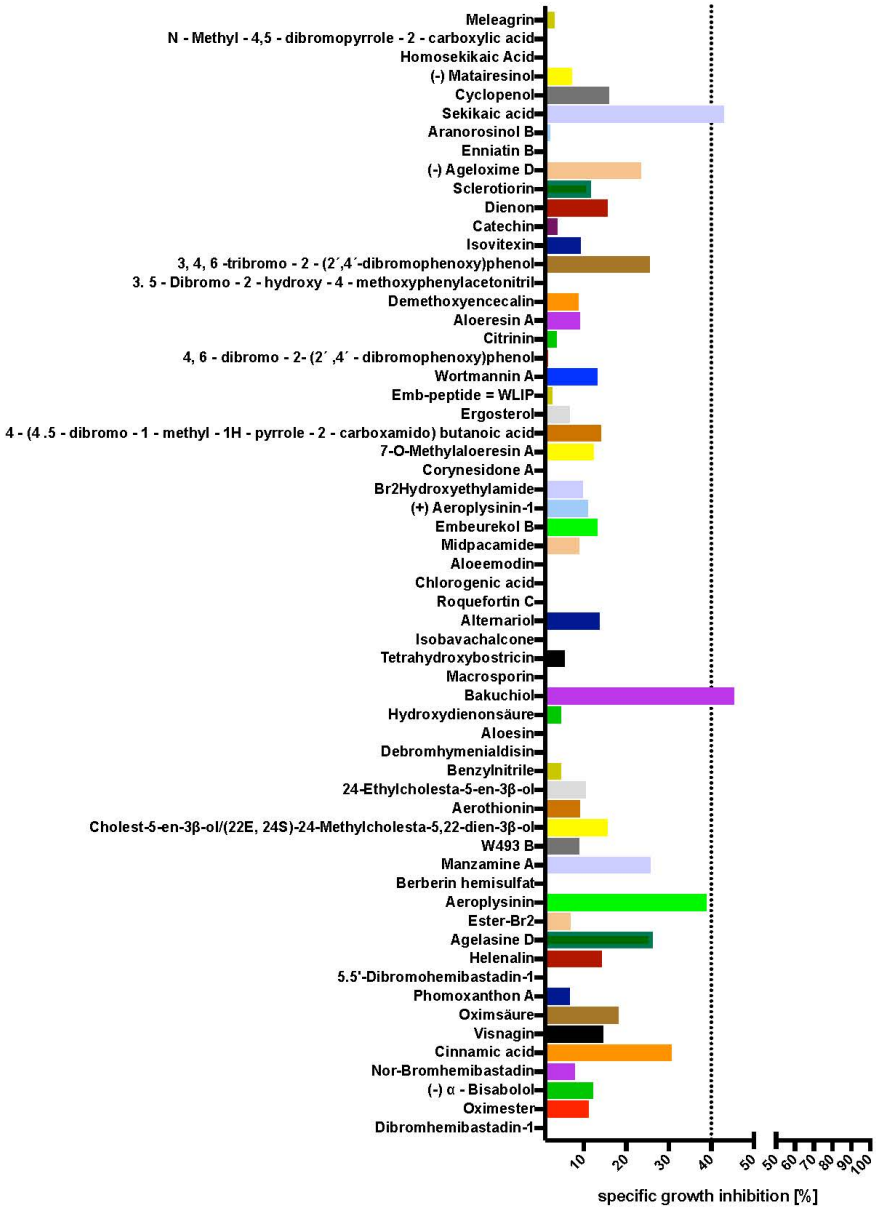

Figure 4: Natural compound screen on *L. lactis* NZ9000 pIL-SV-*Sa*NsrFP. First set of 60 compounds [100 µM] screened on their ability to specifically inhibit the growth of *L. lactis* NZ9000 pIL-SV-*Sa*NsrFP in the presence of 30 nM nisin. Line at 40 % specific growth inhibition shows threshold for further studies. Compounds with no inhibitional effect are shown with no bar.

7

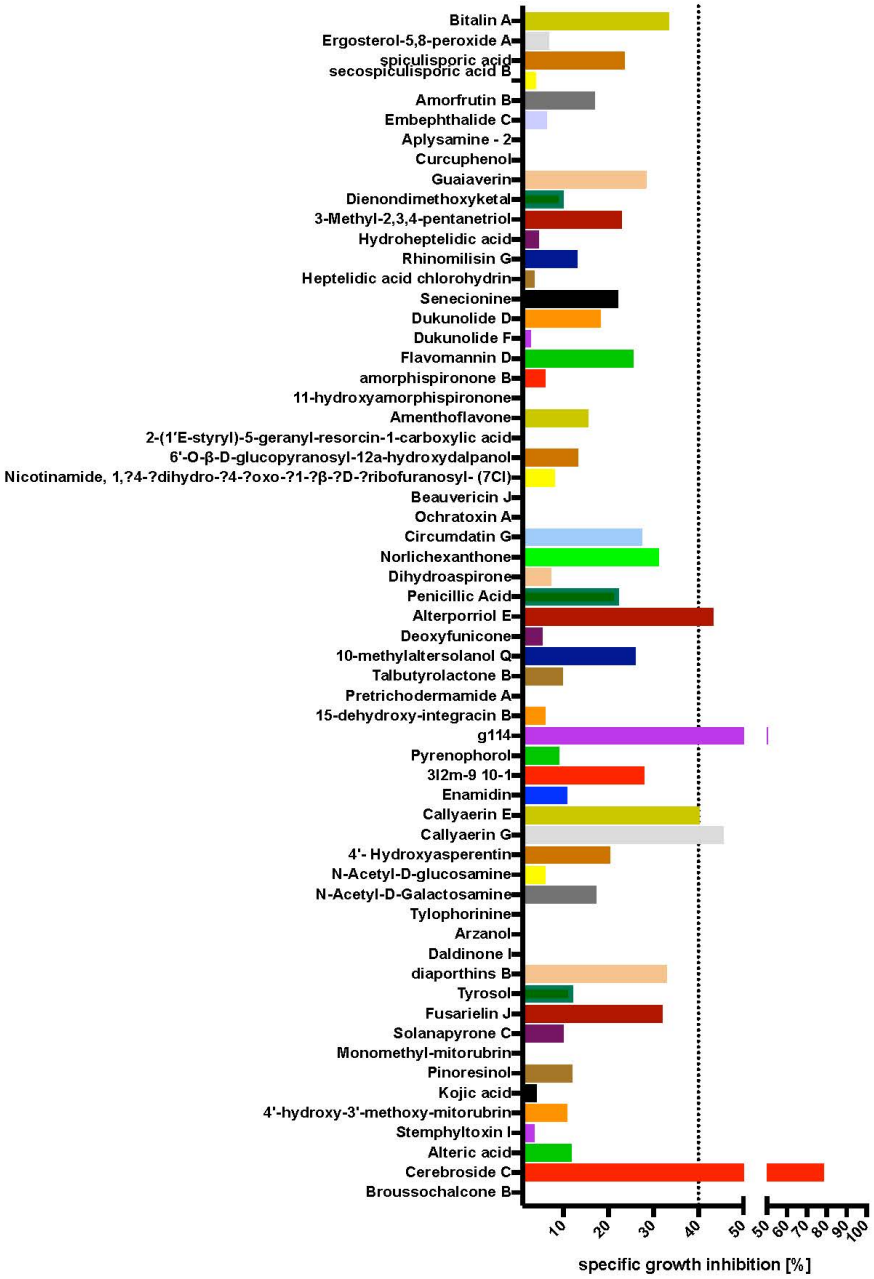

Figure 5: Natural compound screen on *L. lactis* NZ9000 pIL-SV-*Sa*NsrFP. Second set of 60 compounds [100 µM] screened on their ability to specifically inhibit the growth of *L. lactis* NZ9000 pIL-SV-*Sa*NsrFP in the presence of 30 nM nisin. Line at 40 % specific growth inhibition shows threshold for further studies. Compounds with no inhibitional effect are shown with no bar.

Analyzing putative SaNsrFP inhibitors

8

The promising compounds were investigated against *L. lactis* NZ9000NsrFP in the same assay like mentioned above resulting in 8.7 ± 5.5 % specific inhibition for sekikaic acid and 1.4 ± 0.6 % for callyaerin G. More interesting results were obtained for alterporriol E with 19.0 ± 5.6 %, callyaerin E with 27.0 ± 6.5 % and g114 with 38.7 ± 4.7 % specific growth inhibiton of *L. lactis* NZ9000NsrFP. The highest inhibition was detected with Cerebroside C , which gained an value of 83.2 ± 1.0 % specific inhibition, when 100 µM compound were present (Table 1, Figure 6).

Table 1: Measured specific growth inhibition in % of the natural compounds sekikaic acid, Cerebroside C, callyaerin G, callyaerin E, g114 and alterperriol E for *L. lactis* NZ9000 pIL-SV-*Sa*NsrFP.

	Sekikaic acid	Cerebroside C	Callyaerin G	Callyaerin E	g114	Alterporriol E
Specific growth inhibition [%]	8.7 ± 5.5	83.2 ± 1.0	1.4 ± 0.6	27.0 ± 6.5	38.7 ± 4.7	19.0 ± 5.6

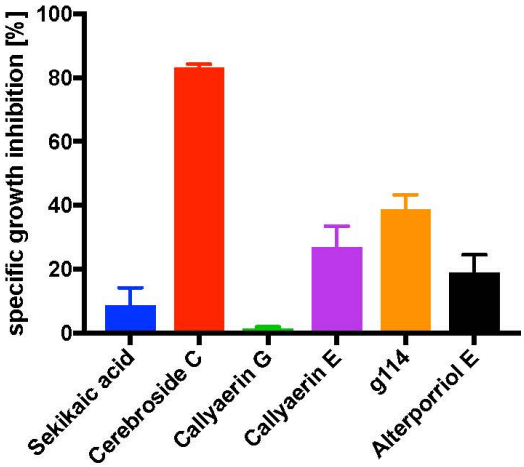

Figure 6: Measured specific growth inhibition in % of the natural compounds sekikaic acid, cerebroside C, callyaerin G, callyaerin E, g114 and alterperriol E for *L. lactis* NZ9000 pIL-SV-*Sa*NsrFP. All values were obtained from at least 4 independent measurements.

Since Cerebroside C gained the highest specific growth inhibition of *L. lactis* NZ9000NsrFP it was further analyzed and compared to Cerebroside D, which only differs in one double bond (Figure 7).

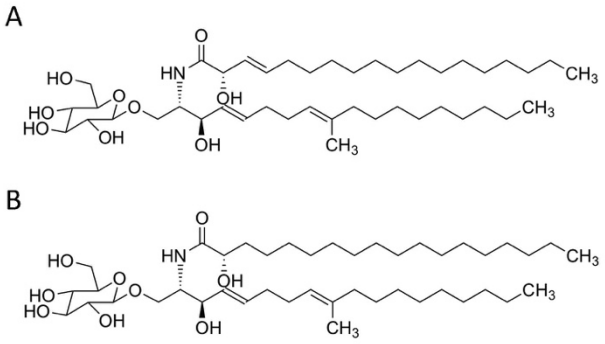

Figure 7: Structures of A) Cerebroside C and B) Cerebroside D.

The growth of *L. lactis* NZ9000NsrFP strain was observed in presence of 30 nM nisin and further compared to the growth of *L.lactis* NZ9000 cells at different concentrations of the Cerebroside variants (Figure 8). Interestingly Cerebroside D (black bars) showed no specific growth inhibition whereas Cerebroside C (blue graph) inhibits the growth of *L. lactis* NZ9000NsrFP even at a concentration of 6.3 µM.

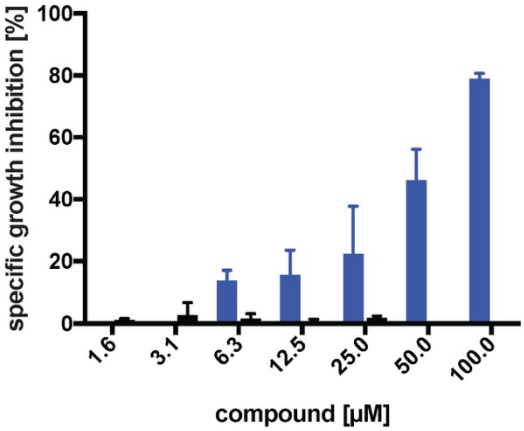

Figure 8: Specific growth inhibition of *L. lactis* NZ9000NsrFP. Normalized and specific growth of *L. lactis* NZ9000NsrFP compared to *L. lactis NZ9000* treated with 30 nM nisin against different concentrations of Cerebroside C (blue) and Cerebroside D (black).

Those results indicate that the inhibition of *Sa*NsrFP is specifically due to Cerebroside C. Cerebroside C, provided by Prof. Dr. Proksch, was analyzed on its purity *via* HPLC-MS measurement (Data not shown). Five different masses where found in the sample, none of them fitting to the mass of Cerebroside C. As the sample

is isolated decades ago, it is thought that the compound degraded over the time. Nevertheless, the sample of Cerebroside C shows a high specific inhibition of the resistance transporter *Sa*NsrFP.

Discussion

Sekikaic acid, which is found in some lichens, was not able to inhibit the nisin resistance ABC-transporter *Sa*NsrFP. Neither was callyaerin G, a cyclic peptide found in *Callyspongia aerizusa* extract, able to inhibit the resistance mediated by *Sa*NsrFP (26). On the contrary callyaerin E, which just differs in three residues in the peptide, gained an specific growth inhibition of 27 %, suggesting that those small differences influence the inhibition property of the peptide (Table 1) (26). The ring structure of the peptide callyaerin E holds a valine residue whereas callyaerin G at this position has a leucine residue. As those amino acids are quite similar, it is very unlikely that this difference influences the inhibition of *Sa*NsrFP. In the peptide side chain two isoleucins in callyaerin E are substituted by a proline and a phenylalanine in callyaerin G resulting in a huge sterically difference which can influence the affinity of the peptide to *Sa*NsrFP. As screenings with the same setup but with *Sa*NSR instead of *Sa*NsrFP resulted in no specific growth inhibition (Figure 2 and 3) mediated by the callyaerins it is very unlikely that callyaerin binds to nisin. To optimize the specific growth inhibition by callyaerins also other nautral variants (A-M) could be tested (26).

The application of alterporriol E resulted in a *L. lactis* NZ9000 pIL-SV-*Sa*NsrFP growth inhibition of 19 % (Table 1). The bianthraquinone from *Alternaria porri* is one of five natural variants, therefore the other natural variants also have to be tested on their ability to inhibit the growth of the *Sa*NsrFP expressing cells (27).
G114, a tricarbocyclic diterpene, causes 39 % inhibition of the *L. lactis* NZ9000 pIL-SV-*Sa*NsrFP growth compared to the control cells. As there is no inhibition for the *L. lactis* NZ9000 pNZ-SV-*Sa*NSR cells it is very likely that g114 binds to the ABC-transporter and thereby interrupts the resistance against nisin. Previous studies suggested an exporting mechanism for *Sa*NsrFP, which led to the assumption that nisin has to be bind by the transporter and therefore g114 could also bind to the same binding site, thereby inhibiting the export of nisin (21). Nevertheless also of this compound more derivates have to be tested.

The best inhibiting compound for the *Sa*NsrFP expressing strain is Cerebroside C with 83 % at a concentration of 100 µM. Cerebrosides consist of a fatty acid and a sphingosine, which together form the ceramide and further a monosaccharide. The ABC-transporter is a membrane protein and Cerebroside C has a high affinity to the membrane because of its lipid structure. It can be assumed that Cerebroside C also has a high affinity to the ABC-transporter. However, Cerebroside D with a similar structure showed no inhibitional effect which indicates rather a specific binding of *Sa*NsrFP.

*Sa*NsrFP is a BceAB-type transporter and several mechanisms have been postulated for this type of transporter. An antimicrobial peptide removal from the membrane (28), an exporting mechanism (21) and a flipping mechanism of undecaprenyl pyrophosphate (29). Although the resistance mechanism of the ABC-transporter family remains unsolved putative inhibition mechanism of Cerebroside C are conceivable. The removal of nisin from the membrane could be disturbed by the lipid-like structure and its affinity to the membrane and eventually to the transporter. This is quite unlikely as Cerebroside D should have the same effect. An exporting mechanism of *Sa*NsrFP could be inhibited by specific binding of Cerebroside C to either the active site of the transporter, resulting in an competitive inhibition, or binding to the non-active part and thereby changing the conformation of *Sa*NsrFP, subsequently affecting the binding of the substrate. For the third putative mechanism of BceAB-type transporter the inhibitional effect of Cerebroside C could be similar to the last mentioned one, except of the substrate. Nevertheless, more ceramide compounds have to be tested on specific growth inhibition.

Conclusively promising candidates of natural compounds where found during this study, ranging from cyclic peptides over diterpenes to ceramides. With a compound concentration of 100 µM specific growth inhibitions from 19 to 83 % could be obtained, showing the high potential of those compounds. Though other derivates of the tested natural compounds have to be investigated.

Acknowledgement

The authors would like to thank Dr. Aleksandra Zivkovic and Prof. Dr. Holger Stark for providing the structures and HPLC-MS analysis. The authors are thankful to the technical assistance for their support during the screening. This work was funded by the Deutsche Forschungsgemeinschaft (DFG, German Research Foundation) – 270650915/GRK 2158.

Bibliography

1. Sahl HG, Bierbaum G. Lantibiotics: biosynthesis and biological activities of uniquely modified peptides from gram-positive bacteria. Annu Rev Microbiol. 1998;52:41-79.
2. Klaenhammer TR. Genetics of bacteriocins produced by lactic acid bacteria. FEMS Microbiol Rev. 1993;12(1-3):39-85.
3. Knerr PJ, van der Donk WA. Discovery, biosynthesis, and engineering of lantipeptides. Annu Rev Biochem. 2012;81:479-505.
4. Chatterjee C, Paul M, Xie L, van der Donk WA. Biosynthesis and mode of action of lantibiotics. Chemical Reviews. 2005;105(2):633-84.
5. Arnison PG, Bibb MJ, Bierbaum G, Bowers AA, Bugni TS, Bulaj G, et al. Ribosomally synthesized and post-translationally modified peptide natural products: overview and recommendations for a universal nomenclature. Nat Prod Rep. 2013;30(1):108-60.

6. Cleveland J, Montville TJ, Nes IF, Chikindas ML. Bacteriocins: safe, natural antimicrobials for food preservation. Int J Food Microbiol. 2001;71(1):1-20.
7. Rogers LA. The Inhibiting Effect of Streptococcus Lactis on Lactobacillus Bulgaricus. J Bacteriol. 1928;16(5):321-5.
8. Wiedemann I, Breukink E, Van Kraaij C, Kuipers OP, Bierbaum G, De Kruijff B, et al. Specific Binding of Nisin to the Peptidoglycan Precursor Lipid II Combines Pore Formation and Inhibition of Cell Wall Biosynthesis for Potent Antibiotic Activity. Journal of Biological Chemistry. 2001;276(3):1772-9.
9. Hsu ST, Breukink E, Tischenko E, Lutters MA, de Kruijff B, Kaptein R, et al. The nisin-lipid II complex reveals a pyrophosphate cage that provides a blueprint for novel antibiotics. Nat Struct Mol Biol. 2004;11(10):963-7.
10. Hasper HE, de Kruijff B, Breukink E. Assembly and stability of nisin-lipid II pores. Biochemistry. 2004;43(36):11567-75.
11. Gebhard S. ABC transporters of antimicrobial peptides in Firmicutes bacteria–phylogeny, function and regulation. Molecular microbiology. 2012;86(6):1295-317.
12. Draper LA, Cotter PD, Hill C, Ross RP. Lantibiotic Resistance. Microbiology and Molecular Biology Reviews. 2015;79(2):171-91.
13. Suárez JM, Edwards AN, McBride SM. The Clostridium difficile cpr locus is regulated by a noncontiguous two-component system in response to type A and B lantibiotics. Journal of bacteriology. 2013;195(11):2621-31.
14. Clemens R, Zaschke-Kriesche J, Khosa S, Smits SHJ. Insight into Two ABC Transporter Families Involved in Lantibiotic Resistance. Front Mol Biosci. 2017;4:91.
15. Reiners J, Abts A, Clemens R, Smits SH, Schmitt L. Stoichiometry and structure of a lantibiotic maturation complex. Sci Rep. 2017;7:42163.
16. Khosa S, AlKhatib Z, Smits SH. NSR from Streptococcus agalactiae confers resistance against nisin and is encoded by a conserved nsr operon. Biol Chem. 2013;394(11):1543-9.
17. Sun Z, Zhong J, Liang X, Liu J, Chen X, Huan L. Novel mechanism for nisin resistance via proteolytic degradation of nisin by the nisin resistance protein NSR. Antimicrob Agents Chemother. 2009;53(5):1964-73.
18. Rawlings ND, Barrett AJ, Thomas PD, Huang X, Bateman A, Finn RD. The MEROPS database of proteolytic enzymes, their substrates and inhibitors in 2017 and a comparison with peptidases in the PANTHER database. Nucleic Acids Res. 2018;46(D1):D624-D32.
19. Khosa S, Frieg B, Mulnaes D, Kleinschrodt D, Hoeppner A, Gohlke H, et al. Structural basis of lantibiotic recognition by the nisin resistance protein from Streptococcus agalactiae. Sci Rep. 2016;6:18679.
20. Liang X, Sun Z, Zhong J, Zhang Q, Huan L. Adverse effect of nisin resistance protein on nisin-induced expression system in Lactococcus lactis. Microbiol Res. 2010;165(6):458-65.
21. Reiners J, Lagedroste M, Ehlen K, Leusch S, Zaschke-Kriesche J, Smits SHJ. The N-terminal Region of Nisin Is Important for the BceAB-Type ABC Transporter NsrFP from Streptococcus agalactiae COH1. Front Microbiol. 2017;8:1643.
22. AlKhatib Z, Lagedroste M, Zaschke J, Wagner M, Abts A, Fey I, et al. The C-terminus of nisin is important for the ABC transporter NisFEG to confer immunity in Lactococcus lactis. Microbiologyopen. 2014;3(5):752-63.
23. Holo H, Nes IF. High-Frequency Transformation, by Electroporation, of Lactococcus lactis subsp. cremoris Grown with Glycine in Osmotically Stabilized Media. Appl Environ Microbiol. 1989;55(12):3119-23.
24. Abts A, Mavaro A, Stindt J, Bakkes PJ, Metzger S, Driessen AJ, et al. Easy and rapid purification of highly active nisin. Int J Pept. 2011;2011:175145.
25. Abts A, Montalban-Lopez M, Kuipers OP, Smits SH, Schmitt L. NisC binds the FxLx motif of the nisin leader peptide. Biochemistry. 2013;52(32):5387-95.

26. Daletos G, Kalscheuer R, Koliwer-Brandl H, Hartmann R, de Voogd NJ, Wray V, et al. Callyaerins from the Marine Sponge Callyspongia aerizusa: Cyclic Peptides with Antitubercular Activity. J Nat Prod. 2015;78(8):1910-25.
27. Suemitsu R, Horiuchi K, Ohnishi K, Kubota M. High-performance liquid chromatographic determination of alterporriol D and E in fermentation of Alternaria porri (Ellis) Ciferri. J Chromatogr. 1990;503(1):282-7.
28. Susanne Gebhard TM. Antimicrobial peptide sensing and detoxification modules:unravelling the regulatory circuitry ofStaphylococcus aureus. Molecular Microbiology. 2011;81:581-7.
29. Kingston AW, Zhao H, Cook GM, Helmann JD. Accumulation of heptaprenyl diphosphate sensitizes Bacillus subtilis to bacitracin: implications for the mechanism of resistance mediated by the BceAB transporter. Mol Microbiol. 2014;93(1):37-49.

4. Discussion

In this thesis the nisin resistance proteins NSR and NsrFP of the human pathogenic strain *S. agalactiae* were investigated. Both resistance proteins are encoded on one operon together with a response regulator and a histidine kinase, combined forming a resistance mechanism (Chapter II).
This operon is also found in many other firmicute bacteria, mostly a BceAB-type ABC transporter is associated and coevolved with a TCS (136). Interestingly those BceAB-type transporter contain a large extracellular domain (ECD), whereas the kinase encoded on the same operon lacks an extracellular sensing domain (1, 7, 146). Since this large ECD is unusual for ABC transporter it is assumed, that the transporter fulfills a dual function: On the one hand it acts as a sensor and on the other hand it mediates the resistance against AMPs (168). Surprisingly, those characteristic ECDs of the BceAB-type transporter share no sequence identities, which raises the question of their function.

Unlike other immunity and resistance transporter BceAB-type transporter confer resistance against structurally very diverse AMPs (Chapter II and (150)). As they are evolutionary connected and fulfill the same function in different bacteria, it is of great interest to solve the overall mechanism of this type of ABC transporter.
In lantibiotic producers a similar operon, named LanFEG, composed of a lipoprotein, a TCS and an ABC transporter is present. The best studied operon is NisFEG of the nisin system, with the lipoprotein NisI, the TCS NisRK and the ABC transporter NisFEG. It was shown that NisFEG is a nisin exporter (158), whereas the lipoprotein NisI binds nisin (157, 169). Further it was shown that the lipoprotein NisI plays a more effective role and is assumed to be the first line of defense, whereas the transporter is the second line (170-172).

Encoded in Bce-like operons just a few additional membrane anchored proteins are known like NSR of *S. agalactiae* or VraH from *S. aureus* (1, 10). Those type of proteins are very interesting since they only confer resistance against one target in contrast to the corresponding transporter. Here it has to be elucidated whether the membrane anchored protein or the ABC transporter operates as the first line of defense.

In this thesis the mechanism of resistance of the ABC transporter *Sa*NsrFP was elucidated. Furthermore, two approaches to overcome the resistance in *Sa*NSR were identified. Here we discuss the achieved findings and their relevance on the previous described context. We will discuss which of the resistance proteins functions as the first line of defense or the second line and further consider the role of the extracellular domain.

4.1. Characterization of *Sa*NsrFP

The ABC transporter NsrFP from *Streptococcus agalactiae* belongs to the BceAB-type transporter (6) and was known to confer resistance against the lantibiotic nisin (1). Several BceAB-type transporter are known which confer resistance against more than one antimicrobial peptide (7-10). Here we first discovered the spectrum of resistance mediated by *Sa*NsrFP. Further the mechanism of the transporter was solved since, although there have been a lot of studies about BceAB-type transporter and it has been assumed that they are involved in antimicrobial peptide removal from the membrane (150), operate as an exporter (147) or flip undecaprenyl pyrophosphate (151), the resistance mechanism of the ABC transporter family remains unsolved.

Resistance of the ABC transporter Sa*NsrFP*

In Chapter I and VI a broad substrate specificity of *Sa*NsrFP was demonstrated. First it was thought the transporter recognizes the N-terminal part of nisin since it confers resistance to all tested nisin variants and also against gallidermin, which is similar in the first lanthionine rings A and B of nisin (Chapter I). Further $nisin_{1\text{-}28}$, the product of the protease *Sa*NSR was tested against NsrFP and resulted in an even higher fold of resistance than wildtype nisin, suggesting that both proteins of the nsr operon work together. Additionally, also $nisin_{C28P}$ was tested, which is able to bypass the protease *Sa*NSR (Chapter III) and is less effective against the transporter *Sa*NsrFP.
In Chapter VI other AMPs targeting lipid II or UDP were tested, demonstrating that *Sa*NsrFP confers resistance against all tested substances but especially against bacitracin, a cyclic peptide able to bind and sequester UPP and thereby prevents the recycling of the lipid carrier and interrupts the lipid II synthesis cycle (Figure 8).

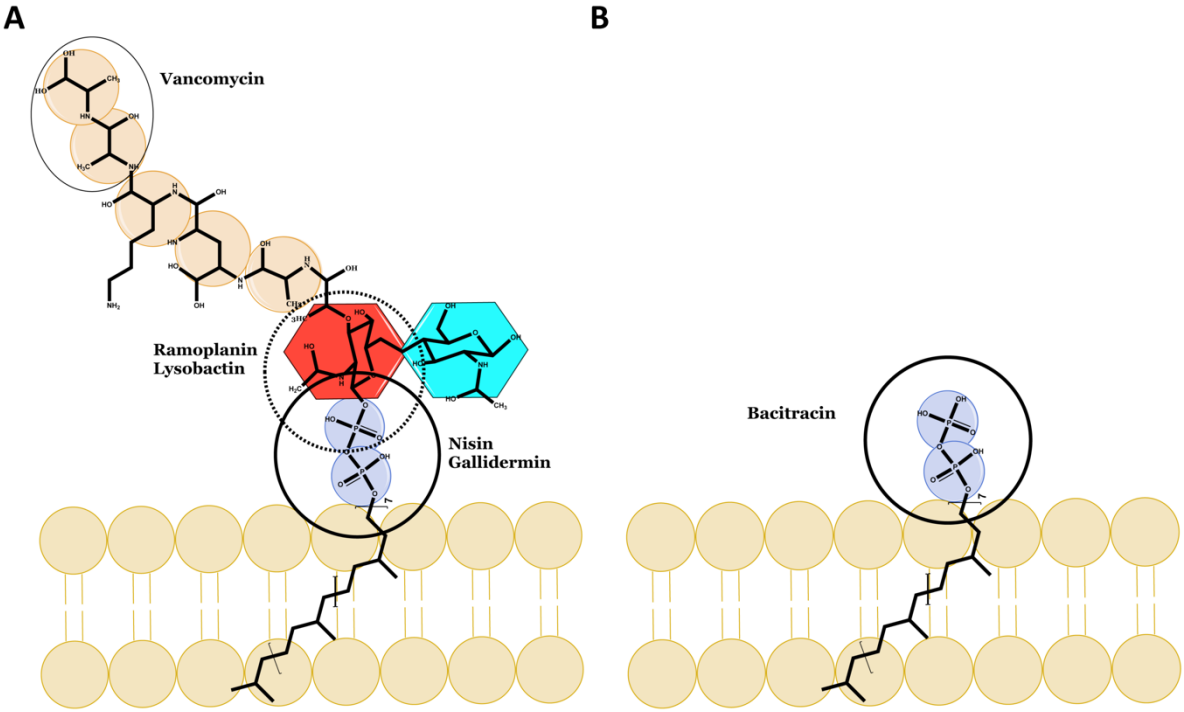

Figure 8: Schematic representation of antibiotics targeting lipid II and UPP.

A) Schematic view of lipid II, anchored to the membrane (yellow) with its undecaprenyl-pyrophosphate (blue), N-acetyl muramic acid (red), N-acetyl glucosamine (turquoise) and the pentapeptide Ala-Glu-Lys-(Asn)-Ala-Ala (orange). Highlighted are the target regions of the nisin and gallidermin (bold), ramoplanin and lysobactin (dashed) and vancomycin (plain). **B)** Schematic view of undecaprenyl-pyrophoshphate with its phosphates (blue), anchored to the membrane (yellow) and highlighted target region of bacitracin (bold) (Taken from Chapter VI).

Interestingly, also other BceAB-type ABC transporter confer a high resistance against bacitracin. In *Listeria monocytogenes* the transporter AnrAB was detected, which was first thought to confer resistance against nisin. AnrAB was tested against other AMPs and showed resistance also against the lantibiotic gallidermin and the highest resistance, of all tested substances, against bacitracin (173). The ABC transporter BceAB of *B. subtilis* showed, besides resistance against nisin and gallidermin, as well the highest resistance against bacitracin (8). Also studies with VraDE of *S. aureus* showed resistance against nisin and gallidermin and also against bacitracin mediated by this transporter (9, 10). As all mentioned transporter confer resistance against the lantibiotic nisin and the cyclic peptide bacitracin, while that share neither structural nor target similarities, it can be assumed that the transporter must share a mechanism involving the lipid II recycling process. In the next part we will discuss the putative mechanism of the BceAB-type transporter.

Mechanism of the ABC transporter Sa*NsrFP*

As mentioned above a common mechanism for BceAB-type ABC transporter is very likely. Here we use NsrFP from *S. agalactiae* as a model system to elucidate their mechanism. In Chapter VI we hypothesize that *Sa*NsrFP flips lipid II back in the cytoplasm, founded by several experimental indications (Figure 9). The first hint was the broad spectrum of antibiotics against which *Sa*NsrFP, and also other BceAB-type transporter, confer resistance. Here it was noticeable that those antibiotics either target lipid II directly or target molecules inside of the lipid II recycling process. Based on these findings we checked the peptidoglycan composition of the *Sa*NsrFP expressing strain, which is altered in the cross-linking bridge compared to our control strains, suggesting a modification of lipid II while flipping inside of the cells.

Since the peptidoglycan synthesis should be disturbed by flipping lipid II inside of the cells an altered growth behavior of the *Sa*NsrFP expressing cells was expected. Our results showed decelerated growth of those cells compared to the control strains, confirming our thesis. Additionally, cell growth was observed in the presence of 100 nM bacitracin, which did not influence the growth of the *Sa*NsrFP expressing cells but result in a breakdown of the control cells growth, supporting the lipid II flipping postulation since the target of bacitracin UPP is absent in *Sa*NsrFP expressing cells (Figure 2).

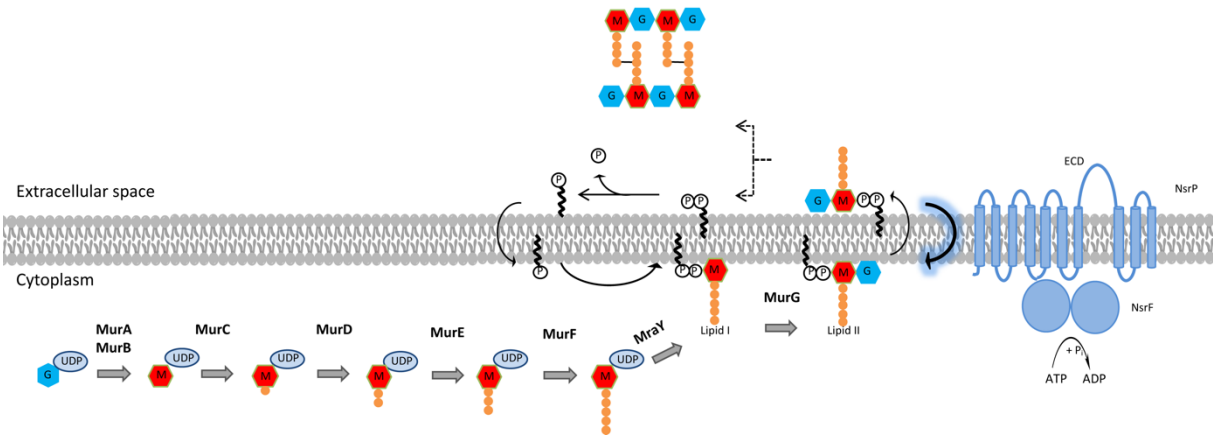

Figure 9: Postulated mechanism of *Sa*NsrFP.

Schematic view of peptidoglycan synthesis Synthesis. Phosphates are marked with a P, undecaprenyl as a black curved line, uridine phosphate (UDP) in light blue, GlcNAc in blue, MurNAc in red and aminoacids of the pentapeptide in orange. The transporter *Sa*NsrFP is demonstrated in blue with a highlighted arrow for the postulated flippase mechanism of lipid II inside of the cytoplasm (Taken from Chapter VI).

Since all these results would influence the lipid II synthesis, it was of major interest to check the proteome of the cells. Interestingly almost all proteins involved in cell wall synthesis are downregulated in *Sa*NsrFP expressing cells (Figure 9: MurA, MurC, MurD, MurE, MurF). Based on the thesis of lipid II flipping subsequently more lipid II is in the cytoplasm and less lipid II has to be synthesized, which would result in less expression rate of the involved proteins.

Overcoming the resistance mediated by Sa*NsrFP*

Since the overall aim is to fight human pathogenic bacteria it is of major interest to overcome the resistance mechanism in those strains. In Chapter VII we demonstrated that natural compounds and derivatives from fungi and marine organisms are able to inhibit the resistance ABC transporter *Sa*NsrFP. The best inhibiting compound was found to be Cerebroside C (Figure 10A), composed of a fatty acid and a sphingosine, which together form the ceramide structure and further a monosaccharide. Since Cerebroside D (Figure 10B), which only differs in one double bound, causes no inhibition of *Sa*NsrFP expressing cells it can be assumed that the effect of Cerebroside C is rather specific than caused by membrane affinity because of its lipid structure.

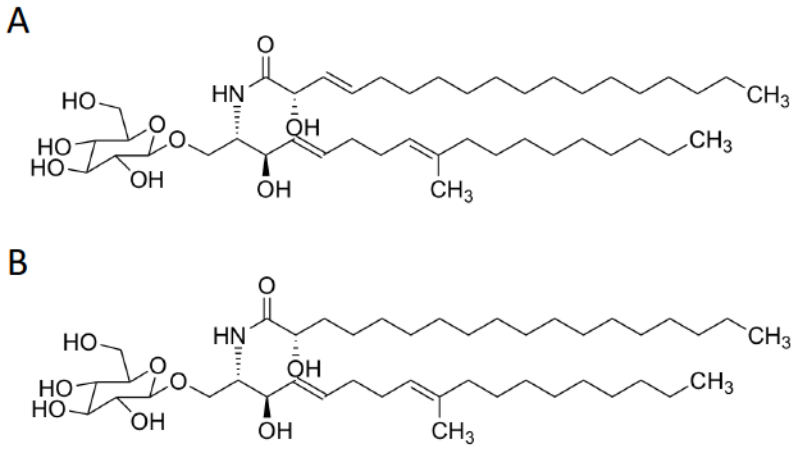

Figure 10:Structures of A) Cerebroside C and B) Cerebroside D (Taken from Chapter VII).

Two putative mechanisms of inhibition were elucidated in Chapter VII. The first one is based on an proposed exporting mechanism of *Sa*NsrFP (147) (Chapter I), which could be inhibited by a specific binding of Cerebroside C to the active site, resulting in competitive inhibition or by binding to the non-active part of the protein and thereby changing its conformation and

preventing substrate binding. Another postulated mechanism of the BceAB-type transporter is a flipping mechanism of undecaprenyl pyrophosphate (151). Here the same putative effects of Cerebroside C are possible, just differing in the substrate of the transporter. Considering Chapter VI and our new postulated mechanism for *Sa*NsrFP it can be assumed that Cerebroside C can not only function as a competitive inhibitor or binding to the non-active part of the transporter but also could be a potential substrate of the ABC transporter due to its structural similarity to lipid II. Nevertheless, this would not explain the specific inhibition of Cerebroside C compared to Cerebroside D. Conclusively the inhibitional effect of this natural compound remains unsolved but creates a great basis for further studies to overcome the resistance mediated by *Sa*NsrFP.

4.2. Overcome the nisin resistance of *Sa*NSR

The nisin resistance protein *Sa*NSR is a C-terminal processing peptidase (CTP) with a specific catalytic dyad mechanism, consisting of a serine and a histidine residue (2, 3). The crystal structure of *Sa*NSR shows a 10 Å width tunnel, which is negatively charged, hydrophobic and binds the last two (methyl–) lanthionine rings D and E of nisin (3). *Sa*NSR confers resistance against nisin by degrading the lantibiotic at its C-terminus, directly after ring E between MeLan28 and Ser29, resulting in a 100 fold less active $nisin_{1\text{-}28}$ fragment (4, 5).

Bypassing SaNSR with an effective nisin derivate

The first approach to overcome this nisin resistance mediated by *Sa*NSR was to find a nisin variant which is still active but cannot be cleaved by *Sa*NSR (Chapter III). We investigated the nisin variant $nisin_{C28P}$, lacking the last lanthionine ring E by substituting the cysteine at position 28 with a proline, and thereby introducing a small ring-like structure which sterically is rather rigid (Figure 11).

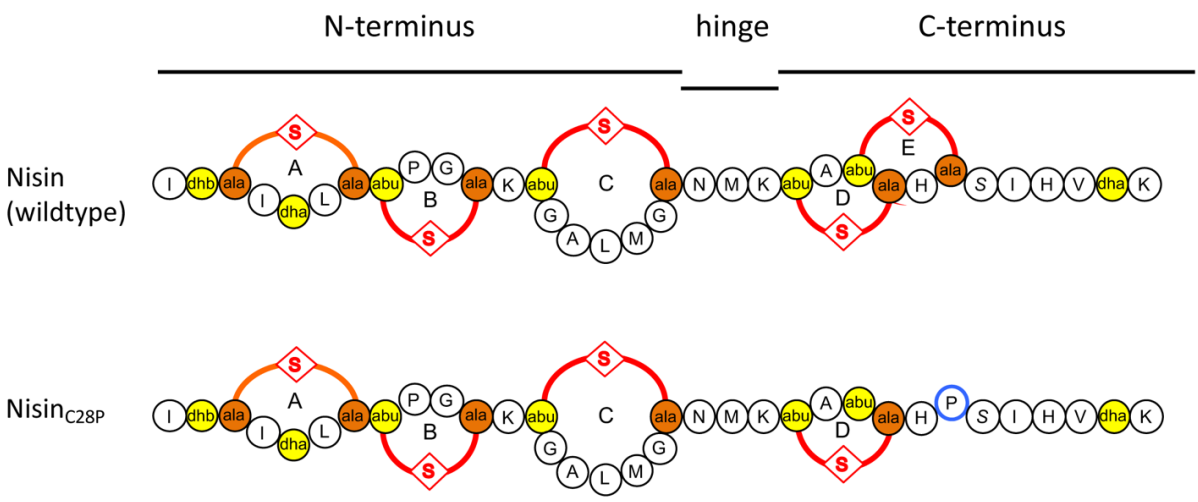

Figure 11: Schematic view of nisin A wildtype and nisin$_{C28P}$.
Introduced mutation at position 28 is highlighted in blue. The (methyl-) lanthionine rings, formed by a cysteine residue sidechain and a dehydrated amino acid residue are highlighted in orange and yellow (rings A, B, C, D and E) (Taken from Chapter III).

Nisin$_{C28P}$ was applied to a *L. lactis* strain expressing the wildtype *Sa*NSR protein as well as to a control strain carrying an empty plasmid and to *Sa*NSR$_{S236A}$ expressing cells, an inactive mutant where the serine of the catalytic dyad is substituted by an alanine. *In vivo* assays showed that nisin$_{C28P}$ is still active in a low nanomolar range and further that the nisin$_{C28P}$ fold of resistance of NZ9000*Sa*NSR as well as of NZ9000*Sa*NSR$_{S236A}$ against the sensitive strain are similar to the nisin fold of resistance of the NZ9000*Sa*NSR$_{S236A}$. These studies suggest that *Sa*NSR is also still able to bind the nisin variant *in vivo* but is not able to cleave it. In comparison to the *Sa*NSR$_{S236A}$ mutant, which is able to bind nisin but not to cleave off the last six amino acids. This assumption also fits to the molecular dynamic studies which showed the interactions between the catalytic domain in *Sa*NSR and the rings D and E of nisin (174).

In vitro assays showed that nisin$_{C28P}$ is still able to form pores in *L. lactis* NZ9000 cells. Further it was shown that the nisin variant forms pores in *L. lactis* NZ9000NSR cells at a concentration of 30 nM, whereas the wildtype nisin shows no pore forming effect at this concentration. In addition it was indicated that pore formation starts slowly when nisin$_{C28P}$ is used, which is consistent with showing that the rings D and E of nisin are, together with the hinge region, responsible for the flipping inside the membrane to form the pores (175).

Compared to previous studies on nisin derivates, the only known mutations leading to a decreased resistance of *Sa*NSR are the results of the nisin$_{C28P}$ variant depicted here and further

the Ser29Pro mutations by Field *et al.* (2018) (176). This study presents a highly potent, pore forming nisin variant as an alternative lantibiotic to bypass *Sa*NSR. Here we detected a lantibiotic with a three times higher activity against *Sa*NSR-expressing *L. lactis* cells than nisin.

Small-molecule inhibitors of Sa*NSR*

The second approach to overcome the nisin resistance mediated by *Sa*NSR was to identify first-in-class small-molecule inhibitors by virtual screening based on a previously derived structural model of the complex of *Sa*NSR with nisin (Chapter V). During this virtual screening first compounds were selected based on shape similarities with the parts of nisin, lanthionine rings D and E as well as Ser29 and Ile30, involved in recognition by *Sa*NSR. Subsequently the best fitting compounds were further analyzed by molecular docking studies to predict their configuration in the binding site of *Sa*NSR and to rank them in accordance with their potential molecular interactions. In the first screening 11 compounds were selected for further testing. In the second screening, with two additional filters, 23 compounds were selected. With those 34 compounds a biological activity assay was performed to gain the specific growth inhibition of the *L. lactis* NZ9000NSR cells mediated by the compounds. The best specific growth inhibition was shown by the compound NPG9, with 58 % at a concentration of 150 µM. NPG9 is a halogenated phenyl-urea derivative. Further a reduced half maximal inhibitory concentration of nisin was measured in presence of 120 µM NPG9 (Figure 12) and results in 50.5 % compared to *L. lactis* NZ9000NSR cells without the compound.

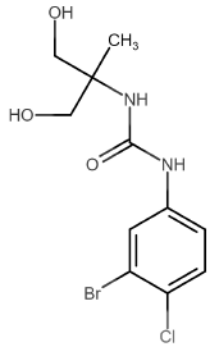

Figure 12: Structure of NPG9.

Based on this derivatives of NPG9 were searched focusing on bioisosteric replacements of halogen atoms or variations of the two hydroxyl groups. None of the 12 NPG9 derivatives shows a higher activity against *Sa*NSR than NPG9.
Molecular docking studies showed that the tunnel of *Sa*NSR is frequently accessible for NPG9. Further STD NMR measurements demonstrate that NPG9 is able to bind the resistance proteins, consistent with the binding mode model. Conclusively the first-in-class small-molecule inhibitor of *Sa*NSR was identified and till date no other biological activities have been reported.
After revealing a strategy to bypass the *Sa*NSR protein with the first approach of this thesis, the second approach shows a direct binding of the resistance protein and thereby an inhibition of its activity, making wildtype nisin more suitable again.

4.3. The nisin resistance machinery in *S. agalactiae*

In this thesis we elucidated the mechanism of the nisin resistance ABC transporter NsrFP from *S. agalactiae* and further exemplified different approaches to overcome *Sa*NsrFP and the serine protease *Sa*NSR.
The serine protease *Sa*NSR is very specific, resulting in inefficient cleavage of nisin derivates like nisin$_{C28P}$ (Chapter III). Further natural, structural unrelated compounds are not able to inhibit this protein (Chapter VII) whereas nisin based modelled small-molecule inhibitors show an inhibitional effect on the serine protease (Chapter V).
In contrast the ABC transporter *Sa*NsrFP confers resistance against lantibiotics, glycopeptides, lipoglycodepsipeptides, acylcyclodepsipeptides and cyclcic peptides, which target either the cell wall precursor lipid II or the peptidoglycan sub product undecaprenyl pyrophosphate (Chapter I and VI). Further we demonstrated that *Sa*NsrFP can be specifically inhibited by some natural compounds, including cyclic peptides, diterpenes and ceramides (Chapter VII).

In Chapter IV we investigated on nisin hinge-region variants, where this region is either partially deleted ($\Delta_{21}MK_{22}$), extended within the hinge-region or at the C-terminus of the hinge-region ($_{20}NIVMK_{24}$ and $_{20}NMKIV_{24}$) (Figure 13). We tested all three variants on the immunity proteins NisI and NisFEG as well as on the resistance proteins *Sa*NSR and *Sa*NsrFP. The nisin hinge-region variant $_{20}NIVMK_{24}$ shows a higher fold of resistance compared to nisin against the immunity proteins NisI and NisFEG, whereas the resistance proteins seemed not to be influenced. On the other hand the nisin variant $\Delta_{21}MK_{22}$ showed a decreased fold of

resistance against the resistance proteins *Sa*NSR and *Sa*NsrFP, whereas the immunity proteins, especially the lipoprotein NisI are not highly influenced by this mutation. Those studies indicate a different mechanism and substrate recognition between the immunity and the resistance system for both, the lipoproteins NisI and *Sa*NSR and the ABC transporter NisFEG and *Sa*NsrFP. Further the nisin variant $_{20}$NMKIV$_{24}$ showed to be less recognized by all tested proteins, demonstrating a great approach for further studies to overcome lantibiotic immunity and resistance, by showing just a slight decrease of pore forming an antimicrobial activity.

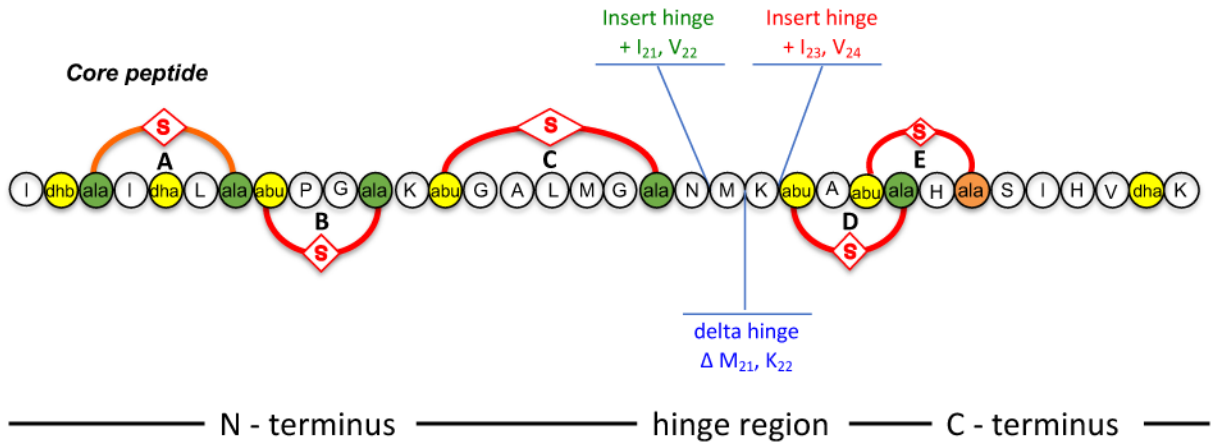

Figure 13: Schematic representation of nisin hinge-region variants.

The (methyl-)lanthionine rings, formed by a cysteine residue side chain and a dehydrated amino acid residue are highlighted in yellow and green. The (methyl-)lanthionine rings A, B, C, D and E are depicted in red (Taken from Chapter IV) Introduced mutations are indicated in green (extension inside hinge-region), red (extension after hinge-region) and blue (partially deletion of the hinge-region).

Considering both resistance proteins as a resistance machinery a few findings stand out. The nisin cleavage product of *Sa*NSR is nisin$_{1-28}$ and it was shown that *Sa*NsrFP still shows resistance against this nisin variant, even with a higher fold than against wildtype nisin, suggesting that both resistance proteins of the nsr operon work together and complement each other. This complementation was also observed for some immunity operons like the nisin operon of *L. lactis* and the subtilin operon in *B. subtilis* (152, 177). Interestingly, nearly all lantibiotic immunity systems are composed out of a lipoprotein LanI, like NisI and SpaI, and an ABC transporter LanFEG, like NisFEG and SpaFEG, independent of their produced lantibiotic (156). The membrane associated LanI lipoproteins confer resistance against just a few substrates by for example binding or sequestering nisin (NisI) or subtilin (SpaI) (157, 169, 177). The immunity ABC transporter NisFEG and SpaFEG are known to transport the substrate (nisin/subtilin) into the extracellular space (152, 177). The only known three-component ABC

transporter, which confers lantibiotic resistance is CprABC from *C. difficile* (148). Together with the TCS CprRK it confers resistance against nisin, gallidermin, subtilin, mutacin 1140 and cinnamycin (155), therefore also showing a broad substrate specificity. Directly in front of this operon a gene encoding a lipoprotein can be found. Although it is uncharacterized yet, it is assumed that it could confer lantibiotic resistance (148, 155).
However, BceAB-type resistance systems almost always lack this lipoprotein, which is assumed to be the first line of defense in lantibiotic immunity systems (170-172). One lipoprotein can be found in the nisin resistance system of *S. agalactiae* (Chapter III-V). Another membrane anchored protein, which is additional to a BceAB-type transporter is VraH of *S. aureus* forming a functional complex with the transporter VraDE. Again the transporter confers resistance against a few antibiotics like gallidermin, nisin and bacitracin, whereas the additional protein VraH only confers resistance against gallidermin and seems to be very substrate specific like *Sa*NSR and the LanI proteins (10) (Chapter II).

Conclusively it can be assumed that in Bce-systems rather the ABC transporter is the first line of defense, protecting the cell against a broad spectrum of antimicrobial peptides with a specific mechanism of flipping the cell wall precursor lipid II and thereby extracting the target from the extracellular space. The characteristic, uncommon large extracellular domain plays a great role in this mechanism, which still has to be elucidated. In contrast to the lantibiotic immunity system the lipoprotein is assumed to be the second line of defense. Since this protein is lacking in many Bce-systems it demonstrates the high effectiveness of the mechanism of the BceAB-type ABC transporter (Figure 14).

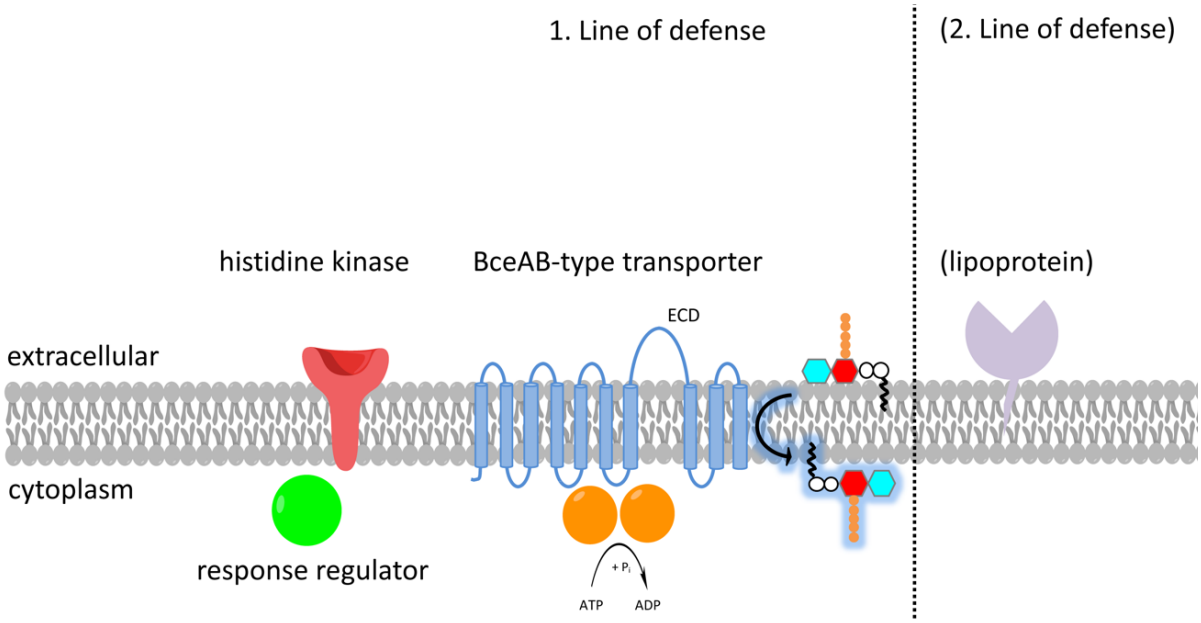

Figure 14: Schematic representation of the proteins encoded on bce-like operons.
The TCS with its histidine kinase (red) and response regulator (green) as well as the BceAB-type transporter with the permease domain (blue) and the NBD (orange) form the first line of defense. The mechanism of BceAB-type transporter is demonstrated by the flipping of lipid II (highlighted in blue). The additional second line of defense with the lipoprotein (purple) is demonstrated as an eventuality, lacking in most of the bce-like operons.

The role and function of the characteristic extracellular domain of BceAB-type ABC transporter is still unknown. They are supposed to recognize the AMPs extracellularly and subsequently induce the TCS-dependent signal transduction within the cell, therefore being crucial for the resistance (9, 146). Further an initial substrate binding of the ECD was postulated based on indirect knockout mutant studies (165). Interestingly, as shown in Figure 15, those ECDs share almost no sequence identity.

```
NsrP      ----SNTQNVVTGLFPKSVSLSIDNSKGDAKNIFEEKILKKLGKSSK---EAITYN----  49
BceB      YISYYSSEKTAEQNVAADFSFMN----EKDAKLFENKLRESNISFVKKATPVLQANVDIA  56
VraE      --SKSNTDQTLTSMAPNEFNVVA----TQDAKQFETKLSQQQITFSKNAYETITVDNVKD  54
               .:::.       ....       .  : ** *: :.  .  *    .:  :

NsrP      QTMISMPVSQSSE------LNITSKNVKHVDITKTGFMYLITQNDFRRLGHRLPKLKDNQ  103
BceB      NIMDGTPKEMQGDPGNMQLAVVSDKDVKGVDVAAGEAVF---------------------  95
VraE      QVITL---ENGSDSGRTNSILSANNKVTGN-----NAII---------------------  85
          : :     .  .:         :.:.*.         :

NsrP      VAYFVQKGDSRLKKINLLGNKFDVVKN-----------LKEAYVPETTNT--YNPGLII  149
BceB      -----SGYTDLLQKIMVFKDSGVIKVKSKHETQPLKYKGLREEFLVSYTFTSGGMPAVIV  150
VraE      -----TNTKSLPNIINIHLNKDLVVKGTKNETFRVTQEDKGRVYPLNLSFN---SPVVEV  137
                    .  : * :  :.  :                 . :  . : .    * : :

NsrP      FANNKQIDNIRKAYLPYTKNINTFPKTFKAYLDLNSQEINSISK-NDIIEVDGKYVGNIS  208
BceB      --DDSLFKQLDKDKDPRI---QLAQSTFIG---VNVKHDDQMEKANELFQQVNKKNEHL-  201
VraE      --SPEKYQQLK------T---QNNVHTFYG---YDIKQTSQKEKAQAIAKQFGDKVITY-  182
            . .  .::           :    ** .    : :. .. .* : : :  ..

NsrP      TKQSFLKEGYQ------     219
BceB      ---SRLDTSAAQKSLFG     215
VraE      ---DEMKKEVD--ATNG     194
             . :.
```

Figure 15: Alignment of representative ECDs.

Alignment of the ECDs of NsrP from *S. agalactiae*, BceB from *B. subtilis* and VraE from *S. aureus* as representatives for BceAB-type ECDs. (Taken from https://www.ebi.ac.uk/Tools/services/web/toolresult.ebi?jobId=clustalo-I20191018-113235-0389-35180401-p1m , 21.10.2019)

Nevertheless, a structural or functional similarity for those characteristic domains is very likely. If this domain acts as a sensor the question arises whether it recognizes just one type of AMPs or several and how does this recognition part look like. Further, if it is responsible for the resistance against diverse AMPs the functional mechanism of this domain has to be elucidated and is of major interest to investigate on novel antibiotics to overcome the resistance mechanisms and to treat infections with related human pathogens.

5. Literature

1. Khosa S, AlKhatib Z, Smits SH. NSR from *Streptococcus agalactiae* confers resistance against nisin and is encoded by a conserved nsr operon. Biol Chem. 2013;394(11):1543-9.

2. Rawlings ND, Barrett AJ, Thomas PD, Huang X, Bateman A, Finn RD. The MEROPS database of proteolytic enzymes, their substrates and inhibitors in 2017 and a comparison with peptidases in the PANTHER database. Nucleic Acids Res. 2018;46(D1):D624-D32.

3. Khosa S, Frieg B, Mulnaes D, Kleinschrodt D, Hoeppner A, Gohlke H, et al. Structural basis of lantibiotic recognition by the nisin resistance protein from *Streptococcus agalactiae.* Sci Rep. 2016;6:18679.

4. Sun Z, Zhong J, Liang X, Liu J, Chen X, Huan L. Novel mechanism for nisin resistance via proteolytic degradation of nisin by the nisin resistance protein NSR. Antimicrob Agents Chemother. 2009;53(5):1964-73.

5. Liang X, Sun Z, Zhong J, Zhang Q, Huan L. Adverse effect of nisin resistance protein on nisin-induced expression system in *Lactococcus lactis*. Microbiol Res. 2010;165(6):458-65.

6. Tsuda H, Yamashita Y, Shibata Y, Nakano Y, Koga T. Genes involved in bacitracin resistance in *Streptococcus mutans*. Antimicrob Agents Chemother. 2002;46(12):3756-64.

7. Ohki R, Giyanto, Tateno K, Masuyama W, Moriya S, Kobayashi K, et al. The BceRS two-component regulatory system induces expression of the bacitracin transporter, BceAB, in *Bacillus subtilis*. Molecular Microbiology. 2003;49(4):1135-44.

8. Staron A, Finkeisen DE, Mascher T. Peptide antibiotic sensing and detoxification modules of *Bacillus subtilis*. Antimicrob Agents Chemother. 2011;55(2):515-25.

9. Hiron A, Falord M, Valle J, Debarbouille M, Msadek T. Bacitracin and nisin resistance in *Staphylococcus aureus*: a novel pathway involving the BraS/BraR two-component system (SA2417/SA2418) and both the BraD/BraE and VraD/VraE ABC transporters. Mol Microbiol. 2011;81(3):602-22.

10. Popella P, Krauss S, Ebner P, Nega M, Deibert J, Gotz F. VraH Is the Third Component of the *Staphylococcus aureus* VraDEH System Involved in Gallidermin and Daptomycin Resistance and Pathogenicity. Antimicrob Agents Chemother. 2016;60(4):2391-401.

11. Flemming A. On the antibacterial action of cultures of a penicillium, with special reference to their use in the isolation of *B. influenza*. British journal of experimental pathology 1929. p. 226–36.

12. van Hoek AH, Mevius D, Guerra B, Mullany P, Roberts AP, Aarts HJ. Acquired antibiotic resistance genes: an overview. Front Microbiol. 2011;2:203.

13. Powers JH. Antimicrobial drug development--the past, the present, and the future. Clin Microbiol Infect. 2004;10 Suppl 4:23-31.

14. Higgins PG, Fluit AC, Schmitz FJ. Fluoroquinolones: structure and target sites. Curr Drug Targets. 2003;4(2):181-90.

15. Drlica K, Zhao X. DNA gyrase, topoisomerase IV, and the 4-quinolones. Microbiol Mol Biol Rev. 1997;61(3):377-92.

16. Hooper DC. Quinolone mode of action. Drugs. 1995;49 Suppl 2:10-5.

17. Yoneyama H, Katsumata R. Antibiotic resistance in bacteria and its future for novel antibiotic development. Biosci Biotechnol Biochem. 2006;70(5):1060-75.

18. Johnston NJ, Mukhtar TA, Wright GD. Streptogramin antibiotics: mode of action and resistance. Curr Drug Targets. 2002;3(4):335-44.

19. Kapoor G, Saigal S, Elongavan A. Action and resistance mechanisms of antibiotics: A guide for clinicians. J Anaesthesiol Clin Pharmacol. 2017;33(3):300-5.

20. Wise R. A review of the mechanisms of action and resistance of antimicrobial agents. Can Respir J. 1999;6 Suppl A:20A-2A.

21. Bozdogan B, Appelbaum PC. Oxazolidinones: activity, mode of action, and mechanism of resistance. Int J Antimicrob Agents. 2004;23(2):113-9.

22. Chapot-Chartier MP. Interactions of the cell-wall glycopolymers of lactic acid bacteria with their bacteriophages. Front Microbiol. 2014;5:236.

23. Muller A, Klockner A, Schneider T. Targeting a cell wall biosynthesis hot spot. Nat Prod Rep. 2017;34(7):909-32.

24. JORDAN DC, INNISS WE. Selective inhibition of ribonucleic acid synthesis in *Staphylococcus aureus* by vancomycin. Nature. 1959;184(Suppl 24):1894-5.

25. ANDERSON JS, MATSUHASHI M, HASKIN MA, STROMINGER JL. LIPID-PHOSPHOACETYLMURAMYL-PENTAPEPTIDE AND LIPID-PHOSPHODISACCHARIDE-PENTAPEPTIDE: PRESUMED MEMBRANE TRANSPORT INTERMEDIATES IN CELL WALL SYNTHESIS. Proc Natl Acad Sci U S A. 1965;53:881-9.

26. Perkins HR. Specificity of combination between mucopeptide precursors and vancomycin or ristocetin. Biochem J. 1969;111(2):195-205.

27. Chatterjee AN, Perkins HR. Compounds formed between nucleotides related to the biosynthesis of bacterial cell wall and vancomycin. Biochem Biophys Res Commun. 1966;24(3):489-94.

28. Montecalvo MA. Ramoplanin: a novel antimicrobial agent with the potential to prevent vancomycin-resistant enterococcal infection in high-risk patients. J Antimicrob Chemother. 2003;51 Suppl 3:iii31-5.

29. Cavalleri B, Pagani H, Volpe G, Selva E, Parenti F. A-16686, a new antibiotic from Actinoplanes. I. Fermentation, isolation and preliminary physico-chemical characteristics. J Antibiot (Tokyo). 1984;37(4):309-17.

30. Hu Y, Helm JS, Chen L, Ye XY, Walker S. Ramoplanin inhibits bacterial transglycosylases by binding as a dimer to lipid II. J Am Chem Soc. 2003;125(29):8736-7.

31. Breukink E, de Kruijff B. Lipid II as a target for antibiotics. Nat Rev Drug Discov. 2006;5(4):321-32.

32. Hamburger JB, Hoertz AJ, Lee A, Senturia RJ, McCafferty DG, Loll PJ. A crystal structure of a dimer of the antibiotic ramoplanin illustrates membrane positioning and a potential Lipid II docking interface. Proc Natl Acad Sci U S A. 2009;106(33):13759-64.

33. O'Sullivan J, McCullough JE, Tymiak AA, Kirsch DR, Trejo WH, Principe PA. Lysobactin, a novel antibacterial agent produced by *Lysobacter sp.* I. Taxonomy, isolation and partial characterization. J Antibiot (Tokyo). 1988;41(12):1740-4.

34. Bonner DP, O'Sullivan J, Tanaka SK, Clark JM, Whitney RR. Lysobactin, a novel antibacterial agent produced by *Lysobacter sp.* II. Biological properties. J Antibiot (Tokyo). 1988;41(12):1745-51.

35. Lee W, Schaefer K, Qiao Y, Srisuknimit V, Steinmetz H, Müller R, et al. The Mechanism of Action of Lysobactin. J Am Chem Soc. 2016;138(1):100-3.

36. Ling LL, Schneider T, Peoples AJ, Spoering AL, Engels I, Conlon BP, et al. A new antibiotic kills pathogens without detectable resistance. Nature. 2015;517(7535):455-9.

37. Kong KF, Schneper L, Mathee K. Beta-lactam antibiotics: from antibiosis to resistance and bacteriology. APMIS. 2010;118(1):1-36.

38. Terico AT, Gallagher JC. Beta-lactam hypersensitivity and cross-reactivity. J Pharm Pract. 2014;27(6):530-44.

39. Konz D, Klens A, Schörgendorfer K, Marahiel MA. The bacitracin biosynthesis operon of *Bacillus licheniformis* ATCC 10716: molecular characterization of three multi-modular peptide synthetases. Chem Biol. 1997;4(12):927-37.

40. Nakano MM, Zuber P. Molecular biology of antibiotic production in Bacillus. Crit Rev Biotechnol. 1990;10(3):223-40.

41. Johnson BA, Anker H, Meleney FL. BACITRACIN: A NEW ANTIBIOTIC PRODUCED BY A MEMBER OF THE *B. SUBTILIS* GROUP. Science. 1945;102(2650):376-7.

42. MELENEY FL, JOHNSON B. Bacitracin therapy; the first hundred cases of surgical infections treated locally with the antibiotic. J Am Med Assoc. 1947;133(10):675-80.

43. Storm DR, Strominger JL. Complex formation between bacitracin peptides and isoprenyl pyrophosphates. The specificity of lipid-peptide interactions. J Biol Chem. 1973;248(11):3940-5.

44. Economou NJ, Cocklin S, Loll PJ. High-resolution crystal structure reveals molecular details of target recognition by bacitracin. Proc Natl Acad Sci U S A. 2013;110(35):14207-12.

45. Hancock RE, Lehrer R. Cationic peptides: a new source of antibiotics. Trends Biotechnol. 1998;16(2):82-8.

46. Malmsten M. Antimicrobial peptides. Ups J Med Sci. 2014;119(2):199-204.

47. Flemming A. On a Remarkable Bacteriolytic Element Found in Tissues and Secretions. Proceedings of the Royal Society B: Biological Sciences: Royal Society; 1922. p. 306-17.

48. Wang G. The Antimicrobial Peptide Database provides a platform for decoding the design principles of naturally occurring antimicrobial peptides. Protein Sci. 2019.

49. Jenssen H, Hamill P, Hancock RE. Peptide antimicrobial agents. Clin Microbiol Rev. 2006;19(3):491-511.

50. Pasupuleti M, Schmidtchen A, Malmsten M. Antimicrobial peptides: key components of the innate immune system. Crit Rev Biotechnol. 2012;32(2):143-71.

51. Nawrocki KL, Crispell EK, McBride SM. Antimicrobial Peptide Resistance Mechanisms of Gram-Positive Bacteria. Antibiotics (Basel). 2014;3(4):461-92.

52. Hale JD, Hancock RE. Alternative mechanisms of action of cationic antimicrobial peptides on bacteria. Expert Rev Anti Infect Ther. 2007;5(6):951-9.

53. Diamond G, Beckloff N, Weinberg A, Kisich KO. The roles of antimicrobial peptides in innate host defense. Curr Pharm Des. 2009;15(21):2377-92.

54. Wang G. Improved methods for classification, prediction, and design of antimicrobial peptides. Methods Mol Biol. 2015;1268:43-66.

55. Klaenhammer TR. Genetics of bacteriocins produced by lactic acid bacteria. FEMS Microbiol Rev. 1993;12(1-3):39-85.

56. Yang S-C, Lin C-H, Sung CT, Fang J-Y. Antibacterial activities of bacteriocins: application in foods and pharmaceuticals. Frontiers in microbiology. 2014;5.

57. Cascales E, Buchanan SK, Duché D, Kleanthous C, Lloubès R, Postle K, et al. Colicin biology. Microbiol Mol Biol Rev. 2007;71(1):158-229.

58. Kleanthous C. Swimming against the tide: progress and challenges in our understanding of colicin translocation. Nat Rev Microbiol. 2010;8(12):843-8.

59. Severinov K, Semenova E, Kazakov A, Kazakov T, Gelfand MS. Low-molecular-weight post-translationally modified microcins. Mol Microbiol. 2007;65(6):1380-94.

60. Cotter PD, Hill C, Ross RP. Bacteriocins: developing innate immunity for food. Nat Rev Microbiol. 2005;3(10):777-88.

61. Cleveland J, Montville TJ, Nes IF, Chikindas ML. Bacteriocins: safe, natural antimicrobials for food preservation. Int J Food Microbiol. 2001;71(1):1-20.

62. B. Jarvis JJ, G.C. Cheeseman. Molecular weight distribution of nisin. Biochim Biophys Acta. 1968;168:153-5.

63. Bierbaum G SC, Josten M, Heidrich C, Kempter C, Jung G, Sahl HG. Engineering of a novel thioether bridge and role of modified residues in the lantibiotic Pep5. Appl Environ Microbiol. 1996;62:385-92.

64. Sahl HG, Bierbaum G. Lantibiotics: biosynthesis and biological activities of uniquely modified peptides from gram-positive bacteria. Annu Rev Microbiol. 1998;52:41-79.

65. Rogers LA. The Inhibiting Effect of *Streptococcus Lactis* on *Lactobacillus Bulgaricus.* J Bacteriol. 1928;16(5):321-5.

66. Rogers LA, Whittier EO. Limiting Factors in the Lactic Fermentation. J Bacteriol. 1928;16(4):211-29.

67. Hastings JW, Sailer M, Johnson K, Roy KL, Vederas JC, Stiles ME. Characterization of leucocin A-UAL 187 and cloning of the bacteriocin gene from *Leuconostoc gelidum*. J Bacteriol. 1991;173(23):7491-500.

68. Marciset O, Jeronimus-Stratingh MC, Mollet B, Poolman B. Thermophilin 13, a nontypical antilisterial poration complex bacteriocin, that functions without a receptor. J Biol Chem. 1997;272(22):14277-84.

69. Kawai Y, Kemperman R, Kok J, Saito T. The circular bacteriocins gassericin A and circularin A. Curr Protein Pept Sci. 2004;5(5):393-8.

70. Knerr PJ, van der Donk WA. Discovery, biosynthesis, and engineering of lantipeptides. Annu Rev Biochem. 2012;81:479-505.

71. Chatterjee C, Paul M, Xie L, van der Donk WA. Biosynthesis and mode of action of lantibiotics. Chemical Reviews. 2005;105(2):633-84.

72. Arnison PG, Bibb MJ, Bierbaum G, Bowers AA, Bugni TS, Bulaj G, et al. Ribosomally synthesized and post-translationally modified peptide natural products: overview and recommendations for a universal nomenclature. Nat Prod Rep. 2013;30(1):108-60.

73. van Heel AJ, de Jong A, Song C, Viel JH, Kok J, Kuipers OP. BAGEL4: a user-friendly web server to thoroughly mine RiPPs and bacteriocins. Nucleic Acids Res. 2018;46(W1):W278-W81.

74. Willey JM, van der Donk WA. Lantibiotics: peptides of diverse structure and function. Annu Rev Microbiol. 2007;61:477-501.

75. Goto Y, Li B, Claesen J, Shi Y, Bibb MJ, van der Donk WA. Discovery of unique lanthionine synthetases reveals new mechanistic and evolutionary insights. PLoS Biol. 2010;8(3):e1000339.

76. Koponen O, Tolonen M, Qiao M, Wahlström G, Helin J, Saris PE. NisB is required for the dehydration and NisC for the lanthionine formation in the post-translational modification of nisin. Microbiology. 2002;148(Pt 11):3561-8.

77. Zhang Q, Yu Y, Vélasquez JE, van der Donk WA. Evolution of lanthipeptide synthetases. Proc Natl Acad Sci U S A. 2012;109(45):18361-6.

78. Okeley NM, Paul M, Stasser JP, Blackburn N, van der Donk WA. SpaC and NisC, the cyclases involved in subtilin and nisin biosynthesis, are zinc proteins. Biochemistry. 2003;42(46):13613-24.

79. Li B, Yu JP, Brunzelle JS, Moll GN, van der Donk WA, Nair SK. Structure and mechanism of the lantibiotic cyclase involved in nisin biosynthesis. Science. 2006;311(5766):1464-7.

80. Lagedroste M, Smits SHJ, Schmitt L. Substrate Specificity of the Secreted Nisin Leader Peptidase NisP. Biochemistry. 2017;56(30):4005-14.

81. Montalban-Lopez M, Deng J, van Heel AJ, Kuipers OP. Specificity and Application of the Lantibiotic Protease NisP. Front Microbiol. 2018;9:160.

82. Pag U, Sahl HG. Multiple activities in lantibiotics--models for the design of novel antibiotics? Curr Pharm Des. 2002;8(9):815-33.

83. Plat A, Kuipers A, Rink R, Moll GN. Mechanistic aspects of lanthipeptide leaders. Curr Protein Pept Sci. 2013;14(2):85-96.

84. Karam L, Jama C, Nuns N, Mamede AS, Dhulster P, Chihib NE. Nisin adsorption on hydrophilic and hydrophobic surfaces: evidence of its interactions and antibacterial activity. J Pept Sci. 2013;19(6):377-85.

85. Zasloff M. Antimicrobial peptides of multicellular organisms. Nature. 2002;415(6870):389-95.

86. Van de Ven FJ, Van den Hooven HW, Konings RN, Hilbers CW. NMR studies of lantibiotics. The structure of nisin in aqueous solution. Eur J Biochem. 1991;202(3):1181-8.

87. Wiedemann I, Breukink E, van Kraaij C, Kuipers OP, Bierbaum G, de Kruijff B, et al. Specific binding of nisin to the peptidoglycan precursor lipid II combines pore formation and inhibition of cell wall biosynthesis for potent antibiotic activity. J Biol Chem. 2001;276(3):1772-9.

88. Gross E, Morell JL. The structure of nisin. J Am Chem Soc. 1971;93(18):4634-5.

89. Wiedemann I, Breukink E, Van Kraaij C, Kuipers OP, Bierbaum G, De Kruijff B, et al. Specific Binding of Nisin to the Peptidoglycan Precursor Lipid II Combines Pore Formation and Inhibition of Cell Wall Biosynthesis for Potent Antibiotic Activity. Journal of Biological Chemistry. 2001;276(3):1772-9.

90. Hsu ST, Breukink E, Tischenko E, Lutters MA, de Kruijff B, Kaptein R, et al. The nisin-lipid II complex reveals a pyrophosphate cage that provides a blueprint for novel antibiotics. Nat Struct Mol Biol. 2004;11(10):963-7.

91. Hasper HE, de Kruijff B, Breukink E. Assembly and stability of nisin-lipid II pores. Biochemistry. 2004;43(36):11567-75.

92. Breukink E, van Kraaij C, Demel RA, Siezen RJ, Kuipers OP, de Kruijff B. The C-terminal region of nisin is responsible for the initial interaction of nisin with the target membrane. Biochemistry. 1997;36(23):6968-76.

93. Breukink E, Wiedemann I, van Kraaij C, Kuipers OP, Sahl HG, de Kruijff B. Use of the cell wall precursor lipid II by a pore-forming peptide antibiotic. Science. 1999;286(5448):2361-4.

94. Abts A, Mavaro A, Stindt J, Bakkes PJ, Metzger S, Driessen AJ, et al. Easy and rapid purification of highly active nisin. Int J Pept. 2011;2011:175145.

95. Hasper HE, Kramer NE, Smith JL, Hillman JD, Zachariah C, Kuipers OP, et al. An alternative bactericidal mechanism of action for lantibiotic peptides that target lipid II. Science. 2006;313(5793):1636-7.

96. Wiedemann I, Benz R, Sahl HG. Lipid II-mediated pore formation by the peptide antibiotic nisin: a black lipid membrane study. J Bacteriol. 2004;186(10):3259-61.

97. Dischinger J, Chipalu SB, Bierbaum G. Lantibiotics: promising candidates for future applications in health care. International Journal of Medical Microbiology. 2014;304(1):51-62.
98. Mota-Meira M, Lapointe G, Lacroix C, Lavoie MC. MICs of mutacin B-Ny266, nisin A, vancomycin, and oxacillin against bacterial pathogens. Antimicrobial agents and chemotherapy. 2000;44(1):24-9.
99. Draper LA, Cotter PD, Hill C, Ross RP. Lantibiotic Resistance. Microbiology and Molecular Biology Reviews. 2015;79(2):171-91.
100. de Freire Bastos MdC, Coelho MLV, da Silva Santos OC. Resistance to bacteriocins produced by Gram-positive bacteria. Microbiology. 2015;161(Pt 4):683-700.
101. Nizet V. Antimicrobial peptide resistance mechanisms of human bacterial pathogens. Curr Issues Mol Biol. 2006;8(1):11-26.
102. Hancock RE, Rozek A. Role of membranes in the activities of antimicrobial cationic peptides. FEMS Microbiol Lett. 2002;206(2):143-9.
103. Huijbregts RP, de Kroon AI, de Kruijff B. Topology and transport of membrane lipids in bacteria. Biochim Biophys Acta. 2000;1469(1):43-61.
104. Verheul A, Russell NJ, Van'T Hof R, Rombouts FM, Abee T. Modifications of membrane phospholipid composition in nisin-resistant *Listeria monocytogenes* Scott A. Appl Environ Microbiol. 1997;63(9):3451-7.
105. Crandall AD, Montville TJ. Nisin resistance in *Listeria monocytogenes* ATCC 700302 is a complex phenotype. Appl Environ Microbiol. 1998;64(1):231-7.
106. Mantovani HC, Russell JB. Nisin resistance of *Streptococcus bovis*. Appl Environ Microbiol. 2001;67(2):808-13.
107. Ming X, Daeschel MA. Nisin Resistance of Foodborne Bacteria and the Specific Resistance Responses of *Listeria monocytogenes* Scott A. J Food Prot. 1993;56(11):944-8.
108. Mazzotta AS, Montville TJ. Nisin induces changes in membrane fatty acid composition of Listeria monocytogenes nisin-resistant strains at 10 degrees C and 30 degrees C. J Appl Microbiol. 1997;82(1):32-8.
109. Martínez B, Rodríguez A. Antimicrobial susceptibility of nisin resistant *Listeria monocytogenes* of dairy origin. FEMS Microbiol Lett. 2005;252(1):67-72.
110. Ernst CM, Staubitz P, Mishra NN, Yang SJ, Hornig G, Kalbacher H, et al. The bacterial defensin resistance protein MprF consists of separable domains for lipid lysinylation and antimicrobial peptide repulsion. PLoS Pathog. 2009;5(11):e1000660.
111. Ernst CM, Peschel A. Broad-spectrum antimicrobial peptide resistance by MprF-mediated aminoacylation and flipping of phospholipids. Mol Microbiol. 2011;80(2):290-9.

112. Peschel A, Jack RW, Otto M, Collins LV, Staubitz P, Nicholson G, et al. *Staphylococcus aureus* resistance to human defensins and evasion of neutrophil killing via the novel virulence factor MprF is based on modification of membrane lipids with l-lysine. J Exp Med. 2001;193(9):1067-76.

113. Kristian SA, Dürr M, Van Strijp JA, Neumeister B, Peschel A. MprF-mediated lysinylation of phospholipids in *Staphylococcus aureus* leads to protection against oxygen-independent neutrophil killing. Infect Immun. 2003;71(1):546-9.

114. Staubitz P, Peschel A. MprF-mediated lysinylation of phospholipids in *Bacillus subtilis*--protection against bacteriocins in terrestrial habitats? Microbiology. 2002;148(Pt 11):3331-2.

115. Bao Y, Sakinc T, Laverde D, Wobser D, Benachour A, Theilacker C, et al. Role of mprF1 and mprF2 in the pathogenicity of E*nterococcus faecalis.* PLoS One. 2012;7(6):e38458.

116. Mishra NN, Bayer AS, Tran TT, Shamoo Y, Mileykovskaya E, Dowhan W, et al. Daptomycin resistance in *enterococci* is associated with distinct alterations of cell membrane phospholipid content. PLoS One. 2012;7(8):e43958.

117. Maloney E, Stankowska D, Zhang J, Fol M, Cheng QJ, Lun S, et al. The two-domain LysX protein of *Mycobacterium tuberculosis* is required for production of lysinylated phosphatidylglycerol and resistance to cationic antimicrobial peptides. PLoS Pathog. 2009;5(7):e1000534.

118. Heath RJ, Rock CO. Enoyl-acyl carrier protein reductase (fabI) plays a determinant role in completing cycles of fatty acid elongation in *Escherichia coli*. J Biol Chem. 1995;270(44):26538-42.

119. Kramer NE, van Hijum SA, Knol J, Kok J, Kuipers OP. Transcriptome analysis reveals mechanisms by which *Lactococcus lactis* acquires nisin resistance. Antimicrob Agents Chemother. 2006;50(5):1753-61.

120. Weidenmaier C, Kristian SA, Peschel A. Bacterial resistance to antimicrobial host defenses--an emerging target for novel antiinfective strategies? Curr Drug Targets. 2003;4(8):643-9.

121. Ward JB. Teichoic and teichuronic acids: biosynthesis, assembly, and location. Microbiol Rev. 1981;45(2):211-43.

122. Weidenmaier C, Peschel A. Teichoic acids and related cell-wall glycopolymers in Gram-positive physiology and host interactions. Nat Rev Microbiol. 2008;6(4):276-87.

123. Neuhaus FC, Heaton MP, Debabov DV, Zhang Q. The dlt operon in the biosynthesis of D-alanyl-lipoteichoic acid in *Lactobacillus casei.* Microb Drug Resist. 1996;2(1):77-84.

124. Peschel A, Otto M, Jack RW, Kalbacher H, Jung G, Götz F. Inactivation of the dlt operon in *Staphylococcus aureus* confers sensitivity to defensins, protegrins, and other antimicrobial peptides. J Biol Chem. 1999;274(13):8405-10.

125. Fabretti F, Theilacker C, Baldassarri L, Kaczynski Z, Kropec A, Holst O, et al. Alanine esters of enterococcal lipoteichoic acid play a role in biofilm formation and resistance to antimicrobial peptides. Infect Immun. 2006;74(7):4164-71.

126. Perego M, Glaser P, Minutello A, Strauch MA, Leopold K, Fischer W. Incorporation of D-alanine into lipoteichoic acid and wall teichoic acid in *Bacillus subtilis*. Identification of genes and regulation. J Biol Chem. 1995;270(26):15598-606.

127. Kovács M, Halfmann A, Fedtke I, Heintz M, Peschel A, Vollmer W, et al. A functional dlt operon, encoding proteins required for incorporation of d-alanine in teichoic acids in gram-positive bacteria, confers resistance to cationic antimicrobial peptides in *Streptococcus pneumoniae*. J Bacteriol. 2006;188(16):5797-805.

128. Giaouris E, Briandet R, Meyrand M, Courtin P, Chapot-Chartier MP. Variations in the degree of D-Alanylation of teichoic acids in *Lactococcus lactis* alter resistance to cationic antimicrobials but have no effect on bacterial surface hydrophobicity and charge. Appl Environ Microbiol. 2008;74(15):4764-7.

129. Abi Khattar Z, Rejasse A, Destoumieux-Garzón D, Escoubas JM, Sanchis V, Lereclus D, et al. The dlt operon of *Bacillus cereus* is required for resistance to cationic antimicrobial peptides and for virulence in insects. J Bacteriol. 2009;191(22):7063-73.

130. McBride SM, Sonenshein AL. The dlt operon confers resistance to cationic antimicrobial peptides in *Clostridium difficile*. Microbiology. 2011;157(Pt 5):1457-65.

131. Schwartz B, Markwalder JA, Wang Y. Lipid II: total synthesis of the bacterial cell wall precursor and utilization as a substrate for glycosyltransfer and transpeptidation by penicillin binding protein (PBP) 1b of *Escherichia coli*. J Am Chem Soc. 2001;123(47):11638-43.

132. Gravesen A, Sørensen K, Aarestrup FM, Knøchel S. Spontaneous nisin-resistant *Listeria monocytogenes* mutants with increased expression of a putative penicillin-binding protein and their sensitivity to various antibiotics. Microb Drug Resist. 2001;7(2):127-35.

133. Stock AM, Zhulin IB. Two-Component Signal Transduction: a Special Issue in the. J Bacteriol. 2017;199(18).

134. Mascher T. Intramembrane-sensing histidine kinases: a new family of cell envelope stress sensors in Firmicutes bacteria. FEMS Microbiol Lett. 2006;264(2):133-44.

135. Mascher T, Margulis NG, Wang T, Ye RW, Helmann JD. Cell wall stress responses in *Bacillus subtilis:* the regulatory network of the bacitracin stimulon. Molecular Microbiology. 2003;50(5):1591-604.

136. Dintner S, Staron A, Berchtold E, Petri T, Mascher T, Gebhard S. Coevolution of ABC transporters and two-component regulatory systems as resistance modules against antimicrobial peptides in Firmicutes Bacteria. J Bacteriol. 2011;193(15):3851-62.

137. Gebhard S. ABC transporters of antimicrobial peptides in Firmicutes bacteria–phylogeny, function and regulation. Molecular microbiology. 2012;86(6):1295-317.

138. Clemens R, Zaschke-Kriesche J, Khosa S, Smits SHJ. Insight into Two ABC Transporter Families Involved in Lantibiotic Resistance. Front Mol Biosci. 2017;4:91.

139. Khosa S, Hoeppner A, Gohlke H, Schmitt L, Smits SH. Structure of the Response Regulator NsrR from *Streptococcus agalactiae,* Which Is Involved in Lantibiotic Resistance. PLoS One. 2016;11(3):e0149903.

140. Jordan S, Junker A, Helmann JD, Mascher T. Regulation of LiaRS-dependent gene expression in *bacillus subtilis*: identification of inhibitor proteins, regulator binding sites, and target genes of a conserved cell envelope stress-sensing two-component system. J Bacteriol. 2006;188(14):5153-66.

141. Mascher T, Zimmer SL, Smith TA, Helmann JD. Antibiotic-inducible promoter regulated by the cell envelope stress-sensing two-component system LiaRS of *Bacillus subtilis*. Antimicrob Agents Chemother. 2004;48(8):2888-96.

142. Bergholz TM, Tang S, Wiedmann M, Boor KJ. Nisin resistance of Listeria monocytogenes is increased by exposure to salt stress and is mediated via LiaR. Appl Environ Microbiol. 2013;79(18):5682-8.

143. Kawada-Matsuo M, Yoshida Y, Zendo T, Nagao J, Oogai Y, Nakamura Y, et al. Three distinct two-component systems are involved in resistance to the class I bacteriocins, Nukacin ISK-1 and nisin A, in *Staphylococcus aureus*. PLoS One. 2013;8(7):e69455.

144. O'Connell-Motherway M, van Sinderen D, Morel-Deville F, Fitzgerald GF, Ehrlich SD, Morel P. Six putative two-component regulatory systems isolated from *Lactococcus lactis subsp. cremoris* MG1363. Microbiology. 2000;146 (Pt 4):935-47.

145. Lutz Schmitt RT. Structure and mechanism of ABC transporters. Current Opinion in Structural Biology. 2002;12:754-60.

146. Rietkötter E, Hoyer D, Mascher T. Bacitracin sensing in *Bacillus subtilis*. Molecular microbiology. 2008;68(3):768-85.

147. Reiners J, Lagedroste M, Ehlen K, Leusch S, Zaschke-Kriesche J, Smits SHJ. The N-terminal Region of Nisin Is Important for the BceAB-Type ABC Transporter NsrFP from *Streptococcus agalactiae* COH1. Front Microbiol. 2017;8:1643.

148. McBride SM, Sonenshein AL. Identification of a genetic locus responsible for antimicrobial peptide resistance in *Clostridium difficile*. Infection and immunity. 2011;79(1):167-76.

149. Bernard R, Guiseppi A, Chippaux M, Foglino M, Denizot F. Resistance to bacitracin in *Bacillus subtilis*: unexpected requirement of the BceAB ABC transporter in the control of expression of its own structural genes. Journal of bacteriology. 2007;189(23):8636-42.

150. Susanne Gebhard TM. Antimicrobial peptide sensing and detoxification modules:unravelling the regulatory circuitry of *Staphylococcus aureus*. Molecular Microbiology. 2011;81:581-7.

151. Kingston AW, Zhao H, Cook GM, Helmann JD. Accumulation of heptaprenyl diphosphate sensitizes *Bacillus subtilis* to bacitracin: implications for the mechanism of resistance mediated by the BceAB transporter. Mol Microbiol. 2014;93(1):37-49.

152. Stein T, Heinzmann S, Solovieva I, Entian K-D. Function of *Lactococcus lactis* nisin immunity genes nisI and nisFEG after coordinated expression in the surrogate host *Bacillus subtilis*. Journal of Biological Chemistry. 2003;278(1):89-94.

153. Otto M, Peschel A, Götz F. Producer self-protection against the lantibiotic epidermin by the ABC transporter EpiFEG of *Staphylococcus epidermidis* Tü3298. FEMS Microbiol Lett. 1998;166(2):203-11.

154. C. Klein KDE. Genes involved in Self-Protection against the Lantibiotic Subtilin Produced by Bacillus subtilis. Appl Environ Microbiol. 1994;60:2793-801.

155. Suárez JM, Edwards AN, McBride SM. The *Clostridium difficile* cpr locus is regulated by a noncontiguous two-component system in response to type A and B lantibiotics. Journal of bacteriology. 2013;195(11):2621-31.

156. Alkhatib Z, Abts A, Mavaro A, Schmitt L, Smits SH. Lantibiotics: how do producers become self-protected? J Biotechnol. 2012;159(3):145-54.

157. AlKhatib Z, Lagedroste M, Fey I, Kleinschrodt D, Abts A, Smits SH. Lantibiotic immunity: inhibition of nisin mediated pore formation by NisI. PLoS One. 2014;9(7):e102246.

158. AlKhatib Z, Lagedroste M, Zaschke J, Wagner M, Abts A, Fey I, et al. The C-terminus of nisin is important for the ABC transporter NisFEG to confer immunity in *Lactococcus lactis*. Microbiologyopen. 2014;3(5):752-63.

159. Peschel A, Schnell N, Hille M, Entian KD, Götz F. Secretion of the lantibiotics epidermin and gallidermin: sequence analysis of the genes gdmT and gdmH, their influence on epidermin production and their regulation by EpiQ. Mol Gen Genet. 1997;254(3):312-8.

160. Repka LM, Chekan JR, Nair SK, van der Donk WA. Mechanistic Understanding of Lanthipeptide Biosynthetic Enzymes. Chem Rev. 2017;117(8):5457-520.

161. Pozzi R, Coles M, Linke D, Kulik A, Nega M, Wohlleben W, et al. Distinct mechanisms contribute to immunity in the lantibiotic NAI-107 producer strain *Microbispora* ATCC PTA-5024. Environ Microbiol. 2016;18(1):118-32.

162. Jarvis B. Resistance to nisin and production of nisin-inactivating enzymes by several Bacillus species. J Gen Microbiol. 1967;47(1):33-48.

163. Jarvis B. Enzymic reduction of the C-terminal dehydroalanyl-lysine sequence in nisin. Biochem J. 1970;119(5):56P.

164. Galesloot TE. Lactic Acid Bacteria Which Destroy The Antibioticum (Nisin) Of *S-Lactis*. Nederlands Melk-En Zuiveltijdschrift1956. p. 143-55

165. Falord M, Karimova G, Hiron A, Msadek T. GraXSR proteins interact with the VraFG ABC transporter to form a five-component system required for cationic antimicrobial peptide sensing and resistance in *Staphylococcus aureus*. Antimicrob Agents Chemother. 2012;56(2):1047-58.

166. Froseth BR, McKay LL. Molecular characterization of the nisin resistance region of *Lactococcus lactis* subsp. lactis biovar diacetylactis DRC3. Appl Environ Microbiol. 1991;57(3):804-11.

167. Schultz J, Milpetz F, Bork P, Ponting CP. SMART, a simple modular architecture research tool: identification of signaling domains. Proc Natl Acad Sci U S A. 1998;95(11):5857-64.

168. Fritz G, Dintner S, Treichel NS, Radeck J, Gerland U, Mascher T, et al. A New Way of Sensing: Need-Based Activation of Antibiotic Resistance by a Flux-Sensing Mechanism. MBio. 2015;6(4):e00975.

169. Stein T, Heinzmann S, Solovieva I, Entian KD. Function of *Lactococcus lactis* nisin immunity genes nisI and nisFEG after coordinated expression in the surrogate host *Bacillus subtilis*. J Biol Chem. 2003;278(1):89-94.

170. Kuipers OP, Beerthuyzen MM, Siezen RJ, De Vos WM. Characterization of the nisin gene cluster nisABTCIPR of *Lactococcus lactis*. Requirement of expression of the nisA and nisI genes for development of immunity. Eur J Biochem. 1993;216(1):281-91.

171. Siegers K, Entian KD. Genes involved in immunity to the lantibiotic nisin produced by *Lactococcus lactis* 6F3. Appl Environ Microbiol. 1995;61(3):1082-9.

172. Khosa S, Lagedroste M, Smits SH. Protein Defense Systems against the Lantibiotic Nisin: Function of the Immunity Protein NisI and the Resistance Protein NSR. Front Microbiol. 2016;7:504.

173. Collins B, Curtis N, Cotter PD, Hill C, Ross RP. The ABC transporter AnrAB contributes to the innate resistance of *Listeria monocytogenes* to nisin, bacitracin, and various beta-lactam antibiotics. Antimicrob Agents Chemother. 2010;54(10):4416-23.

174. Khosa S, Frieg B, Mulnaes D, Kleinschrodt D, Hoeppner A, Gohlke H, et al. Structural basis of lantibiotic recognition by the nisin resistance protein from *Streptococcus agalactiae*. Scientific Reports. 2016;6:18679.

175. Hasper HE, de Kruijff B, Breukink E. Assembly and stability of nisin-lipid II pores. Biochemistry. 2004;43(36):11567-75.

176. Field D, Blake T, Mathur H, O'Connor PM, Cotter PD, Ross RP, et al. Bioengineering Nisin to overcome the Nisin Resistance Protein. Mol Microbiol. 2018.

177. Stein T, Heinzmann S, Düsterhus S, Borchert S, Entian K-D. Expression and functional analysis of the subtilin immunity genes spaIFEG in the subtilin-sensitive host *Bacillus subtilis* MO1099. Journal of bacteriology. 2005;187(3):822-8.

6. Curriculum Vitae

Personal Data

Date of birth	20.03.1989, Dormagen
Nationality	German

Academic studies

Since 04.10.2016	PhD student at the Institute of Biochemistry, Heinrich Heine-University Düsseldorf with Prof. Dr. Lutz Schmitt and Dr. Sander Smits
April 2014 – April 2016	Master of Science (M.Sc.) Graduation Master of Biochemistry at the Heinrich Heine University Düsseldorf
23.03.2015 – 30.05.2015	Internship at the institute of Biochemistry of Mahidol University, Bangkok Supported by “Hedwig und Waldemar Hort” scholarship foundation
October 2011 – March 2014	Bachelor of Science (B.Sc.) Graduation Bachelor of Biochemistry at the Heinrich Heine University Düsseldor

Work experience

18.07.2011 – 30.09.2011	Grünenthal Pharma GmbH, Technician in biological test laboratory for quality control
19.12.2010 – 30.06.2011	Grünenthal Pharma GmbH, Technician in biological test laboratory for quality control

Education

01.08.2008 – 19.12.2010	Training for biological laboratory technician at Grünenthal GmbH & Co.KG
1999 – 2008	Abitur, Heinrich-Mann-Gymnasium, Köln

Professional Membership

2016 - present	Member, Interdisciplinary Graduate and Research Academy Duesseldorf

Workshops and Conferences

May 2019	Symposium of the graduate school GRK2158, Duesseldorf
April 2019	First international RiPPs Conference, Granada, Spain
September 2018	Symposium of the graduate school GRK2158, Bejing, China
March 2018	Gordon Research Conference New antibacterial discovery and development, Ventura, USA
March 2018	Gordon Research Seminar, New antibacterial discovery and development, Ventura, USA
September 2017	Symposium of the graduate school GRK2158, Duesseldorf
July 2017	FEMS 2017, 7th Congress of European Microbiologists, Valencia, Spain

7. List of publications

AlKhatib, Z., Lagedroste, M., **Zaschke, J.**, Wagner, M., Abts, A., Fey, I., Kleinschrodt, D. & Smits, S. H. (2014). The C-terminus of nisin is important for the ABC transporter NisFEG to confer immunity in Lactococcus lactis. Microbiologyopen, 3(5), 752-763. doi:10.1002/mbo3.205

Reiners, J., Lagedroste, M., Ehlen, K., Leusch, S., **Zaschke-Kriesche, J.**, & Smits, S. H. J. (2017). The N-terminal Region of Nisin Is Important for the BceAB-Type ABC Transporter NsrFP from Streptococcus agalactiae COH1. Front Microbiol, 8, 1643. doi:10.3389/fmicb.2017.01643

Clemens, R., **Zaschke- Kriesche, J.**, Khosa, S., & Smits, S. H. J. (2017). Insight into Two ABC Transporter Families Involved in Lantibiotic Resistance. Front Mol Biosci, 4, 91. doi:10.3389/fmolb.2017.00091

Zaschke-Kriesche, J., Behrmann, L. V., Reiners, J., Lagedroste, M., Gröner, Y., Kalscheuer, R., & Smits, S. H. J. (2019). Bypassing lantibiotic resistance by an effective nisin derivative. Bioorg Med Chem, 27(15), 3454-3462. doi:10.1016/j.bmc.2019.06.031

Zaschke-Kriesche, J., Reiners, J., Lagedroste, M., & Smits, S. H. J. (2019). Influence of nisin hinge-region variants on lantibiotic immunity and resistance proteins. Bioorg Med Chem, 27(17), 3947-3953. doi:10.1016/j.bmc.2019.07.014

Porta, N., **Zaschke-Kriesche, J.**, Frieg, B., Gopalswamy, M., Zivkovic, A., Etzkorn, M., Stark, H., Smits, S. H. J., Gohlke, H. (2019). Small-molecule inhibitors of nisin resistance protein NSR from the human pathogen Streptococcus agalactiae. Bioorg Med Chem, 27(20), 1-9, https://doi.org/10.1016/j.bmc.2019.115079

8. Acknowledgement

Am Ende meiner Dissertation möchte ich mich noch bei den Menschen bedanken, die mich auf dem Weg unterstützt haben.

Als aller erste möchte ich Dr. Sander Smits danken, dass er mich überhaupt dazu gebracht hat zu promovieren. Vielen Dank für das tolle Projekt und die Unmengen an guten Diskussionen und Ideen. Wir waren oft nicht einer Meinung aber ich glaube genau das hat die Diskussionen so fruchtbar gemacht. Danke für die Unterstützung bei den Veröffentlichungen und auch für das Korrektur lesen dieser Arbeit. Und vor allem vielen Dank für die Ehrlichkeit und den Einsatz für mich. Die letzten Jahre waren eine tolle Zeit und ich werde sie nie vergessen.

Des Weiteren danke ich Prof. Dr. Lutz Schmitt für die Möglichkeit diese Promotion in seinem Institut machen zu können und vor allem für die vielen guten Denkanstöße in unseren Gruppenmeetings. Ich danke ihm auch sehr dafür immer eine „offene Tür“ zu haben, egal worum es gerade geht.

Ein weiterer Dank geht an PD Dr. Ulrich Schulte für die gute Betreuung während des Studiums. Während der Betreuungs-Gespräche ist mir klar geworden dass ich weiter machen möchte und überhaupt den Master in Biochemie machen möchte. Außerdem möchte ich ihm für die gute Praktikumskoordination danken, irgendwie konnte immer alles geregelt werden.

Ich möchte mich bei Prof. Dr. Holger Gohlke für die Übernahme des Koreferats und die gute Zusammenarbeit innerhalb des GRK2158 bedanken.

Ich danke meiner liebsten Kaffeerunde für all die tollen Gespräche, Aufmunterungen, Lösungsvorschläge und auch einfach für die tolle Zeit.
Katja ich danke dir für die vielen tollen Gespräche während unserer Laufeinheiten und auch, dass du das mit mir durch gezogen hast.
Isa möchte ich danken dass sie immer ehrlich ist und oft sehr vernünftig an Probleme ran geht. Die Zeit mit dir im Büro fehlt mir jetzt schon, du hast mir so viel geholfen auch wenn es oft nur Kleinigkeiten waren.

Ich danke Dir, Oli, für sehr viel Spaß und Unmengen an guten Gesprächen. Mit dir ist es immer bunt und lustig aber gleichzeitig weiß ich dass ich mich auf dich verlassen kann wenn ich dich brauche.
Ein besonderer Dank geht an Rebecca, meine „Leidensgenossin“, die auch nach ihrer Promotion immer ein offenes Ohr für mich hat. Danke, dass ich immer meinen Frust bei dir abladen durfte und du mir immer versuchst zu helfen. Und natürlich Danke, dass du immer so organisiert bist und mich damit schon das ein oder andere Mal gerettet hast.
Ich danke euch für diese unvergessliche Zeit, gerade in den anstrengenden oder stressigen Phasen der Promotion waren die Kaffeepausen mit euch Gold wert. Vielen Dank!

Ich möchte Martina für Alles danken. Du bist immer ansprechbar und hilfsbereit und einfach eine Bereicherung für das ganze Institut.

Jens möchte ich danken für seine unglaublich Hilfsbereitschaft, egal ob an der HPLC oder im Büro. Du hast immer viele gute Ideen und Lösungsvorschläge und versuchst immer zu helfen auch wenn du eigentlich schon aus dem Labor raus bist.

Sakshi I would like to thank first of all for this great project she passed to me. Thank you for the great introduction and the help during the first steps in the lab. Thank you for showing me your tricks and for always being helpful.

Ich möchte mich bei Marcel bedanken für all die guten Ratschläge bei allem was mit Lactis zu tun hat. Du hast mir oft sehr geholfen und umsetzbare Vorschläge gemacht.

Außerdem möchte ich Silke danken, du warst immer sehr hilfsbereit und hast mir im Screening viel Arbeit ab genommen.

Bei Martin möchte ich mich bedanken für die lustigen Gespräche und das du unser Büro wieder was lebhafter gemacht hast.

Tobi, dir danke ich für all dein „unnützes Wissen“ und die daraus resultierenden interessanten Gespräche und Diskussionen über jedes mögliche Thema.

Außerdem möchte ich Tim danken, für seine Frohnatur und die netten Gespräche. Mit dir ist es immer lustig und du bist immer gut gelaunt.

Ich möchte auch Stefanie und Astrid danken für die gute Unterstützung bei all den Kristallisationsversuchen in meinem ersten Jahr. Es ist schön wieviel gute Laune und Optimismus ihr versprüht.

Des Weiteren möchte ich gerne meinen Studenten Hans, Lara und Tri danken. Es hat mir viel Freude bereitet euch während eurer Bachelor- bzw. Masterarbeiten zu betreuen und ihr habt nicht nur gute Ergebnisse erzielt sondern mir auch nebenbei viel im Labor geholfen. Vielen Dank für Alles und ich hoffe (und glaube) dass der ein oder andere von euch Spaß an der Wissenschaft gefunden hat und weiter macht.

Ich würde gerne allen „neueren“ Kollegen danken. Ihr habt unser Labor und die Küche wieder lebhafter gemacht. Vivien mit dem wahnsinnig guten Projekt, danke dass du mich in meiner zeitweise einsamen Nisin-Gruppe unterstützt hast. Florestan und Manuel danke, dass ihr so hilfsbereit seid und ein wenig Ordnung in unser Chaos bringt. Auch Steffi, Alex und Zoreh möchte ich danken für schöne Gespräche und ihre Hilfsbereitschaft. Und auch bei unserer neuen Arbeitsgruppe mit Alexej, Maryna, Michael und Athanasios möchte ich mich für all die lustigen Gesprächen bedanken.

Und auch allen „älteren“ Kollegen möchte ich danken. Manuel, auch wenn du noch nicht ganz weg bist, Kalpana, die immer ein offenes Ohr hatte, Katharina, Sandra, Hilke, José, Jan-Peter und Andreas, Diana, die bei allen Klonierungsfragen helfen konnte, Michael der mir seinen Platz und seinen Stress-Max überlassen hat und vor allem Sven, bei dem ich gelernt habe mit Frust um zu gehen und immer einen Plan zu haben. Es hat immer sehr viel Spaß gemacht mit euch zusammen zu arbeiten.

Außerdem möchte ich Frau Blum und Frau Platz danken, dass alle Verwaltungsangelegenheiten mit Ihnen immer so unkompliziert sind.

Ich möchte meinen Freunden danken für ihr Verständnis wenn ich Verabredungen absagen musste weil ich zu lange im Labor war, wenn ich später kam oder wenn ich zeitweise auch sehr angespannt war. Danke, dass ihr mich immer unterstützt und verstanden habt.

Auch meiner Familie möchte ich danken, meiner alten Familie mit meinen Eltern, Fabian und Meike und auch meiner neuen Familie mit meinen Schwiegereltern, Patrick und Bea. Danke, dass ihr mich immer unterstützt habt und mir den Rückhalt gegeben habt den ich brauchte. Danke dass ihr euch immer dafür interessiert habt wo ich stehe und wie es weiter geht und danke, dass ihr auch Verständnis dafür hattet wenn ich mal keine Lust hatte zu reden.

Zu guter Letzt möchte ich meinem Mann danken. Du hast mich immer unterstützt und aufgebaut. Danke, dass du oft lange mit mir diskutiert hast und immer versucht hast meine Problematiken zu verstehen. Danke, dass du so viel Verständnis für mich hattest wenn ich kaum zu Hause war. Danke, dass du immer versucht hast mir zu helfen und mir Ratschläge zu geben, die meine Situation verbessern können. Danke, dass du mir immer den Rücken frei gehalten hast und vor allem dass du mich immer ausgehalten hast, ich weiß es war nicht immer ganz einfach. Danke!

9. Declaration

Ich, Julia Schumacher, geb. Zaschke-Kriesche, versichere an Eides statt, dass die vorliegende Dissertation von mir selbstständig und ohne unzulässige fremde Hilfe unter Beachtung der „Grundsätze zur Sicherung guter wissenschaftlicher Praxis an der Heinrich-Heine-Universität Düsseldorf“ erstellt worden ist.
Diese Dissertation wurde in der vorgelegten oder in ähnlicher Form noch bei keiner anderen Institution eingereicht. Ich habe bisher keine erfolglosen Promotionsversuche unternommen.

Düsseldorf,

(Julia Schumacher)